AD_____

Award Number: W81XWH-04-1-0286

TITLE: The Role of the Sonic Hedgehog Pathway for Prostate Cancer Progression

PRINCIPAL INVESTIGATOR: Jingwu Xie

CONTRACTING ORGANIZATION: University of Texas Medical Branch
Galveston, TX 77555-1048

REPORT DATE: February 2008

TYPE OF REPORT: Final Addendum

PREPARED FOR: U.S. Army Medical Research and Materiel Command
Fort Detrick, Maryland 21702-5012

REPORT DOCUMENTATION PAGE

Form Approved
OMB No. 0704-0188

1. REPORT DATE	2. REPORT TYPE	3. DATES COVERED
01-02-2008	Final Addendum	30 Jan 2007– 29 Jan 2008

4. TITLE AND SUBTITLE

The Role of the Sonic Hedgehog Pathway for Prostate Cancer Progression

5a. CONTRACT NUMBER

5b. GRANT NUMBER
W81XWH-04-1-0286

5c. PROGRAM ELEMENT NUMBER

6. AUTHOR(S)

Jingwu Xie

Email: jinxie@utmb.edu

5d. PROJECT NUMBER

5e. TASK NUMBER

5f. WORK UNIT NUMBER

7. PERFORMING ORGANIZATION NAME(S) AND ADDRESS(ES)

University of Texas Medical Branch
Galveston, TX 77555-1048

8. PERFORMING ORGANIZATION REPORT NUMBER

9. SPONSORING / MONITORING AGENCY NAME(S) AND ADDRESS(ES)
U.S. Army Medical Research and Materiel Command
Fort Detrick, Maryland 21702-5012

10. SPONSOR/MONITOR'S ACRONYM(S)

11. SPONSOR/MONITOR'S REPORT NUMBER(S)

12. DISTRIBUTION / AVAILABILITY STATEMENT
Approved for Public Release; Distribution Unlimited

13. SUPPLEMENTARY NOTES
Original contains colored plates: ALL DTIC reproductions will be in black and white.

14. ABSTRACT Prostate cancer is a predominant cancer in men in the US, with an annual incidence of 170, 000. Only a minority of the tumor progress rapidly into advanced cancer. Thus, identification of the signaling pathways involved in prostate cancer progression is essential for designing strategies to combat prostate cancer. Based on our preliminary data, we hypothesize that Su(Fu) gene is a novel tumor suppressor gene for human prostate cancer. In this study, we determine that activation of the sonic hedgehog pathway is high in advanced prostate cancer. Several tumors with activated hedgehog signaling lack expression of Su(Fu). Our studies have also extended to other types of tumors including lung and liver cancers. We further determine he mechanisms by which Su(Fu) exerts its tumor suppressing effects using cell lines. Similarly, we have shown that there are several mechanisms of regulating Gli transcriptional factor in addition to Su(Fu). Furthermore, We show that constitutive activation of hedgehog signaling alone in the prostate is not sufficient to drive tumor 3-6 month mice. These studies reveal that hedgehog signaling is a major pathway altered in prostate cancer and it functions mainly in tumor progression, not in tumor initiation.

15. SUBJECT TERMS
Prostate cancer, Suppressor of fused, hedgehog, Patched

16. SECURITY CLASSIFICATION OF:			17. LIMITATION OF ABSTRACT	18. NUMBER OF PAGES	19a. NAME OF RESPONSIBLE PERSON
a. REPORT	b. ABSTRACT	c. THIS PAGE			USAMRMC
U	U	U	UU	115	19b. TELEPHONE NUMBER *(include area code)*

Table of Contents

Introduction

This proposal is to evaluate the role of the hedgehog pathway in prostate cancer in clinical specimens, and to identify the molecular basis of hedgehog mediated tumor formation and to examine the in vivo role of hedgehog signaling in prostate cancer development.

Body

We made great accomplishments on this project. All the specific aims have been accomplished. In total, we have generated 12 publications in the last four years with support from this grant. Some of the studies have been used for three News Releases in our institution. Major accomplishments include being one of the first groups linking hedgehog signaling activation to prostate cancer and hepatocellular carcinomas; identification of the role of Su(Fu) in cancer cell proliferation and establishment of prostate-specific activation of hedgehog signaling in mouse model.

Task 1: Activation of hedgehog signaling activation in prostate cancer (Molecular Cancer 3: 29, 2004)

We have successfully collected over 200 prostate cancer specimens. Fifty five of them are TURP (transurethral resection of the prostate) specimens, and the rest are from prostatectomy of patients with different stages of prostate cancer. We mainly focused on these 55 TURP specimens in our studies because of the following reasons. First, prostatectomy specimens are heterogeneous, with variations within a paraffin block. In contrast, TURP specimens are relatively homogeneous in tumor morphology. Second, TURP specimens can be used for other analyses such as real-time PCR and Western blotting.

Through examination of these 55 TURP specimens using specific antibodies, we found that 27 specimens contain activated hedgehog signaling (see Table 1 below), 11 tumors with no detectable Su(Fu). In addition, we discovered that Shh expression was elevated in 28 specimens (see **Table 1** for details).

Figure 1 shows immunohistostaining of PTCH1 in two tumors. One tumor had no expression of PTCH1 (**Fig. 1a**) whereas the other with a high level of PTCH1 (**Fig. 1b**). The staining was specific to the PTCH1 peptide from which the antibodies were made (**Fig. 1c**) because no positive signals were seen in the presence of excess of the PTCH1 peptide.

Table 1 Summary of protein expression in prostate cancer specimens

Tumor grade											
Gleason 3-6 (**18**) 4/18				Gleason 7 (**15**) 7/15				Gleason 8-10 (**22**) 16/22			
18 Su(Fu) Positive	4 PTCH1 Positive	4 HIP positive	10 Shh positive 10/18	13 Su(Fu) Positive	7 PTCH1 Positive	7 HIP positive	4 Shh positive 4/15	13 Su(Fu) Positive	16 PTCH1 Positive	16 HIP positive	14 Shh positive 14/22
18/18				13/15				13/22			

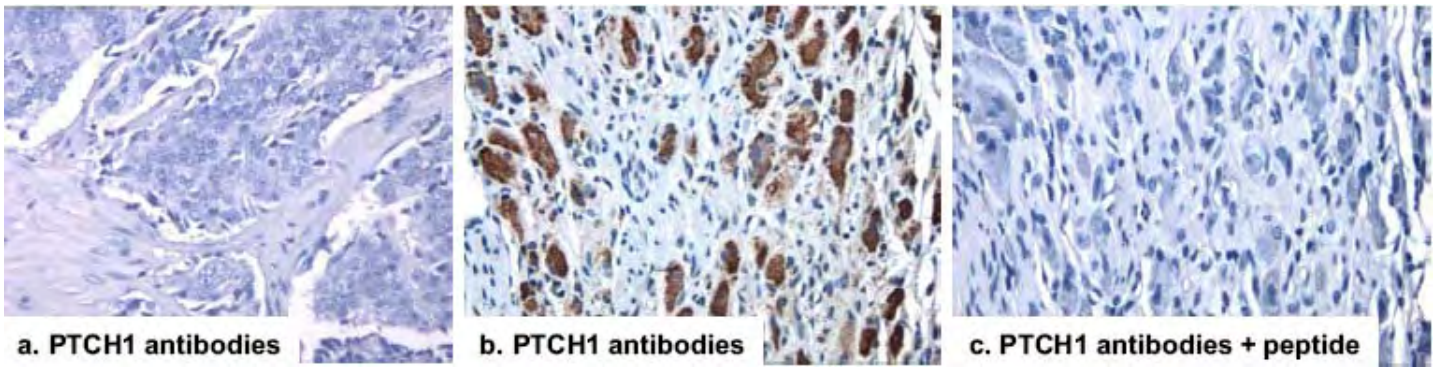

Fig.1 Detection of PTCH1 in prostate cancers PTCH1 protein expression was detected by immunohistochemistry PTCH1 specific antibodies (Santa Cruz Biotechnology Inc Cat# 6149; 1:50 dilution).

To confirm the data from PTCH1, we examined expression of another hedgehog target gene, HIP (hedgehog-interacting protein) in these prostate cancer specimens (**Fig.2**). We found that HIP was highly expressed in tumors with PTCH1 expression (see **Table 1**), and the pattern of HIP expression is very similar to that of PSA (prostate specific antigen), a sensitive marker for early prostate cancer. Thus, it appears that hedgehog signaling is frequently activated in prostate cancer.

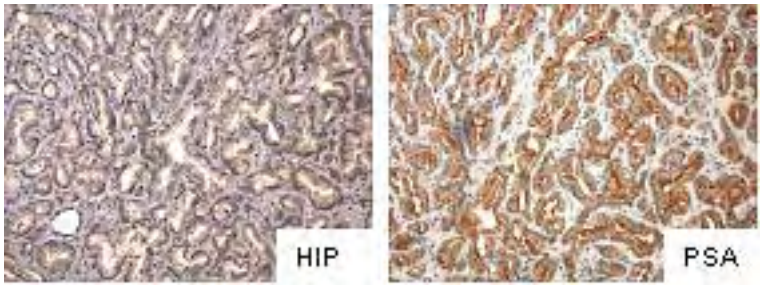

Fig. 2 Detection of HIP expression in prostate cancers Expression of HIP, another hedgehog target gene and a component of hedgehog signaling pathway, was detected using HIP specific antibodies (R&D systems, Cat# AF1568; 1:50 dilution). The pattern of HIP expression was similar to that of PSA, a serum marker for prostate cancer.

In these specimens (n=55), expression of hedgehog target genes, PTCH1 and HIP, occur only in the tumor, not in the adjacent normal prostate tissues or in the stroma (data not shown here), indicating that hedgehog signaling is mainly activated in the tumor.

Further analysis indicates that hedgehog signaling is more frequently activated in tumors with high Gleason scores (see **Table 1** and **Fig.3)**. In tumors with Gleason scores 4-6, four out of eighteen (22.2%) tumors had activated hedgehog signaling. Seven of fifteen tumors (46.7%) with Gleason scores 7 had elevated hedgehog signaling while sixteen out of twenty two (72.7%) tumors with Gleason scores 8-10 had hedgehog signaling activation. Statistic analysis using Binomial Proportions showed that the differences among different groups are significant (p values below 0.05). These data indicate hedgehog signaling activation is associated with prostate cancer progression.

Expression of Su(Fu) and sonic hedgehog in prostate cancer

Next we evaluate expression of Su(Fu) and sonic hedgehog in these prostate cancer specimens. Using antibodies specific to Su(Fu) (Santa Cruz Biotechnology Inc. Cat# 10933, 1:40 dilution), we detected Su(Fu) in all 18 prostate cancer specimens with low Gleason scores (**Table 1**). However, we only found Su(Fu) expression in only 26 of 37 tumors with Gleason scores 7-10 (**Table 1**). The differences were significant (P value < 0.05, using using Binomial Proportions analysis). Loss of detectable Su(Fu) was correlated with elevated expression of PTCH1 and HIP proteins, suggesting that Su(Fu) loss may be responsible for hedgehog signaling activation in these tumors.

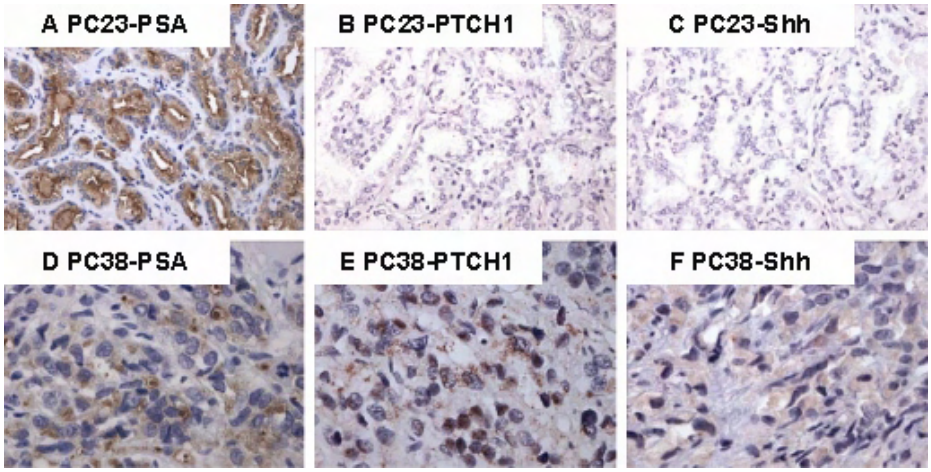

Fig. 3 Expression of PTCH1, Shh and PSA in prostate cancer Expression of PTCH1, Shh and PSA was detected by immunohistochemistry. The protein expression patterns of PTCH1 and Shh were compared with that of PSA, a marker for prostater cancer. PC23 had no detecatble expression of PTCH1 and Shh whereas PC38 has elevated expression of PTCH1, Shh and HIP. Positive signals were in brown.

These data indicate that activation of the hedgehog pathway is quite common in prostate cancer. Tumors with activated hedgehog signaling either over-express the positive regulator Shh, or lack protein expression of the negative regulator Su(Fu) (**Table 1** and **Fig.4**).

Mutation analysis of Su(Fu) in prostate cancer

To confirm the immunohistochemistry data, we performed immunoblotting analyses using several dissected TURP (Transurethral resection of the prostate) specimens in which tumor portion can be as high as 70% of the tissue mass. As shown in **Fig. 5A**, two tumors (PC48 and PC51) had no detectable Su(Fu) protein, which are consistent with our immunohistostaining. The matched normal tissues, however, retained expression of Su(Fu), indicating that alteration of Su(Fu) is a somatic event. Sequence analyses of these two tumors revealed genetic mutations in *Su(Fu)*, which are predicted to create STOP codons in the coding sequence (**Fig. 5B**). In PC48, a homozygous deletion of A1315 was detected, which results in a STOP codon at +1318 bp (**Fig. 5B**). In PC51, we detected two types of mutations, one with a deletion of C255, which results in a STOP codon at +294 bp whereas another with a deletion of C198, create a STOP codon (Picture not shown here, see Table 1). These mutations were confirmed with 6 independent clones from two separate experiments, which exclude the possibility of PCR errors. No mutations were detected from the matched benign tissues, indicating the somatic nature of the mutations. Real-time PCR analyses indicated that target genes of the hedgehog pathway, PTCH1 and Gli1, were all elevated in these tumors (**Fig. 5C**), confirming activation of the hedgehog pathway in these tumors. Thus, Su(Fu) inactivation appears to contribute to activation of hedgehog signaling in these prostate tumors.

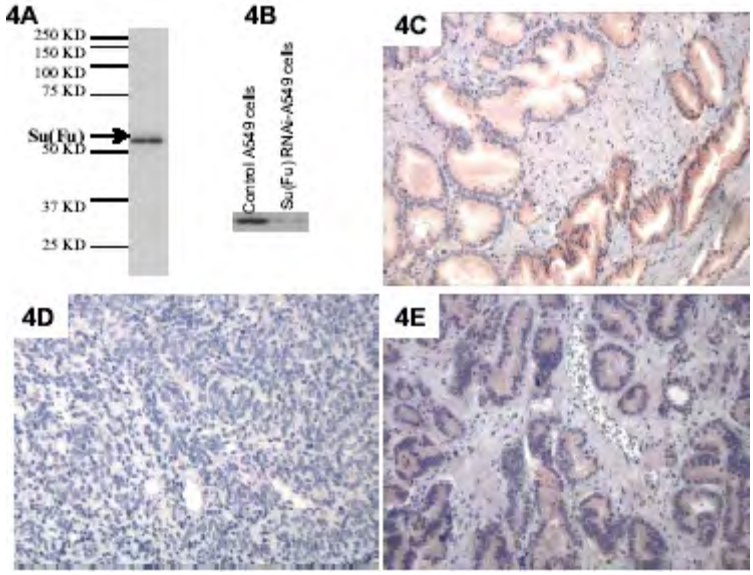

Fig. 4 Detection of Su(Fu) in prostate cancer specimens Su(Fu) antibodies (Santa Cruz Biotechnology Cat# 10933) recognized only one single band (54-Kd) in D283 cells (A). Following treatment of a specific SiRNA of Su(Fu), the endogenous Su(Fu) band was greatly reduced (B). Immunohistostaining with Su(Fu) antibodies in prostate cancer specimens revealed positive (C, in red, 200×), negative (D, 200×) or weak staining (E, red, 200×).

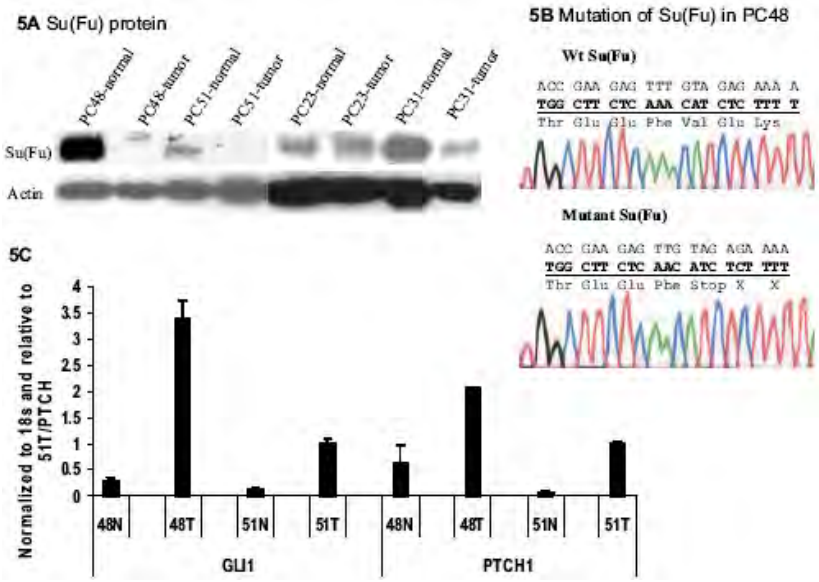

Fig. 5 Inactivation of Su(Fu) in prostate cancer. Two TURP specimens were examined for Su(Fu) protein by immunoblotting. Consistent with loss of Su(Fu) in the tissue, we did not detect Su(Fu) protein in these two tumors (PC48 and PC51 (5A). Further analysis revealed mutations of Su(Fu) in the tumor (PC48, 5B), which created a STOP codon in Su(Fu). We further found that tumor with mutant Su(Fu) had high levels of hedgehog target genes, PTCH1 and Gli1 (5C), indicatiing that hedgehog isignaling is activated.

In addition, we have discovered another mechanism by which hedgehog signaling is activated in human cancer, including prostate cancer. We found that sonic hedgehog, the ligand of hedgehog pathway, is frequently up-

regulated in prostate cancer cells. **Fig. 6** shows a luciferase reporter gene analysis using sonic hedgehog promoter construct in LNCaP cells.

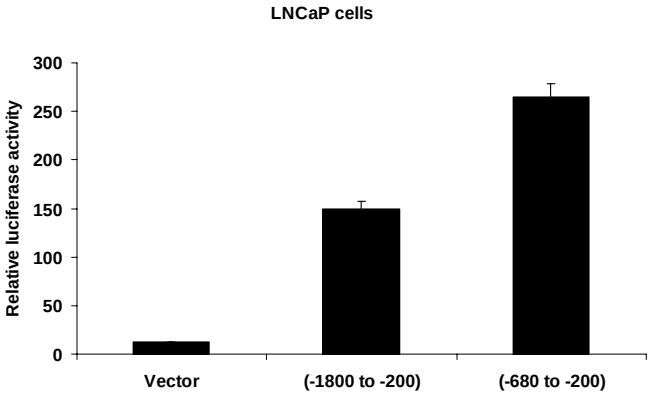

Fig. 6 Analysis of Shh promoter reporter activity in prostate cancer cells. We cloned human two sonic hedgehog promoter fragments (-1,800 to -200 and -680 to -200) into the luciferase reporter plasmid pGL4.14. 48 hr following transfection of the sonic hedgehog promoter constructs or the control vector (together with renilla luciferase reporter plasmid as the transfection control), we performed dual luciferase analyses. Consistent with elevated expression of sonic hedgehog in our previous study (Sheng et al, 2004, Molecular Cancer 3, 29), we found a high sonic hedgehog promoter activity in LNCaP cells. We found that a short fragment of sonic hedgehog promoter region (-680 to -200) retains a high level of promoter activity.

These data provide strong evidence that hedgehog signaling activation occurs in prostate cancer, through loss of Su(Fu) or over-expression of Shh.

Furthermore, we have extended our findings in prostate cancer to other types of human cancer, including skin, esophageal, gastric, liver, lung and colon cancers (Can Res 60:7545-52, 2004; Mol Carcinogenesis 42:18-28, 2005; Carcinogenesis 26: 1698-1705, 2005; 27:1334-40, 2006; Int J Cancer 118: 139-0148, 2006; Cancer Letters 244: 53-60, 2006; World J Gastroenterology 12: 3965-9, 2006; 13: 1659-65, 2007). All the reprints have been attached with this report.

Task 2: Determine the molecular basis of Su(Fu) function in cancer cell lines

Inhibition of hedgehog signaling for cell growth and cell invasiveness (Molecular Cancer 3: 29, 2004)
Identification of Shh over-expression was unexpected in the proposal. Because of the availability of hedgehog signaling inhibitor, cyclopamine, the effects of hedgehog signaling activation on cell proliferation and invasiveness was demonstrated in several prostate cancer cell lines, in which Shh is over-expressed. In the presence of hedgehog signaling inhibitor, cyclopamine, both cell proliferation and cell invasiveness was dramatically reduced, indicating that the hedgehog pathway is required for both cell proliferation and cell invasiveness of prostate cancer cells.

Following treatment with 5 μM cyclopamine in PC3 cells, expression of hedgehog target genes were dramatically inhibited (data not shown here), which was accompanied with a significant reduction of BrdU positive cells (see Molecular Cancer 3, 29, 2004). This effect is specific because addition of tomotidine, a non specific compound with a similar structure to cycloapmine, had no effects on either target gene expression or DNA synthesis. The prostate epithelial RWPE-1 cells which have no activated hedgehog signaling, on the other hand, were not sensitive to cyclopamine (data not shown here), indicating that cyclopamine specifically affects cells with elevated hedgehog signaling. LN-CAP, Du145 and TSU cells, like PC3 cells were also sensitive to cyclopamine treatment (see Molecular Cancer 3, 29, 2004 for details).

Prostate cancer progression is accompanied by increased cell invasiveness. Because the hedgehog signaling activation occurs frequently in advanced prostate cancer, we examined if inhibition of the hedgehog signaling can reduce cell invasiveness. Using BD Bio-coat cell invasion chambers, we found that treatment of cyclopamine in PC3 cells reduced the percentage of invasive cells by 70% (**Fig. 7A**). Similar data were also observed in Du145, LN-CAP and TSU cells (**Fig. 7B**). Under the same condition, RWPE-1 cells were not very invasive. Thus, hedgehog signaling activation regulates both cell proliferation as well as cell invasiveness of prostate cancer cells.

The role of Su(Fu) on cell proliferation (Cancer Letters 244: 53-60, 2006)

On the other hand, the only cancer cell line with no detectable expression of Su(Fu) is a lung cancer cell line. We have demonstrated that re-expression of Su(Fu) slowed cell growth of this cell line, and reduced the percentage of S phase cell population (see **Fig. 7**).

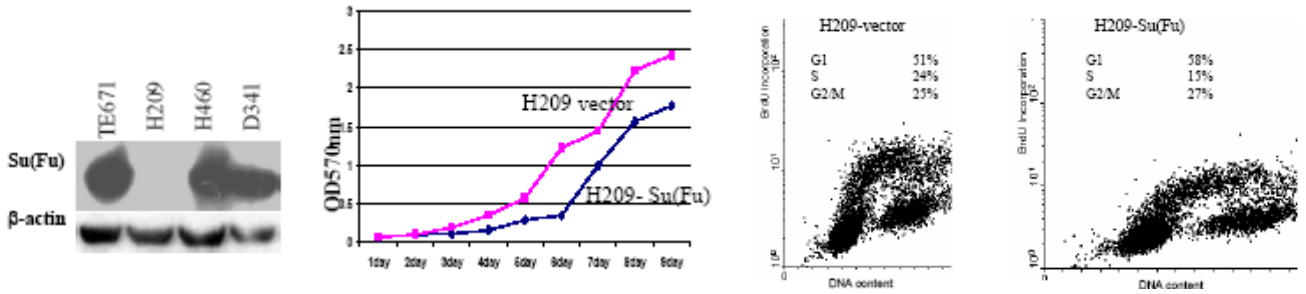

Fig. 7 Effects of Su(Fu) on DNA synthesis and cell growth of H209 cells. Of 30 cell lines screened, only one lung cancer cell line, H209, was shown to lack Su(Fu) protein expression by Western blotting (**left**). Stable expression of Su(Fu) leads to reduced cell growth (**middle**). In consistence with cell growth, Su(Fu) reduced the percentage of S phase cell population (**right**).

The role of PKA in regulation of Gli functions (J. Biological Chemistry 281:9-12, 2006)

In addition to Su(Fu), the PKA/cAMP axis is also involved in regulation of Gli1 functions (see Fig.8 for details). Based on our data, we proposed a model for PKA-mediated Gli1 regulation. Hedgehog signaling activation leads to elevated expression of Gli1, which shuttles to the nucleus through the NLS signal. When cells accumulate cAMP, which results increased PKA activity in the cell, Gli1 will be phosphorylated at T374. As a result, the local positive charge nearby the NLS is reduced, which prevents the proper function of the NLS. Consequently, Gli1 will be sequestered in the cytoplasm. Because a high conservation of T374 residue among all Gli molecules, we believe that other Gli proteins utilize this same mechanism for regulation of Gli1 localization.

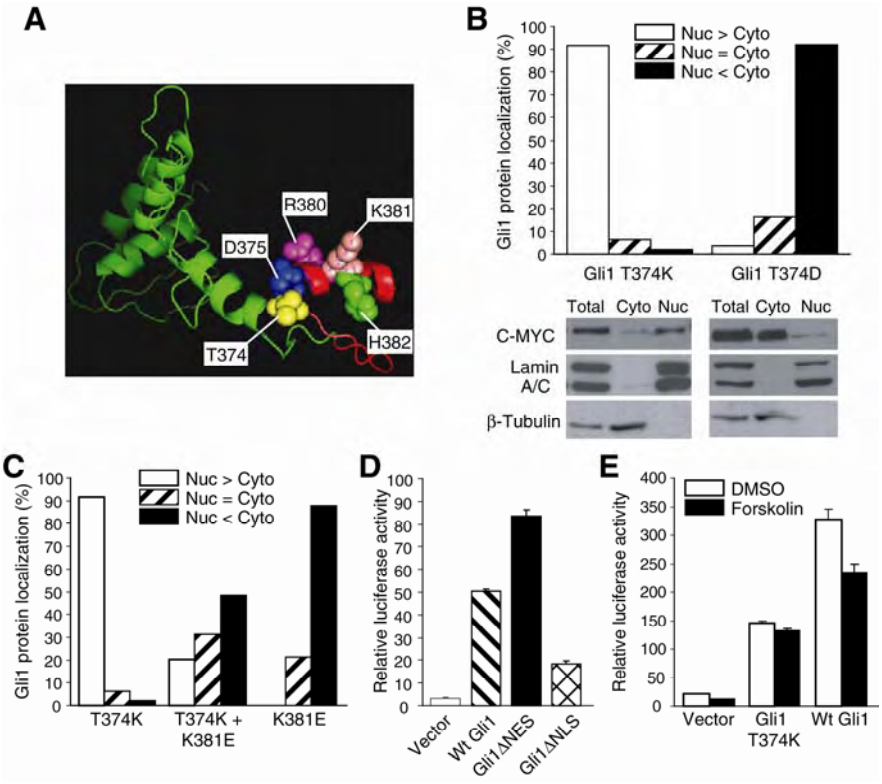

Fig. 8 The effect of T374 in regulation of Gli1 transcriptional activity. 8A shows the site of T374. Mutations of T374 were examined for their localization (**8B**). When the NLS signal was disrupted by K381E mutation, T374 Gli1 becomes cytoplasmic (**8C**). Consistence of Gli1 localization with its transcriptional activity was examined in NIH3T3 cells with stable expression of a Gli-responsive luciferase reporter **(8D**). Transcriptional activity of Gli1/T374V was not responsive to forskolin treatment. In contrast, the wild type Gli1 transcriptional activity was reduced by 60% by forskolin (**8E**)..

Task 3: The in vivo role of the hedgehog pathway for prostate cancer progression

Because nearly 50% of Ptch1+/- mice die of medulloblastomas or rhabdomyosarcomas, we have established two systems for activated hedgehog signaling in the prostate. In the first system, we established keratin 14 promoter-driven Ptch1 knock/out, which will allow activation of hedgehog signaling in prostate and other keratin 14-expressing epithelial tissues. In the second system, we expressed activated SMO molecule, SMO-

m2, in a tissue specific manner also under the control of keratin 14 promoter. **Fig. 9** shows our genotyping of allelic recombination of the Ptch1 locus.

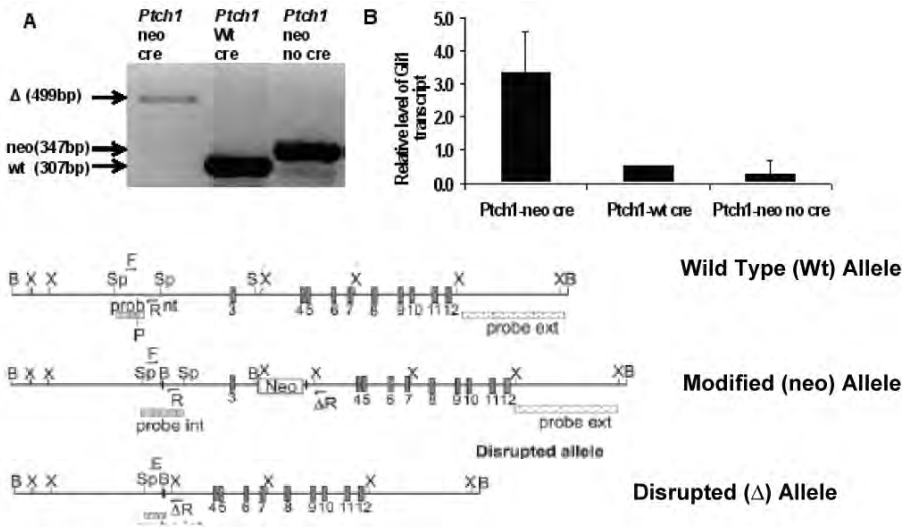

Fig 9: Genetic recombination occurred in Ptc^{floxp} keratinocytes following expression of Keratin 14 promoter driven cre to generate a 499 bp PCR product (**A**); wild-type cells expressing K14- or Ptc^{floxp} keratinocytes without cre expression do not yield this PCR product. Genetically Ptch1 knockdown cells were expected to have activated Hh signaling and therefore increased Gli1 expression (**B**). This approach can be used to generate prostate-specific Ptch1 knockdown to study the role of Hh signaling in prostate cancer. Wild-type, modified and disrupted Ptch1 allele were described previously.

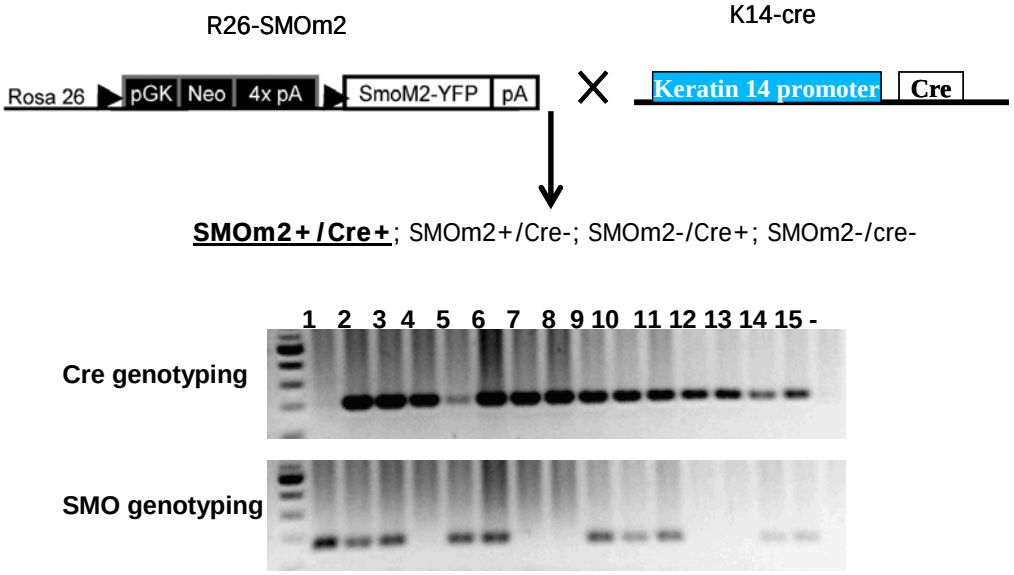

Fig. 10 Genetic recombination occurred in R26-SMOm2 mouse keratinocytes following expression of Keratin 14 promoter driven cre to generate mice with expression of activated SMO and subsequently pathway activation. Genotyping with primers of SMOm2 and Cre gives four groups of mice. Only double positive mice will used for this study.

In the last two years, we have examined mice from both systems and found no abnormalities in the prostate in all the mice examined. Most of these mice die around 6 months due to other lesions. There might be many reasons for this result. First, development of prostate cancer occurs often in older mice (even in the PTEN knockout mice). Thus, we may find hyperplasia or tumor in the prostate in the old animals. Second, since activation of the hedgehog pathway is frequently found in advanced and metastatic cancers of prostate. It is possible that hedgehog signaling plays an important role in tumor metastasis, but not tumor initiation.

Key Research Accomplishments

We made great accomplishments on this project. All the specific aims have been accomplished. In total, we have generated 12 publications in the last four years with support from this grant. Some of the studies have been used for three News Releases in our institution. Major accomplishments include being one of the first groups linking hedgehog signaling activation to prostate cancer and hepatocellular carcinomas; identification of the role of Su(Fu) in cancer cell proliferation and establishment of prostate-specific activation of hedgehog signaling in mouse model.

Reportable outcomes

12 peer-reviewed publications (see references for details)

Conclusions

In summary, we have data to indicate that hedgehog signaling activation is associated with several types of human cancer, including prostate cancer. This activation can be achieved either through elevated expression of hedgehog ligands or altered expression of downstream genes. Su(Fu) can affect cell functions through regulation of Gli transcription factors to interfere with hedgehog target gene expression and cell proliferation. Although hedgehog signaling is activated in advanced and metastatic prostate cancer, targeted activation of hedgehog signaling in the prostate of mice has no abnormality in prostate tissue, suggesting that hedgehog signaling activation alone can not drive development of prostate cancer in mice.

References

1. Athar M, Li C-X, Chi S, Tang X, Kim A-L, Norris, B.A., Tyring, S.K., Kopelovich, L., Epstein, E.H. Jr., Bickers, D.R. and Xie, J. Inhibition of *smoothened* signaling prevents ultraviolet B-induced basal cell carcinomas through induction of fas expression and apoptosis (The first two authors contribute equally). *Cancer Research* 60: 7545-52, 2004.

2. Sheng, T*, Li C-X*, Zhang X*, Chi S., He N., Chen, K., McCormick, F., Gatalica, Z. and Xie, J. Activation of the hedgehog pathway in advanced prostate cancer. *Molecular Cancer* 3: 29, 2004.

3. He N., Li C-X, Zhang X., Sheng T, Chi S, Chen K, Wang Q, Vertrees R, Logrono R. and **Xie, J**. Regulation of lung cancer cell invasion by β-TRCP. *Molecular Carcinogenesis* 42: 18-28, 2005.

4. Ma, X.L*, Chen, K*, Huang S.H*, Sheng, T., Zhang, X., Evers, B.M., Adegygoga, P., Zhang H.W. and **Xie J** (2005). Frequent activation of the hedgehog pathway in advanced gastric adenocarcinomas. *Carcinogenesis* 26(10):1698-1705. Epub 2005 May 19.

5. Ma, X.L*, Sheng, T*, Zhang, Y.X., Huang S.H., He, J., Chen, K., Zhang, X., Zhang H.W. and **Xie J.** Hedgehog signaling is activated in subsets of esophageal cancers *International Journal of Cancer* 118(1): 139-148, 2006. Epub 2005 July 7.

6. Sheng T, Chi S, Zhang X and Xie J, Regulation of Gli1 localization by the cAMP/ PKA signaling axis through a site near the nuclear localization signal. *J. Biological Chemistry* 281: 9-12, 2006.

7. Chi S*, Huang S-H*, Zhang X, Li C-X, Haque AK, Zwischenberger J, Tyring SK, Logrono R, Bhutani M, Zhang H-W, **Xie J**. Expression of sonic hedgehog and its target genes in lung cancers. *Cancer Lett* 2006 Nov 28;244(1):53-60. Epub 2006 Jan 30.

8. Huang S*, He J*, Zhang X*, Bian X, Yang L, Xie G, Zhang K, Tang W, Stelter AA, Wang Q, Zhang HW, Xie J. Activation of the hedgehog pathway in human hepatocellular carcinomas. *Carcinogenesis* 27(7):1334-40 (Epub ahead of print on Feb. 25, 2006), 2006.

9. Tang WW, Stelter AA, French S, Shen S, Qiu S, Venegas R, Wen J, Wang H-Q and **Xie J,** L0ss of Cell-Adhesion Molecule Complexes in Solid Pseudopapillary Tumor of Pancreas. *Modern Pathology* 20(5):509-13, 2007

10. Bian Y, Huang S, Yang L, Ma X, **Xie J** and Zhang HW, The sonic hedgehog-Gli1 pathway in colorectal adenocarcinomas. *World J Gastroenterol* 13(11):1659-65, 2007

11. Xie, **J**. (2005) Hedgehog Signalling in prostate cancer. *Future Oncology* 1(3): 331-338.

12. Xie, J., (2008) Implications of Hedgehog signaling antagonists for cancer therapy. *Acta Biochimica et Biophysica Sinica (Shanghai)* 40(7):670-80.

Appendices

1. Reprint of *Cancer Research* 60: 7545-52, 2004
2. Reprint of *Molecular Cancer* 3: 29, 2004
3. Reprint of *Carcinogenesis* 26(10):1698-1705, 2005
4. Reprint of *International Journal of Cancer* 118(1): 139-148, 2006
5. Reprint of *J. Biological Chemistry* 281: 9-12, 2006.
6. Reprint of *Cancer Lett* 244(1):53-60, 2006
7. Reprint of *Carcinogenesis* 27(7):1334-40 (Epub ahead of print on Feb. 25, 2006), 2006
8. Reprint of *World J Gastroenterol* 13(11):1659-65, 2007
9. Reprint of *Future Oncology* 1(3): 331-338, 2005.
10. Reprint of ***Acta Biochimica et Biophysica Sinica (Shanghai)*** 40(7):670-80, 2008.

[CANCER RESEARCH 64, 7545–7552, October 15, 2004]

Inhibition of *Smoothened* Signaling Prevents Ultraviolet B-Induced Basal Cell Carcinomas through Regulation of Fas Expression and Apoptosis

Mohammad Athar,[1] Chengxin Li,[5,6] Xiuwei Tang,[1] Sumin Chi,[5,6] Xiaoli Zhang,[6] Arianna L. Kim,[1] Stephen K. Tyring,[4] Levy Kopelovich,[2] Jennifer Hebert,[3] Ervin H. Epstein Jr.,[3] David R. Bickers,[1] and Jingwu Xie[5]

[1]Department of Dermatology, College of Physicians and Surgeons, Columbia University, New York, New York; [2]Division of Cancer Prevention, National Cancer Institute, Bethesda, Maryland; [3]Department of Dermatology and Comprehensive Cancer Center, University of California San Francisco, San Francisco, California; [4]Department of Dermatology, University of Texas Health Science Center, Houston, Texas; [5]Sealy Centers for Cancer Cell Biology and Environmental Health, Department of Pharmacology and Toxicology, University of Texas Medical Branch at Galveston, Galveston, Texas; and [6]Xijing Hospital, Xi'an 710032, China

ABSTRACT

Abnormal activation of the hedgehog-signaling pathway is the pivotal abnormality driving the growth of basal cell carcinomas (BCCs), the most common type of human cancer. Antagonists of this pathway such as cyclopamine may therefore be useful for treatment of basal cell carcinomas and other hedgehog-driven tumors. We report here that chronic oral administration of cyclopamine dramatically reduces (~66%) UVB-induced basal cell carcinoma formation in *Ptch1*$^{+/-}$ mice. Fas expression is low in human and murine basal cell carcinomas but is up-regulated in the presence of the smoothened (SMO) antagonist, cyclopamine, both *in vitro* in the mouse basal cell carcinoma cell line ASZ001 and *in vivo* after acute treatment of mice with basal cell carcinomas. This parallels an elevated rate of apoptosis. Conversely, expression of activated SMO in C3H10T1/2 cells inhibits Fas expression. Fas/Fas ligand interactions are necessary for cyclopamine-mediated apoptosis in these cells, a process involving caspase-8 activation. Our data provide strong evidence that cyclopamine and perhaps other SMO antagonists are potent *in vivo* inhibitors of UVB-induced basal cell carcinomas in *Ptch1*$^{+/-}$ mice and likely in humans because the majority of human basal cell carcinomas manifest mutations in PTCH1 and that a major mechanism of their inhibitory effect is through up-regulation of Fas, which augments apoptosis.

INTRODUCTION

The *hedgehog* (Hh) pathway plays a critical role in embryonic development and tissue polarity (1). Secreted Hh molecules bind to the receptor patched (PTC), thereby alleviating PTC-mediated suppression of smoothened (SMO), a putative seven-transmembrane protein. SMO signaling triggers a cascade of intracellular events, leading to activation of the pathway through GLI-dependent transcription (2). Considerable insight into the role of the Hh pathway in vertebrate development and human cancers has come from the discovery that mutations of the *patched* gene (*PTCH1*) underlie the basal cell nevus syndrome, a rare hereditary disorder in which patients are highly susceptible to the development of large numbers of basal cell carcinomas and other tumors (3, 4). Activation of Hh signaling, usually due to loss-of-function somatic mutations of *PTCH1* and less often to activating mutations of *SMO*, is the pivotal abnormality in sporadic basal cell carcinomas (5–7). Therefore, targeted inhibition of SMO signaling should afford mechanistically based prevention/therapy of basal cell carcinomas, as well as of other tumors driven by Hh signaling abnormalities, including certain medulloblastomas, small-cell lung carcinomas, and gastrointestinal tract cancers (8–11). One such inhibitor is the naturally occurring plant extract cyclopamine, and there are additional synthetic compounds that directly associate with the transmembrane domains of SMO (12–14). Therefore, these small molecular weight compounds have significant promise for the prevention and treatment of basal cell carcinomas and other human malignancies.

Ptch1$^{+/-}$ mice (15) provided the first practical animal model for inducing basal cell carcinomas using UV and ionizing radiation (16). We report here that chronic oral administration of cyclopamine dramatically inhibits basal cell carcinoma growth in these mice. We also have tested the *in vitro* effects of cyclopamine and of the synthetic SMO inhibitor Cur61414 on the mouse basal cell carcinoma cell line ASZ001 and have demonstrated that both compounds elevate Fas expression and augment apoptosis. The clinical relevance of our data for treatment of basal cell carcinomas is supported by the low baseline Fas expression in basal cell carcinomas of both humans and mice and by the *in vivo* induction of high level Fas expression by short-term administration of cyclopamine in murine basal cell carcinomas. Thus, our studies support the idea that treatment of human basal cell carcinomas with specific inhibitors of the Hh pathway may offer a mechanism-driven approach to the chemoprevention of these tumors.

MATERIALS AND METHODS

Animals. *Ptch1*$^{+/-}$ heterozygous knockout mice have been developed by deleting exons 1 and 2 and inserting the LacZ gene at the deletion site (15). *Ptch1-lacZ*-transgenic mice were genotyped by PCR amplification of genomic DNA extracted from tail biopsies (15, 16). The animals were housed under standard conditions (fluorescent lighting 12 hours per day, room temperature 23°C to 25°C, and relative humidity 45 to 55%). The mice were provided tap water and Purina Laboratory Chow 5001 diet (Ralston-Purina Co., St. Louis, MO).

UV Light Source. An UV Irradiation unit (Daavlin Co., Bryan, OH) equipped with an electronic controller to regulate dosage was routinely used for these studies. The UVB source consisted of eight FS72T12-UVB-HO lamps emitting UVB (290 to 320 nm, 75 to 80% of total energy) and UVA (320 to 380 nm, 20 to 25% of total energy). We used a Kodacel cellulose film (Kodacel TA401/407) to eliminate UVC radiation. A UVC sensor (Oriel's Goldilux UVC Probe) was used during each exposure to confirm the lack of UVC emission. The UVB dose was quantified using a UVB Spectrum 305 Dosimeter obtained from the Daavlin Co. The radiation was additionally calibrated using an IL1700 Research Radiometer/Photometer from International Light, Inc. (Newburyport, MA). The distance between the radiation source and targets was maintained at 30 cm. The irradiation assembly is kept in an air-conditioned room, and a fan is placed inside the exposure chamber to minimize temperature fluctuations during irradiation.

Carcinogenesis Protocol and Statistical Analyses. Mice were irradiated with a UV Irradiation unit (240 mJ/cm^2 three times a week) from age 6 to 32 weeks, at which time, ~50% of the animals had one or more visible skin tumors. The mice (25 mice per group) were given either cyclopamine (10 μg/day as a cyclodextran complex) or the vehicle control in drinking water,

Received 4/20/04; revised 6/20/04; accepted 8/18/04.

Grant support: National Cancer Institute Grants CA 94160 (J. Xie), CA81888 (M. Athar, A. Kim, J. Hebert, E. Epstein, D. Bickers), and CA101061 (M. Athar), Department of Defense Grant PC030429 (J. Xie), the American Cancer Society (J. Xie), the National Institute of Environmental Health Sciences Center at University of Texas Medical Branch (J. Xie), and the John Sealy Memorial Endowment Fund for Biomedical Research (J. Xie).

The costs of publication of this article were defrayed in part by the payment of page charges. This article must therefore be hereby marked *advertisement* in accordance with 18 U.S.C. Section 1734 solely to indicate this fact.

Note: M. Athar and C. Li contributed equally to this article.

Requests for reprints: Jingwu Xie, Sealy Center for Cancer Cell Biology, Department of Pharmacology and Toxicology, University of Texas Medical Branch at Galveston, 301 University Blvd., Galveston, TX 77555-1048. E-mail: jinxie@utmb.edu; or Mohammad Athar, Department of Dermatology, College of Physicians and Surgeons, Columbia University, 630 West 168th Street, New York, NY 10032. E-mail: ma493@columbia.edu

and the number of tumors was recorded weekly. Mice treated with cyclopamine or with the vehicle control were sacrificed at 52 weeks, their dorsal skin removed, and tumors harvested and collected for the histologic and immunohistochemical studies. The microscopic basal cell carcinoma areas were assessed by histologic evaluation of three dorsal skin sections per mouse from a total of seven mice ($n = 7$) in the vehicle-treated water group and a total of six mice ($n = 6$) in the cyclopamine-treated group. The basal cell carcinoma areas were measured by microscopic assessment using the Axiovision 3.1 analysis program (Carl Zeiss MicroImaging, Inc., Thornwood, NY). Results were analyzed using the Student's t test or a nonparametric test (Mann-Whitney test): $P < 0.05$ was considered statistically significant.

For evaluation of Fas expression and apoptosis *in vivo*, cyclopamine was injected (at 100 pg s.c. or intratumorally) into mice with visible basal cell carcinomas (>1 cm in diameter). Seventy-two hours later, basal cell carcinomas were embedded in OCT compound (Tissue-Tek; Sakura, Torrance, CA), and stored in −20°C for additional analyses. Stromal cells were used as the control for basal cell carcinoma cells.

β-Galactosidase Staining. Tissues were fixed in 0.2% glutaraldehyde (Sigma-Aldrich, St. Louis, MO)/2% formaldehyde (Fisher Scientific Co., Pittsburgh, PA) in 1× PBS for 20 minutes at 4°C, then washed twice in 1× PBS. Tissues were incubated with 5% 5-bromo-4-chloro-3-indolyl-β-D-galactopyranoside in 95% iron buffer solution for 24 hours at 37°C using a β-galactosidase staining set (Roche Applied Science, Indianapolis, IN), according to the manufacturer's guideline. The tissues were washed twice in 3% DMSO in 1× PBS and then three times in 70% etomidate. The tissues were embedded in paraffin and processed for counterstaining.

Terminal Deoxynucleotidyl Transferase-Mediated Nick End Labeling (TUNEL) and Immunofluorescent Staining. TUNEL analysis was performed using a kit from Roche Applied System according to the manufacturer's guideline. Immunofluorescent staining of Fas in basal cell carcinomas was performed with an antibody specific to mouse Fas (M20; Santa Cruz Biotechnology, Inc., Santa Cruz, CA).

Cell Culture and Cell Viability Assay. The mouse basal cell carcinoma cell line ASZ001 was maintained in 154CF medium as reported previously (17). Ectopic expression of Gli1 in ASZ001 cells was induced using LipofectAmine 2000, and the transfected cells were enriched by cell sorting after coexpression of green fluorescence protein and Gli1 (green fluorescence protein to Gli1 plasmid ratio = 1:4). C3H10T1/2 cells were cultured in basal medium containing 10% heat-inactivated fetal bovine serum. GLI-transformed baby rat kidney cells were cultured in DMEM containing 10% fetal bovine serum (18). ASZ001 cells were first treated with 2 μmol/L 3-keto-N-aminoethylaminoethylcaproyldihydrocinnamoyl cyclopamine (KAAD-cyclopamine) for 36 hours in the presence or absence of 10 μg/mL epidermal growth factor or platelet-derived growth factor (PDGF)-AA (R&D Systems, Inc., Minneapolis, MN) or treated with U0126 alone (10 μmol/L; EMD Biosciences, Inc., San Diego, CA) for 36 hours. Cells were then harvested for protein expression and cell viability analyses. Cell viability was assessed by trypan blue exclusion and colorimetric 3-(4,5-dimethylthiazol-2-yl)-2,5-diphenyltetrazolium bromide assay (19). The proliferation inhibition was calculated by dividing the mean test value by the respective PBS control. The background absorbance, obtained from the wells treated with DMSO only, was subtracted from the test- and control-well values to yield corrected absorbance. Triplicates for each sample were used, and all experiments were performed in triplicate (19).

Flow Cytometry and Cell Sorting. Cells were plated at 3,000,000 cells per 10-cm plate in 154CF without growth supplements the day before treatment. KAAD-cyclopamine (Toronto Research Chemicals, Inc., North York, Ontario, Canada) was added to the medium to achieve a final concentration of 2 μmol/L, and the cells were incubated for 36 hours. Epidermal growth factor and PDGF-A were used at a final concentration of 10 μg/mL, U0126 at a final concentration of 10 μmol/L, and Fas ligand (FasL)–neutralizing antibodies at a final concentration of 20 μg/mL were added to the medium. Subsequently, cells were collected and fixed overnight in 70% etomidate and treated with 50 ng/mL propidium iodide in the presence of 10 μg/mL RNase A (in PBS). Cell cycle profiles were determined by a fluorescence-activated cell sorter (FACSCaliber; Becton Dickinson, Franklin Lakes, NJ). At least 20,000 gated events were recorded for each sample, and the data were analyzed with Multicycle software for Windows (Phoenix Flow Systems, San Diego, CA). ASZ001 cells with ectopic Gli1 expression were enriched through cell sorting, resulting in >90% of the cells with Gli1 expression (from a starting population of 5% positive cells). Both positive and negative fractions were collected for Western blot analysis.

Western Blot Analysis and ELISA. Western blotting was performed as previously reported (17), with specific antibodies [anti-PDGFR-α and anti-mouse Fas antibodies from Upstate Biotechnology (Lake Placid, NY); anti-Erk, anti-phospho-Erk and anti-caspase-3 antibodies from Cell Signaling Technology (Beverly, MA); anti-β-actin from Sigma-Aldrich (St. Louis, MO); and antihuman Fas and anti-FasL from BD Transduction Laboratories (San Diego, CA)]. ELISA detection of secreted FasL protein in the growth medium was performed using a kit from R&D Systems, Inc., according to the manufacturer's protocol.

Real-time PCR Analyses. Total RNAs from ASZ001 cells were extracted using RNAqueous from Ambion, Inc. (Austin, TX). We used Applied Biosystems' (Foster City, Ca) assays-by-design 20× assay mix of primers and TaqMan probes (carboxyfluorescein dye-labeled probe) for the target genes [mouse Gli1, hedgehog interacting protein (HIP)] and predeveloped 18S rRNA (VIC dye-labeled probe) TaqMan assay reagent (P/N 4319413E) for an internal control. Mouse Gli1 and HIP primers are designed to span exon-exon junctions so as not to detect genomic DNA, and the primers and probe sequences were searched against the Celera database to confirm specificity. The primer and probe sequences of mouse Gli1 and HIP are as follows.

To obtain the relative quantitation of gene expression, a validation experiment was performed to test the efficiency of the target amplification and the efficiency of the reference amplification. All absolute values of the slope of log input amount *versus* ΔC_T were <0.1. Separate tubes (singleplex) one-step reverse transcription-PCR was performed with 20 ng of RNA for both target gene (mGli1 or mHIP) and endogenous control. The reagent we used was TaqMan one-step reverse transcription-PCR master mix reagent kit (P/N 4309169). The cycling parameters for one-step reverse transcription-PCR was reverse transcription 48°C for 30 minutes, AmpliTaq activation 95°C for 10 minutes, denaturation 95°C for 15 seconds, and annealing/extension 60°C for 1 minute (repeat 40 times) on ABI7000. Triplicate C_T values were analyzed in Microsoft Excel using the comparative C_T ($\Delta\Delta C_T$) method as described by the manufacturer (Applied Biosystems). The amount of target ($2^{-\Delta\Delta CT}$) was obtained by normalization to an endogenous reference (18 rRNA) and relative to a calibrator.

RESULTS

Cyclopamine Inhibits Basal Cell Carcinoma Development in *Ptch1*$^{+/-}$ Mice. The Hh pathway is constitutively activated in essentially all human and mouse basal cell carcinomas (3, 20). Because PTCH1, which is frequently inactivated in human basal cell carcinomas, is known to be upstream of SMO (21), inhibiting SMO functions should be an effective way to treat basal cell carcinomas. To test the effects of a SMO antagonist on development of basal cell carcinomas, we administered cyclopamine orally to basal cell carcinoma-bearing *Ptch1*$^{+/-}$ mice. We UV-irradiated *Ptch1*$^{+/-}$ mice from age 6 to 32 weeks, at which time, approximately half of the mice had developed one or more macroscopic tumors: basal cell carcinomas, squamous cell carcinomas, and/or spindle cell tumors (fibrosarcomas). UV irradiation was then stopped and the mice were randomized (25 mice per group) to receive either vehicle or cyclopamine (as cyclodextran complex) in the drinking water for the ensuing 20 weeks. The survival of these two groups of animals was similar, indicating that cyclopamine does not affect the overall survival of *Ptch*1$^{+/-}$ mice (data not shown). At age 52 weeks, we measured microscopic basal cell carcinoma areas per tissue area (mm^2) in these two groups after β-galactosidase staining (see Materials and Methods for details) and found a 90% reduction of microscopic basal cell carcinomas in the cyclopamine-treated animals (Fig. 1, *A* and *B*). Cyclopamine-treated mice also had fewer visible basal cell carcinomas at age 52 weeks than did the vehicle-treated controls (Fig. 2, *A* and *B*). Thus, the mice receiving vehicle alone continued to develop visible tumors, and the number of tumors had tripled by week 52. We

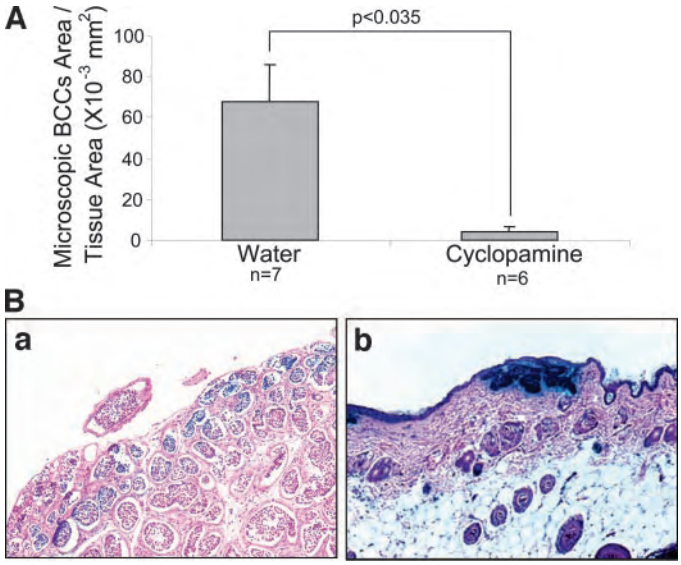

Fig. 1. Effect of cyclopamine on UVB-induced microscopic basal cell carcinomas (BCCs) in *Ptch1*$^{+/-}$ mice. *A*, effect of orally administered cyclopamine on the number of UVB-induced microscopic BCC-like lesions in *Ptch1*$^{+/-}$ mice. Microscopic BCC-like lesions were counted as total tumor area/mm^2 skin and assessed by histologic evaluation of three dorsal skin sections per mouse from a total of seven mice ($n = 7$) in the vehicle-treated group and a total of 6 mice ($n = 6$) in the cyclopamine-treated group. Results of microscopic BCCs in the two groups were statistically analyzed using the Student's *t* test (two-tailed): $P < 0.05$ was considered statistically significant. *B*, β-galactosidase and H&E staining showing the effect of orally administered cyclopamine on UVB-induced microscopic BCC lesions in *Ptch1*$^{+/-}$ mice. Representative staining from UVB-irradiated (*a*) and UVB-irradiated cyclopamine-treated (*b*) *Ptch1*$^{+/-}$ mice. These skin samples were fixed in 10% buffered formalin before staining with H&E and detection of β-galactosidase activities.

found that mice receiving cyclopamine developed 50% fewer new basal cell carcinomas than did the control group at week 52 (Fig. 2, *A* and *C*), and the difference is statistically significant ($P = 0.0078$ by nonparametric test, Mann-Whitney test). More importantly, the number of visible squamous cell carcinomas and spindle cell tumors did not differ between the two groups, showing the specificity of cyclopamine for basal cell carcinomas in this mouse model (Fig. 2*C*).

Cyclopamine Inhibits the Hh Pathway and Induces Apoptosis in Basal Cell Carcinoma Cells. To investigate the mechanism whereby cyclopamine prevents basal cell carcinoma development in *Ptch1*$^{+/-}$ mice, we used the mouse basal cell carcinoma cell line ASZ001, which is derived from basal cell carcinoma-bearing *Ptch1*$^{+/-}$ mice. Both copies of the *Ptch1* gene are lost in this cell line, resulting in constitutive activation of the Hh pathway (16, 17). Incubation with 2 μmol/L KAAD-cyclopamine, a cyclopamine analogue, for 12 hours reduced the levels of Hh target genes (Gli1 and Hip) by >70% (Fig. 3*A*), confirming that cyclopamine inhibits the Hh pathway in these cells. Treatment of ASZ001 cells for 36 hours with cyclopamine or Cur61414 caused a dose-dependent decrease in cell viability (Fig. 3*B*). A SMO antagonist, Cur61414, showed an effect similar to that of cyclopamine (Fig. 3*B*). A similar result was also obtained from the trypan blue exclusion analysis (data not shown). The closely related compound tomatidine, which does not affect SMO signaling and thus served as a negative control, had little discernible effect on the viability of the ASZ001 cells (Fig. 3*B*). Additional evidence that cyclopamine-mediated inhibition of cell growth is dependent on activated Hh signaling came from studies in primary mouse keratinocytes (Hh pathway inactivated), which did not respond to cyclopamine treatment (data not shown). In ASZ001 cells, cyclopamine treatment did not promote cellular differentiation, and hence, the dramatic reduction in the number of living cells suggested that cyclopamine might be inducing apoptosis.

We next assessed cyclopamine-induced apoptosis using flow cytometry analysis and found that treatment of cells with cyclopamine for 36 hours caused a 3-fold increase in the sub-G_1 cell population and a decrease in the S phase (Fig. 3*C*), suggesting that cyclopamine is a potent inducer of apoptosis in basal cell carcinomas. Treatment of ASZ001 cells with either cyclopamine or Cur61414 for 36 hours (see Materials and Methods for details) increased the level of activated caspase-3, a major executioner of cysteinyl aspartate-specific proteinases for apoptosis (Fig. 3*C*).

Confirming our *in vitro* findings, direct injection of cyclopamine into basal cell carcinoma-bearing mice for 72 hours enhanced apoptosis (an increase in TUNEL-positive cells) of basal cell carcinoma tumor cells *in vivo* (Fig. 3*D*).

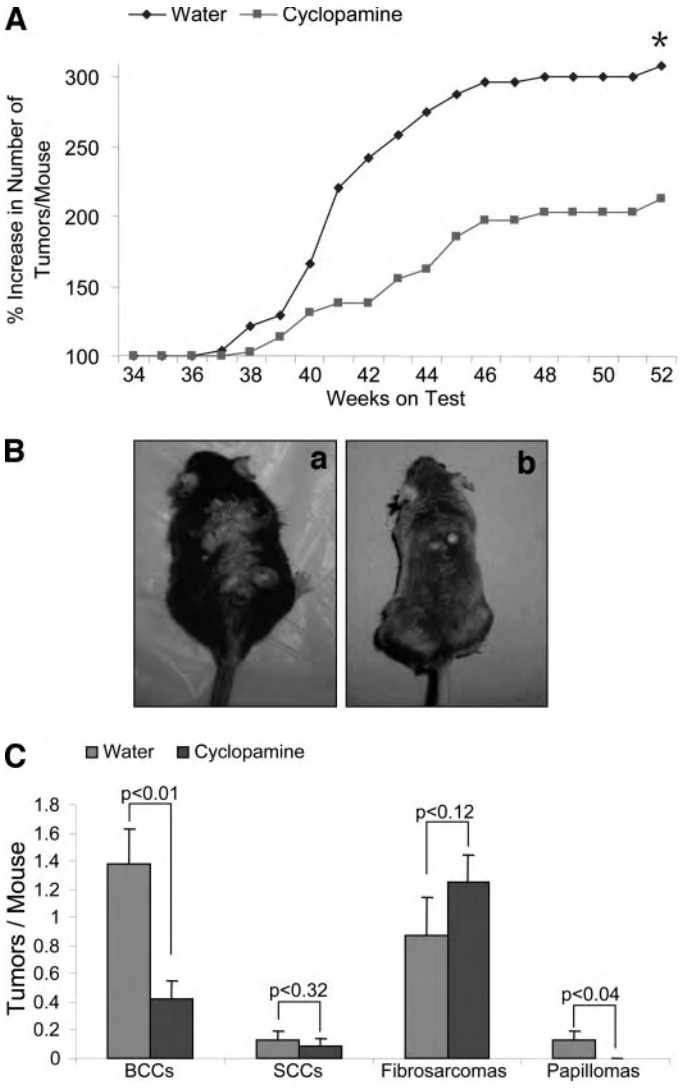

Fig. 2. Effect of cyclopamine on UVB-induced macroscopic basal cell carcinomas (BCCs) in *Ptch1*$^{+/-}$ mice. *A*, effect of cyclopamine administration on the growth of UVB-induced skin tumors in *Ptch1*$^{+/-}$ mice is shown as percent increase in number of tumors per mouse. The statistical analysis was performed using the nonparametric Mann-Whitney test (two-tailed) and obtained $P = 0.0078$ (*) at week 52. $P < 0.05$ is considered statistically significant. *B*, *Ptch1*$^{+/-}$ mice showing effects of cyclopamine treatment on UVB-induced skin tumors. Representative pictures of UVB-irradiated, vehicle-treated control mouse (*a*) and UVB-irradiated, cyclopamine-treated (*b*) mouse at week 52. *C*, effect of orally administered cyclopamine on the growth of UVB-induced BCCs, squamous cell carcinomas (SCCs), and fibrosarcomas in *Ptch1*$^{+/-}$ mice. The statistical analysis was performed using the Student's *t* test: $P < 0.05$ is considered statistically significant.

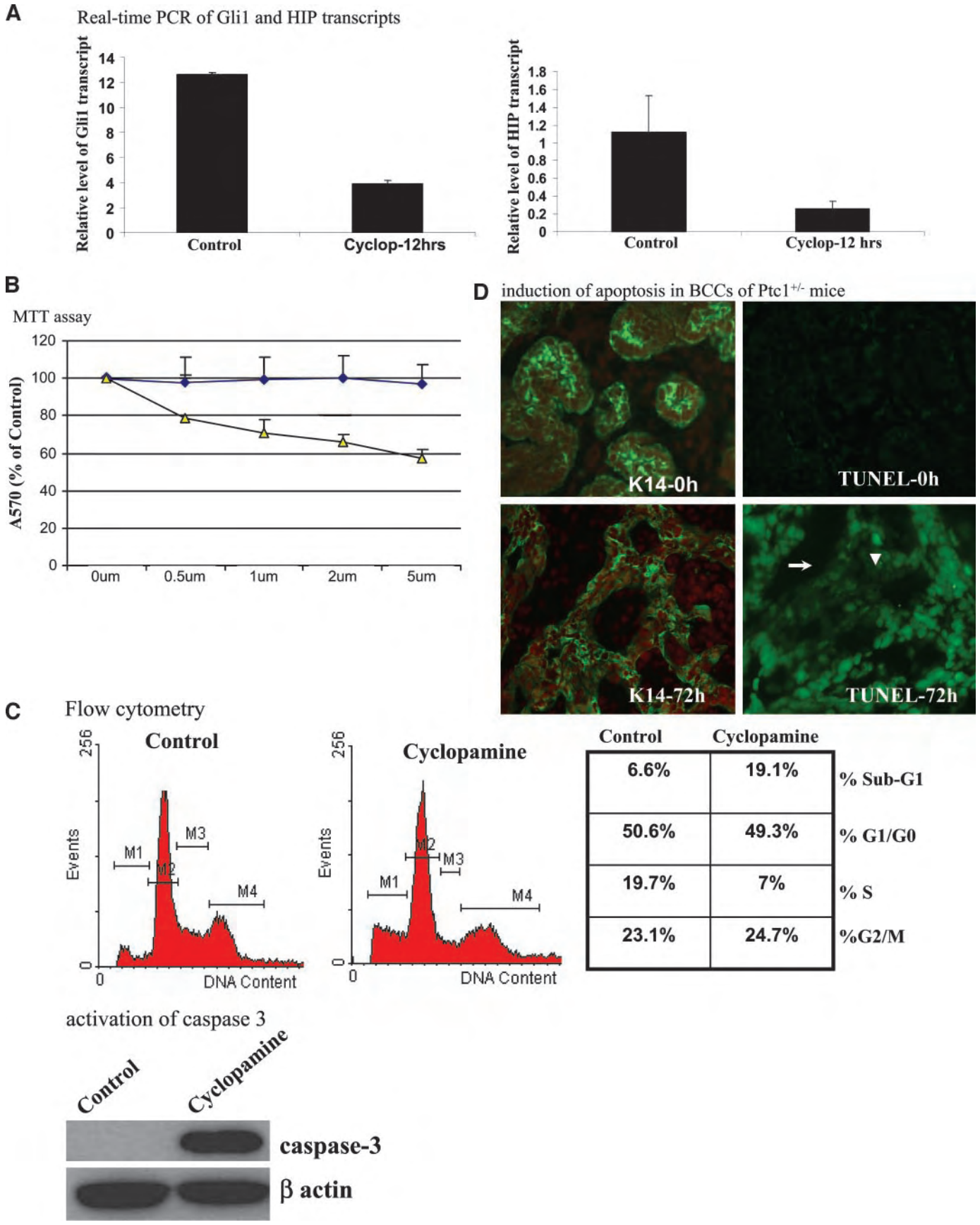

Fig. 3. Cyclopamine inhibits the Hh pathway and induces apoptosis in ASZ001 cells. *A*. Gli1 and HIP transcripts were detected by real-time PCR analysis. Cells were treated with 2 μmol/L KAAD-cyclopamine for 12 hours. After RNA extraction, real-time PCR analysis was performed (see Materials and Methods for details). *B*, 3-(4,5-dimethylthiazol-2-yl)-2,5-diphenyltetrazolium bromide (MTT) assay of ASZ001 cells in the presence of SMO antagonists. ASZ001 cells were treated with cyclopamine, or the control compound tamotidine for 36 hours, and the cell viability was examined by MTT assay. *C*, cell cycle and protein analyses of ASZ001 cells. The percentage of cell population in each cell cycle

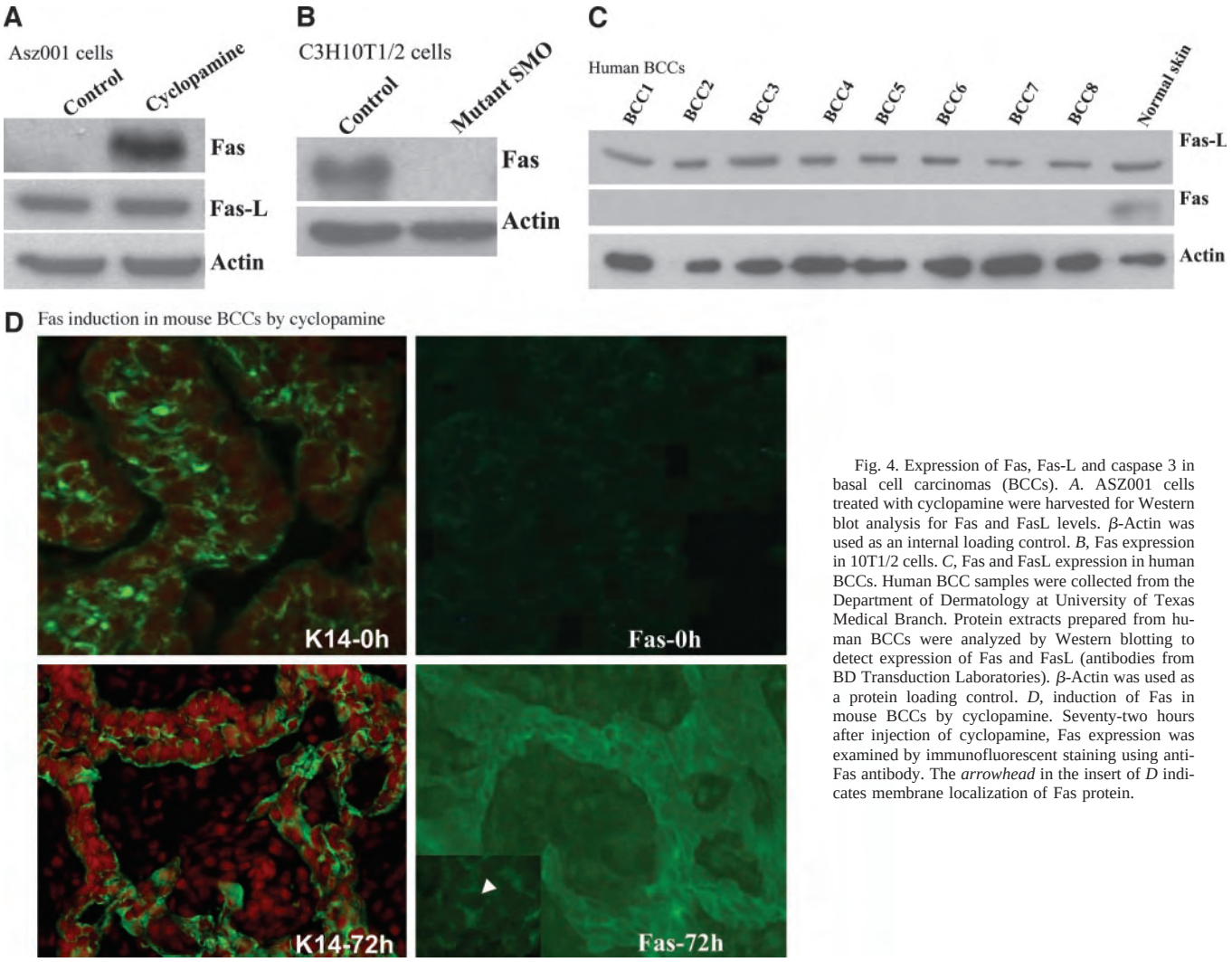

Fig. 4. Expression of Fas, Fas-L and caspase 3 in basal cell carcinomas (BCCs). *A.* ASZ001 cells treated with cyclopamine were harvested for Western blot analysis for Fas and FasL levels. β-Actin was used as an internal loading control. *B,* Fas expression in 10T1/2 cells. *C,* Fas and FasL expression in human BCCs. Human BCC samples were collected from the Department of Dermatology at University of Texas Medical Branch. Protein extracts prepared from human BCCs were analyzed by Western blotting to detect expression of Fas and FasL (antibodies from BD Transduction Laboratories). β-Actin was used as a protein loading control. *D,* induction of Fas in mouse BCCs by cyclopamine. Seventy-two hours after injection of cyclopamine, Fas expression was examined by immunofluorescent staining using anti-Fas antibody. The *arrowhead* in the insert of *D* indicates membrane localization of Fas protein.

Active Fas/FasL Interactions Are Necessary for Cyclopamine-induced Cell Death. Because treatment of human basal cell carcinomas with IFN-α may be accompanied by increased Fas expression in the tumor (19, 22), we tested whether cyclopamine, too, can augment Fas expression. Indeed, cyclopamine substantially increased the level of Fas protein in ASZ001 cells (Fig. 4*A*). In contrast, we detected FasL protein irrespective of cyclopamine treatment (Fig. 4*A*). Using an ELISA assay, we detected FasL in the culture medium of ASZ001 cells, indicating that these basal cell carcinoma cells indeed secrete FasL protein (see Fig. 5*B* for details). Thus, Fas would appear to be the limiting factor for the FasL/Fas signaling axis in this basal cell carcinoma cell line. Conversely, Fas is down-regulated in C3H10T1/2 cells with stable expression of activated SMO via retrovirus-mediated gene transfer (Fig. 4*B*).

The *in vivo* relevance of the data obtained from the experiments with the ASZ001 cell line is supported by the low level baseline expression of Fas in human basal cell carcinomas (refs. 23, 24; Fig. 4*C*) and the induction of Fas expression and apoptosis in *Ptch1*$^{+/-}$ mouse basal cell carcinomas by treatment with either cyclopamine (Fig. 4*D*) or by Cur 61414 (data not shown). Specifically, Fas protein expression increased after cyclopamine injection (either s.c. injection or intratumoral injection), and this was accompanied by increased TUNEL-positive cells (Figs. 3*F* and 4*D*). Immunofluorescent staining revealed a membrane localization of Fas protein in basal cell carcinoma cells (indicated by the arrowhead in the insert of Fig. 4*D*). Thus, it appears that Fas expression is elevated in the presence of SMO antagonists both in cultured cell lines and in basal cell carcinomas induced in *Ptch1*$^{+/-}$ mice.

On the basis of these results, we predicted that either (*a*) interruption of the FasL/Fas signaling axis or (*b*) inhibition of the downstream apoptosis-effector caspase 8 activity would prevent cyclopamine-induced apoptosis. To test this hypothesis, we inactivated FasL/Fas signaling using neutralizing antibodies against FasL. By depleting FasL molecules (Fig. 5*B*), the cyclopamine-mediated decrease in cell viability was rescued (Fig. 6, *C* and *D*). Neutralizing antibodies against FasL also decreased the level of caspase-3 (Fig. 5*C*). Furthermore, administration of the caspase-8 inhibitor Z-IETD-FMK (25) abrogated the cyclopamine-mediated activation of caspase-3 (Fig. 5*C*). Thus, our data provide direct evidence that the FasL/Fas signaling axis is an important mediator of cyclopamine-induced apoptosis in basal cell carcinomas.

phase was shown at the bottom. The level of caspase-3 in ASZ001 cells, a marker for apoptosis, was detected by immunoblotting with a specific antibody from Cell Signaling Technology (*C*). *D*, TUNEL analyses of basal cell carcinomas (BCCs) from *Ptch1*$^{+/-}$ mice. BCCs were induced in *Ptch1*$^{+/-}$ mice as reported previously (16). Cyclopamine was injected s.c. into BCC-bearing *Ptch1*$^{+/-}$ mice or directly into the tumor. Tumor specimens were collected at 72 hours after injection and embedded in OCT. Cryostat tissue sections were used for TUNEL analysis. *Green,* TUNEL or K14; *red,* nuclear staining. —◆—, Tomatidine; —■—, Cur61414; —△—, Cyclopamine.

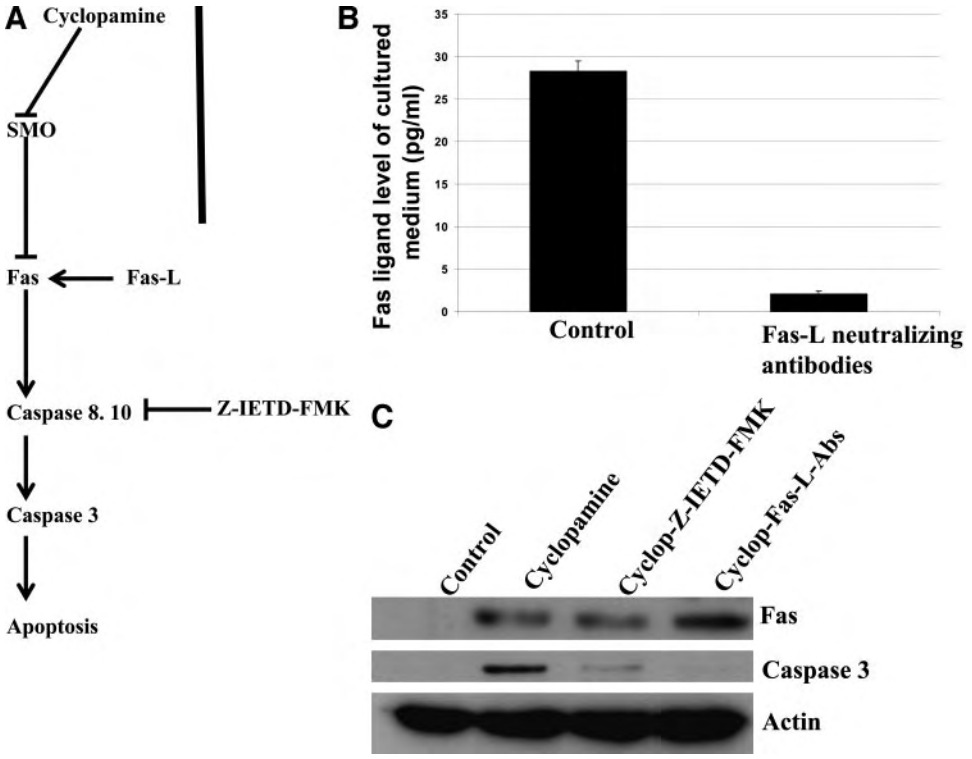

Fig. 5. Inhibition of cyclopamine-induced apoptosis by FasL-neutralizing antibodies. *A*, pathway for cyclopamine-mediated apoptosis. *B*. ASZ001 cells were cultured in 154CF medium without growth supplements during treatment with 2 μmol/L cyclopamine. The level of FasL in the culture medium of ASZ001 cells was detected by ELISA with a kit from R&D Systems, Inc. *C*, detection of Fas and caspase-3 in ASZ001 cells by Western blotting.

The Molecular Basis of Cyclopamine-mediated Induction of Fas. To investigate the mechanism whereby inhibition of the Hh pathway induces Fas expression, we assessed whether this regulation occurs directly as opposed to indirectly by altering other signaling pathways. It has been reported that several signaling pathways, including the Ras-Erk pathway and the p53 pathway, can regulate Fas expression (26–28). We have previously reported that Hh activation augments Ras-Erk signaling (17). Consistent with those findings, we observed that cyclopamine decreased the levels of PDGFR-α and phospho-Erk, indicating an inhibitory effect on Ras-Erk signaling in ASZ001 cell (Fig. 6*B*). As a result, PDGF-A had no effect on cyclopamine-mediated caspase-3 activation, Fas induction, or cell death (see Fig. 6, *D* and *E*, for details). In contrast, epidermal growth factor, which can activate the Ras-Erk pathway through the epidermal growth factor receptor, did inhibit cyclopamine-mediated accumulation of the sub-G_1 population (Fig. 6*C*), Fas expression (Fig. 6*D*), caspase-3 activation (Fig. 6*D*), and cell death (Fig. 6*E*). Furthermore, addition of the mitogen-activated protein kinase kinase inhibitor U0126 alone was sufficient to induce caspase-3 in ASZ001 cells (Fig. 6*D*). Consistent with these data, ASZ001 cells in which PDGFR-α and active Raf were overexpressed resisted cyclopamine treatment (data not shown), providing additional information that inhibition of PDGFR-α and subsequent down-regulation of Ras-Erk signaling is an important mechanism whereby cyclopamine induces apoptosis in basal cell carcinomas.

Our model predicts that overexpression of Gli1 in ASZ001 cells under a strong promoter (such as the cytomegalovirus promoter) would constitutively activate the Hh pathway, which could render these basal cell carcinoma cells resistant to cyclopamine treatment. Indeed, cyclopamine did not induce apoptosis in constitutive Gli1-expressing ASZ001 cells, as indicated by lack of TUNEL staining and of procaspase-3 cleavage (Fig. 6, *F* and *G*). As a result of constitutive Gli1 overexpression, PDGFR-α remained unchanged even after cyclopamine treatment (Fig. 6*G*). In addition, Fas protein was not induced by cyclopamine in constitutive Gli1-expressing ASZ001 cells (Fig. 6*G*). The ability of Gli-1 overexpression to abrogate cyclopamine-mediated cell death was additionally confirmed by flow cytometry analysis (data not shown). Although cyclopamine caused an increase in the sub-G_1 population in Gli1-negative cells, no such change was observed in Gli1-expressing ASZ001 cells. These data indicate that ectopic expression of Gli1 under the cytomegalovirus promoter prevents cyclopamine-induced changes in the expression of PDGFR-α, Fas, and apoptosis.

DISCUSSION

The identification of SMO antagonists has created the opportunity to consider mechanism-driven anticancer strategies for effective treatment of common malignancies in which Hh activation is thought to be important, including basal cell carcinomas, as well as subsets of medulloblastomas, lung cancer, and gastrointestinal cancers (3, 8–11). Basal cell carcinomas frequently contain mutations of the *PTCH1* gene, most of which lead to inactivated *PTCH1* and consequently uncontrolled SMO signaling. Because PTCH1 is upstream of SMO (21),[7] we reasoned that administration of the SMO inhibitor cyclopamine to *Ptch1*$^{+/-}$ mice could specifically and effectively inhibit the development of basal cell carcinomas *in vivo*. Our studies indicate that orally administered cyclopamine is a potent inhibitor of basal cell carcinomas in *Ptch1*$^{+/-}$ mice and that this natural substance does not cause significant toxicity because the overall survival of the treated mice was unaffected. These data are consistent with the observation in sheep that cyclopamine toxicity is limited to Hh signaling-dependent teratogenicity (2, 29) and with the fact that most normal adult mouse and human tissues appear to have very low expression of Hh target genes (30). Basal cell carcinomas would appear to be good candidates for the cutaneous application of SMO antagonists because our data indicate that direct injection of cyclopamine into mouse basal cell carcinomas induces Fas expression and apoptosis. Thus, it should be possible to design topical formulations of

[7] Unpublished observation.

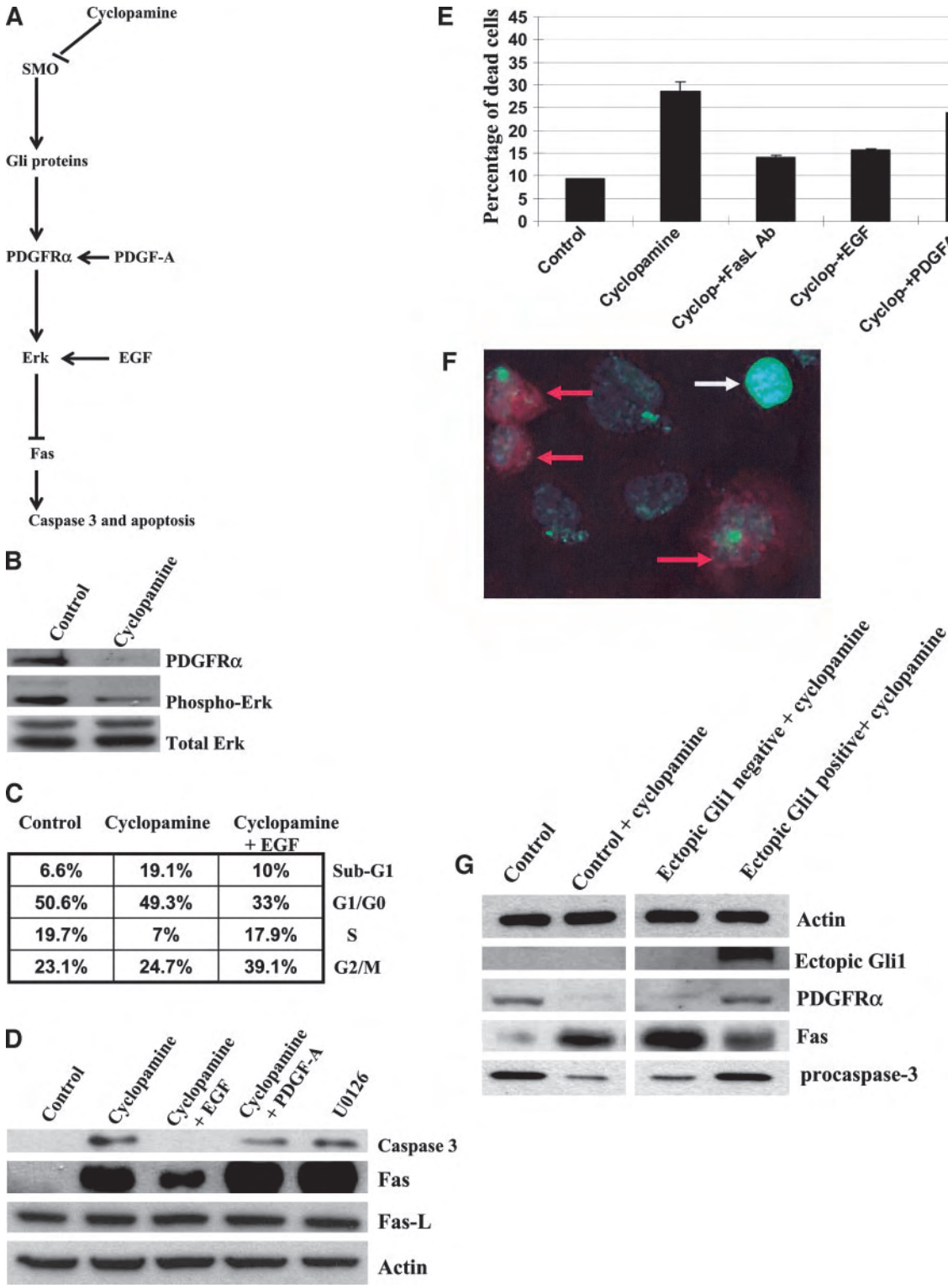

Fig. 6. Regulation of Fas expression by cyclopamine through the Ras-Erk pathway. *A*, pathway for cyclopamine-mediated apoptosis. *B*. In the presence of cyclopamine, the levels of PDGFR-α and phospho-Erk were down-regulated. *C*, epidermal growth factor (EGF) abrogated cyclopamine-mediated sub-G_1 accumulation in ASZ001 cells. *D*. The protein levels of Fas, FasL, and activated caspase-3 were detected by Western blotting after 36 hours treatment with 2 μmol/L KAAD-cyclopamine in the presence of other reagents or with U0126 alone (10 μmol/L). *E*. Cell viability was assessed by trypan blue analysis. Each experiment was repeated three times with similar results. *F*, detection of apoptosis by TUNEL assay in ASZ001 cells with Gli1 expression under the cytomegalovirus promoter. *Red arrows* indicate Gli1-positive cells, and the *white arrow* indicates TUNEL-positive cells. *G*. After enrichment of Gli1-overexpressing cells through cell sorting, the protein levels of PDGFR-α, Fas, and caspase-3 were detected by Western blotting.

cyclopamine or other SMO antagonists for treating basal cell carcinomas, initially in *Ptch1*$^{+/-}$ mice and eventually in humans.

Our data indicate that cyclopamine inhibits the Hh pathway in basal cell carcinomas, as indicated by down-regulation of the target genes HIP and Gli1 (Fig. 3, *A* and *B*). We additionally demonstrate that induction of Fas expression (both the protein and the RNA levels) and consequent activation of the FasL/Fas signaling axis is necessary for cyclopamine-mediated apoptosis because cell death is blocked *in vitro*

by anti-FasL antibodies. Thus, it appears that Fas expression is suppressed by the activity of the Ras-Erk pathway in basal cell carcinoma cells, and overexpression of Gli1, PDGFR-α, or active Raf (all downstream of Ptch1) renders ASZ001 cells resistant to cyclopamine-induced apoptosis (Fig. 6, *E* and *F*).[8] Furthermore, addition of a mitogen-activated protein kinase kinase inhibitor U0126 alone is sufficient to induce Fas expression and apoptosis in ASZ001 cells (Fig. 6, *C* and *D*). We have analyzed promoter sequences of human and mouse Fas genes and found multiple copies of serum response elements and Ras-responsive elements, suggesting that the Ras/Erk pathway can regulate transcription of murine and human Fas directly.[9] These data are consistent with a previous report showing that cyclopamine causes apoptosis in subsets of small-cell lung cancer and medulloblastomas in the presence of low concentrations of newborn bovine serum in which growth factor content is quite low (9, 11).[10] Because Fas is regulated at multiple levels, it will be interesting to determine whether other mechanisms, including altered Fas membrane translocation, could be involved in cyclopamine-mediated Fas up-regulation.

Because cyclopamine exerts its effects through direct association with SMO, tumors with genetic mutations downstream of SMO may not be sensitive to cyclopamine treatment. We have found that cyclopamine does not cause apoptosis in ASZ001 cells with Gli1 overexpression under the cytomegalovirus promoter (Fig. 6, *F* and *G*) or in Gli1-transformed RK3E cells.[11] Similarly, cells expressing activated SMO are resistant to cyclopamine (31). Thus, studies on the genetic mutations in specific target tumors could be helpful in predicting the effectiveness of cyclopamine treatment. Effective treatment of tumors with mutations of genes encoding proteins acting downstream of Smo will require identification of novel small molecular weight compounds acting downstream of SMO signaling. However, because most basal cell carcinomas do contain loss-of-function mutations of PTCH1, cyclopamine should represent an effective and specific agent for basal cell carcinoma therapy, as well as for those visceral cancers with Hh signaling activation, which thus far appears to be driven by overexpression of sonic Hh.

In summary, our results indicate that chronic administration of the SMO antagonist cyclopamine is effective in preventing basal cell carcinoma development *in vivo*. We demonstrate that cyclopamine inhibits Hh signaling and thereby exerts its effects through induction of Fas expression, leading to activation of the FasL/Fas signaling axis and apoptosis. It is likely that SMO antagonists capable of inhibiting Hh activation and inducing Fas expression hold great promise as a mechanism-directed approach for the treatment of basal cell carcinomas.

ACKNOWLEDGMENTS

We thank Brent Norris and Huiping Guo for technical support and Drs. Michelle Azsterbaum, Eric Fearon, and William Gaffield for providing reagents. We also thank Nonggao He, Tao Sheng, and Josh Sultz for support.

[8] Unpublished data.
[9] Unpublished observation.
[10] Unpublished data.
[11] J. Xie and C. Li, unpublished data.

REFERENCES

1. Ingham PW. Transducing Hedgehog: the story so far. EMBO J 1998;17:3505–11.
2. Taipale J, Beachy PA. The Hedgehog and Wnt signalling pathways in cancer. Nature (Lond.) 2001;411:349–54.
3. Epstein E Jr. Genetic determinants of basal cell carcinoma risk. Med Pediatr Oncol 2001;36:555–8.
4. Toftgard R. Hedgehog signalling in cancer. Cell Mol Life Sci 2000;57:1720–31.
5. Johnson RL, Rothman AL, Xie J, et al. Human homolog of patched, a candidate gene for the basal cell nevus syndrome Science (Wash. DC) 1996;272:1668–71.
6. Hahn H, Wicking C, Zaphiropoulous PG, et al. Mutations of the human homolog of Drosophila patched in the nevoid basal cell carcinoma syndrome. Cell 1996;85:841–51.
7. Xie J, Murone M, Luoh SM, et al. Activating Smoothened mutations in sporadic basal-cell carcinoma Nature (Lond.) 1998;391:90–2.
8. Thayer SP, di Magliano MP, Heiser PW, et al. Hedgehog is an early and late mediator of pancreatic cancer tumorigenesis. Nature (Lond.) 2003;425:851–6.
9. Berman DM, Karhadkar SS, Hallahan AR, et al. Medulloblastoma growth inhibition by hedgehog pathway blockade. Science (Wash. DC) 2002;297:1559–61.
10. Berman DM, Karhadkar SS, Maitra A, et al. Widespread requirement for Hedgehog ligand stimulation in growth of digestive tract tumours. Nature (Lond.) 2003;425:846–51.
11. Watkins DN, Berman DM, Burkholder SG, Wang B, Beachy PA, Baylin SB. Hedgehog signalling within airway epithelial progenitors and in small-cell lung cancer. Nature (Lond.) 2003;422:313–7.
12. Chen JK, Taipale J, Cooper MK, Beachy PA. Inhibition of Hedgehog signaling by direct binding of cyclopamine to Smoothened. Genes Dev 2002;16:2743–8.
13. Williams JA, Guicherit OM, Zaharian BI, et al. Identification of a small molecule inhibitor of the hedgehog signaling pathway: effects on basal cell carcinoma-like lesions. Proc Natl Acad Sci USA 2003;100:4616–21.
14. Frank-Kamenetsky M, Zhang XM, Bottega S, et al. Small-molecule modulators of Hedgehog signaling: identification and characterization of Smoothened agonists and antagonists. J Biol 2002;1:10.
15. Goodrich LV, Milenkovic L, Higgins KM, Scott MP. Altered neural cell fates and medulloblastoma in mouse patched mutants. Science (Wash. DC) 1997;277:1109–13.
16. Aszterbaum M, Epstein J, Oro A, et al. Ultraviolet and ionizing radiation enhance the growth of BCCs and trichoblastomas in patched heterozygous knockout mice. Nat Med 1999;5:1285–91.
17. Xie J, Aszterbaum M, Zhang X, et al. A role of PDGFRalpha in basal cell carcinoma proliferation. Proc Natl Acad Sci USA 2001;98:9255–9.
18. Louro ID, Bailey EC, Li X, et al. Comparative gene expression profile analysis of GLI and c-MYC in an epithelial model of malignant transformation. Cancer Res 2002;62:5867–73.
19. Li C, Chi S, He N, et al. IFNalpha induces Fas expression and apoptosis in hedgehog pathway activated BCC cells through inhibiting Ras-Erk signaling. Oncogene 2004;23:1608–17.
20. Bonifas JM, Pennypacker S, Chuang PT, et al. Activation of expression of hedgehog target genes in basal cell carcinomas. J Investig Dermatol 2001;116:739–42.
21. Zhang XM, Ramalho-Santos M, McMahon AP. Smoothened mutants reveal redundant roles for Shh and Ihh signaling including regulation of L/R asymmetry by the mouse node. Cell 2001;105:781–92.
22. Buechner SA, Wernli M, Harr T, Hahn S, Itin P, Erb P. Regression of basal cell carcinoma by intralesional interferon-alpha treatment is mediated by CD95 (Apo-1/Fas)-CD95 ligand-induced suicide. J Clin Investig 1997;100:2691–6.
23. Lee S, Jang JJ, Lee JY, et al. Fas ligand is expressed in normal skin and in some cutaneous malignancies. Br J Dermatology 1998;139:186–91.
24. Filipowicz E, Adegboyega P, Sanchez RL, Gatalica Z. Expression of CD95 (Fas) in sun-exposed human skin and cutaneous carcinomas. Cancer (Phila.) 2002;94:814–9.
25. Thornberry NA, Lazebnik Y. Caspases: enemies within. Science (Wash. DC) 1998;281:1312–6.
26. Fenton RG, Hixon JA, Wright PW, Brooks AD, Sayers TJ. Inhibition of Fas (CD95) expression and Fas-mediated apoptosis by oncogenic Ras. Cancer Res 1998;58:3391–400.
27. Kannan KAN, Rechavi G, Jakob-Hirsch J, et al. DNA microarrays identification of primary and secondary target genes regulated by p53. Oncogene 2001;20:2225–34.
28. Kazama H, Yonehara S. Oncogenic K-Ras and basic fibroblast growth factor prevent Fas-mediated apoptosis in fibroblasts through activation of mitogen-activated protein kinase. J Cell Biol 2000;148:557–66.
29. Cooper MK, Porter JA, Young KE, Beachy PA. Teratogen-mediated inhibition of target tissue response to Shh signaling. Science (Wash. DC) 1998;280:1603–7.
30. Hu Z, Bonifas JM, Aragon G, et al. Evidence for lack of enhanced hedgehog target gene expression in common extracutaneous tumors. Cancer Res 2003;63:923–8.
31. Taipale J, Chen JK, Cooper MK, et al. Effects of oncogenic mutations in Smoothened and Patched can be reversed by cyclopamine. Nature (Lond.) 2000;406:1005–9.

Molecular Cancer

BioMed Central

Research

Open Access

Activation of the hedgehog pathway in advanced prostate cancer

Tao Sheng[†1], Chengxin Li[†1,2], Xiaoli Zhang[†1], Sumin Chi[1,2], Nonggao He[1], Kai Chen[1], Frank McCormick[3], Zoran Gatalica[4] and Jingwu Xie*[1]

Address: [1]Sealy Centers for Cancer Cell Biology and Environmental Health, Department of Pharmacology and Toxicology, University of Texas Medical Branch, Galveston, Texas, 77555-1048, USA, [2]Department of Dermatology, Xijing hospital, Xi'an 710032, China, [3]UCSF Cancer Center, 2340 Sutter Street, San Francisco, CA 94115, USA and [4]Department of Pathology, Creighton University Medical Center, 601 N 30th St. Omaha, NE 68131, USA

Email: Tao Sheng - tasheng@utmb.edu; Chengxin Li - cxli66@yahoo.com; Xiaoli Zhang - xiaolzha@utmb.edu; Sumin Chi - chisumin@yahoo.com; Nonggao He - nhe@utmb.edu; Kai Chen - kachen@utmb.edu; Frank McCormick - mccormick@cc.ucsf.edu; Zoran Gatalica - zgatalica@pathology.creighton.edu; Jingwu Xie* - jinxie@utmb.edu

* Corresponding author †Equal contributors

Published: 13 October 2004

Molecular Cancer 2004, **3**:29 doi:10.1186/1476-4598-3-29

Received: 22 September 2004
Accepted: 13 October 2004

This article is available from: http://www.molecular-cancer.com/content/3/1/29

Abstract

Background: The hedgehog pathway plays a critical role in the development of prostate. However, the role of the hedgehog pathway in prostate cancer is not clear. Prostate cancer is the second most prevalent cause of cancer death in American men. Therefore, identification of novel therapeutic targets for prostate cancer has significant clinical implications.

Results: Here we report that activation of the hedgehog pathway occurs frequently in advanced human prostate cancer. We find that high levels of hedgehog target genes, PTCH1 and hedgehog-interacting protein (HIP), are detected in over 70% of prostate tumors with Gleason scores 8–10, but in only 22% of tumors with Gleason scores 3–6. Furthermore, four available metastatic tumors all have high expression of PTCH1 and HIP. To identify the mechanism of the hedgehog signaling activation, we examine expression of Su(Fu) protein, a negative regulator of the hedgehog pathway. We find that Su(Fu) protein is undetectable in 11 of 27 PTCH1 positive tumors, two of them contain somatic loss-of-function mutations of *Su(Fu)*. Furthermore, expression of sonic hedgehog protein is detected in majority of PTCH1 positive tumors (24 out of 27). High levels of hedgehog target genes are also detected in four prostate cancer cell lines (TSU, DU145, LN-Cap and PC3). We demonstrate that inhibition of hedgehog signaling by smoothened antagonist, cyclopamine, suppresses hedgehog signaling, down-regulates cell invasiveness and induces apoptosis. In addition, cancer cells expressing Gli1 under the CMV promoter are resistant to cyclopamine-mediated apoptosis. All these data suggest a significant role of the hedgehog pathway for cellular functions of prostate cancer cells.

Conclusion: Our data indicate that activation of the hedgehog pathway, through loss of Su(Fu) or overexpression of sonic hedgehog, may involve tumor progression and metastases of prostate cancer. Thus, targeted inhibition of hedgehog signaling may have significant implications of prostate cancer therapeutics.

Background

The *hedgehog* (Hh) pathway plays a critical role in embryonic development and tissue polarity [1]. Secreted Hh molecules bind to the receptor *patched* (PTC-PTCH1, PTCH2), thereby alleviating PTC-mediated suppression of *smoothened* (SMO), a putative seven-transmembrane protein. SMO signaling triggers a cascade of intracellular events, leading to activation of the pathway through GLI-dependent transcription [2]. The hedgehog receptor PTCH1 is also a target gene of this pathway, which forms a negative feedback mechanism to maintain the pathway activity at an appropriate level in a given cell. Activation of Hh signaling through loss-of-function somatic mutations of PTCH1 in human basal cell carcinomas (BCCs) disrupts this feedback regulation, leading to uncontrolled SMO signaling. Activating mutations of SMO in BCCs, on the other hand, are resistant to PTCH1-mediated inhibition, leading to an outcome similar to PTCH1 inactivation [3-6]. More recently, abnormal activation of the sonic hedgehog pathway, through over-expression of sonic hedgehog, has been implicated in the development of subsets of medulloblastomas, small cell lung cancer and gastrointestinal tract (GI) cancers [7-10].

Development of prostate requires hedgehog signaling. Although the initial formation of prostate buds does not require sonic hedgehog signaling (shh), shh is critical for maintaining appropriate prostate growth, proliferation and tissue polarity [11-14]. In the adult prostate, however, the activity of the hedgehog pathway is quite low. It remains to be tested whether this hedgehog pathway is activated during development of prostate cancer, the second most prevalent cause of cancer death in American men. Activation of the hedgehog pathway is often indicated by elevated levels of PTCH1 and HIP. In addition to PTCH1 mutation, SMO activation and hedgehog over-expression, loss of Su(Fu) can result in activation of the hedgehog pathway. In the human, the Su(Fu) gene is localized at chromosome 10q24, a region with LOH in several types of cancer including prostate cancer, lung cancer, breast cancer and medulloblastomas [15,16]. As a negative regulator of the hedgehog pathway, Su(Fu) inhibits the function of Gli molecules, leading to inactivation of this pathway [17-19]. Su(Fu) is also reported to affect beta-catenin function [20]. In addition, over-expression of sonic hedgehog is shown to be involved in the development of GI cancers [9,10]. Here we report our findings that activation of the hedgehog pathway occurs frequently in advanced prostate cancers, possibly through loss of Su(Fu) protein or over-expression of sonic hedgehog.

Results

Elevated expression of hedgehog target genes in prostate cancer specimens

As an important regulator of tissue polarity, active hedgehog signaling is required for ductual morphogenesis and proliferation during prostate development [11-14]. The adult prostate, on the other hand, does not contain active hedgehog signaling. Because hedgehog signaling is an important regulator for epithelial-mesenchymal interaction, an event critical during prostate cancer development, we examined whether the hedgehog-signaling pathway is activated in prostate cancer.

Activation of hedgehog signaling causes elevated expression of target genes PTCH1 and HIP. Thus, increased protein expression of PTCH1 and HIP indicates activation of the hedgehog pathway. Using PTCH1 antibodies [10], we examined 59 prostate cancer samples for hedgehog signaling activation (see Table 1, Additional file 1 for details). We first tested the specificity of the PTCH1 antibodies in MEF cells. *Ptch1* null MEF cells have no active *Ptch1* gene, thus should not have positive staining with PTCH1 antibodies. Indeed, no staining was seen in *Ptch1* null MEF cells (Fig. 1A). After transfection of *PTCH1* expressing plasmid, transfected cells showed positive staining (Fig. 1A), indicating that the PTCH1 antibodies are specific to PTCH1. Furthermore, PTCH1 immunohistostining was abolished after addition of the specific peptide, from which the antibodies were raised (Fig. 1B,1c). We found that percentage of PTCH1 positive staining tumors increased in high grade tumors (Table 1, Additional file 1). In prostate cancers with Gleason scores 3–6, 4 out of 18 specimens were positive for PTCH1 (22%), whereas 16 out of 22 undifferentiated carcinomas (Gleason Scores of 8–10) expressed PTCH1 (73%, see Table 1, Additional file 1), suggesting that the hedgehog pathway is frequently activated in advanced prostate cancer. To confirm this data, we found that all four available metastatic prostate cancer specimens were all positive for PTCH1 staining.

To further confirm our data, we detected HIP protein expression, another marker of the hedgehog signaling activation. After transfection of HIP expressing plasmid into 293 cells, HIP antibodies recognize a single band around 75 KD (Fig. 3A), and an endogenous HIP protein with a similar size was also detected in two cancer tissues, in which hedgehog signaling is known to be activated (Fig. 3B and data not shown here). In contrast, the matched normal tissue did not express detectable HIP. Thus, HIP expression appears to be a good marker for hedgehog signaling activation. Immunohistostaining with HIP antibodies in prostate cancer specimens revealed a similar pattern to prostate specific antigen (PSA) and PTCH1 (Fig. 3C and Table 1, Additional file 1), further confirming that hedgehog pathway is activated in

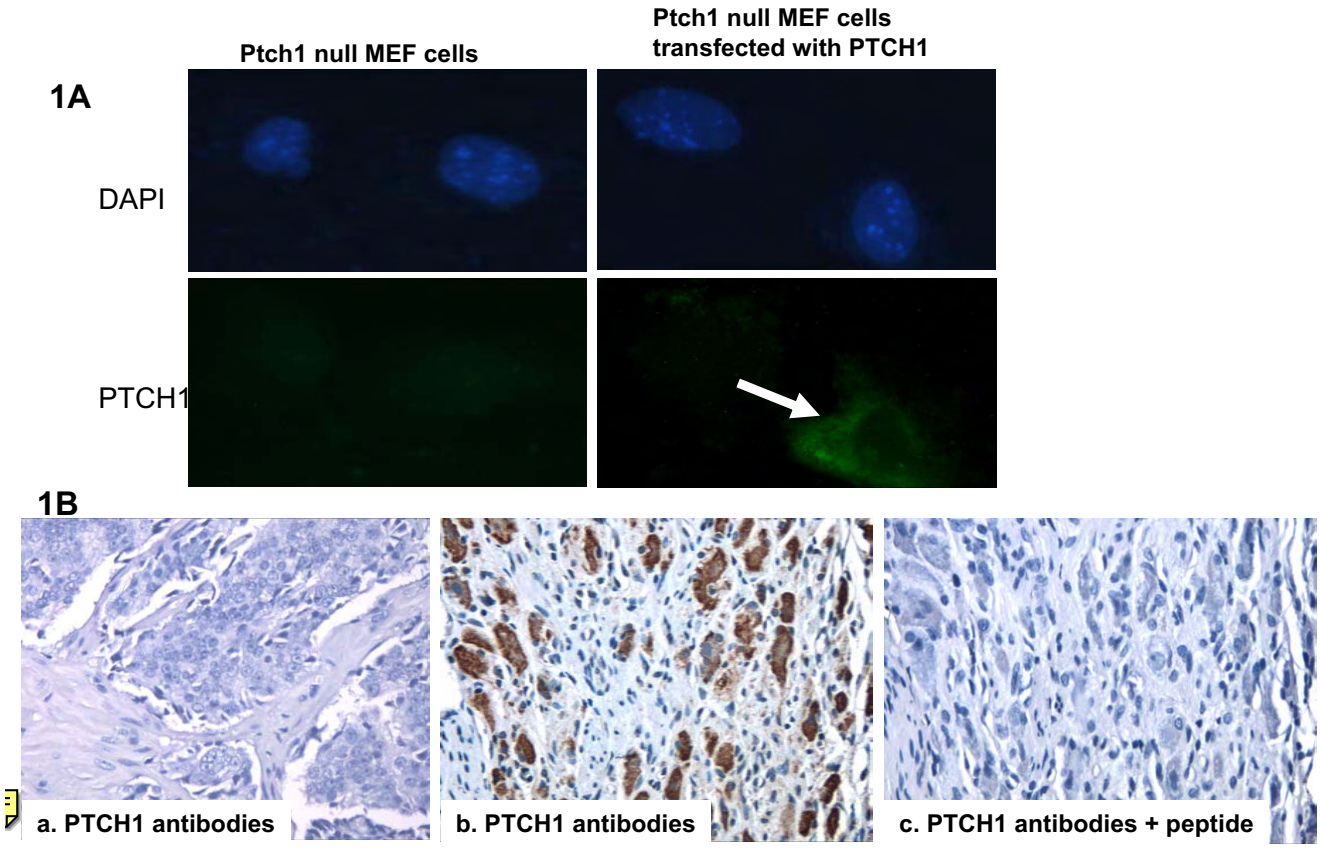

Figure 1
Detection of PTCH1 expression in prostate cancers. Protein expression of PTCH1 was detected by immunostaining. PTCH1 antibodies (Santa Cruz Biotechnology Cat# 9149) were tested in *Ptch1*$^{-/-}$ null MEF cells (**A**). While *Ptch1*$^{-/-}$ null MEF cells had no positive fluorescent staining with PTCH1 antibodies, transfection of PTCH1 expressing plasmid lead to positive staining (green, indicated by an arrow, 400×). Immunohistochemistry of prostate cancer specimens with PTCH1 gave negative (**B-a,** 200×) or positive (Red in **B-b,** 200×) signals. When PTCH1 antibodies were pre-incubated with the very peptide for raising the antibodies, no positive signals could be observed (**B-c**).

advanced prostate cancers. Thus the hedgehog pathway appears to be frequently activated in advanced or metastatic prostate cancers.

Altered expression of Su(Fu) and Shh in prostate cancer specimens

There are several mechanisms by which the hedgehog pathway in these prostate tumors can be activated, including loss of Su(Fu) or over-expression of hedgehog [6-10]. The Su(Fu) gene is localized at 10q24, a region with a frequent LOH in prostate cancer [15,16,18]. Mutations of Su(Fu) have been reported in other human cancers [6]. To test whether loss of Su(Fu) function is responsible for hedgehog signaling activation, we examined expression of Su(Fu) protein in these prostate cancer specimens. The antibodies of Su(Fu) recognize a single band at 52-kD in Western blotting analyses (Fig. 4A), which was reduced following treatment with Su(Fu) SiRNA (Fig. 4B), indicating the specificity of the antibodies. Furthermore, addition of the peptide, from which the antibodies were raised, prevented the antibody binding, further confirming the specificity of our Su(Fu) antibodies (data not shown). Of the 16 PTCH1 positive prostate cancer specimens with Gleason scores 8–10, 9 have no detectable Su(Fu) protein (Fig. 4C,4D,4E and Table 1, Additional file 1). In total, 11 of 27 PTCH1 positive prostate cancer specimens have no detectable Su(Fu) protein. Prostate cancers with low Gleason scores, however, frequently have

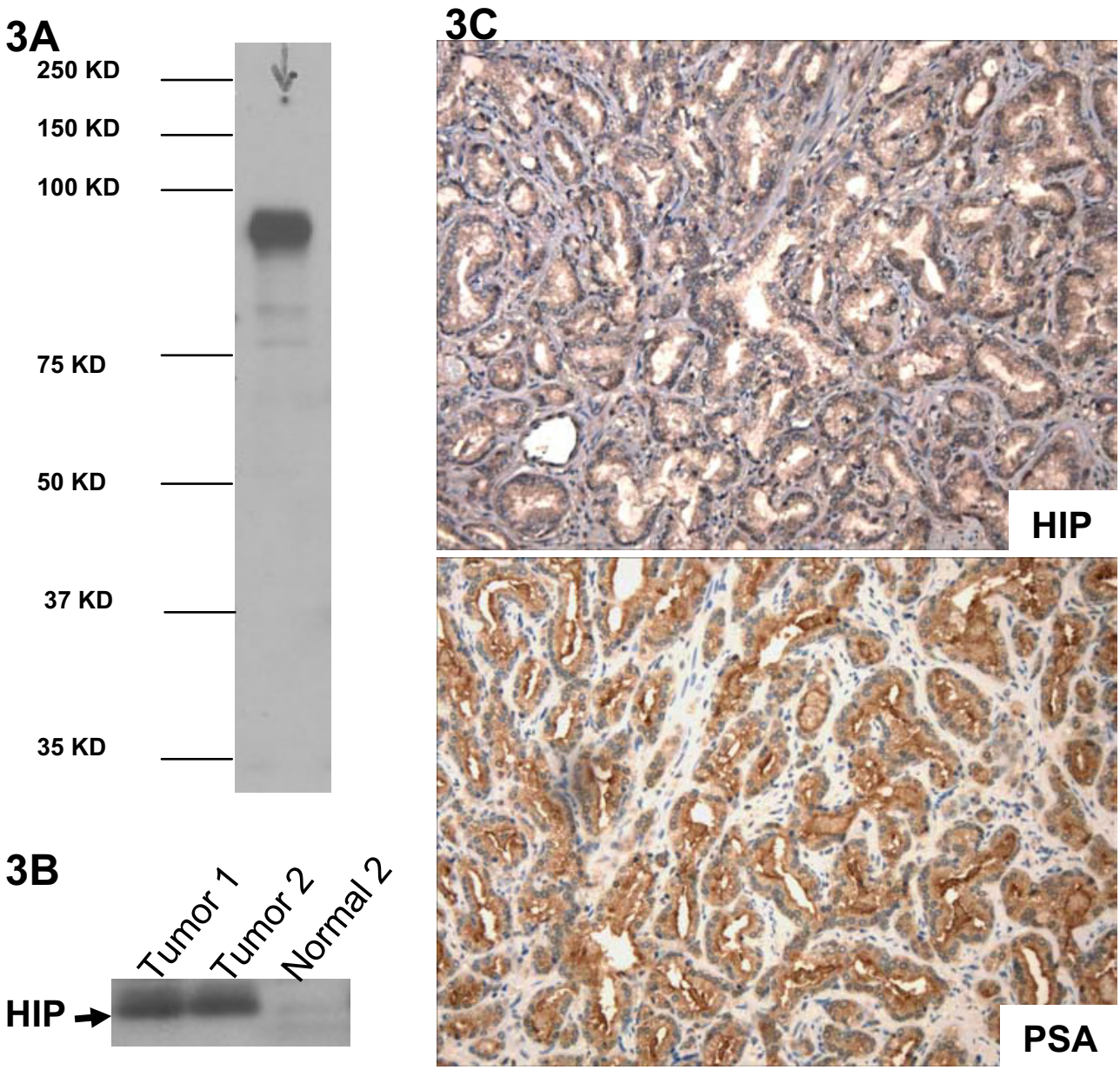

Figure 3
Detection of HIP in human cancer specimens. By Western blotting, HIP antibodies (R&D systems Cat# AF1568) recognized one band between 75 and100 KD (**A**). Expression of endogenous HIP was detected in two GI cancer tissues, which were known to contain activated hedgehog signaling (data not shown here), but not in the matched normal tissue (**B**). Immunohistostaining of HIP I prostate cancer showed a similar pattern to PSA (**C**, 200×)

detectable Su(Fu) protein (see Table 1, Additional file 1), suggesting that loss of Su(Fu) protein may be associated with prostate cancer progression.

To confirm the immunohistochemistry data, we performed immunoblotting analyses using several dissected TURP (Transurethral resection of the prostate) specimens in which tumor portion can be as high as 70% of the tissue mass. Prostatectomy specimens (most of our tumors), however, often contain a small percentage (5–10%) of tumor tissue and are therefore not suitable for Western blotting or real-time PCR analyses. As shown in Fig. 5A,

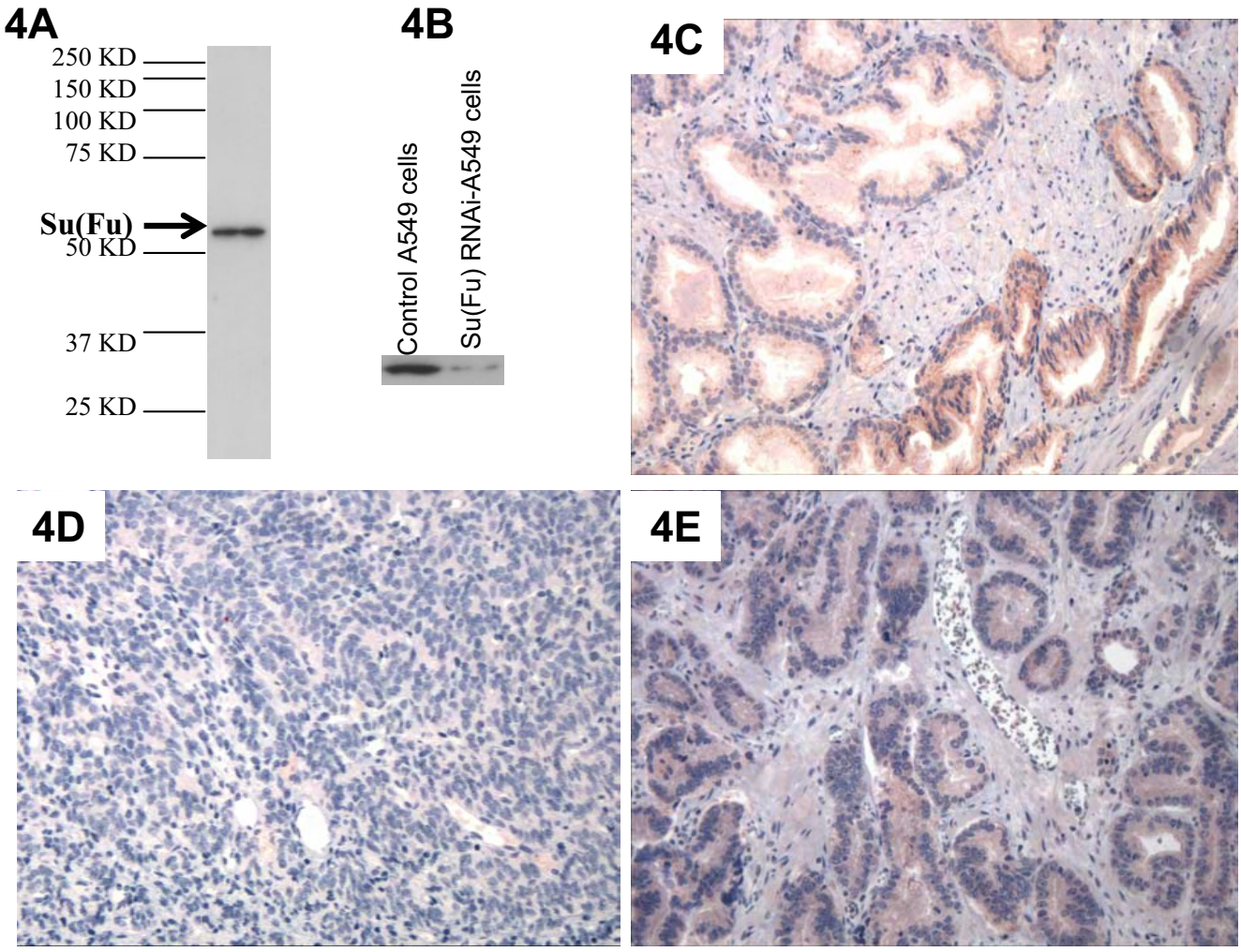

Figure 4
Detection of Su(Fu) in prostate cancer specimens. Su(Fu) antibodies (Santa Cruz Biotechnology Cat# 10933) recognized only one single band (54-Kd) in D283 cells (**A**). Following treatment of a specific SiRNA of Su(Fu), the endogenous Su(Fu) band was greatly reduced (**B**). Immunohistostaining with Su(Fu) antibodies in prostate cancer specimens revealed positive (**C**, in red, 200×), negative (**D**, 200×) or weak staining (**E**, red, 200×).

two tumors (PC48 and PC51) had no detectable Su(Fu) protein, which are consistent with our immunohistostaining, suggesting loss of Su(Fu) may be responsible for hedgehog pathway activation in these tumors. The matched normal tissues, however, retained expression of Su(Fu), indicating that alteration of Su(Fu) is a somatic event. Sequence analyses of these two tumors revealed genetic mutations in *Su(Fu)*, which are predicted to create STOP codons in the coding sequence (Fig. 5B and Table 1, Additional file 1). In PC48, a homozygous deletion of A1315 was detected, which results in a STOP codon at +1318 bp (Fig. 5B). In PC51, we detected two types of mutations, one with a deletion of C255, which results in a STOP codon at +294 bp whereas another with a deletion of C198, create a STOP codon (Picture not shown here, see Table 1, Additional file 1). These mutations were confirmed with 6 independent clones from two separate experiments, which exclude the possibility of PCR errors. No mutations were detected from the matched benign tissues, indicating the somatic nature of the mutations. Real-time PCR analyses indicated that target genes of the hedgehog pathway, PTCH1 and Gli1, were all elevated in these tumors (Fig. 5C), confirming activation of the hedgehog pathway in these tumors. Thus, Su(Fu) inactivation appears to contribute to activation of hedgehog signaling in these prostate tumors.

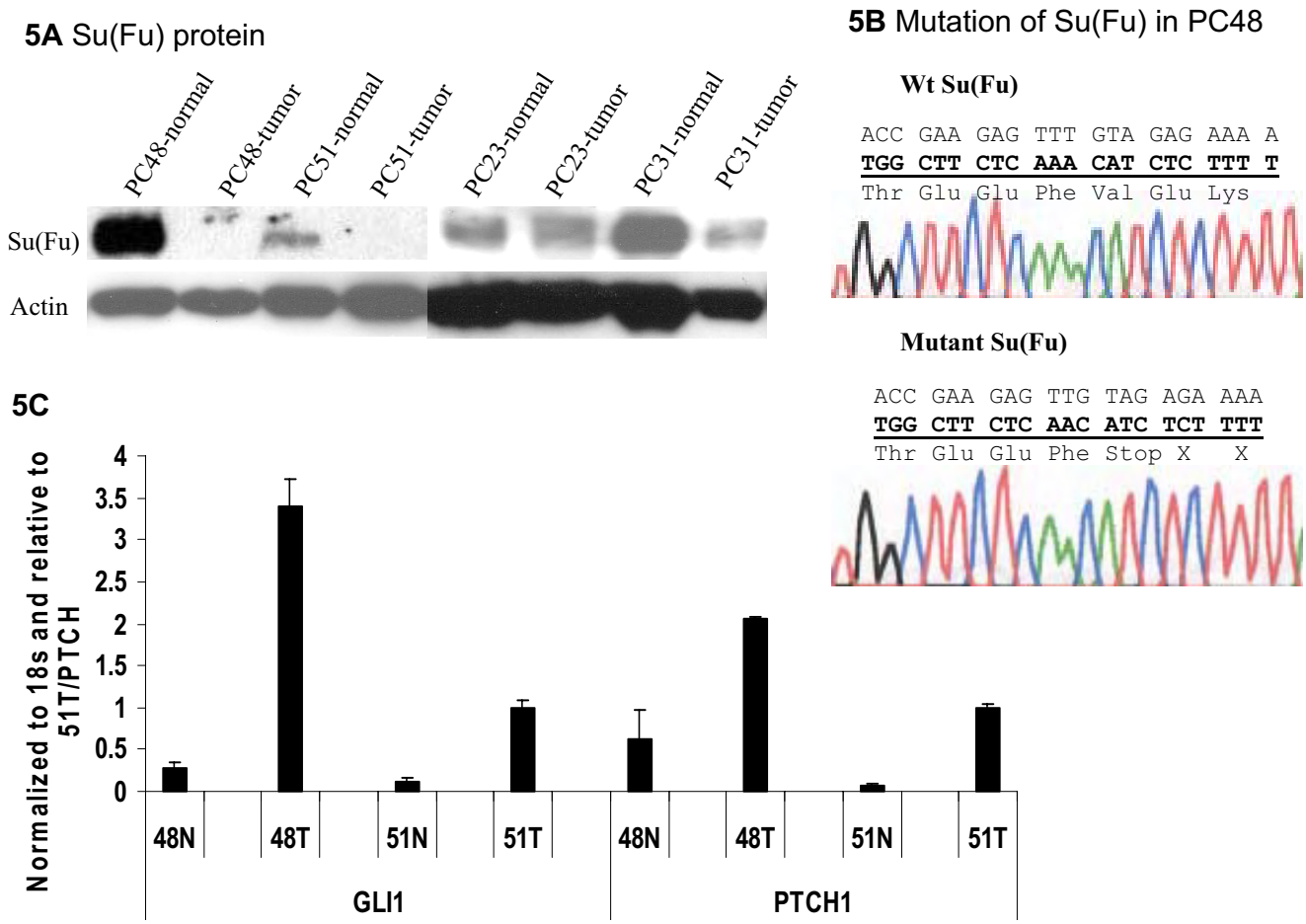

Figure 5

Inactivation of Su(Fu) in prostate cancer. Two TURP (Transurethral resection of the prostate) tumors with loss of Su(Fu) expression were confirmed by Western blotting (**A**). One mutation of Su(Fu) found in prostate cancer PC48 is shown in **B**, which is predicted to create a STOP codon in the Su(Fu) coding sequence +1318. The levels of Gli1 and PTCH1 transcripts in prostate tissues were detected by real-time PCR (see methods for details) (**C**). Tumor tissues had higher levels of the target gene transcripts.

For tumors with high level of PTCH1 expression, but no changes in Su(Fu) protein expression, we examined expression of sonic hedgehog. It is reported that expression of hedgehog may be responsible for hedgehog signaling activation in lung cancer and GI cancers. Immunohistostaining with sonic hedgehog antibodies indicate that sonic hedgehog is highly expressed in 24 of 27 advanced prostate tumors with elevated expression of PTCH1 and HIP (see Fig. 2 and Table 1, Additional file 1). Thus, activation of the hedgehog pathway, as indicated by elevated PTCH1 and HIP expression, is associated with loss of Su(Fu) expression or elevated hedgehog expression.

The role for activated hedgehog signaling for cellular functions of prostate cancer

To demonstrate the role of hedgehog pathway in prostate cancer, we screen five available cell lines for the expression of Gli1, PTCH1 and HIP. TSU, LNCap, Du145 and PC3 are prostate cancer cell lines whereas RWPE-1 is a prostate epithelial cell line. We found that the hedgehog target genes were significantly elevated in all cancer cell lines (Fig. 6A). Thus, we predicted that inhibition of the hedgehog pathway by smoothened antagonist, cyclopamine, would suppress cell proliferation and cell invasiveness.

Following treatment with 5 μM cycloapmine in PC3 cells, expression of hedgehog target genes were dramatically inhibited (data not shown here), which was accompanied

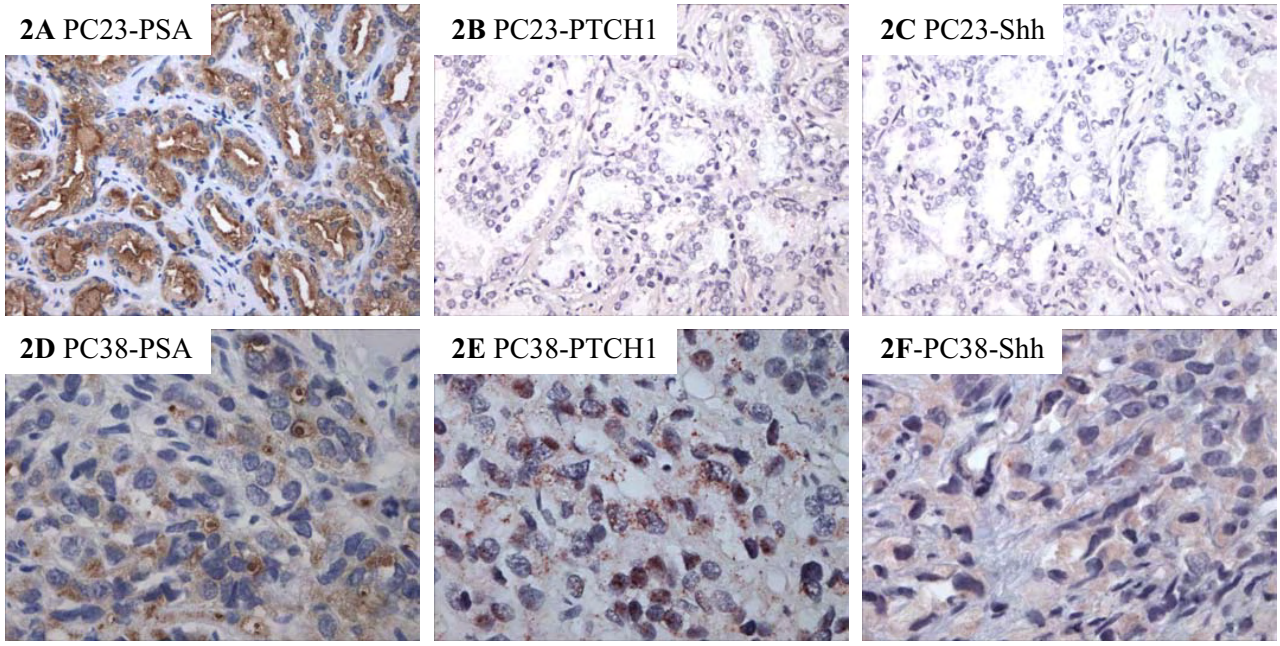

Figure 2
Co-expression of PTCH1, PSA and Shh in prostate cancer specimens. Immunohistochemistry of prostate cancer specimens with PSA was used to confirm the cancer region. Positive staining was in red. Positive staining patterns of PTCH1 and Shh antibodies (Santa Cruz Biotechnology Cat# 9024) were similar to that of PSA staining. PC23 (**A-C**) was from tumors with Gleason score 7 (200×). PC38 (**D-F**) was a tumor from Gleason score 10 (400×) (**see** Table 1, Additional file 1 for details).

with a significant reduction of BrdU positive cells (see Fig. 6B for details). This effect is specific because addition of tomotidine, a non specific compound with a similar structure to cycloapmine, had no effects on either target gene expression or DNA synthesis (indicated by BrdU labeling in Fig. 6B and 6C). The prostate epithelial RWPE-1 cells which have no activated hedgehog signaling, on the other hand, were not sensitive to cyclopamine (data not shown here), indicating that cyclopamine specifically affects cells with elevated hedgehog signaling. LN-CAP, Du145 and TSU cells, like PC3 cells were also sensitive to cyclopamine treatment (Fig. 6C).

Prostate cancer progression is accompanied by increased cell invasiveness. Because the hedgehog signaling activation occurs frequently in advanced prostate cancer, we examined if inhibition of the hedgehog signaling can reduce cell invasiveness. Using BD Bio-coat cell invasion chambers, we found that treatment of cyclopamine in PC3 cells reduced the percentage of invasive cells by 70% (Fig. 7A). Similar data were also observed in Du145, LN-CAP and TSU cells (Fig. 7B). Under the same condition, RWPE-1 cells were not very invasive. Thus, hedgehog signaling activation regulates both cell proliferation as well as cell invasiveness of prostate cancer cells.

It has been shown that cyclopamine induced apoptosis in cancer cells with activated hedgehog signaling [21]. We have shown that Gli1 down-regulation is necessary for cyclopamine-mediated apoptosis in basal cell carcinoma cells [21]. To test the significant role of Gli1, the downstream effector and the target gene of the hedgehog pathway, in cyclopamine-mediated apoptosis, we first transfected Gli1 expressing plasmid in to PC3 cells, and then treated the cells with 5 μM cyclopamine for 36 h. Since Gli1 is expressed under the control of the CMV promoter, we predicted that ectopic Gli1-expressing cells should be resistant to apoptosis, which is detected by TUNEL staining. As shown in Fig. 8, we found that all Gli1 positive cells (n = 500) were TUNEL negative, supporting our hypothesis that down-regulation of Gli1 may be an important mechanism by which cyclopamine mediates apoptosis in prostate cancer cells with activated hedgehog signaling.

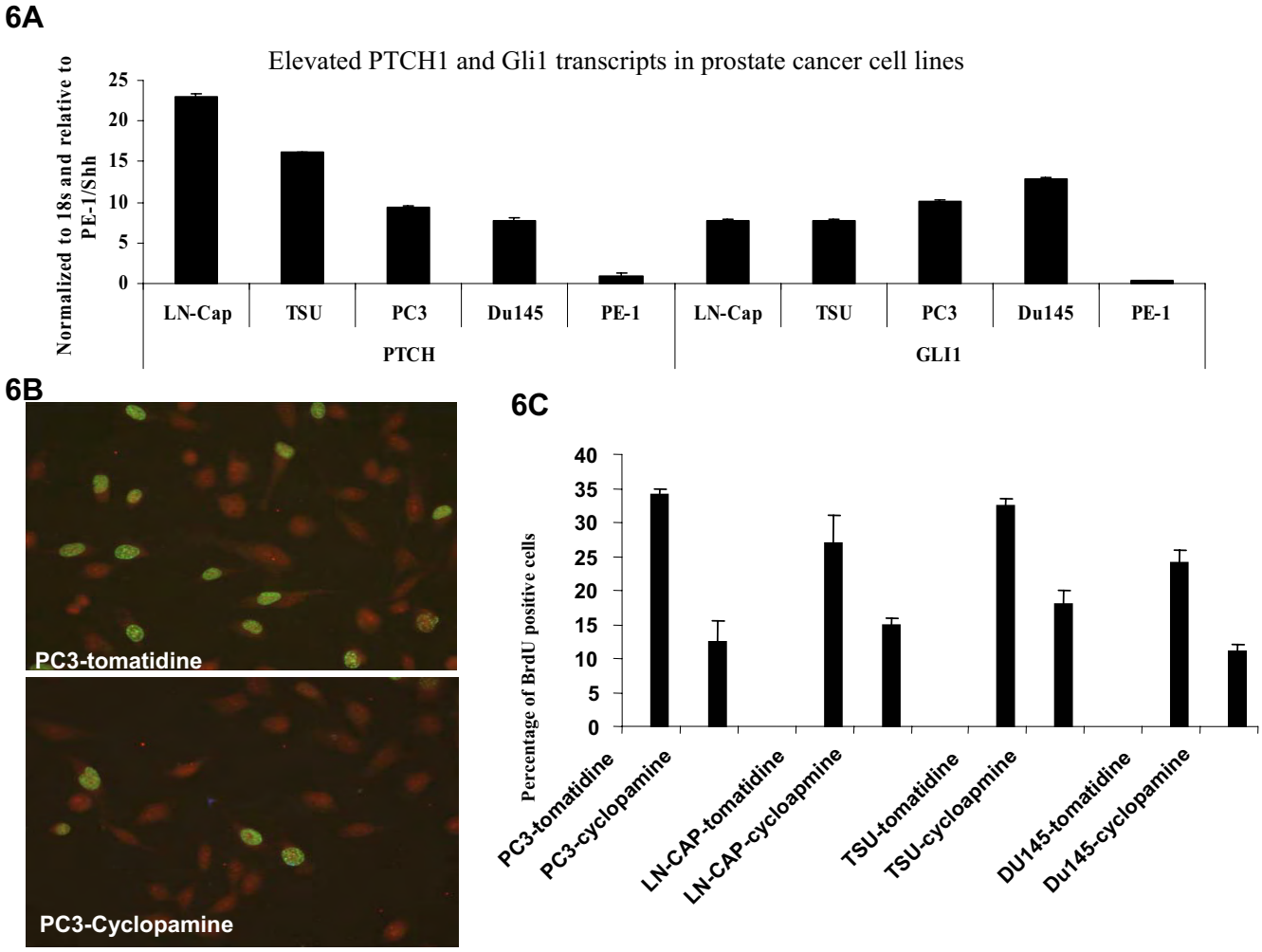

Figure 6

Cellular functions of the hedgehog pathway in prostate cancer cells. Expression of hedgehog target genes, PTCH1 and Gli1, were detected by real-time PCR (**A**). DNA synthesis was detected by BrdU labeling (**B**). Over 1000 cells were counted under fluorescent microscope for the percentage of BrdU positive cells, and the experiment was repeated twice (**C**).

All these data indicate that the hedgehog pathway is activated in advanced prostate cancers, as indicated by high expression of PTCH1 and HIP. Our results also indicate that hedgehog signaling is required for cell proliferation and cell invasion of prostate cancer cells. Thus, targeted inhibition of the hedgehog pathway may be effective in future prostate cancer therapeutics.

Discussion

Hedgehog signaling pathway regulates cell proliferation, tissue polarity and cell differentiation during normal development. Abnormal signaling of this pathway has been reported in a variety of human cancers, including basal cell carcinomas, medulloblastomas, small cell lung cancer and GI cancers [3,4,6-10,22,23]. Our findings in this report indicate a role of the sonic hedgehog pathway in prostate cancer. We detected a high expression of hedgehog target genes, PTCH1 and HIP, in advanced or metastatic prostate cancers. In contrast, only 22% of prostate tumors with Gleason scores 3–6 have elevated expression of PTCH1 and HIP. While our manuscript is being reviewed, three independent groups have recently reported similar results [24-26]. Thus, the hedgehog signaling pathway is frequently activated in advanced or metastatic prostate cancers.

Alterations of genes in the hedgehog pathway in prostate cancer

In our studies, we found that some prostate tumors had no detectable Su(Fu) protein expression while others

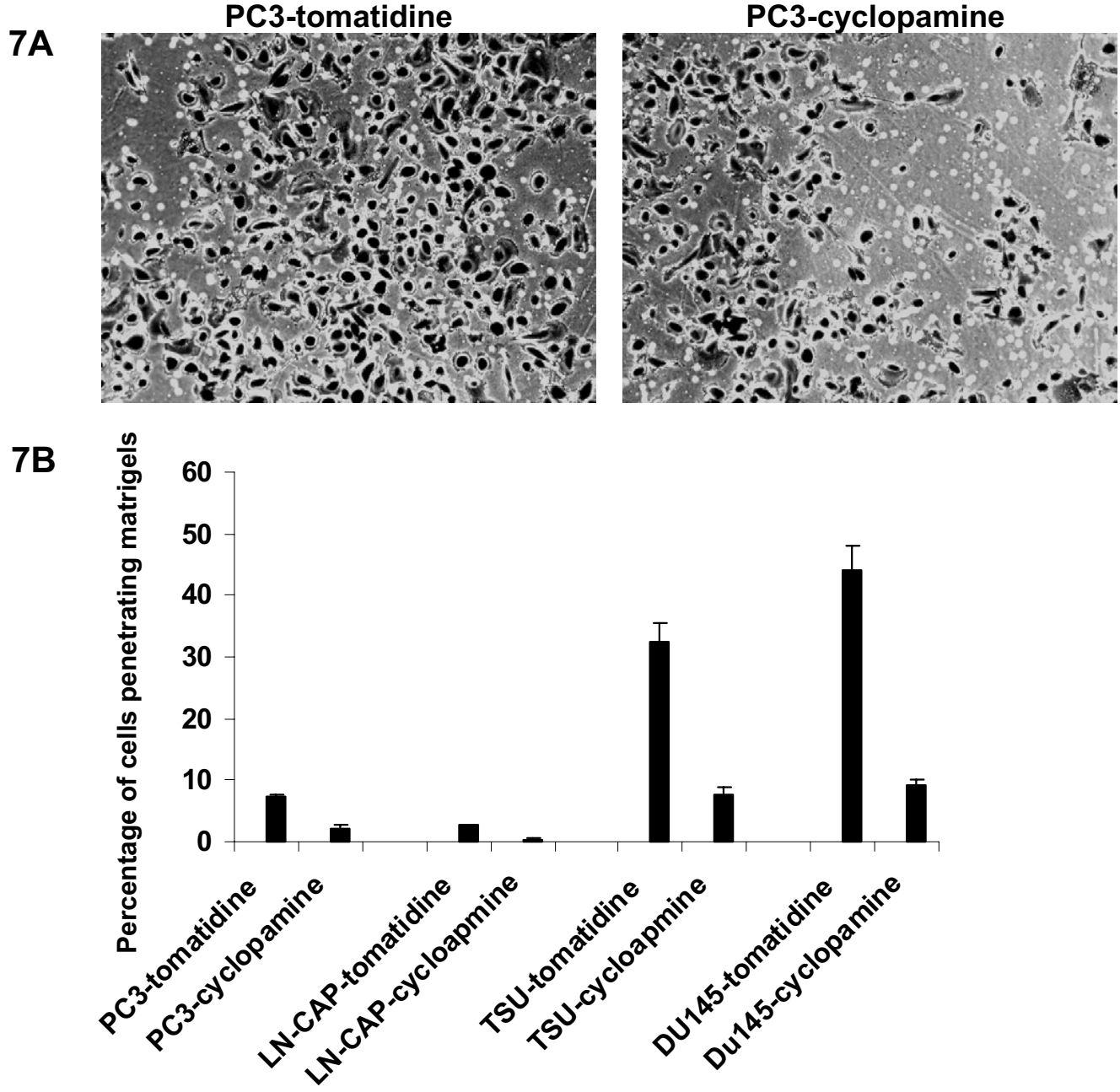

Figure 7
Effects of cyclopamine on cell invasiveness of prostate cancer cells. Cell invasion assay of prostate cancer cells was performed using BD Bio-coat cell invasion chambers (**A**). The rate of cell invasion was calculated by dividing cell numbers penetrated the matrigels by the number of cell in the control chambers (without matrigels) (**B**).

contained high levels of Shh protein expression. We further identified inactivated mutations of *Su(Fu)* in two prostate cancers. In addition to inactivated mutations in the coding region, Su(Fu) may be inactivated through promoter methylation. The heterogeneous nature of prostate cancer makes it difficult to screen prostate cancer specimens for Su(Fu) mutations since the tumor content is often less than 5% of the specimens. Future improve-

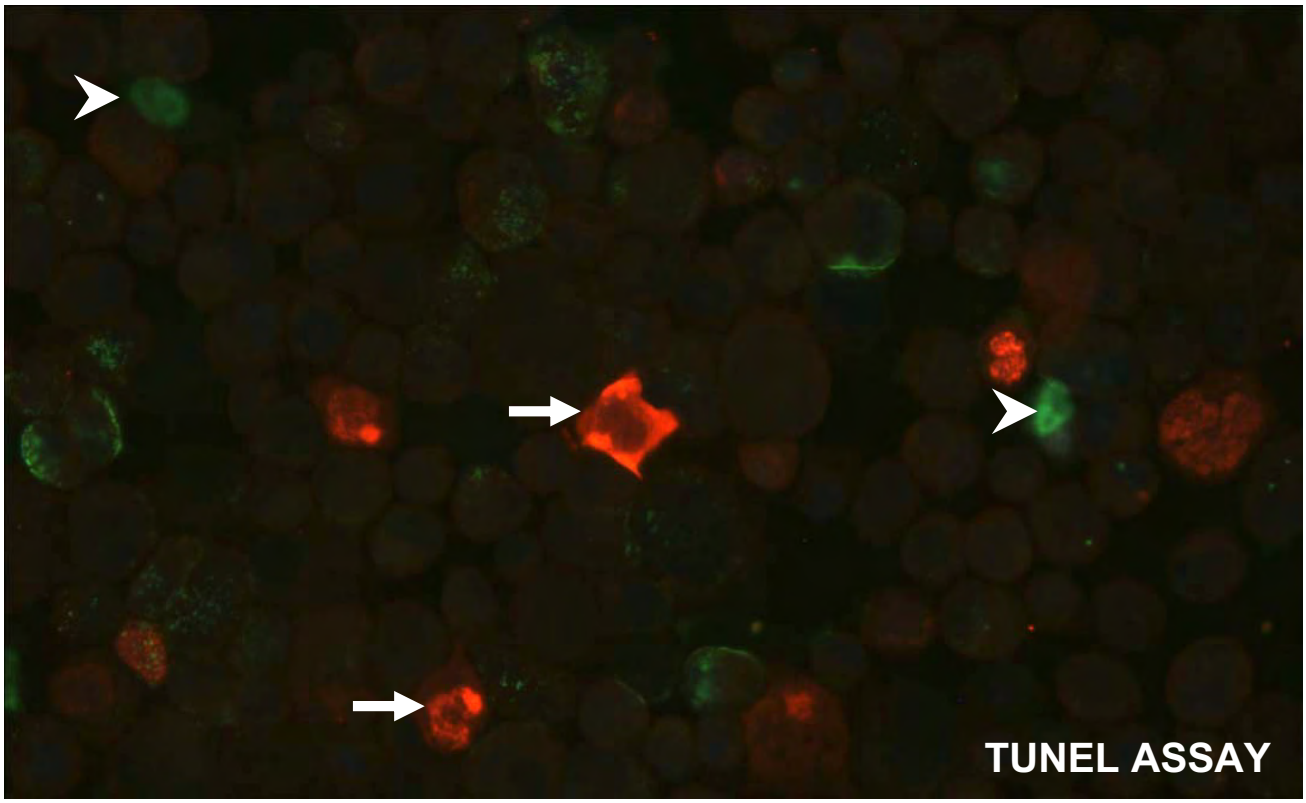

Figure 8
Cyclopamine induces apoptosis in prostate cancer cells. Cyclopamine-mediated apoptosis in prostate cancer cells was analyzed by TUNEL assay. TUNEL positive cells were indicated by arrowheads. Cells with expression of Gli1 under the CMV promoter (indicated by the arrows) did not undergo apoptosis (n = 500).

ment can be achieved using microdissection techniques for collecting pure population of tumor cells in gene mutation analysis.

Since all available prostate cancer cell lines express Su(Fu) at a high level, the role of Su(Fu) on cellular functions of prostate cancer cannot be investigated in these cells. It appears that over-expression of sonic hedgehog may be responsible for hedgehog signaling activation in these cell lines [our unpublished data and [24-26]]. After screening over 30 human cancer cell lines, we identified non-prostate cancer cell line with elevated hedgehog target genes and no detectable Su(Fu) expression (data not shown here). The growth suppression effects of Su(Fu) was demonstrated in this cell line, in which Su(Fu) expression down-regulated hedgehog target genes, inhibited DNA synthesis and cell growth (data not shown here). Thus, inactivation of Su(Fu) can contribute to active hedgehog signaling in prostate cancer.

Su(Fu) is reported to affect β-catenin signaling [27,28]. We analyzed expression of β-catenin and E-cadherin in our prostate cancer array and detected cytoplasmic distribution of E-cadherin and β-catenin only in PC51 (data not shown), indicating that Su(Fu) may be able to affect both the wnt pathway and the hedgehog pathway in prostate cancer.

In addition to Su(Fu) inactivation, over-expression of Shh is another mechanism by which the hedgehog pathway is activated in cancer [7-10]. We noticed that sonic hedgehog expression varies from tumor to tumor, which may be resulted from the heterogeneity of prostate cancer. Our immunohistostaining also revealed that three tumors (PC14, PC20 and PC36) expressed PTCH1 and HIP at high levels, but had no alterations of Shh and Su(Fu). This could be due to elevated expression of indian hedgehog, or even alterations of other components of the pathway (such as Rab23 or Fused).

Once hedgehog pathway is activated, the target gene expression will be up-regulated. Thus, analysis of target gene expression using immunohistochemistry will be an effective way to detect hedgehog pathway activation in prostate cancer. Currently, PTCH1, Gli1 and HIP are good markers for the hedgehog pathway.

Perspectives on prostate cancer therapy

Our findings not only provide novel basic understanding of prostate cancer, but also allow us to design new ways to treat prostate cancer. With a specific SMO antagonist, cyclopamine, it will be possible in the future to treat prostate cancers, which have over-expressed sonic hedgehog. However, as a downstream molecule, tumors with Su(Fu) inactivation may not respond to cyclopamine treatment. Therefore, additional small molecule inhibitors appear to be necessary to treat Su(Fu) inactivated prostate cancer. One possibility is to use Gli1 SiRNA since we have indicated that down-regulation of Gli1 may be an important mechanism by which inhibition of the hedgehog pathway by cyclopamine induces apoptosis (Fig. 8). Sanchez et al also indicated that Gli1 SiRNA down-regulated DNA synthesis in prostate cancer cells [24].

Conclusion

Taken together, our findings suggest that activation of the hedgehog pathway involves prostate cancer progression. There might be several mechanisms by which the hedgehog pathway is activated in advanced prostate cancers, including loss of Su(Fu) protein expression, over-expression of sonic hedgehog or other alterations. We demonstrate that activation of the hedgehog pathway is associated with DNA synthesis and cell invasiveness in prostate cancer cells. Inhibition of the hedgehog pathway, on the other hand, causes apoptosis possibly through down-regulation of Gli1. Our studies predict that targeted inhibition of the hedgehog pathway may be an effective way to prevent prostate cancer progression.

Materials and methods

Tissue Microarray of Prostate Cancer

A total of 55 paraffin-embedded tissue blocks from patients with prostate cancer were obtained from UTMB Surgical pathology with approval from the Institutional Review Board (IRB). Pathological reports, H#E staining of each specimen were reviewed to determine the nature of the disease and the Gleason scores. Of 55 specimens, 18 were from tumors with Gleason scores 3–6, 15 with Gleason score 7 and 22 with Gleason scores 8–10. The tumor area was first identified before tissue microarray (1.5 mm in diameter for specimens) was assembled with Beecher's Tissue arrayer-I® according to manufacturer's instruction http://www.beecherinstruments.com.

Immunohistochemistry and Western blotting

A standard avidin-biotin immunostaining technique was performed using a kit from Vector laboratories using specific antibodies to Su(Fu) (Santa Cruz Biotechnology Cat# 10933), PTCH1 (Santa Cruz Biotechnology Cat# 6149), HIP (R&D systems Cat# AF1568) and Shh (Santa Cruz Biotechnology Cat# 9024) and PSA (Vector laboratories). Positive staining was in red or brown. The specificity of antibodies was tested using the very peptide used for raising the antibodies, which abolished the specific staining. Hematoxylin was used for counterstaining (in blue). Protein was analyzed by Western analysis with appropriate antibodies [Su(Fu) antibodies were from Santa Cruz, beta-actin antibody was purchased from Sigma). The signals were visualized with the enhanced chemiluminescence detection system (Amersham).

Cell lines and Cell invasion assay

Cell lines (RWPE-1, Du145, PC3, LN-CAP were purchase from ATCC and cultured according to the suggested conditions. TSU was kindly provided by Dr. Allen Gao. Cell invasion assay was performed with BD Bio-coat cell invasion chambers according to manufacturer's instruction (BD Bioscience, Inc., Franklin Lakes, NJ), with triplicates for each sample and the experiment was repeated three times with the similar results. Cell were treated with 5 μM cyclopamine (or tomatidine) before (for 12 h) and during cell invasion assay (for 24 h). The rate of cell invasion was calculated by dividing cell numbers penetrated the matrigels by the number of cell in the control chambers (without matrigels).

RT-PCR and sequencing analysis

Total RNA was isolated using Trizol® reagent (Invitrogen), and RT-PCR was performed using Promega's RT-PCR system according to the manufacturer's protocol. Two pairs of Su(Fu) primers were used (the first set with the forward primer 5'-cctacgcaccccgatggcg-3" and the reverse primer 5'-agccaaaaccactacctcca-3'; the second set with the forward primer 5'-tccaggttaccgctatcgtc-3' ad the reverse primer 5'-tagtgtagcggactgtcg-3'). PCR products were first purified using Qiagen's Gel Extraction Kit. Due to existence of possible Su(Fu) splicing isoforms in humans, Su(Fu) genetic mutations were screened after the PCR products were cloned into TOPO® TA cloning vectors (Invitrogen). Several independent clones (from three experiments) of each PCR product were selected for sequencing analysis in UTMB sequencing facility. All mutations were confirmed by at least six independent clones.

Real-time PCR We used Applied Biosystems' assays-by-demand 20× assay mix of primers and TaqMan probes (FAM™ dye-labeled) for the target genes (human Gli and PTCH1, the sequences have been patented by Applied Biosystems, Foster City, CA) and pre-developed 18S rRNA

(VIC™-dye labled probe) TaqMan® assay reagent (P/N 4319413E) for an internal control. The primers are designed to span exon-exon junctions so as not to detect genomic DNA and the primers and probe sequences were searched against the Celera database to confirm specificity. To obtain the relative quantitation of gene expression, a validation experiment was performed to test the efficiency of the target amplification and the efficiency of the reference amplification. All absolute values of the slope of log input amount vs. ΔC_T were <0.1. Separate tubes (singleplex) one-step RT-PCR was performed with 20 ng RNA for both target genes and endogenous control. The reagent we used was TaqMan one-step RT-PCR master mix reagent kit (P/N 4309169). The cycling parameters for one-step RT-PCR was: reverse transcription 48°C for 30 min, AmpliTaq activation 95°C for 10 min, denaturation 95°C for 15 sec and annealing/extension 60°C for 1 min (repeat 40 times) on ABI7000. Triplicate C_T values were analyzed in Microsoft Excel using the comparative $C_T(\Delta\Delta C_T)$ method as described by the manufacturer(Applied Biosystems, Foster City, CA). The amount of target ($2^{-\Delta\Delta CT}$) was obtained by normalization to an endogenous reference (18sRNA) and relative to a calibrator.

BrdU labeling and TUNEL assay

BrdU labeling was performed using an *in situ* cell proliferation kit (Roche Molecular Biochemicals) [22]. Cells were treated with 5μM cyclopamine (or tomatidine) for 12 h before BrdU labeling (1 h at 37°C). The percentage of BrdU positive cells was obtained by counting over 1000 cells under microscope, and the experiment was repeated twice with similar results. TUNEL assay was performed using an *in situ* cell death kit (Roche Molecular Biochemicals) [21,29]. Cells were treated with 5 μM cyclopamine (or tomatidine) for 36 h before TUNEL assay).

List of abbreviations

PSA – prostate specific antigen; HIP – hedgehog-interacting protein; Su(Fu) – suppressor of fused; PTCH1 – human homologue of *patched* 1; Shh – sonic hedgehog; SMO – smoothened, BCC – basal cell carcinoma.

Authors' contributions

Tao Sheng contributed to Figures 6, 7, 8, cellular functions of the hedgehog pathway in prostate cancer cells. Chegxin Li contributed to primary tumor protein expression, particularly on Su(Fu) expression. Xiaoli Zhang contributed to mutation analyses of Su(Fu) in prostate cancer and real-time PCR analyses. Sumin Chi contributed to HIP antibody test (Fig. 3A and 3B). Nonggao He contributed to HIP antibody staining (Fig. 3C). Kai Chen contributed to PTCH1 antibody test (Fig. 1A). Frank McCormick involved in the initial project discussion. Zoran Gatalica contributed to prostate cancer histology and Gleason scores of the tumors.

Additional material

Additional File 1

Table 1 Prostate cancer specimens and protein expression. *Prostate cancer specimens and expression of several hedgehog signaling proteins are summarized in this table (A). A total of 55 specimens were used in this study. The Gleason scores and protein expression of Shh, PTCH1 and Su(Fu) are shown (B).*

Click here for file

[http://www.biomedcentral.com/content/supplementary/1476-4598-3-29-S1.doc]

Acknowledgements

we thank Dr. Huiping Guo for technical support of real-time PCR. J.X. was supported by grants from a NIH R01 grant, a DOD grant and the Sealy Foundation for biomedical Sciences.

References

1. Ingham PW: **Transducing Hedgehog: the story so far.** *Embo J* 1998, **17:**3505-3511.
2. Taipale J, Beachy PA: **The Hedgehog and Wnt signalling pathways in cancer.** *Nature* 2001, **411:**349-354.
3. Johnson RL, Rothman AL, Xie J, Goodrich LV, Bare JW, Bonifas JM, Quinn AG, Myers RM, Cox DR, Epstein E. H., Jr., Scott MP: **Human homolog of patched, a candidate gene for the basal cell nevus syndrome.** *Science* 1996, **272:**1668-1671.
4. Hahn H, Wicking C, Zaphiropoulous PG, Gailani MR, Shanley S, Chidambaram A, Vorechovsky I, Holmberg E, Unden AB, Gillies S, Negus K, Smyth I, Pressman C, Leffell DJ, Gerrard B, Goldstein AM, Dean M, Toftgard R, Chenevix-Trench G, Wainwright B, Bale AE: **Mutations of the human homolog of Drosophila patched in the nevoid basal cell carcinoma syndrome.** *Cell* 1996, **85:**841-851.
5. Xie J, Murone M, Luoh SM, Ryan A, Gu Q, Zhang C, Bonifas JM, Lam CW, Hynes M, Goddard A, Rosenthal A, Epstein E. H., Jr., de Sauvage FJ: **Activating Smoothened mutations in sporadic basal-cell carcinoma.** *Nature* 1998, **391:**90-92.
6. Taylor MD, Liu L, Raffel C, Hui CC, Mainprize TG, Zhang X, Agatep R, Chiappa S, Gao L, Lowrance A, Hao A, Goldstein AM, Stavrou T, Scherer SW, Dura WT, Wainwright B, Squire JA, Rutka JT, Hogg D: **Mutations in SUFU predispose to medulloblastoma.** *Nat Genet* 2002, **31:**306-310.
7. Berman DM, Karhadkar SS, Hallahan AR, Pritchard JI, Eberhart CG, Watkins DN, Chen JK, Cooper MK, Taipale J, Olson JM, Beachy PA: **Medulloblastoma growth inhibition by hedgehog pathway blockade.** *Science* 2002, **297:**1559-1561.
8. Watkins DN, Berman DM, Burkholder SG, Wang B, Beachy PA, Baylin SB: **Hedgehog signalling within airway epithelial progenitors and in small- cell lung cancer.** *Nature* 2003, **422:**313-317.
9. Berman DM, Karhadkar SS, Maitra A, Montes De Oca R, Gerstenblith MR, Briggs K, Parker AR, Shimada Y, Eshleman JR, Watkins DN, Beachy PA: **Widespread requirement for Hedgehog ligand stimulation in growth of digestive tract tumours.** *Nature* 2003, **425:**846-851.
10. Thayer SP, Di Magliano MP, Heiser PW, Nielsen CM, Roberts DJ, Lauwers GY, Qi YP, Gysin S, Fernandez-Del Castillo C, Yajnik V, Antoniu B, McMahon M, Warshaw AL, Hebrok M: **Hedgehog is an early and late mediator of pancreatic cancer tumorigenesis.** *Nature* 2003, **425:**851-856.
11. Berman DM, Desai N, Wang X, Karhadkar SS, Reynon M, Abate-Shen C, et al.: **Roles for Hedgehog signaling in androgen production and prostate ductal morphogenesis.** *Dev Biol* 2004, **267:**: 387-398.

12. Podlasek CA, Barnett DH, Clemens JQ, Bak PM, Bushman W: **Prostate development requires Sonic hedgehog expressed by the urogenital sinus epithelium.** *Dev Biol* 1999, **209:**28-39.
13. Wang BE, Shou J, Ross S, Koeppen H, De Sauvage FJ, Gao WQ: **Inhibition of epithelial ductal branching in the prostate by sonic hedgehog is indirectly mediated by stromal cells.** *J Biol Chem* 2003, **278:**18506-18513.
14. Freestone SH, Marker P, Grace OC, Tomlinson DC, Cunha GR, Harnden P and Thomson AA.: **Sonic hedgehog regulates prostatic growth and epithelial differentiation.** *Dev Biol* 2003, **264:**: 352-362.
15. Latini JM, Rieger-Christ KM, Wang DS, Silverman ML, Libertino JA, Summerhayes IC: **Loss of heterozygosity and microsatellite instability at chromosomal sites 1Q and 10Q in morphologically distinct regions of late stage prostate lesions.** *J Urol* 2001, **166:**1931-1936.
16. Leube B, Drechsler M, Muhlmann K, Schafer R, Schulz WA, Santourlidis S, Anastasiadis A, Ackermann R, Visakorpi T, Muller W, Royer-Pokora B: **Refined mapping of allele loss at chromosome 10q23-26 in prostate cancer.** *Prostate* 2002, **50:**135-144.
17. Ding Q, Fukami S, Meng X, Nishizaki Y, Zhang X, Sasaki H, et al.: **Mouse suppressor of fused is a negative regulator of sonic hedgehog signaling and alters the subcellular distribution of Gli1.** *Curr Biol* 1999, **9:**1119-1122.
18. Kogerman P, Grimm T, Kogerman L, Krause D, Unden AB, Sandstedt B, et al.: **Mammalian suppressor-of-fused modulates nuclear-cytoplasmic shuttling of Gli-1.** *Nat Cell Biol* 1999, **1:**312-319.
19. Stone DM, Murone M, Luoh S, Ye W, Armanini MP, Gurney A, Phillips H, Brush J, Goddard A, de Sauvage FJ, Rosenthal A: **Characterization of the human suppressor of fused, a negative regulator of the zinc-finger transcription factor Gli.** *J Cell Sci* 1999, **112:**4437-4448.
20. Meng X, Poon R, Zhang X, Cheah A, Ding Q, Hui CC, Alman B: **Suppressor of fused negatively regulates beta-catenin signaling.** *J Biol Chem* 2001, **276:**40113-40119.
21. Athar M, Li CX, Chi S, Tang X, Zhang X, Kim AL, Tyring SK, Kopelovich L, Epstein EH Jr, Blickers DR, Xie J: **Inhibition of smoothened signaling prevents ultraviolet B-induced basal cell carcinomas through induction of fas expression and apoptosis.** *Cancer Res* 2004, **64:**7545-7552.
22. Xie J, Aszterbaum M, Zhang X, Bonifas JM, Zachary C, Epstein E, McCormick F: **A role of PDGFRalpha in basal cell carcinoma proliferation.** *Proc Natl Acad Sci U S A* 2001, **98:**9255-9259.
23. Xie J, Johnson RL, Zhang X, Bare JW, Waldman FM, Cogen PH, Menon AG, Warren RS, Chen LC, Scott MP, Epstein E. H., Jr.: **Mutations of the PATCHED gene in several types of sporadic extracutaneous tumors.** *Cancer Res* 1997, **57:**2369-2372.
24. Sanchez P, Hernandez AM, Stecca B, Kahler AJ, DeGueme AM, Barrett A, et al.: **Inhibition of prostate cancer proliferation by interference with SONIC HEDGEHOG-GLI1 signaling.** *Proc Natl Acad Sci U S A* 2004, **101:**12561-12566.
25. Karhadkar SS, Steven Bova G, Abdallah N, Dhara S, Gardner D, Maitra A, et al.: **Hedgehog signalling in prostate regeneration, neoplasia and metastasis.** *Nature* 2004, **431:**707-712.
26. Fan L, Pepicelli CV, Dibble CC, Catbagan W, Zarycki JL, Laciak R, et al.: **Hedgehog signaling promotes prostate xenograft tumor growth.** *Endocrinology* 2004, **145:**3961-3970.
27. Meng X, Poon R, Zhang X, Cheah A, Ding Q, Hui CC and Alman B.: **Suppressor of fused negatively regulates beta-catenin signaling.** *J Biol Chem* 2001, **276:**40113-40119.
28. Taylor MD, Zhang X, Liu L, Hui CC, Mainprize TG, Scherer SW, et al.: **Failure of a medulloblastoma-derived mutant of SUFU to suppress WNT signaling.** *Oncogene* 2004, **23:**4577-4583.
29. Li C, Chi S, He N, Zhang X, Guicherit O, Wagner R, Tyring S, Xie J: **IFNalpha induces Fas expression and apoptosis in hedgehog pathway activated BCC cells through inhibiting Ras-Erk signaling.** *Oncogene* 2004, **23:**1608-1617.

Carcinogenesis vol.26 no.10 pp.1698–1705, 2005
doi:10.1093/carcin/bgi130
Advance Access publication May 19, 2005

Frequent activation of the hedgehog pathway in advanced gastric adenocarcinomas

Xiaoli Ma[1,†], Kai Chen[2,†], Shuhong Huang[1,†], Xiaoli Zhang[2], Patrick A.Adegboyega[3], B.Mark Evers[4], Hongwei Zhang[1] and Jingwu Xie[2,*]

[1]Institute of Developmental Biology, School of Life Sciences, Shandong University, Jinan, PR China, [2]Department of Pharmacology, [3]Department of Pathology and [4]Department of Surgery, Sealy Center for Cancer Cell Biology, University of Texas Medical Branch, Galveston, TX 77555-1048, USA

[*]To whom correspondence should be addressed. Tel: +1 409 747 1845; Fax: +1 409 747 1938;
Email: jinxie@utmb.edu or zhw@sdu.edu.cn

The hedgehog pathway plays a critical role in the development of the foregut. Recent studies indicate that the hedgehog pathway activation occurs in the stomach and other gastrointestinal cancers. However, the association of hedgehog pathway activation with tumor stage, differentiation and tumor subtype is not well documented. Here, we report our findings that the elevated expression of hedgehog target genes human patched gene 1 (PTCH1) or Gli1 occurs in 63 of the 99 primary gastric cancers. Activation of the hedgehog pathway is associated with poorly differentiated and more aggressive tumors. The sonic hedgehog (Shh) transcript is localized to the cancer tissue, whereas expression of Gli1 and PTCH1 is observed both in the cancer and in the surrounding stroma. Treatment of gastric cancer cells with KAAD-cyclopamine, a hedgehog signaling inhibitor, decreases expression of Gli1 and PTCH1, resulting in cell growth inhibition and apoptosis. Overexpression of Gli1 under the control of the cytomegalovirus (CMV) promoter renders these cells resistant to cyclopamine-induced apoptosis. Thus, our analysis of *in vivo* tissues indicates that the hedgehog pathway is frequently activated in advanced gastric adenocarcinomas; our *in vitro* studies suggest that hedgehog signaling contributes to gastric cancer cell growth. These data predict that targeted inhibition of the hedgehog pathway may be effective in the prevention and treatment of advanced gastric adenocarcinomas.

Introduction

The hedgehog pathway plays a critical role in embryonic development, tissue polarity and carcinogenesis (1,2). Secreted hedgehog molecules bind to the receptor patched (PTC–PTCH1, PTCH2), thereby alleviating PTC-mediated suppression of smoothened (SMO), a putative seven-transmembrane protein. SMO signaling triggers a cascade of intracellular events, leading to the activation of the pathway through GLI-dependent transcription (2). Activation of hedgehog signaling, through loss-of-function mutations of PTCH1 or activated mutations of SMO, occurs frequently in human basal cell carcinomas (BCCs) and medulloblastomas (3–7). More recently, abnormal activation of the sonic hedgehog pathway has been reported in subsets of small cell lung cancer, pancreatic cancer, prostate cancer and gastrointestinal (GI) cancers (8–14).

Gastric cancer is the second most common cancer worldwide in terms of incidence and mortality (15). Patients with gastric cancer usually present at late stages and have a poor prognosis. Thus, identification of specific drug targets in the tumor is an essential step to reduce the mortality. A previous study indicated that activation of the hedgehog pathway occurred in all nine primary gastric cancers (10). To determine if hedgehog signaling activation can be utilized for the diagnosis and treatment of gastric cancer, we performed a comprehensive study to assess the hedgehog pathway activation in 99 primary gastric cancers using *in situ* hybridization, real-time PCR and immunohistochemistry.

Through the assessment of sonic hedgehog and its target genes Gli1 and PTCH1, we find that activation of the hedgehog pathway varies among different subtypes of gastric cancer. Tubular and papillary adenocarcinomas, but not signet-ring cell carcinomas, frequently harbor activated hedgehog signaling. Protein expression of the hedgehog and its target genes is not only detected in the tumor, but also in the stroma. We further demonstrate that targeted inhibition of the hedgehog pathway slows cell growth and induces apoptosis in gastric cancer cells. Thus, our studies indicate that activation of the hedgehog pathway is an important event during the progression of gastric cancer. We predict that targeted inhibition of the hedgehog pathway may be an effective method for the treatment of patients with gastric cancer.

Materials and methods

Tumor samples

A total of 117 specimens of gastric tissues were used in our study (99 cancer specimens and 18 normal or inflamed gastric tissues). From the Surgery Department at the Shan Dong Qi Lu Hospital, Jinan, China, or from the UTMB Surgical Pathology, 54 specimens were received as discarded materials with the approval from the Institutional Review Board (IRB). In addition, we purchased a tissue microarray, which contains 63 specimens of gastric cancer, from Chaoying Biotechnology Co., Ltd (Xi'an, China). Pathological reports, H and E staining of each specimen were reviewed to determine the nature of the disease and the tumor histology. In addition, immunohistochemistry with keratin antibodies was used to confirm the tumor pathology. The randomly sorted samples with masked identity were evaluated by at least two independent certified pathologists. Gastric cancers were divided into three major subtypes according to the WHO guideline (16): tubular adenocarcinoma, papillary adenocarcinoma and signet-ring cell carcinomas. This study also includes specimens for normal stomach tissues ($n = 11$), gastritis ($n = 4$) and other stomach tissues ($n = 3$) (see Supplementary Table 1A for more information).

In situ hybridization

Gli1 (X07384) was cloned into pBluescript M13+KS, the direction of insert is *Hind*III-5′ and *Xba*I-3′. The plasmid was digested with *Nru*I to generate the

Abbreviations: BCC, basal cell carcinoma; CMV, cytomegalovirus; PTC, patched; PTCH1, human patched gene 1; Shh, sonic hedgehog; SMO, smoothened; Su(Fu), suppressor of fused.

[†]These authors contributed equally to this work.

sense fragment (412 bp) and with *Nde*I to generate the antisense fragment (682 bp). PTCH1 (U59464) (cloned into *Xba*I5′ and *Cla*I3′ of pRK5) was digested with *Dra*III to generate a small cDNA fragment (590 bp). Gli3 (M57609) was initially cloned into *Sst*I (5′) and *Sal*I (3′) of pBluescript-SK. *Sna*BI was used to generate the sense fragment (552 bp) and *Psh*AI to generate the antisense fragment (770 bp). Sense and antisense probes were obtained by T3 and T7 *in vitro* transcription using a DIG RNA labeling kit from Roche (Mannheim, Germany). Tissue sections (6 μm thick) were mounted onto poly-L-lysine slides (19). Following deparaffinization, the tissue sections were rehydrated in a series of dilutions of ethanol. To enhance the signal and facilitate probe penetration, sections were immersed in 0.3% Triton X-100 solution for 15 min at room temperature and in proteinase K (20 μg/ml) solution for 20 min at 37°C, respectively. The sections were then incubated with 4% (v/v) paraformaldehyde/phosphate-buffered saline (PBS) for 5 min at 4°C. After washing with PBS and 0.1 M triethanolamine, the slides were incubated with prehybridization solution (50% formamide, 50% 4× SSC) for 2 h at 37°C. The probe was added to each tissue section at a concentration of 1 μg/ml and hybridized overnight at 42°C. After high stringency washing (2× SSC twice, 1× standard saline citrate twice and 0.5× SSC twice at 37°C) the sections were incubated with an alkaline phosphatase-conjugated sheep anti-digoxigenin antibody, which catalyzed a color reaction with the NBT/BCIP (Nitro-Blue-Tetrazolium/5-bromo-4-chloro-3-indolyl phosphate) substrate (Roche, Mannheim, Germany). Blue indicated strong hybridization. As negative controls, sense probes were used in all hybridizations and no positive signal was observed.

RNA isolation and quantitative PCR

Total RNA of the cells was extracted using an RNA extraction kit from Promega according to the manufacturer's instruction (Promega, Madison, WI). For this analysis, we selected only tumors in which 70% of the tissue mass was actually tumor tissue. For quantitative PCR analyses, we detected transcripts of sonic hedgehog, Gli1 and PTCH1 using the Applied Biosystems' assays-by-demand assay mixtures (the sequences for human Gli1, HIP and PTCH1 have been patented by Applied Biosystems, Foster City, CA) and pre-developed 18S rRNA (VIC™-dye labeled probe) TaqMan® assay reagent (P/N 4319413E) as an internal control. The primers were designed to span exon–exon junctions so as not to detect genomic DNA, and the primers and probe sequences were searched against the Celera database to confirm specificity. To obtain the relative quantitation of gene expression, a validation experiment was performed to test the efficiency of the target amplification and the efficiency of the reference amplification. All absolute values of the slope of log input amount versus ΔC_T were <0.1. Separate tubes (single-plex) one-step RT–PCR was performed with 20 ng RNA for both target genes and the endogenous control using TaqMan one-step RT–PCR master mix reagent kit (P/N 4309169). The cycling parameters for one-step RT–PCR were reverse transcription at 48°C for 30 min, AmpliTaq activation at 95°C for 10 min, denaturation at 95°C for 15 s and annealing/extension at 60°C for 1 min (repeat 40 times) on ABI7000. Triplicate C_T values were analyzed in Microsoft Excel using the comparative $C_T(\Delta\Delta C_T)$ method as described by the manufacturer (Applied Biosystems, Foster City, CA). The amount of target ($2^{-\Delta\Delta CT}$) was obtained by normalization to an endogenous reference (18S RNA) and relative to a calibrator.

Immunohistochemistry

Representative formalin fixed and paraffin embedded tissue sections (6 μm thickness) were used for immunohistochemistry with specific antibodies to human Shh and PTCH1 (Cat. no. 9024 for Shh and Cat. no. 6149 for PTCH1, Santa Cruz Biotechnology Inc., Santa Cruz, CA). First, tissue sections were deparaffinized, followed by rehydration with decreased concentrations of ethanol, and immersed in 3% H_2O_2 (in distilled H_2O) for 10 min (to inhibit endogenous peroxidase activity). Following antigen retrieval in citrate buffer (pH 6.0), the tissue sections were incubated with normal goat serum to block nonspecific antibody binding (20 min at room temperature). The sections were then incubated with primary antibodies (at 1:200 dilution) at 37°C in humid chambers for 2 h. After washing with PBS three times, the sections were incubated with the biotinylated secondary antibody (goat anti-rabbit IgG or monkey anti-goat IgG) and streptavidin conjugated to horseradish peroxidase for 20 min at 37°C, followed by PBS wash. The sections were incubated with the DAB substrate for less than 30 min. Haematoxylin was used for counterstaining. Negative controls were performed in all cases by omitting the first antibodies. All primary antibodies have been previously tested for immunohistostaining (9,11,18).

Cell culture, MTT assay and TUNEL assay

Cell lines (AGS, SIIA and RKO) were cultured in F12 Medium with 10% FBS (AGS and SIIA) or DMEM with 10% FBS (RKO), respectively. Colorimetric MTT assay was performed according to our published protocol in the presence of 0.5% FBS (19). Cells were treated with 2 μM of Keto-*N*-aminoethylaminocaproyldihydrocinnamoyl-cyclopamine (KAAD-cyclopamine) for specific times (see Figure 6 for details). Ectopic expression of Gli1, under the control of the cytomegalovirus (CMV) promoter, in AGS cells was achieved by the transient transfection with LipofectAmine 2000 (20,21), and Gli1 was detected by immunofluorescent staining with the Myc tag antibody 9e10 (Sigma, St Louis, MO) (19). TUNEL assay was performed using a kit from Roche according to the manufacturer's instructions (19,21).

Statistical analysis

Student's *t*-test for two samples was performed for the difference between the tumor groups: $P < 0.05$ was considered statistically significant. For example (Table I), the difference between Stage I and Stage III tumors for expression of Shh and PTCH1 was statistically significant with a P value of 0.01923. Similarly, the difference between well-differentiated (WD) and poorly differentiated (PD) tumors for expression of Shh and PTCH1 was significantly

Table I. Summary of gastric specimens: clinical pathological data and the hedgehog pathway activation*

	Tumor number	Expression of Shh	Expression of PTCH1	Expression of Gli1
Overall	99	64/99 (∼65%)	63/99 (∼64%)	22/32 (∼69%)
Gender				
Male	77	50/77 (∼65%)	47/77 (∼61%)	15/25 (60%)
Female	22	14/22 (∼64%)	16/22 (∼73%)	7/8
Stage[a]				
I	22	12/22 (∼55%)	11/22 (50%)	5/6
II	22	17/22 (∼77%)	15/22 (∼68%)	4/6
III	41	30/41 (∼73%)	32/41 (∼78%)	11/16 (∼69%)
IV	5	5/5	5/5	2/2
WHO classification				
Adenocarcinomas	90	64/90 (∼71%)	63/90 (70%)	22/28 (79%)
Tubular	43	27/43 (∼63%)	25/43 (∼58%)	7/12 (∼58%)
Papillary	7	5/7	4/7	3/4
PD	40	32/40 (80%)	34/40 (85%)	11/11 (100%)
Signet-ring cell carcinomas	9	0/9	0/9	0/9
Differentiation[b]				
Well differentiated (WD)	18	7/18 (∼39%)	7/18 (∼39%)	1/4
Moderately differentiated (MD)	25	20/25 (80%)	18/25 (72%)	7/9
Poorly differentiated (PD)	40	32/40 (80%)	34/40 (85%)	11/11 (100%)

*Statistical analysis was performed using student's *t*-test for two samples: $P < 0.05$ was considered statistically significant (see Materials and methods for details).
[a]Signet-ring cell carcinomas were excluded from this analysis.
[b]Only tubular adenocarcinomas were used in this analysis.

different (P value = 0.006028). The P value comparing WD and moderately differentiated (MD) tumors for Shh and PTCH1 expression was 0.02993. Furthermore, the difference between tubular and PD tumors on Shh and PTCH1 expression was significant with a P value of 0.01059. There was no significant difference between MD and PD tumors in Shh and PTCH1 expression (P value = 1).

Results

Increased hedgehog target gene expression in gastric cancers

Hedgehog is a critical endodermal signal for the epithelial–mesodermal interactions during the development of the vertebrate gut. In the adult stomach, hedgehog signaling is either undetectable or its expression is restricted to the fundus (18). A previous report using nine primary gastric cancers identified hedgehog pathway activation in all tumors (10). To test whether hedgehog signaling activation can be used for diagnosis of gastric cancers, a comprehensive study is needed to examine the frequency of hedgehog signaling activation in a large number of primary gastric cancers. Toward that end, we examined expression of hedgehog target genes Gli1 and PTCH1 in 117 gastric specimens (99 cancer specimens and 18 non-cancerous specimens, see Supplementary Table 1A for more information). As the target genes of the hedgehog pathway, increased levels of PTCH1 and Gli1 transcripts indicates hedgehog signaling activation (1). We used three methods to assess hedgehog signaling activation in our collected tissues (n = 54): *in situ* hybridization, immunohistochemistry and real-time PCR analyses. Expression of sonic hedgehog and PTCH1 was also examined in the tissue array specimens (n = 63) by *in situ* hybridization and immunohistostaining (Supplementary Table 1A and B).

Using *in situ* hybridization, we detected PTCH1 expression in 63 of the 99 (~64%) tumor specimens, suggesting that activation of the hedgehog pathway is quite common in gastric cancer (Figure 1A and B and Supplementary Figure A). In contrast, all normal stomach tissues did not have a detectable level of PTCH1, indicating that the hedgehog pathway is not activated in these normal tissues (Figure 1C). Our data are consistent with a previous report that Shh signaling is restricted to the fundic stomach of humans and mice (18). The results of Gli1 expression were consistent with those of PTCH1 expression (see Figure 1E and F, Supplementary Figure B and Supplementary Table 1A). The frequency of hedgehog signaling activation appears to differ in different subtypes of gastric cancer (see Table I). In adenocarcinomas of gastric cancer, 63 of the 90 (70%) specimens demonstrated high levels of PTCH1 (or Gli1) transcripts (Figure 1 and Table I for details). However, signet-ring cell carcinomas (n = 9) had no detectable expression of these target genes, suggesting that activation of the hedgehog pathway may not be a frequent event in this subtype of gastric cancer (Table I). Thus, our results indicate that the hedgehog pathway is frequently activated in gastric cancer and the frequency of activation varies among different subtypes of tumors.

Further analysis of the data revealed an association of hedgehog signaling activation with poor differentiation in tubular adenocarcinomas. Only 7 out of 18 (~39%) well-differentiated adenocarcinomas had a high level of PTCH1 transcript, whereas 18 out of 25 (72%) moderately differentiated adenocarcinomas and 34 out of the 40 (85%) poorly differentiated adenocarcinomas expressed the target genes (see Table I). Thus, activation of hedgehog signaling appears to be inversely associated with tumor differentiation. As poor differentiation of the tumor is often associated with prognosis, our findings suggest that activation of the hedgehog pathway may serve as a valuable prognostic biomarker for gastric cancer. This hypothesis predicts that activation of the hedgehog pathway may be more common in advanced stages of gastric cancer. Indeed, 11 out of the 22 Stage I gastric adenocarcinomas (50%) had elevated levels of the target gene transcripts, 78% of Stage III tumors had detectable expression of the target genes (Table I).

To confirm the *in situ* hybridization data, we performed real-time PCR analyses in selected tumors, in which >70% of the tissue mass was actually tumor tissue, to detect the levels of Gli1 and PTCH1 expression. In the tumors with elevated Gli1 and PTCH1 transcripts, we found an approximate 5- to 20-fold increase in levels of Gli1 and PTCH1 expression compared with the matched normal tissues (Figure 2), indicating that the *in situ* hybridization results are in agreement with real-time PCR data. Furthermore, we detected the PTCH1 protein by immunohistochemistry (11). We found that PTCH1 protein was detected in primary gastric cancer, but not in the normal tissues (Figure 3). The data from the immunohistochemical analysis are consistent with the results from real-time PCR and *in situ* hybridization analyses. Taken together, these data indicate that the hedgehog pathway is frequently activated in advanced gastric adenocarcinomas.

Expression of sonic hedgehog in gastric cancer

It is reported that overexpression of sonic hedgehog may be responsible for the activation of the hedgehog pathway in pancreatic cancer, subsets of small cell lung cancer, prostate cancer and several primary gastric cancers (8–14). To test this possibility, we examined expression of sonic hedgehog in gastric specimens by *in situ* hybridization. Many cancers had a high level of sonic hedgehog transcript (Figure 4, Supplementary Figure C and Supplementary Table 1A). In most of the cases, elevated levels of Shh were consistent with elevated levels of PTCH1 and Gli1 expression (see Supplementary Table 1A and B). We found that elevated sonic hedgehog expression is associated with poor differentiation of the tumor and higher tumor grades (Table I). Also in agreement with lack of PTCH1 and Gli1 expression in signet-ring cell carcinomas, there was no detectable expression of sonic hedgehog in any of the signet-ring cell carcinomas analyzed (Table I). In contrast, sonic hedgehog expression was undetectable or very low in normal and inflamed gastric tissues (Figure 4). To confirm the *in situ* hybridization data, we detected the sonic hedgehog protein by immunohistochemistry (9,11). In agreement with the *in situ* hybridization data, we found that tumors with increased sonic hedgehog mRNA expression had high levels of the sonic hedgehog protein (Figure 5). The correlation of sonic hedgehog expression with Gli1 and PTCH1 transcripts indicates an important role of sonic hedgehog in the activation of the hedgehog pathway in gastric adenocarcinomas.

Hedgehog signaling and cellular functions of gastric cancers

If hedgehog pathway activation is required for gastric cancer development, gastric cancer cells should be susceptible to the treatment using the SMO antagonist, cyclopamine. All available gastric cancer cell lines have elevated hedgehog signaling (10), we chose a GI cancer cell line RKO as the negative control [RKO cells do not have elevated levels of Gli1 and

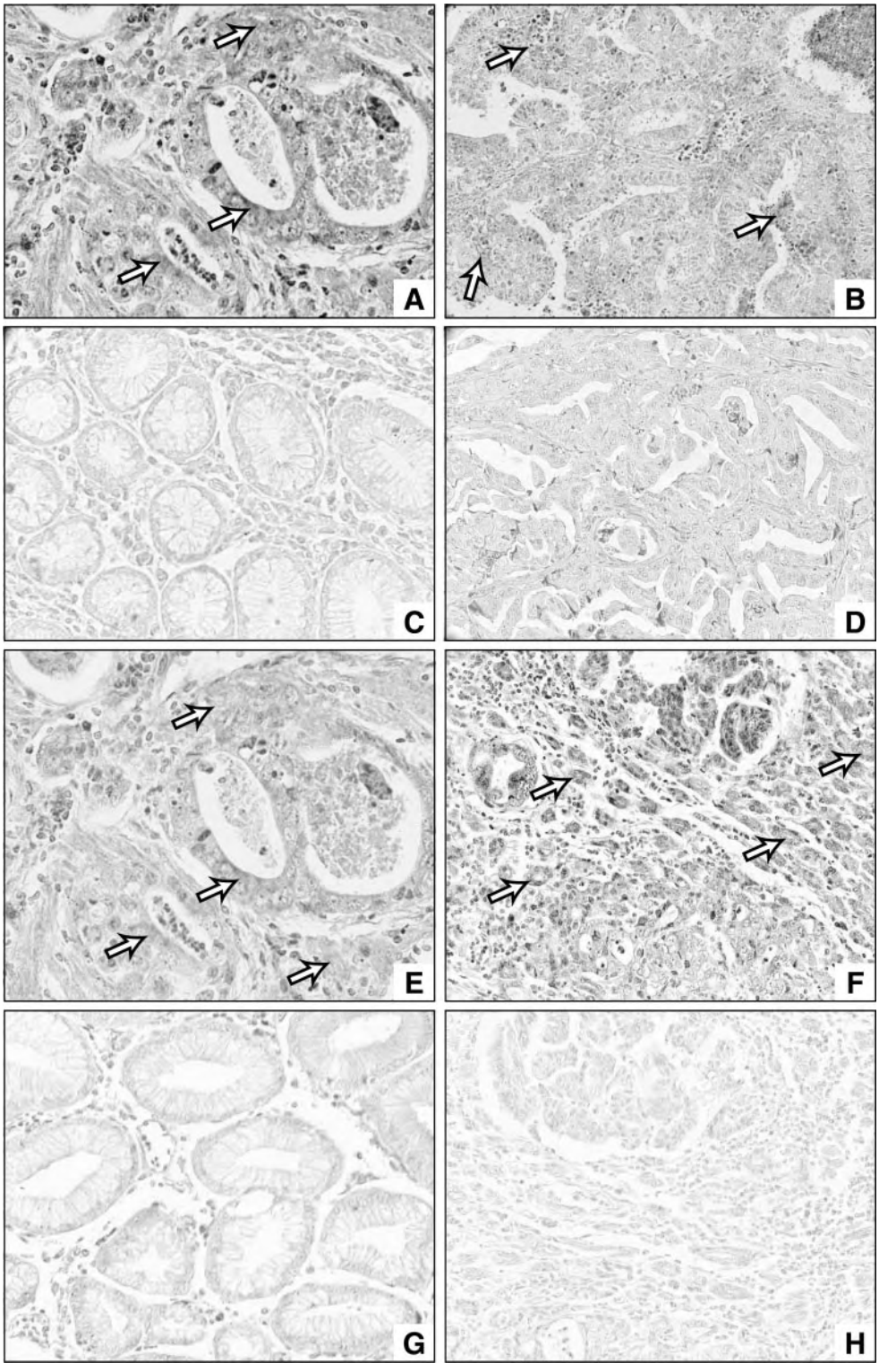

Fig. 1. Detection of Gli1 and PTCH1 expression in primary gastric cancers by *in situ* hybridization. *In situ* hybridization detection of PTCH1 expression (denoted by arrows) in gastric cancers (**A** and **B**) and normal gastric tissue (**C**). **D** is the sense probe control of **B**. Expression of Gli1 was similar to PTCH1 in gastric cancer (**E** and **F**) and normal gastric tissue (**G**) (denoted by arrows). **H** is the sense probe control of **F**. The pattern of Gli1 and PTCH1 expression is very similar in the same tumor (comparing **A** and **E**), further affirming that the hedgehog pathway is activated in the tumor. See online Supplementary material for a color version of this figure.

PTCH1, unpublished data and (10)]. In this experiment, we used two gastric cancer cell lines (AGS and SIIA) to test KAAD-cyclopamine sensitivity.The addition of KAAD-cyclopamine (2 μM) greatly decreased the levels of Gli1 and PTCH1 mRNA expression in both the cell lines (Figure 6A shows the data for Gli1 expression in SIIA and RKO cells), indicating inhibition of the hedgehog pathway by KAAD-cyclopamine. The closely related compound tomatidine,

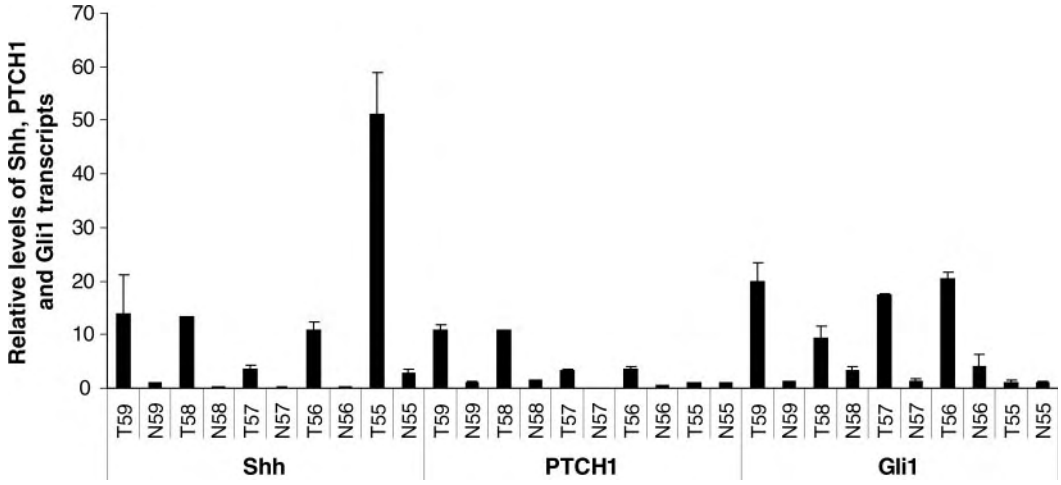

Fig. 2. Real-time PCR analysis of Shh, Gli1 and PTCH1 transcripts in primary gastric cancers. Total RNAs were extracted from the primary tumors in which 70% of the tissue mass was actually tumor tissue. The levels of Shh, Gli1 and PTCH1 were measured in our Real-time PCR Core Facility (see Materials and methods for details), and the experiment was repeated twice with similar results. The relative amount of target was obtained by normalization to an endogenous reference (18S RNA) and relative to a calibrator. T59 stands for tumor from patient no. 59 and N59 stands for the matched normal control from patient no. 59. The data from this analysis are consistent with those from *in situ* hybridization.

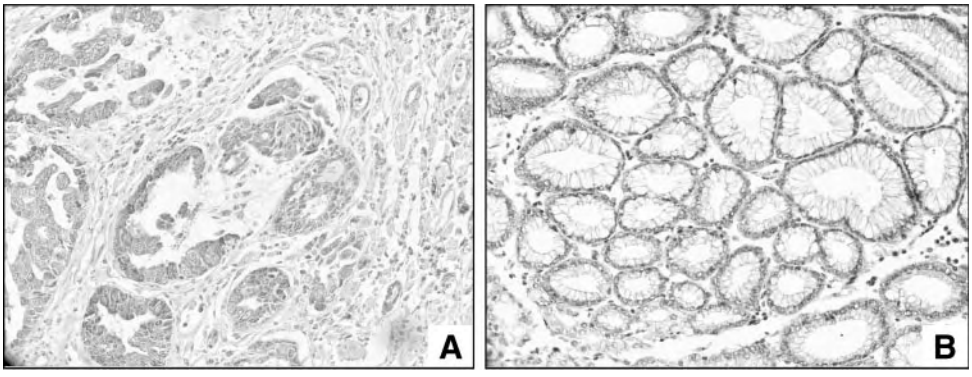

Fig. 3. Detection of PTCH1 protein in gastric tissues. Ptch1 protein was detected by immunohistostaining in gastric cancer (**A**) and normal tissue (**B**). See online Supplementary material for a color version of this figure.

which does not affect SMO signaling and thus served as a negative control, had little discernible effect on these target genes. As expected, we found that cell growth of SIIA and AGS (Figure 6B) cells was inhibited by KAAD-cyclopamine (2 μM). In addition, we detected apoptosis in AGS cells following the treatment with cyclopamine (Figure 6C). Tomatidine did not induce apoptosis in AGS cells (Figure 6C). Similar data were also observed in SIIA cells (data not shown). In contrast, RKO cells, which do not have active hedgehog signaling, were not affected by KAAD-cyclopamine treatment (Figure 6B), with no detectable apoptosis (Figure 6C). These data indicate that inhibition of the hedgehog pathway by KAAD-cyclopamine dramatically decreases cell growth, and induces apoptosis in gastric cancer cells.

Our model predicts that overexpression of Gli1 in AGS cells under the control of a strong promoter (such as the CMV promoter) would constitutively activate the hedgehog pathway, which could render these cancer cells resistant to cyclopamine treatment. Indeed, cyclopamine did not induce apoptosis in constitutive Gli1-expressing AGS cells, as indicated by lack of TUNEL staining in all Gli1 positive cells ($n = 500$) (Figure 6D). Thus, ectopic expression of Gli1 under the control of the CMV promoter prevents KAAD-cyclopamine-induced apoptosis in gastric cancer cells.

Taken together, our findings indicate that activation of the hedgehog pathway is quite common in advanced gastric adenocarcinomas, and this activation differs among different subtypes of gastric cancer. Elevated expression of Gli1 and PTCH1 is associated with decreased tumor differentiation and more advanced tumor stages in tubular adenocarcinomas. Inhibition of the hedgehog pathway in gastric cancer cell lines, however, decreases cell growth and induces apoptosis. Thus, our data indicate that activation of the hedgehog pathway may be an important event in the progression of gastric adenocarcinomas.

Discussion

Activation of the hedgehog pathway in gastric cancer

Hedgehog signaling pathway regulates cell proliferation, tissue polarity and cell differentiation during normal development. Abnormal signaling of this pathway has been reported in a variety of human cancers, including BCCs, medulloblastomas, small cell lung cancer, pancreatic cancer, prostate cancer and

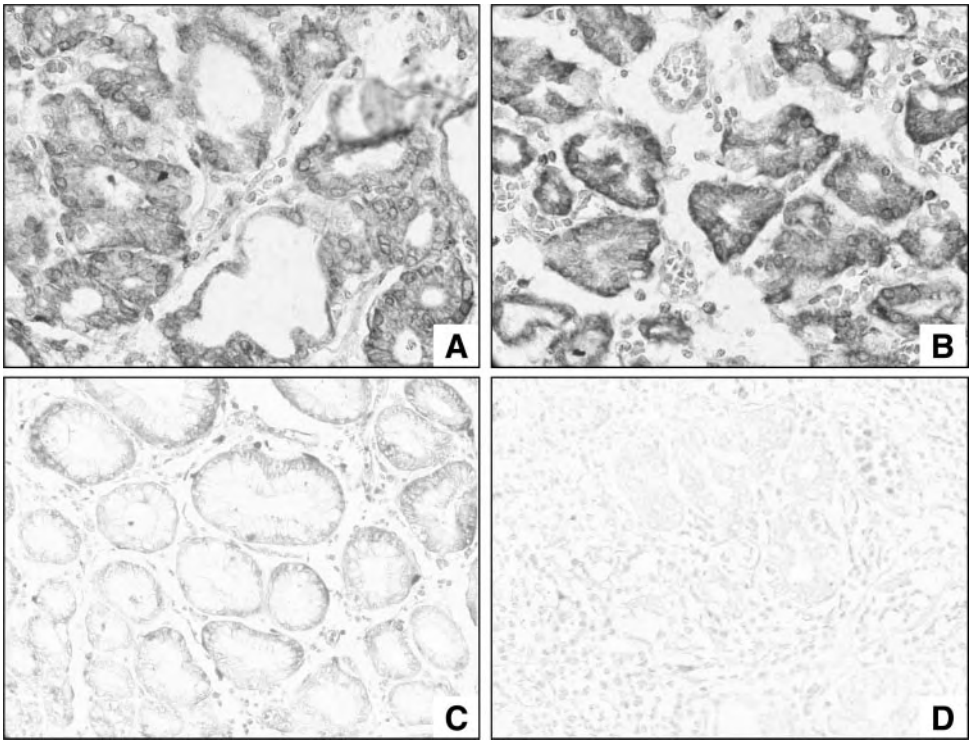

Fig. 4. Expression of Shh in primary gastric cancers. *In situ* hybridization was performed to detect Shh expression in gastric cancers (**A** and **B**) and normal gastric tissue (**C**). (**D**) The sense probe control for the sample shown in (**B**) and did not reveal any positive signals. See online Supplementary material for a color version of this figure.

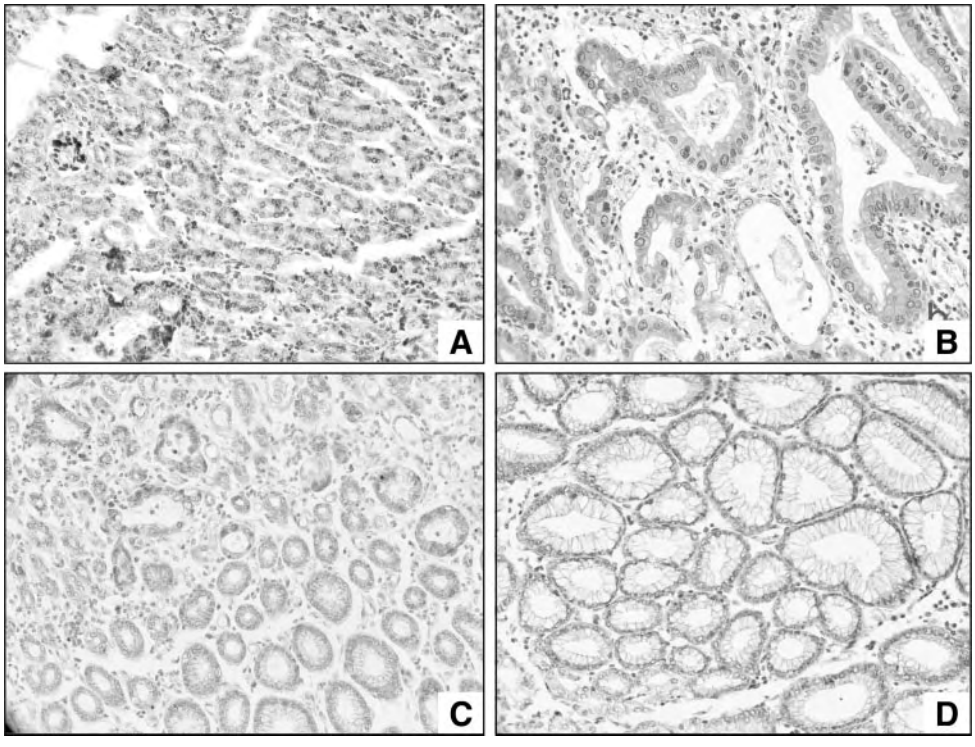

Fig. 5. Protein expression of Shh in primary gastric cancers. *In situ* hybridization was confirmed by immunohistostaining in gastric cancers (**A**–**C**) and normal gastric tissue (**D**). See online Supplementary material for a color version of this figure.

several primary gastric tumors (3–14). Our findings in this report indicate that activation of the hedgehog pathway occurs frequently in advanced gastric adenocarcinomas. We have detected high levels of hedgehog targets PTCH1 and Gli1 in $>60\%$ of gastric cancers. Further analyses of our data indicate an association of the hedgehog pathway activation with poor differentiation of gastric tumors. In a previous report, hedgehog signaling activation was detected in all nine primary

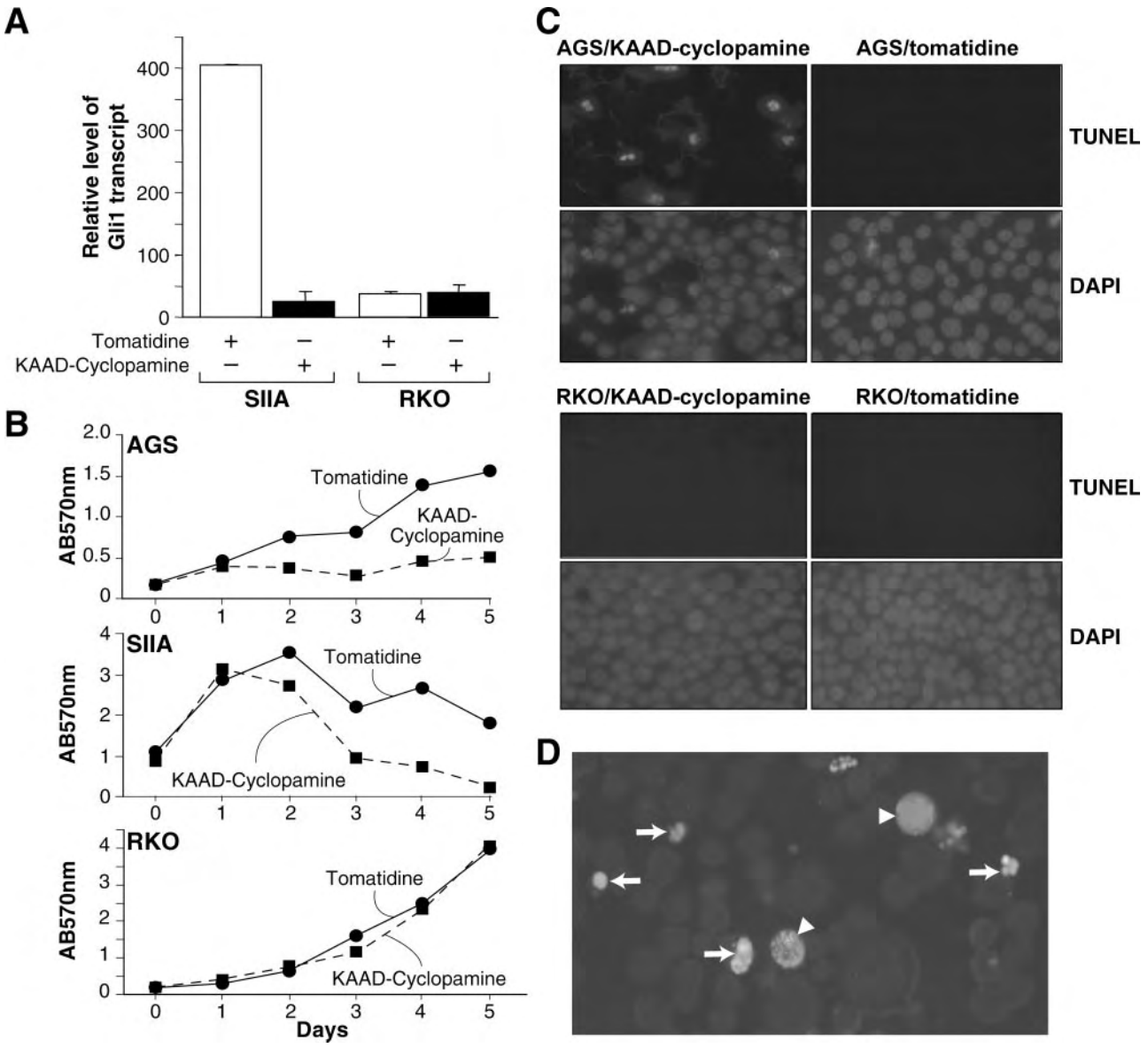

Fig. 6. Hedgehog signaling is required for growth of gastric cancer cells. In the presence of the SMO antagonist KAAD-cyclopamine (2 μM), Gli1 expression was decreased in SIIA cells (**A**). Unlike RKO cells, which do not have active hedgehog signaling, AGS and SIIA cells are sensitive to KAAD-cyclopamine treatment (2 μM) (**B**). TUNEL assay revealed apoptosis (indicated by arrows) in AGS cells but not in RKO cells (**C**). Following the expression of Gli1 under the control of the CMV promoter, AGS cells became resistant to KAAD-cyclopamine treatment (**D**). No apoptosis was detected in >500 Gli1 over-expressing cells (indicated by arrowheads), whereas 10–20% of Gli1 negative cells underwent apoptosis after the cyclopamine treatment (indicated by arrows). See online Supplementary material for a color version of this figure.

tumors using real-time PCR analysis (10). This discrepancy may be owing to specimen selection. As we have indicated in our study, hedgehog signaling activation is associated with poorly differentiated tumors (tubular adenocarcinoma subtype). Another factor may be the sample size. Since signet-ring carcinomas are not a common subtype of gastric cancer, a large number of tumor specimens may be necessary to verify the results in our study.

In all the tumors with elevated levels of Gli1 and PTCH1 we detected expression of Shh, thus suggesting that overexpression of Shh may be responsible for elevated expression of Gli1 and PTCH1 in gastric cancer. However, a high level of sonic hedgehog expression was not always accompanied by elevated Gli1 and PTCH1 expression in tumors (Table I and Supplementary Table 1A), suggesting additional regulatory mechanisms for the hedgehog pathway activation. We speculate that, in addition to the hedgehog overexpression, other genetic alterations are required to activate the hedgehog pathway in gastric cancers.

Therapeutic perspective of gastric cancer through targeted inhibition of the hedgehog pathway

Our studies using gastric cancer cells indicate that the SMO antagonist, cyclopamine, may be effective in the future treatment of gastric cancers. We further demonstrate that over-expression of Gli1 under the control of the CMV promoter prevents cyclopamine-mediated apoptosis, further supporting the specificity of cyclopamine. Our recent studies indicate that chronic oral administration of cyclopamine to Ptch1$^{+/-}$ mice did not affect the overall survival of the mice (21), which

provides a possibility of clinical trials using cyclopamine for gastric cancers. Thus, in the future, it may be possible to treat the subsets of gastric cancer in which the hedgehog pathway is activated with a specific SMO antagonist (e.g. cyclopamine).

Supplementary material

Supplementary material can be found at: http://carcin.oxfordjournals.org/

Acknowledgements

This research was supported by grants from the NIH (R01-CA94160), Department of Defense (DOD-PC030429), the Sealy Foundation for Biomedical Sciences and National Science Foundation of China (30228031). We thank Huiping Guo for technical support in real-time PCR analysis, Karen K.Martin, Brenda Rubio and David Gosky for helping with the manuscript.

Conflict of Interest Statement: None declared.

References

1. Pasca di Magliano,M. and Hebrok,M. (2003) Hedgehog signalling in cancer formation and maintenance. *Nat. Rev. Cancer*, **3**, 903–911.
2. Taipale,J. and Beachy,P.A. (2001) The Hedgehog and Wnt signalling pathways in cancer. *Nature*, **411**, 349–354.
3. Johnson,R.L., Rothman,A.L., Xie,J. *et al.* (1996) Human homolog of patched, a candidate gene for the basal cell nevus syndrome. *Science*, **272**, 1668–1671.
4. Hahn,H., Wicking,C., Zaphiropoulous,P.G. *et al.* (1996) Mutations of the human homolog of *Drosophila* patched in the nevoid basal cell carcinoma syndrome. *Cell*, **85**, 841–851.
5. Xie,J., Murone,M., Luoh,S.M. *et al.* (1998) Activating smoothened mutations in sporadic basal-cell carcinoma. *Nature*, **391**, 90–92.
6. Xie,J., Johnson,R.L., Zhang,X. *et al.* (1997) Mutations of the PATCHED gene in several types of sporadic extracutaneous tumors. *Cancer Res.*, **57**, 2369–2372.
7. Berman,D.M., Karhadkar,S.S., Hallahan,A.R. *et al.* (2002) Medulloblastoma growth inhibition by hedgehog pathway blockade. *Science*, **297**, 1559–1561.
8. Watkins,D.N., Berman,D.M., Burkholder,S.G., Wang,B., Beachy,P.A. and Baylin,S.B. (2003) Hedgehog signaling within airway epithelial progenitors and in small-cell lung cancer. *Nature*, **422**, 313–317.
9. Thayer,S.P., Di Magliano,M.P., Heiser,P.W. *et al.* (2003) Hedgehog is an early and late mediator of pancreatic cancer tumorigenesis. *Nature*, **425**, 851–856.
10. Berman,D.M., Karhadkar,S.S., Maitra,A. *et al.* (2003) Widespread requirement for Hedgehog ligand stimulation in growth of digestive tract tumours. *Nature*, **425**, 846–851.
11. Sheng,T., Li,C.-X., Zhang,X., Chi,S., He,N., Chen,K., McCormick,F., Gatalica,Z. and Xie,J. (2004) Activation of the hedgehog pathway in advanced prostate cancer. *Mol. Cancer*, **3**, 29.
12. Sanchez,P., Hernandez,A.M., Stecca,B. *et al.* (2004) Inhibition of prostate cancer proliferation by interference with SONIC HEDGEHOG-GLI1 signaling. *Proc. Natl Acad. Sci. USA*, **101**, 12561–12566.
13. Fan,L., Pepicelli,C.V., Dibble,C.C. *et al.* (2004) Hedgehog signaling promotes prostate xenograft tumor growth. *Endocrinology*, **145**, 3961–3970.
14. Karhadkar,S., Bova,G., Abdallah,N. *et al.* (2004) Hedgehog signaling in prostate regeneration, neoplasia and metastasis. *Nature*, **2431**(7009), 707–712.
15. Pisani,P., Parkin,D.M., Bray,F. and Ferlay,J. (1999) Estimates of the worldwide mortality from 25 cancers in 1990. *Int. J. Cancer*, **83**, 18–29.
16. Borchard,F. (1990) Classification of gastric carcinoma. *Hepatogastroenterology*, **37**, 223–232.
17. Unden,A.B., Zaphiropoulos,P.G., Bruce,K., Toftgard,R. and Stahle-Backdahl,M. (1997) Human patched (PTCH) mRNA is overexpressed consistently in tumor cells of both familial and sporadic basal cell carcinoma. *Cancer Res.*, **57**, 2336–2340.
18. van den Brink,G.R., Hardwick,J.C., Nielsen,C., Xu,C., ten Kate,F.J., Glickman,J., van Deventer,S.J., Roberts,D.J. and Peppelenbosch,M.P. (2002) Sonic hedgehog expression correlates with fundic gland differentiation in the adult gastrointestinal tract. *Gut*, **51**, 628–633.
19. Li,C., Chi,S., He,N., Zhang,X., Guicherit,O., Wagner,R., Tyring,S. and Xie,J. (2004) IFNalpha induces Fas expression and apoptosis in hedgehog pathway activated BCC cells through inhibiting Ras-Erk signaling. *Oncogene*, **23**, 1608–1617.
20. Xie,J., Aszterbaum,M., Zhang,X., Bonifas,J.M., Zachary,C., Epstein,E. and McCormick,F. (2001) A role of PDGFRalpha in basal cell carcinoma proliferation. *Proc. Natl Acad. Sci. USA*, **98**, 9255–9259.
21. Athar,M., Li,C.-X., Chi,S. *et al.* (2004) Inhibition of smoothened signaling prevents ultraviolet B-induced basal cell carcinomas through induction of fas expression and apoptosis. *Cancer Res.*, **60**, 7545–7552.

Received January 28, 2005; revised May 4, 2005; accepted May 13, 2005

Int. J. Cancer: **118,** 139–148 (2006)

Hedgehog signaling is activated in subsets of esophageal cancers

Xiaoli Ma[1], Tao Sheng[2], Yuanxin Zhang[1], Xiaoli Zhang[2], Jing He[2], Shuhong Huang[1], Kai Chen[2], Josh Sultz[2], Patrick A. Adegboyega[2], Hongwei Zhang[1]* and Jingwu Xie[2]*

[1]*Institute of Developmental Biology, School of Life Sciences, Shandong University, Jinan, China*
[2]*Sealy Center for Cancer Cell Biology, Departments of Pharmacology, Toxicology and Pathology, University of Texas Medical Branch, Galveston, TX, USA*

The hedgehog pathway plays a critical role in the development of the foregut. However, the role of the hedgehog pathway in primary esophageal cancers is not well studied. Here, we report that elevated expression of hedgehog target genes occurs in 14 of 22 primary esophageal cancers. The hedgehog signaling activation is not associated with tumor subtypes, stages, or differentiation. While the sonic hedgehog (Shh) transcript is localized to the tumor tissue, expression of *Gli1* and *PTCH1* is observed both in the tumor and in the stroma. We discovered that 4 esophageal squamous cell carcinomas, which overexpress Shh, have genomic amplification of the *Shh* gene. Treatment of esophageal cancer cells with smoothened antagonist, KAAD-cyclopamine, or the neutralizing antibodies of Shh reduces cell growth and induces apoptosis. Overexpression of Gli1 under the CMV promoter renders these cells resistant to the treatments. Thus, our results indicate that elevated expression of Shh and its target genes is quite common in esophageal cancers. Our data also indicate that downregulation of Gli1 expression may be an important mechanism by which KAAD-cyclopamine inhibits growth and induces apoptosis in esophageal cancer cells (supplementary material for this article can be found on the *International Journal of Cancer* website at http://www.interscience.wiley.com/jpages/0020-7136/suppmat/index.html).

Key words: sonic hedgehog; cyclopamine; smoothened; esophageal cancer; GI cancer

The hedgehog pathway plays a critical role in embryonic development, tissue polarity and carcinogenesis.[1] Secreted Hedgehog molecules bind to the receptor *patched* (PTC-PTCH1, PTCH2), thereby alleviating PTC-mediated suppression of *smoothened* (SMO), a putative 7-transmembrane protein. SMO signaling triggers a cascade of intracellular events, leading to activation of the pathway through GLI-dependent transcription.[2,3] Activation of Hedgehog signaling, through loss-of-function mutations of *PTCH1* or activated mutations of *SMO*, occurs frequently in human basal cell carcinomas (BCCs) and medulloblastomas.[4–9] More recently, abnormal activation of the hedgehog pathway is also reported in subsets of small cell lung cancer, pancreatic cancer, gastric cancers, prostate cancer and several esophageal cancer cell lines.[10–15]

Esophageal cancer is the 6th most frequent cause of cancer death worldwide.[16] In the United States, the incidence of esophageal adenocarcinoma has nearly quadrupled over the past few decades despite a decline in the overall incidence of cancers in esophagus. Most esophageal cancers remain clinically silent until late in the disease process. Thus, these cancers are often associated with later diagnoses, poorer prognoses, significant morbidities and high mortality rates. Although an early report indicates activation of the hedgehog pathway in several esophageal cancer cell lines, it is not clear if primary tumors of esophagus have activated hedgehog signaling.[12]

To examine the significance of hedgehog pathway activation in esophageal cancers, we have analyzed expression of sonic hedgehog (Shh) and its target genes in 22 primary esophageal tumors using *in situ* hybridization, real-time PCR and immunohistochemistry. Through the assessment of the hedgehog target genes, we find that activation of the hedgehog pathway occurs in 14 of 22 esophageal cancers. We discover genomic amplification of *Shh* in 4 squamous cell carcinomas with elevated Shh expression. These data indicate that activation of the hedgehog pathway can be used as a valuable biomarker for diagnosis and molecular classification of esophageal cancers. Our results further suggest that targeted inhibition of the hedgehog signaling by KAAD-cyclopamine or Shh neutralizing antibodies may be effective in chemoprevention and treatment of esophageal cancers.

Material and methods

Tumor sample

Specimens from 22 cases of esophageal cancers (tumors and the matched adjacent normal tissues) and 1 case of normal esophageal tissue were received as discarded materials from the Shandong Qi Lu Hospital, Jinan, China, or from University of Texas Medical Branch Surgical Pathology with approval from the institutional review board. Pathology reports and H&E staining of each specimen were reviewed to determine the nature of the disease and the tumor histology. Esophageal cancers were divided into 2 major subtypes according to the WHO guideline[17] as follows: adenocarcinoma (4 cases) and squamous cell carcinomas (18 cases).

In situ *hybridization*

Gli1 (X07384) was cloned into pBluescript M13 + KS using *Hind*III (5′) and *Xba*I (3′). The plasmid was digested with *Nru*I to generate the sense fragment (412 bp) and with *Nde*I to generate the antisense fragment (682 bp). PTCH1 (U59464; cloned into *Xba*I5′ and *Cla*I3′ of pRK5) was digested with *Dra*III to generate a small cDNA fragment (590 bp). Sense and antisense probes were obtained by T3 and T7 *in vitro* transcription using a kit from Roche (Mannheim, Germany). Tissue sections (6 μm thick) were mounted onto poly-L-lysine slides.[18] Following deparaffinization, tissue sections were rehydrated in a series of dilutions of ethanol. To enhance signal and facilitate probe penetration, sections were immersed in 0.3% Triton X-100 solution for 15 min at room temperature, followed by treatment with proteinase K (20 μg/ml) for 20 min at 37°C. The sections were then incubated with 4% (v/v) paraformaldehyde/PBS for 5 min at 4°C. After washing with PBS and 0.1M triethanolamine, the slides were incubated with prehybridization solution (50% formamide, 50% 4 × SSC) for 2 hr at 37°C. The probe was added to each tissue section at a concentration of 1 μg/ml and hybridized overnight at 42°C. After high-stringency washing (2 × SSC twice, 1 × standard saline citrate twice, 0.5 × SSC twice at 37°C), sections were incubated with an alkaline phosphatase-conjugated sheep antidigoxigenin antibody, which cata-

Grant sponsor: The National Institutes of Health; Grant number: R01-CA94160; Grant sponsor: The Department of Defense; Grant number: DOD-PC030429; Grant sponsor: The American Cancer Society; Grant sponsor: The Sealy Foundation for Biomedical Sciences; Grant sponsor: The National Science Foundation of China; Grant number: 30228031.
***Correspondence to:** Jingwu Xie, Sealy Center for Cancer Cell Biology, Departments of Pharmacology, Toxicology and Pathology, University of Texas Medical Branch, Galveston, TX 77555. Fax: +409-747-1938. E-mail: jinxie@utmb.edu or to Hongwei Zhang, Institute of Developmental Biology, School of Life Sciences, Shandong University, Jinan, China 250100. E-mail: zhu@sdu.edu.cn
[†]The first three authors contributed equally to this work.
Received 7 October 2004; Accepted after revision 8 April 2005
DOI 10.1002/ijc.21295
Published online 7 July 2005 in Wiley InterScience (www.interscience.wiley.com).

TABLE I – LIST OF ESOPHAGEAL CANCERS AVAILABLE FOR OUR STUDIES

Number	Age	Sex	Pathology diagnosis	Stage	Gli1/PTCH1	Shh
Control-1			Normal esophagus	Normal	−	−
EC-1	66	F	Squamous cell carcinoma (M)	II	+	+
EC-2	69	F	Squamous cell carcinoma (M)	I	−	−
EC-3	60	M	Squamous cell carcinoma (W)	II	+	+
EC-4	57	F	Squamous cell carcinoma (W)	III	−	−
EC-5	57	M	Squamous cell carcinoma (W)	II	+	+[1]
EC-6	65	M	Squamous cell carcinoma (W)	II	+	+
EC-7	68	M	Squamous cell carcinoma (W)	II	−	−
EC-8	56	F	Squamous cell carcinoma (M)	III	+	+[1]
EC-9	64	M	Squamous cell carcinoma (M)	II	−	−
EC-10	51	M	Squamous cell carcinoma (M)	II	+	+
EC-11	47	F	Squamous cell carcinoma (M)	II	−	−
EC-12	64	F	Squamous cell carcinoma (P)	II	+	+
EC-13	54	M	Squamous cell carcinoma (P)	III	+	+[1]
EC-14	38	F	Squamous cell carcinoma (P)	III	+	+[1]
EC-15	55	M	Squamous cell carcinoma (P)	II	−	−
EC-16	73	M	Squamous cell carcinoma (P)	II	+	+
EC-17	68	M	Squamous cell carcinoma (P)	II	−	−
EC-18	66	M	Squamous cell carcinoma (P)	II	+	+
EC-19	50	M	Adenocarcinomas of thoracic esophagus (M)	I	+	+
EC-20	52	F	Adenocarcinomas of gastroesophageal junction (M)	II	+	+
EC-21	52	M	Adenocarcinomas of lower esophagus (M)	IV	+	+
EC-22	55	M	Adenocarcinomas of lower esophagus (M)	II	+	+

Esophageal cancer specimens and summary of *Shh*, *PTCH1* and *Gli1* expression. These data were derived from *in situ* hybridization, Real-time PCR analyses and immunohistochemistry. Since our data from these 3 approaches were consistent with each other, a list of the data from each method was not necessary. –[1]*Shh* genomic DNA amplification was observed in these tumors (confirmed by real-time PCR and regular PCR). W, well-differentiated tumor; M, moderately differentiated tumor; P, poorly differentiated tumor; EC, esophageal cancer.

lyzed a color reaction with the NBT/BCIP (nitro-blue-tetrazolium/5-bromo-4-chloro-3-indolyl phosphate) substrate (Roche). Blue indicated strong hybridization. As negative controls, sense probes were used in all hybridization and no positive signals were observed.

RNA isolation, PCR and quantitative PCR

Total RNAs were extracted using an RNA extraction kit from Promega (Madison, WI) according to the manufacturer's instructions. The exon II of the *Shh* gene was amplified with the forward primer 5′-TAACGTGTCCGTCGGTGGG -3′ and the reverse primer 5′-TGCTTTCACCGAGCAGTGG-3′ using the following cycles: 96°C for 4 min, 25 cycles of 96°C for 30 sec, 57°C for 45 sec and 72°C for 45 sec, plus 72°C for 5 min (50 ng of total genomic DNA in 25 μl PCR cocktail). D10S222 was amplified using the same condition but with 27 cycles. For real-time PCR analyses, we detected the levels of Shh, Gli1 and PTCH1 transcripts using the Applied Biosystems' assays-by-demand assay mixtures (Applied Biosystems, Foster City, CA) and predeveloped 18S rRNA (VIC dye-labeled probe) TaqMan assay reagent (P/N 4319413E) as an internal control. The procedure was described previously.[13] Rnase P was used as the internal control for detecting genomic amplification of the *Shh* gene. The sequences for primers and probes are available upon request. The amount of target ($2^{-\Delta\Delta CT}$) was obtained by normalization to an endogenous reference (18sRNA or Rnase P) and relative to a calibrator.

Immunohistochemistry

Representative formalin-fixed and paraffin-embedded tissue sections (6 μm thickness) were used for immunohistochemistry with specific antibodies to human Shh and PTCH1 (catalog number 9024 for Shh and 6149 for PTCH1; Santa Cruz Biotechnology, Santa Cruz, CA). All primary antibodies have been previously tested for immunohistostaining.[11,13,19] Immunohistochemistry was carried out as previously reported.[13]

Cell culture, MTT assay, BrdU incorporation, flow cytometry and TUNEL assay

Cell lines (KYSE-180 and KYSE-270, purchased from German Collection of Microorganisms and Cell Cultures, Braunschweig, Germany; and RKO, purchased from American Type Culture Collection, Manassas, VA) were cultured in RPMI-1640 with 10% FBS (KYSE-180), F12/RPMI-1640 (1:1) with 2% FBS (KYSE-270), or DMEM with 10% FBS (RK0), respectively. Cells (0.5% FBS) were treated with KAAD-cyclopamine (at a final concentration of 2 or 5 μM) or Shh neutralizing antibodies (5E1 monoclonal antibody was purchased from the Hybridoma Bank, University of Iowa, and was used at the concentrations of 0.1 or 0.5 μg/ml). For colorimetric MTT assay, culture media (including KAAD-cyclopamine) were changed every 24 hr, and the assay was performed according to our published protocol in the presence of 0.5% FBS.[19] BrdU[20,21] and flow cytometry[20] was performed as previously reported. Ectopic expression of Gli1, under the control of the CMV promoter, in KYSE-180 and KYSE-270 cells was achieved by transient transfection with lipofectAmine 2000,[19,20] and Gli1 was detected by immunofluorescent staining with the Myc tag antibody 9e10 (Sigma, St. Louis, MO).[20] TUNEL assay was performed using a kit from Roche according to the manufacturer's instructions.[19,20]

Results

Expression of hedgehog target genes in esophageal cancers

Hedgehog is a critical endodermal signal for the epithelial-mesodermal interactions during development of the vertebrate gut. In adult esophagus, hedgehog signaling is undetectable.[22,23] To test if hedgehog signaling is activated in primary esophageal cancers, we examined expression of hedgehog target genes *Gli1* and *PTCH1* in 22 cases of esophageal specimens (see Table I for specimen information). Increased levels of PTCH1 and Gli1 transcripts indicate activation of the hedgehog pathway.[1]

We first detected Gli1 and PTCH1 transcripts using *in situ* hybridization. In agreement with published reports,[23] we found that the normal esophageal tissue did not have detectable levels of Gli1 and PTCH1, indicating that the hedgehog pathway is not normally activated in adult esophageal tissues (Fig. 1*a*). In contrast, we detected Gli1 and PTCH1 transcripts in 14 of 22 (∼ 64%) tumor specimens, suggesting that activation of the hedgehog pathway is a common event in esophageal cancers. We observed activation of the hedgehog pathway both in adenocarcinomas and in squamous cell carcinomas. In squamous cell carcinomas, 10 of 18 (∼ 56%) specimens had high levels of Gli1 and PTCH1 transcripts

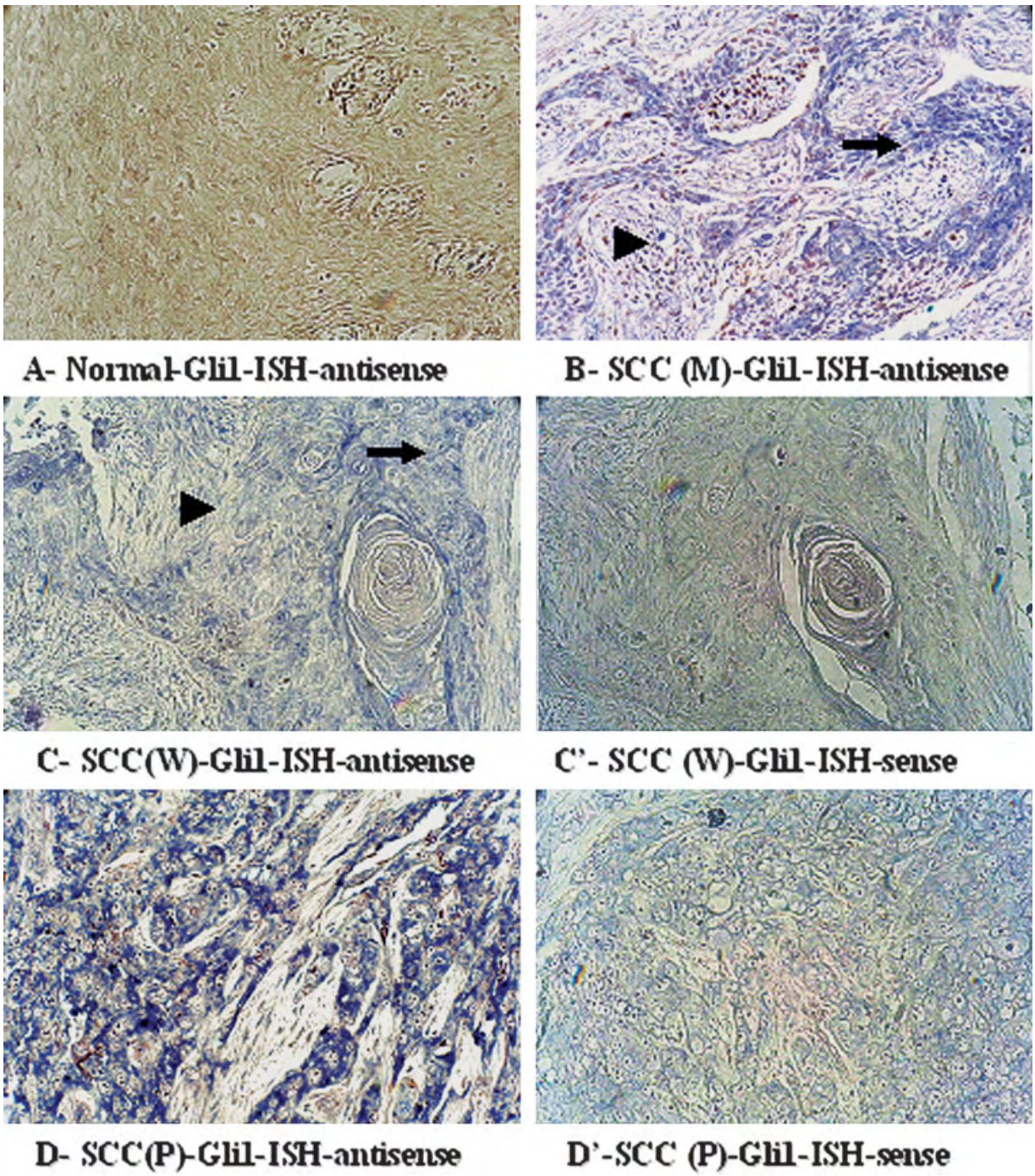

FIGURE 1 – Elevated expression of Gli1 and PTCH1 in primary esophageal tumors. Gli1 transcript (blue as positive) was detected by *in situ* hybridization in the normal control (*a*) and esophageal cancers (*b–d*). (*c′*) and (*c*) are from the same tumor, with (*c′*) being derived from the Gli1 sense probe. Similarly, (*d′*) is the sense probe control of (*d*). Expression of Gli1 transcript was strong in the tumor (indicated by arrows) and weak in the stroma (indicated by arrowheads). The pattern of PTCH1 transcript was similar to those of Gli1 (figures not shown), indicating activation of the hedgehog pathway in esophageal cancers. The data are summarized in Table I.

(see Table I for details). All 4 adenocarcinomas had detectable expression of Gli1 and PTCH1 (Table I). These data indicate that activation of the hedgehog pathway occurs frequently in esophageal cancers.

Further analyses did not reveal any association of hedgehog target gene expression with the tumor stage or differentiation. *In situ* hybridization data indicate that transcripts of Gli1 (Fig. 1*b* and *c*) and PTCH1 (not shown here) are detectable both in the tumor (indicated by arrows) and in the adjacent stroma tissue (indicated by arrowheads). These data suggest that hedgehog signaling may involve epithelium/stroma interactions during development of esophageal cancer.

To confirm the *in situ* hybridization data, we performed real-time PCR analyses to detect the levels of Gli1 and PTCH1 transcripts. We found that Gli1 and PTCH1 transcripts from esophageal tumors were several folds higher than those from

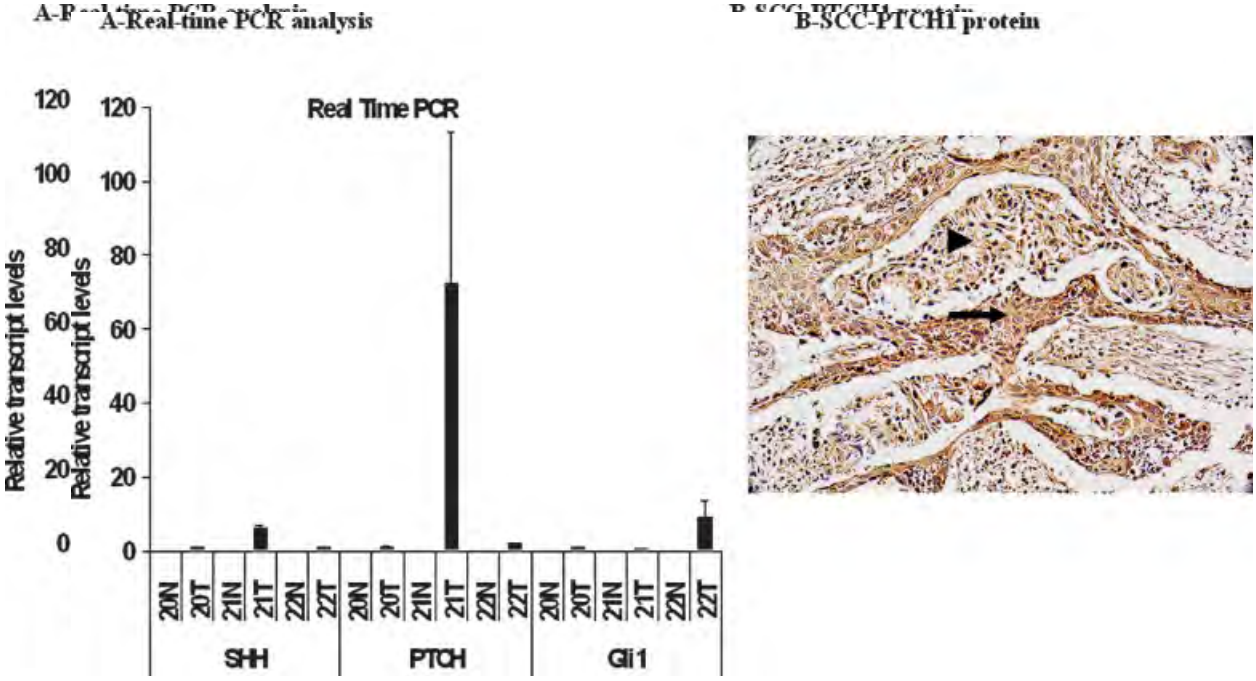

Figure 2 – Elevated PTCH1 transcript and PTCH1 protein in esophageal cancers. To confirm the *in situ* hybridization data, we performed real-time PCR analyses on Shh, PTCH1 and Gli1. Shh, PTCH1 and Gli1 transcripts (*a*) were elevated in 3 primary esophageal tumors. We found that real-time data are consistent with our *in situ* hybridization data. To confirm elevated PTCH1, we performed immunohistochemistry with PTCH1 antibodies.[15] (*b*) shows positive staining of PTCH1 protein (positive in brown) both in the tumor (indicated by an arrow) and in the stroma (indicated by an arrowhead). Our data from real-time PCR analyses are consistent with those derived from *in situ* hybridization, which

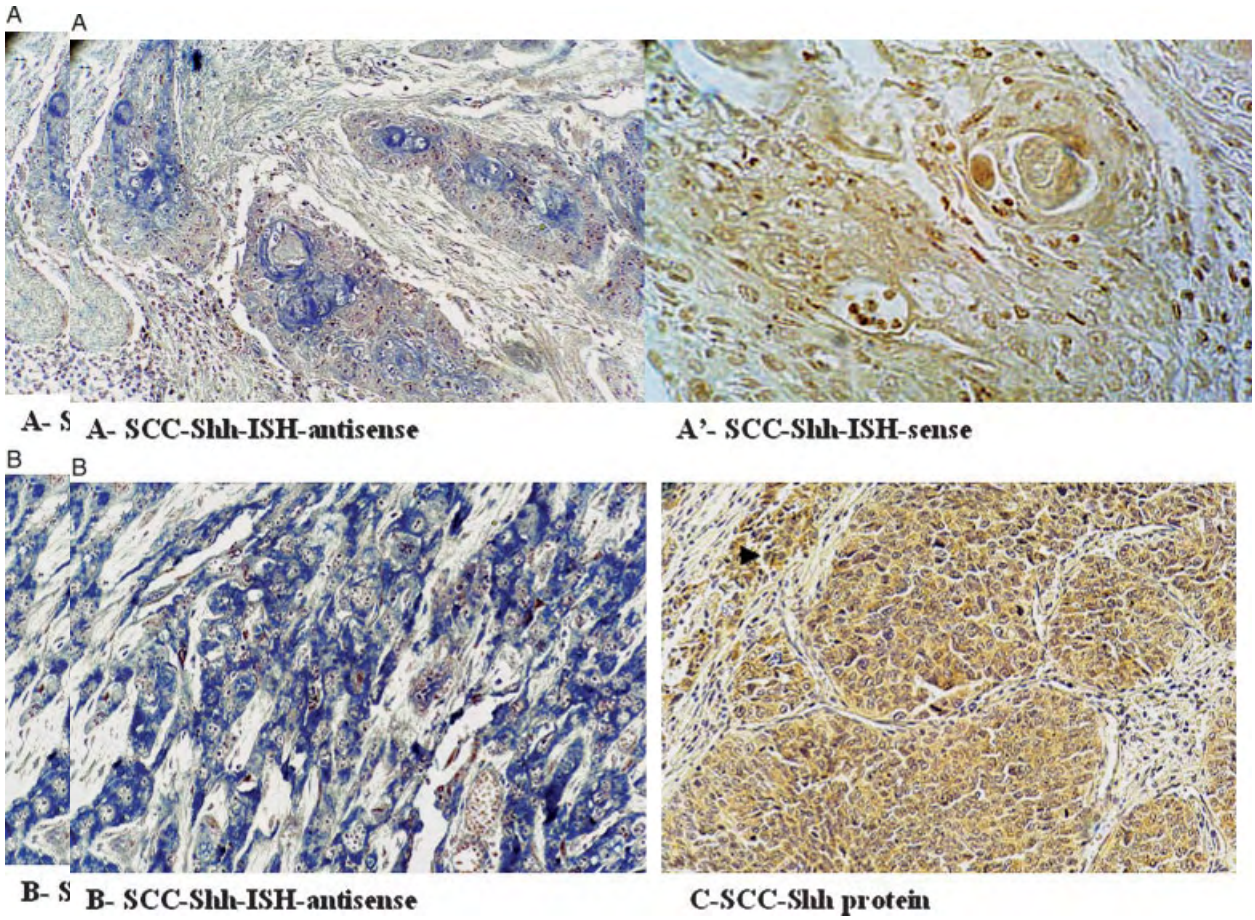

Figure 3 – Expression of Shh in esophageal tumors. *In situ* hybridization was performed to detect Shh transcript in cancerous (*a* and *b*) tissues (positive in blue), and the sense probe did not reveal any positive signals. (*a*′) is the sense probe control of (*a*). Note that no stroma localization of Shh transcript was seen. *In situ* hybridization was confirmed by immunohistostaining of tumor tissues (*c*; positive in brown). Arrowhead indicates stroma expression of Shh protein.

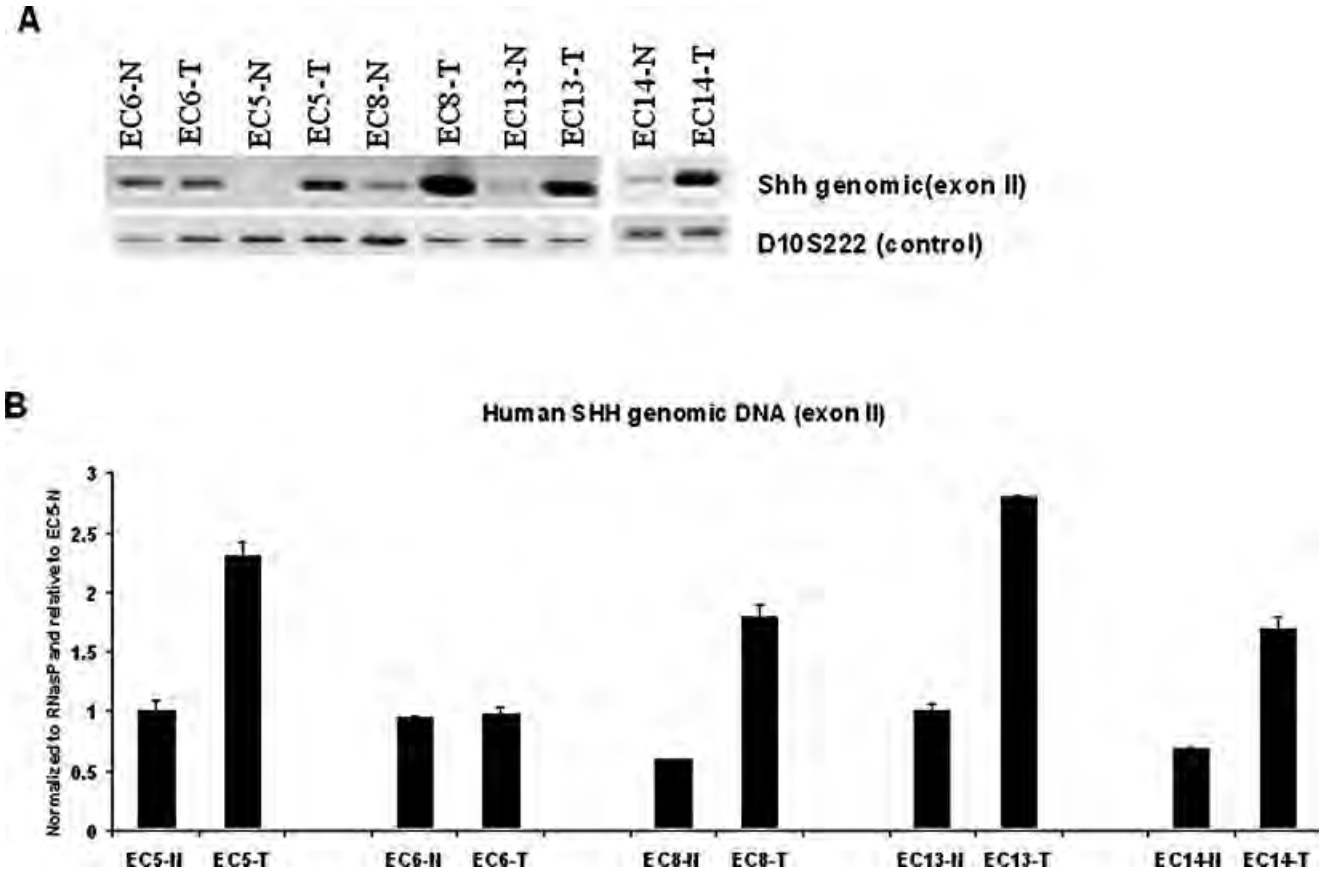

FIGURE 4 – Genomic amplification of the *Shh* exon II in esophageal squamous cell carcinomas. The exon II of *Shh* genomic DNA was initially amplified by regular PCR (see text for details; 25 cycles; nonquantitative PCR). Under the same PCR condition, the levels of PCR products from tumors as well as the matched normal tissues were shown in (*a*). The PCR was repeated 3 times with similar results, suggesting that the *Shh* gene may be amplified in some esophageal tumors. No elevated PCR products were seen from tumors without *Shh* overexpression. To confirm this observation, we performed real-time PCR (see text for details; quantitative analyses). The level of *Shh* genomic fragment was normalized using Rnase P. We noticed that 4 of the esophageal squamous cell carcinomas had 2- to 4-fold increase of *Shh* genomic DNAs over the matched normal tissues (*b*).

the matched normal tissues (Fig. 2*a* shows levels of Shh, PTCH1 and Gli1), confirming that expression of PTCH1 and Gli1 is elevated in the tumor tissues. Expression of PTCH1 in the tumor was further confirmed by immunohistochemistry (Fig. 2*b*).[11,13] All tissues with detectable PTCH1 protein had elevated PTCH1 transcript. In agreement with the *in situ* hybridization results, PTCH1 protein was detected both in the tumor (indicated by an arrow in Fig. 2*b*) and in the stroma (indicated by an arrowhead in Fig. 2*b*). Data derived from *in situ* hybridization, real-time PCR and immunohistochemistry analyses all indicate that activation of the hedgehog pathway is a common event in esophageal cancers.

Expression of Shh in esophageal cancers

It is reported that Shh overexpression may be responsible for activation of the hedgehog pathway in pancreatic cancer and several primary gastric cancers.[11,12] To test this possibility in esophageal cancer, we first examined expression of Shh in esophageal specimens by *in situ* hybridization. As expected, Shh expression was undetectable in the normal esophageal tissue (data not shown). In contrast, many of the primary tumors expressed a high level of Shh transcript (Figs. 2*a* and 3*a* and *b*, Table I). The Shh transcript was detectable specifically in the tumor, not in the stroma (Fig. 3*a* and *b*), suggesting that the tumor cells are the source for Shh expression. Shh expression was associated with detectable levels of Gli1 and PTCH1 transcripts, suggesting an important role of Shh in activating hedgehog pathway in esophageal cancers.

Furthermore, we detected Shh protein by immunohistochemistry using specific antibodies.[11] In agreement with the *in situ* hybridization data, we found that tumors with Shh transcript had higher levels of Shh protein (Fig. 3*c*). As a secreted molecule, sonic hedgehog protein was also detected in the stroma (indicated as arrowhead in Fig. 3*c*). We believe that the secreted sonic hedgehog protein may be responsible for elevated expression of Gli1 and PTCH1 transcripts in the tumor as well as in the stroma (Fig. 1). These results suggest a paracrine signaling mechanism of sonic hedgehog in esophageal cancers.

To identify the mechanisms by which the *Shh* gene was overexpressed in the tumor, we compared genomic DNA of *Shh* from the tumor with that from the adjacent normal tissue. We found that 4 of these tumors with Shh overexpression also had more genomic DNAs (Fig. 4). This observation was initially made using regular PCR amplification PCR (25 cycles, not quantitative) and was confirmed by real-time PCR (quantitative analyses). *Shh* genomic DNA from these tumors, on average, was 3 times more than that from the adjacent normal tissues (Fig. 4*b*). In contrast, we did not observe any elevated *Shh* genomic DNAs in adenocarcinomas of esophagus. These data are in agreement with previous findings that chromosome 7q is frequently overrepresented in esophageal squamous cell carcinomas,[24,25] suggesting that genomic amplifica-

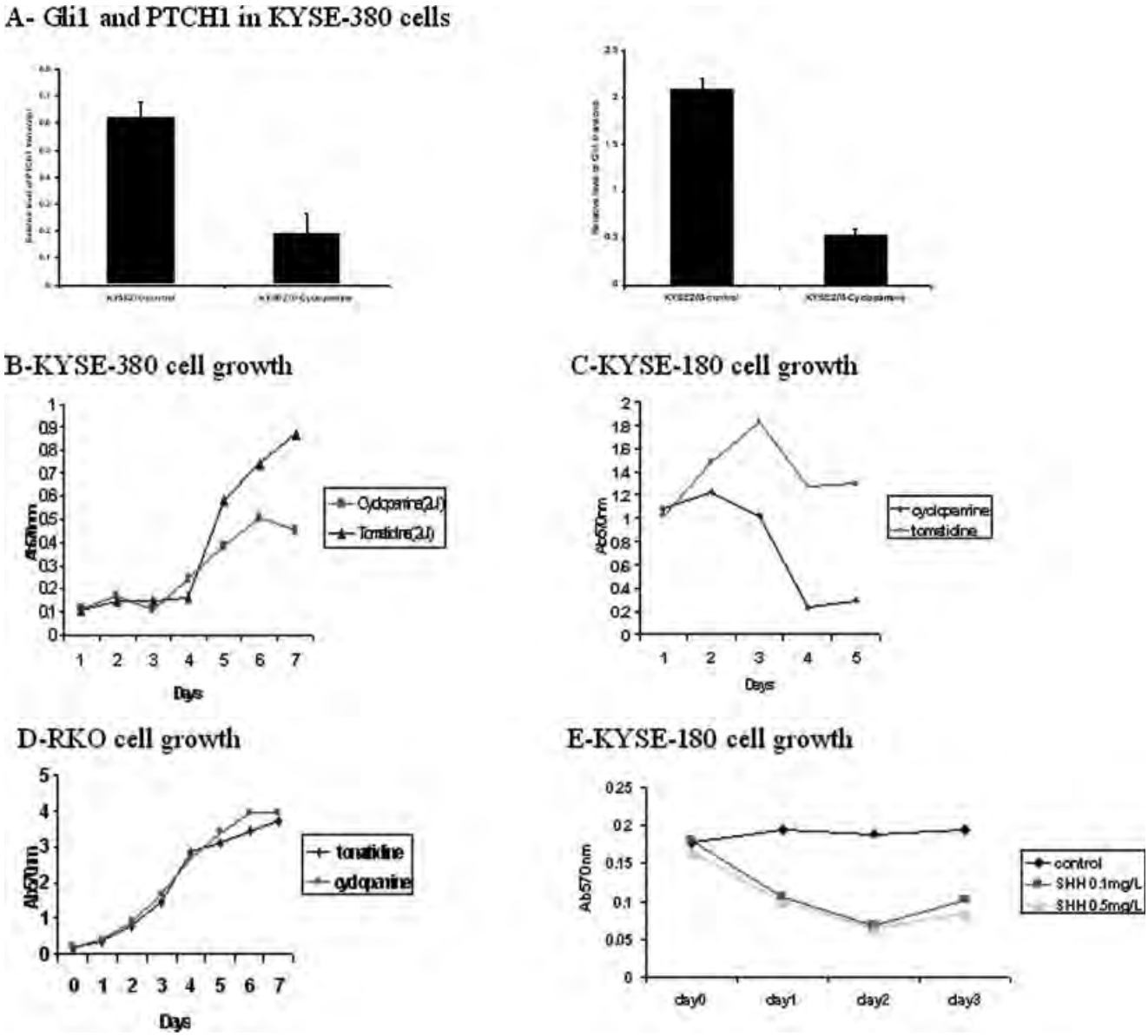

FIGURE 5 – Hedgehog signaling is required for growth of esophageal cancer cells. In the presence of SMO antagonist, KAAD-cyclopamine, the levels of hedgehog pathway target genes (Gli1 and PTCH1) were downregulated (*a* shows data from KYSE-270). Similar data were also obtained from KYSE-180 cells (not shown here). Unlike RKO cells (*d*), which do not have active hedgehog signaling, growth of KYSE-180 (*b*) and KYSE-270 (*c*) cells was inhibited by 2 μM KAAD-cyclopamine. Due to space limit, KAAD-cyclopamine was labeled as cyclopamine. Similarly, incubation of Shh neutralizing antibody 5E1 (0.1 and 0.5 μg/ml) inhibited cell growth of KYSE-180 (*e*) and KYSE-270 (not shown here).

tion of the *Shh* gene in some of these esophageal cancers may be responsible for Shh overexpression.

Targeted inhibition of hedgehog pathway and esophageal cancer cells

If hedgehog pathway activation is required for esophageal cancer development, esophageal cancer cells should be susceptible to treatment of SMO antagonist, KAAD-cyclopamine. Since all available esophageal cancer cell lines have elevated hedgehog signaling,[12] we chose a GI cancer cell line RKO as the negative control (RKO cells do not have elevated levels of Gli1 and PTCH1; data not shown and Berman *et al.*[12]). In this experiment, we used 2 esophageal cancer cell lines (KYSE-180 and KYSE-270) to test the effects of KAAD-cyclopamine. Addition of KAAD-cyclopamine at a final concentration of 2 μM significantly decreased the levels of Gli1 and PTCH1 in both cell lines (Fig. 5*a* shows the data from KYSE-270 cells), indicating that KAAD-cyclopamine inhibits the hedgehog pathway in these cells. The closely related compound tomatidine (2 μM), which does not affect SMO signaling and thus served as a negative control, had little discernible effect on these target genes. As expected, we found that cell growth of esophageal cancer cells, but not RKO cells, was greatly inhibited by KAAD-cyclopamine (Fig. 5*b–d*). We found that cell toxicity of KAAD-cyclopamine at 2 or 5 μM was low (see Fig. S2 for details; supplementary material for this article can be found on the *International Journal of Cancer* website at http://www.interscience.wiley.com/jpages/0020-7136/suppmat/index.html). KAAD-cyclopamine-mediated growth inhibition of KYSE-180 and KYSE-270 cells was dose-dependent (see Fig. S3). Further-

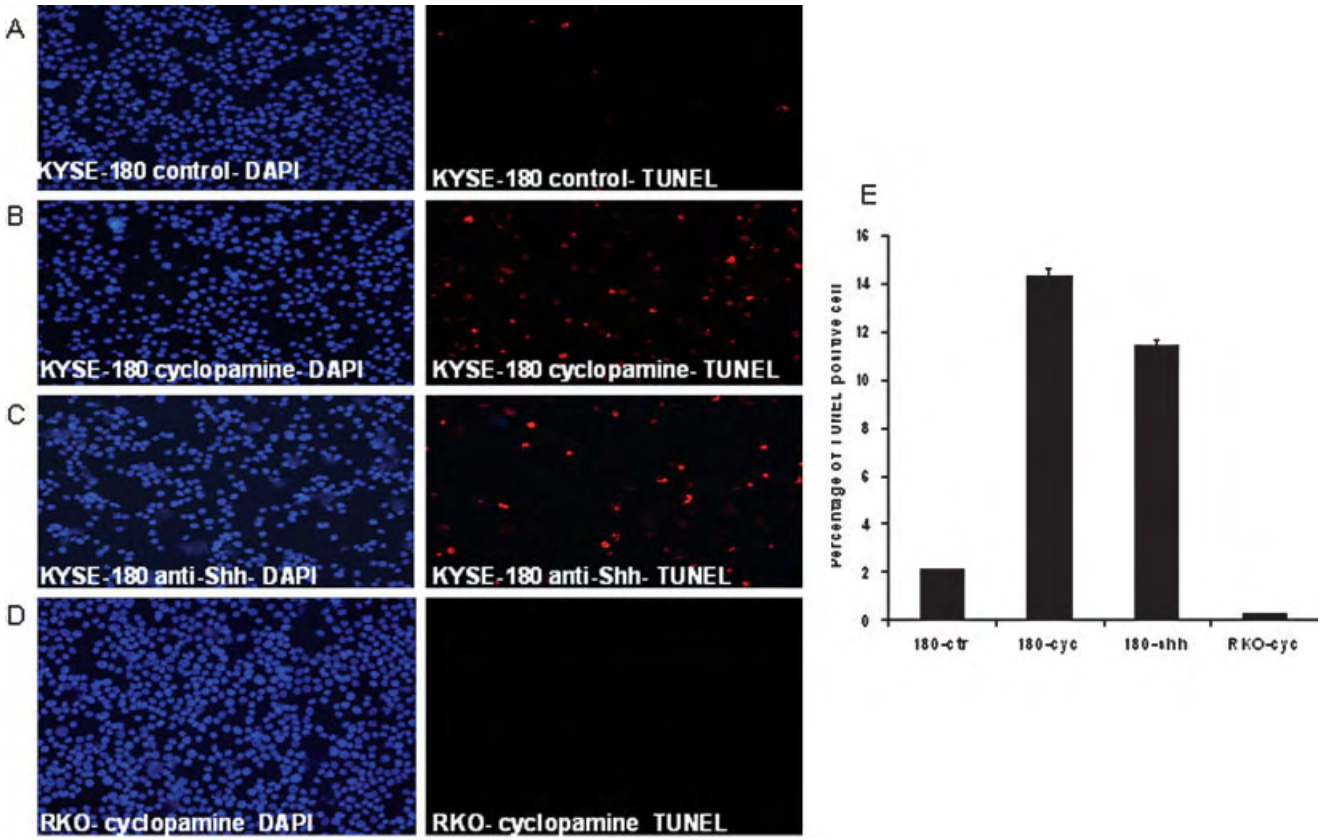

FIGURE 6 – KAAD-cyclopamine and Shh neutralizing antibodies induce apoptosis in esophageal cancer cells. TUNEL assay revealed apoptosis (red) in KYSE180 (*b*) cells, but not in RKO cells (*d*), after treatment with KAAD-cyclopamine (labeled as cyclopamine due to space) for 36 hr. The tomatidine-treated control group had very few TUNEL positive cells (*a* and *e*). Similarly, Shh neutralizing antibody 5E1 (0.1 μg/ml) also caused cell death in KYSE-180 cells (*c*). (*e*) shows the percentage of TUNEL positive cells in each cell lines.

more, KYSE-180 (Fig. 6*b* and *e*) and KYSE-270 cells (not shown here) were TUNEL-positive, indicative of apoptosis after treatment with KAAD-cyclopamine (cell confluence was 15% upon treatment). No apoptosis was observed in RKO cells following addition of 2 μM KAAD-cyclopamine (Fig. 6*d*). Apoptosis was further confirmed by accumulation of sub-G1 cell population (Fig. 7*b*). These results indicate that inhibition of the hedgehog pathway by KAAD-cyclopamine dramatically attenuates the growth of esophageal cancer cells following inhibition of Gli1 and PTCH1 expression, resulting in apoptosis.

If Shh is responsible for hedgehog signaling activation in esophageal cancer cells, inhibition of Shh functions by neutralizing antibodies should reduce cell growth. Indeed, Shh neutralizing antibody 5E1 (at final concentrations of 0.1 μg/ml and 0.5 μg/ml, respectively) significantly inhibited the growth of KYSE-180 cells (Fig. 5*e*), but not that of RKO cells (data not shown). 5E1 IgG also reduced BrdU incorporation in KYSE-180 cells (see Fig. S1). Similar data were also obtained in KYSE-270 cells (data not shown). Flow cytometry analyses indicate an accumulation of sub-G1 cell population after addition of 5E1 IgG in KYSE-180 cells (Fig. 7*c*). This observation was further confirmed by TUNEL analyses (Fig. 6*c*), demonstrating that KYSE-180 cells undergo apoptosis following treatment with 5E1 IgG. Thus, our data support that Shh is responsible for hedgehog-mediated cell proliferation in esophageal cancers.

Our model predicts that overexpression of Gli1 in esophageal cancer cells under a strong promoter (such as the CMV promoter) would constitutively activate the hedgehog pathway, which could render these cancer cells resistant to KAAD-cyclopamine treatment. Indeed, KAAD-cyclopamine did not induce apoptosis in Gli1-expressing KYSE-180 cells, as indicated by lack of TUNEL staining (Fig. 8). Thus, downregulation of Gli1 expression may be an important mechanism by which KAAD-cyclopamine inhibits growth and induces apoptosis of esophageal cancer cells.

Taken together, our findings indicate that activation of the hedgehog pathway is common in esophageal cancers. Activation of the hedgehog pathway is not associated with any specific tumor features (tumor stage, tumor differentiation and tumor subtype). The Shh gene amplification is observed in several esophageal tumors with Shh overexpression. Our data also suggest that downregulation of Gli1 expression is an important mechanism by which KAAD-cyclopamine controls esophageal cancer cell growth. Thus, detection of hedgehog signaling activation may be very useful in cancer diagnosis and targeted cancer treatment of esophageal cancers.

Discussion

Hedgehog signaling activation in esophageal cancers

Hedgehog signaling pathway regulates cell proliferation, tissue polarity and cell differentiation during normal development. Abnormal signaling of this pathway has been reported in a variety of human cancers, including basal cell carcinomas, medulloblastomas, small cell lung cancer and pancreatic cancer.[1] Our findings in this report indicate an important role of the Shh pathway in esophageal cancers. However, not all esophageal squamous cell carcinomas (EC-SCCs) have activated hedgehog signaling, and activation of the hedgehog pathway is not associated with tumor stages or tumor differentiation. In contrast, we found that hedgehog signaling activation in gastric cancers is associated with more

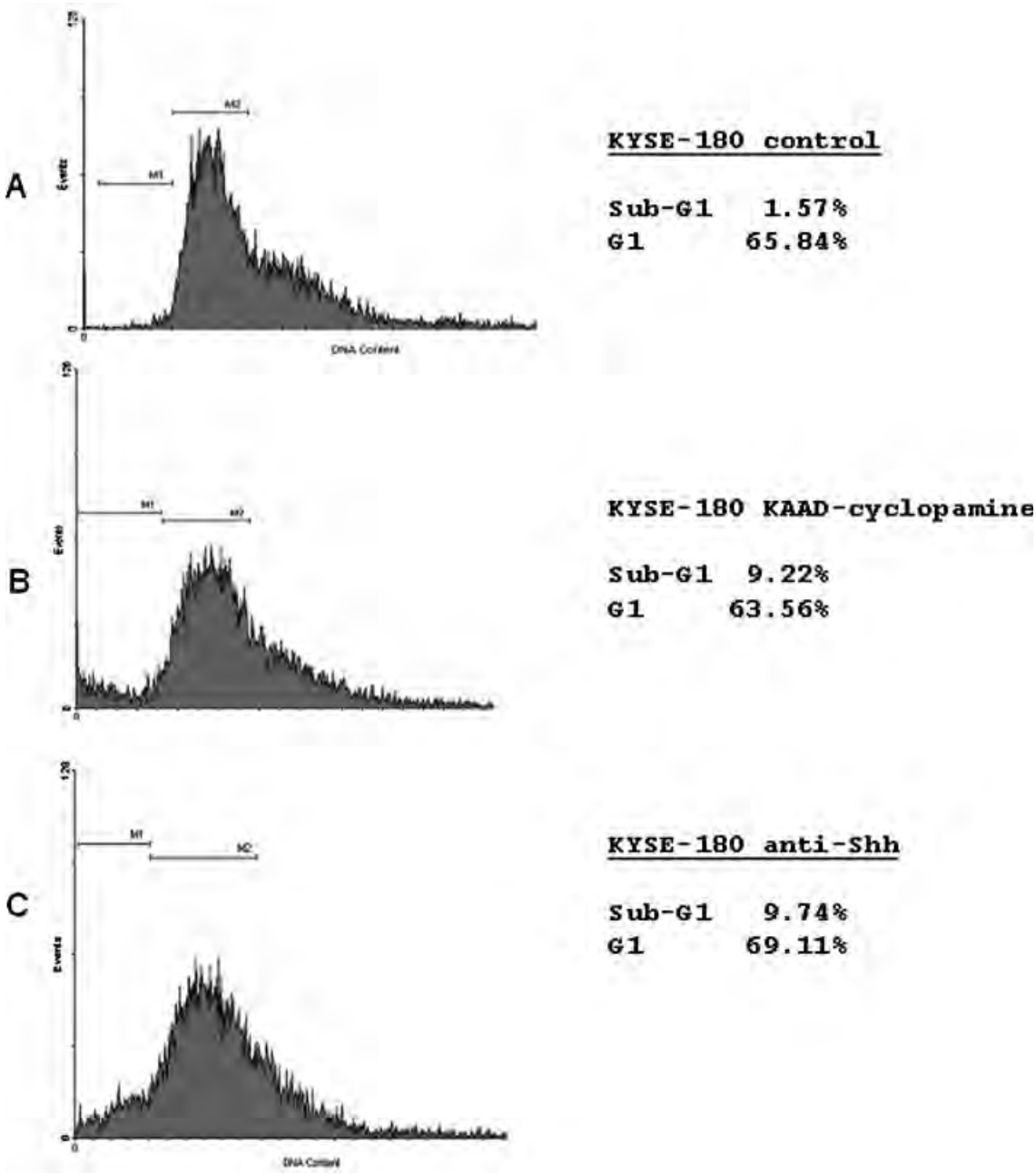

FIGURE 7 – Accumulation of sub-G1 cell population in esophageal cancer cells after hedgehog signaling inhibition. Cells (medium with 0.5% FBS) were treated with 2 μM KAAD-cyclopamine or 0.1 μg/ml Shh neutralizing antibodies for 36 hr before harvest. Flow cytometry was performed as previously reported.[20] KAAD-cyclopamine or Shh neutralizing antibodies increased sub-G1 cell population over 4-fold, from 1.57% to nearly 10% (*a–c*).

poorly differentiated and more aggressive tumors (data not shown). We hypothesize that tumors with activated hedgehog signaling may represent a distinct group of EC-SCCs. Thus, it may be possible to use hedgehog signaling for future molecular classification of EC-SCCs. The actual frequency of hedgehog signaling activation in esophageal cancers, however, should be determined with a large number of primary tumors. It should be interesting to examine the fluency of hedgehog pathway activation in other GI cancers, such as liver, stomach and colon cancers.

Development of esophageal cancer is a multiple-step process, including tumor precursors (Barrett's metaplasia for adenocarcinomas and squamous dysplasia for squamous cell carcinomas), early tumors and tumor metastases. It is of great interests to understand if hedgehog signaling is activated in precursors of esophageal cancers. Similarly, further work is needed to examine if hedgehog signaling is involved in tumor metastases of esophageal cancers. Future understanding of the possible interactions of the hedgehog pathway with other morphogenetic signaling pathways (including wnt and notch pathways) in esophageal cancers will improve our understanding of the etiology of esophageal cancer.

We demonstrated in our studies that amplification of the *Shh* gene may be one mechanism by which Shh is overexpressed in the tumor. Our data are consistent with previous studies, which indicate that gain of 7q is a frequent event in EC-SCCs. Thus, direct detection of

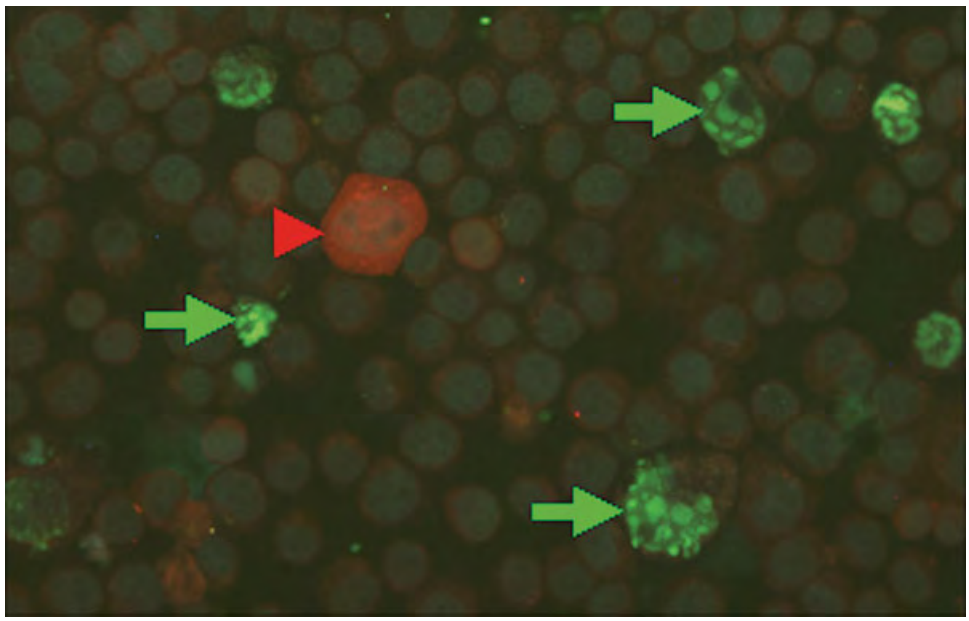

Figure 8 – Ectopic expression of Gli1 and cyclopamine sensitivity in esophageal cancer cells. Following ectopic expression of Gli1 under the CMV promoter, KYSE-180 cells became resistant to KAAD-cyclopamine treatment. No apoptosis was detected in over 500 ectopic Gli1 expressing cells (red; indicated by arrowheads), whereas 10–20% Gli1-negative cells underwent apoptosis after KAAD-cyclopamine treatment (green; indicated by arrows).

Shh expression in primary esophageal cancer specimens may be an effective way for diagnosis for subsets of EC-SCC.

Therapeutic perspective of esophageal cancer through targeted inhibition of hedgehog pathway

Addition of smoothened antagonist, KAAD-cyclopamine, or Shh neutralizing antibodies in culture medium of esophageal cancer cells causes inhibition of cell growth, resulting in apoptosis. These data suggest that hedgehog signaling inhibitors may be effective in future treatment of esophageal cancers. Our preliminary data further indicate that activation of caspases-8 and -3 occurs in KYSE-180 cells after treatment with Shh antibodies (data not shown), suggesting that a death receptor pathway is activated. Additional understanding of apoptotic mechanisms will be helpful for future design of novel drugs for esophageal cancers.

We further demonstrated that overexpression of Gli1 prevents cyclopamine-mediated apoptosis in esophageal cancer cells, further supporting the specificity of KAAD-cyclopamine. Our recent studies indicated that chronic oral administration of KAAD-cyclopamine of Ptch1$^{+/-}$ mice did not affect the overall survival of the mice,[20] which provides a foundation for clinical trials of KAAD-cyclopamine on esophageal cancers. Thus, it is quite possible in the future, with availability of a specific SMO antagonist, KAAD-cyclopamine, to treat the subsets of esophageal cancer in which the hedgehog pathway is activated.

Acknowledgements

The authors thank Huiping Guo for technical support in real-time PCR analysis.

References

1. Pasca di Magliano M, Hebrok M. Hedgehog signalling in cancer formation and maintenance. Nat Rev Cancer 2003;3:903–11.
2. Taipale J, Beachy PA. The hedgehog and Wnt signalling pathways in cancer. Nature 2001;411:349–54.
3. Ingham PW. Transducing hedgehog: the story so far. EMBO J 1998; 17:3505–11.
4. Hahn H, Wicking C, Zaphiropoulous PG, Gailani MR, Shanley S, Chidambaram A, Vorechovsky I, Holmberg E, Unden AB, Gillies S, Negus K, Smyth I, *et al*. Mutations of the human homolog of Drosophila patched in the nevoid basal cell carcinoma syndrome. Cell 1996;85:841–51.
5. Johnson RL, Rothman AL, Xie J, Goodrich LV, Bare JW, Bonifas JM, Quinn AG, Myers RM, Cox DR, Epstein EH Jr, Scott MP. Human homolog of patched, a candidate gene for the basal cell nevus syndrome. Science 1996;272:1668–71.
6. Xie J, Johnson RL, Zhang X, Bare JW, Waldman FM, Cogen PH, Menon AG, Warren RS, Chen LC, Scott MP, Epstein EH Jr. Mutations of the PATCHED gene in several types of sporadic extracutaneous tumors. Cancer Res 1997;57:2369–72.
7. Raffel C, Jenkins RB, Frederick L, Hebrink D, Alderete B, Fults DW, James CD. Sporadic medulloblastomas contain PTCH mutations. Cancer Res 1997;57:842–5.
8. Xie J, Murone M, Luoh SM, Ryan A, Gu Q, Zhang C, Bonifas JM, Lam CW, Hynes M, Goddard A, Rosenthal A, Epstein EH Jr, *et al*. Activating smoothened mutations in sporadic basal-cell carcinoma. Nature 1998;391:90–2.
9. Taylor MD, Liu L, Raffel C, Hui CC, Mainprize TG, Zhang X, Agatep R, Chiappa S, Gao L, Lowrance A, Hao A, Goldstein AM, *et al*. Mutations in SUFU predispose to medulloblastoma. Nat Genet 2002; 31:306–10.
10. Watkins DN, Berman DM, Burkholder SG, Wang B, Beachy PA, Baylin SB. Hedgehog signalling within airway epithelial progenitors and in small-cell lung cancer. Nature 2003;422:313–7.
11. Thayer SP, Di Magliano MP, Heiser PW, Nielsen CM, Roberts DJ, Lauwers GY, Qi YP, Gysin S, Fernandez-Del Castillo C, Yajnik V, Antoniu B, McMahon M, *et al*. Hedgehog is an early and late mediator of pancreatic cancer tumorigenesis. Nature 2003;425:851–6.
12. Berman DM, Karhadkar SS, Maitra A, Montes De Oca R, Gerstenblith MR, Briggs K, Parker AR, Shimada Y, Eshleman JR, Watkins DN, Beachy PA. Widespread requirement for Hedgehog ligand stimulation in growth of digestive tract tumours. Nature 2003; 425:846–51.
13. Sheng T, Li C-X, Zhang X, Chi S, He N, Chen K, McCormick F, Gatalica Z, Xie J. Activation of the hedgehog pathway in advanced prostate cancer. Mol Cancer 2004;3:29.
14. Sanchez P, Hernandez AM, Stecca B, Kahler AJ, DeGueme AM, Barrett A, Beyna M, Datta MW, Datta S, Ruiz i Altaba A. Inhibition of prostate cancer proliferation by interference with SONIC HEDGEHOG-GLI1 signaling. Proc Natl Acad Sci USA 2004;101:12561–6.
15. Karhadkar SS, Bova GS, Abdallah N, Dhara S, Gardner D, Maitra A, Isaacs JT, Berman DM, Beachy PA. Hedgehog signalling in prostate regeneration, neoplasia and metastasis. Nature 2004;431:707–12.
16. Pisani P, Parkin DM, Bray F, Ferlay J. Estimates of the worldwide mortality from 25 cancers in 1990. Int J Cancer 1999;83:18–29.
17. Sarbia M, Becker KF, Hofler H. Pathology of upper gastrointestinal malignancies. Semin Oncol 2004;31:465–75.
18. Unden A, Zaphiropoulos PG, Toftgard R, Stahle-Backdahl M. Human patched (PTCH) mRNA is overexpressed consistently in tumor cells of both familial and sporadic basal cell carcinoma. Cancer Res 1997; 57:2336–40.

19. Li C, Chi S, He N, Zhang X, Guicherit O, Wagner R, Tyring S, Xie J. IFNalpha induces Fas expression and apoptosis in hedgehog pathway activated BCC cells through inhibiting Ras-Erk signaling. Oncogene 2004;23:1608–17.
20. Athar M, Li C, Tang X, Chi S, Zhang X, Kim AL, Tyring SK, Kopelovich L, Hebert J, Epstein EH Jr, Bickers DR, Xie J. Inhibition of smoothened signaling prevents ultraviolet B-induced basal cell carcinomas through regulation of Fas expression and apoptosis. Cancer Res 2004;64:7545–52.
21. Xie J, Aszterbaum M, Zhang X, Bonifas JM, Zachary C, Epstein E, McCormick F. A role of PDGFRalpha in basal cell carcinoma proliferation. Proc Natl Acad Sci USA 2001;98:9255–9.
22. van den Brink GR, Hardwick JC, Nielsen C, Xu C, ten Kate FJ, Glickman J, van Deventer SJ, Roberts DJ, Peppelenbosch MP. Sonic hedgehog expression correlates with fundic gland differentiation in the adult gastrointestinal tract. Gut 2002;51:628–33.
23. Arsic D, Keenan J, Quan QB, Beasley S. Differences in the levels of Sonic hedgehog protein during early foregut development caused by exposure to adriamycin give clues to the role of the Shh gene in oesophageal atresia. Pediatr Surg Int 2003;19:463–6.
24. Yen CC, Chen YJ, Chen JT, Hsia JY, Chen PM, Liu JH, Fan FS, Chiou TJ, Wang WS, Lin CH. Comparative genomic hybridization of esophageal squamous cell carcinoma: correlations between chromosomal aberrations and disease progression/prognosis. Cancer 2001;92:2769–77.
25. Walch AK, Zitzelsberger HF, Bruch J, Keller G, Angermeier D, Aubele MM, Mueller J, Stein H, Braselmann H, Siewert JR, Hofler H, Werner M. Chromosomal imbalances in Barrett's adenocarcinoma and the metaplasia-dysplasia-carcinoma sequence. Am J Pathol 2000;156:555–66.

ACCELERATED PUBLICATION

This paper is available online at www.jbc.org

THE JOURNAL OF BIOLOGICAL CHEMISTRY VOL. 281, NO. 1, pp. 9–12, January 6, 2006

Regulation of Gli1 Localization by the cAMP/Protein Kinase A Signaling Axis through a Site Near the Nuclear Localization Signal*[S]

Received for publication, June 28, 2005, and in revised form, November 14, 2005
Published, JBC Papers in Press, November 17, 2005, DOI 10.1074/jbc.C500300200

Tao Sheng, Sumin Chi, Xiaoli Zhang, and Jingwu Xie[1]

From the Sealy Center for Cancer Cell Biology and Department of Pharmacology, University of Texas Medical Branch, Galveston, Texas 7555-1048

The *hedgehog* (Hh) pathway plays a critical role during development of embryos and cancer. Although the molecular basis by which protein kinase A (PKA) regulates the stability of hedgehog downstream transcription factor cubitus interruptus, the *Drosophila* homologue of vertebrate Gli molecules, is well documented, the mechanism by which PKA inhibits the functions of Gli molecules in vertebrates remains elusive. Here, we report that activation of PKA retains Gli1 in the cytoplasm. Conversely, inhibition of PKA activity promotes nuclear accumulation of Gli1. Mutation analysis identifies Thr^{374} as a major PKA site determining Gli1 protein localization. In the three-dimensional structure, Thr^{374} resides adjacent to the basic residue cluster of the nuclear localization signal (NLS). Phosphorylation of this Thr residue is predicted to alter the local charge and consequently the NLS function. Indeed, mutation of this residue to Asp (Gli1/T374D) results in more cytoplasmic Gli1 whereas a mutation to Lys (Gli1/T374K) leads to more nuclear Gli1. Disruption of the NLS causes Gli1/T374K to be more cytoplasmic. We find that the change of Gli1 localization is correlated with the change of its transcriptional activity. These data provide evidence to support a model that PKA regulates Gli1 localization and its transcriptional activity, in part, through modulating the NLS function.

Hedgehog (Hh)[2] proteins are a group of secreted proteins whose active forms are derived from a unique protein cleavage process and at least two post-translational modifications (1, 2). Secreted Hh molecules bind to the receptor patched (PTC), thereby alleviating PTC-mediated suppression of smoothened (SMO) (2, 3). Expression of sonic hedgehog (Shh) appears to stabilize SMO protein possibly through post-translational modification of SMO (4). The effect of hedgehog molecules can be inhibited by hedgehog-interacting protein (HIP) through competitive association with PTC (5, 6). In *Drosophila*, SMO stabilization triggers complex formation with Costal-2, Fused, and Gli homologue cubitus interruptus (CI), which prevents CI degradation and formation of a transcriptional repressor (7–10). SMO ultimately activates transcription factors of the Gli family. Gli molecules enter nucleus through a nuclear localization signal (11, 12), but little is known about the regulatory mechanism for this process. As transcriptional factors, Gli molecules can regulate target gene expression by direct association with a consensus binding site (5′-tgggtggtc-3′) located in the promoter region of the target genes (13, 14).

Protein kinase A (PKA) was first identified as an inhibitory component of the Hh pathway in *Drosophila* (15–19). PKA fulfills its negative role by phosphorylating full-length Ci (Ci155) at several Ser/Thr residues, priming it for further phosphorylation by glycogen synthase kinase 3 (GSK3) and casein kinase I (CKI) (20–22). Hyperphosphorylation of Ci155 targets it for proteolytic processing to generate the repressor form (Ci75) (23). Consistent with this, overexpressing a constitutively active form of PKA catalytic subunit (PKAc), mC*, blocks Ci155 accumulation and Hh target gene expression (24). In addition to its inhibitory effects, PKA phosphorylation at the C terminus of SMO in *Drosophila*, but not in mammals, enhances hedgehog-mediated signaling (25, 26).

While the regulation of CI cleavage by PKA phosphorylation is well documented, very little is known about the role of PKA in Gli regulation. In vertebrates, there are three Gli molecules, Gli1, Gli2, and Gli3. Gli3 can be processed in a manner similar to CI, a process regulated by PKA (27, 28). The fact that Gli3 expression is often not detectable in human cancer suggests that Gli3 does not play a significant role in hedgehog-driven carcinogenesis (29–31). In contrast, Gli1 and Gli2 are expressed in tumors with activated hedgehog signaling (2, 29–36). Here, we report that the cAMP/PKA signaling axis regulates Gli1 protein localization, in part, through phosphorylation of Gli1 at a site near the nuclear localization signal (NLS). We propose that this unique regulation is an important mechanism by which PKA inhibits transcriptional activity of Gli molecules.

MATERIALS AND METHODS

Cell Culture and Plasmids—COS7 and NIH3T3 cells were purchased from the American Type Culture Collection (Manassas, VA) and were maintained in Dulbecco's modified Essential medium supplemented with 10% fetal bovine serum (Invitrogen). Transfection was performed using Lipofectamine 2000 (Invitrogen) according to the manufacturer's instructions (the ratio of plasmid (μg) to lipid (μl) was 1:2.5). Stable expression of a luciferase reporter under the control of Gli responsive elements in NIH3T3 cells was achieved through selection with G418 for 3 weeks after transient transfection with Lipofectamine 2000 (Invitrogen). Two clones with good responses to Gli1 expression (over 20-fold) were selected from a total of 80 clones.

Cells with expression of Gli1 (with C-MYC tag) were treated with 10 μM H89 (Calbiochem) or 0.4 ng/ml leptomycin B (LMB, Sigma) for 8 h. For forskolin treatment (20 μM for 8 h), cells were pretreated with phosphodiesterase inhibitor IBMX (100 μM) for 30 min before addition of forskolin. Immunofluorescent detection of C-MYC-tagged Gli1 was performed as described previously with Cy3-conjugated MYC antibody 9e10 (Sigma) (1:100 dilution) (37). Gli1 localization was detected under a fluorescent microscope; the percentage of Gli1 in the nucleus or the cytoplasm was calculated for each experiment from over 200 Gli1-expressing cells, and the experiment was repeated three times.

Gli1 cDNA was generously provided by Dr. Bert Vogelstein and cloned into pCDNA3.1 with a C-MYC tag at the N terminus. Gli1-GFP construct was made by subcloning Gli1 cDNA into pEGFP-3C using *BamHI* (5′) and NotI (3′) sites. Point mutations of Gli1 were made by *in situ* mutagenesis in our DNA Recombinant Laboratory Core Facility or by PCR-based mutagenesis. All mutations were confirmed by sequencing of the entire coding region. Clones containing only the targeted mutations were used in the studies.

Immunoprecipitation and in Vitro Kinase Assay—Cells were lysed using Nonidet P-40 cell lysis buffer 48 h following Gli1 transfection. C-MYC-tagged Gli1 proteins were immunoprecipitated with an anti-MYC 9B11 antibody (Cell Signaling Inc.) for 3 h followed by incubation with A/G plus beads (Bethyl Laboratories, Inc.) for 1 h. The immunocomplexes were divided into two portions. One portion (20%) was separated by 10% SDS-PAGE and analyzed by Western blotting using an anti-MYC antibody 9B11. The remaining 80% of them were incubated with 0.6 ng of recombinant PKA catalytic subunit with ADBI buffer (20 mM MOPS, pH 7.2, 25 mM β-glycerol phosphate, 5 mM EGTA, 1 mM sodium orthovanadate, 1 mM dithionthreitol) containing 1 mg/ml bovine serum albumin, and 10 μCi of [γ-^{32}P]ATP at 30 °C for 30 min. The kinase reactions were terminated by adding 4× SDS sample buffer, and the samples were separated by 10% SDS-PAGE. Gels were dried on Whatman

* This work was supported by NCI/National Institutes of Health Grant R01CA94160, Department of Defense Grant DOD-PC030429, and NIEHS/National Institutes of Health Grant ES06676. The costs of publication of this article were defrayed in part by the payment of page charges. This article must therefore be hereby marked "*advertisement*" in accordance with 18 U.S.C. Section 1734 solely to indicate this fact.

[S] The on-line version of this article (available at http://www.jbc.org) contains a supplemental figure.

[1] To whom correspondence should be addressed: Sealy Center for Cancer Cell Biology, MRB 9.104, UTMB, 301 University Blvd., Galveston, TX 77555-1048. Tel.: 409-747-1845; Fax: 409-747-1938; E-mail: jinxie@utmb.edu.

[2] The abbreviations used are: Hh, hedgehog; PTC, patched; SMO, smoothened; PKA, protein kinase A; CI, cubitus interruptus; Shh, sonic hedgehog; NLS, nuclear localization signal; NES, nuclear export signal; aa, amino acid; LMB, leptomycin B; IBMX, isobutylmethylxanthine; GFP, green fluorescent protein; MOPS, 4-morpholinepropanesulfonic acid.

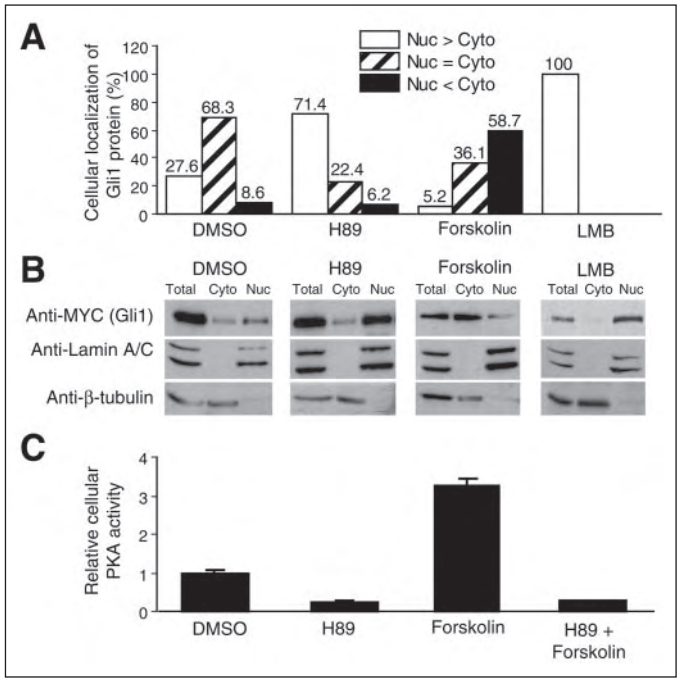

FIGURE 1. **Regulation of Gli1 localization by forskolin-mediated PKA activation in COS7 cells.** *A*, Gli1 was detected by immunofluorescent staining. Following treatment with forskolin (8 h), H89 (8 h), or LMB (8 h) (see "Materials and Methods"), Gli1 protein localization was assessed under a fluorescent microscope in over 200 Gli1-expressing cells, and the experiment was repeated three times with similar results. The percentage of Gli1 in each cellular compartment was calculated from these experiments (see supplemental figure for typical pictures of Gli1 staining). *Nuc > Cyto* indicates preferential nuclear localization, *Nuc = Cyto* indicates localization both in the nucleus and in the cytoplasm, and *Nuc < Cyto* indicates predominant cytoplasmic localization. *B*, Gli1 was detected after cell fractionation (see "Materials and Methods"). Both the nuclear fraction and the cytoplasmic fraction were collected for Western blotting analysis. The purity of cell fractionation was assessed using lamin A/C for the nuclear fraction and β-tubulin for the cytoplasmic fraction. *C*, the cellular PKA activity in COS7 cells was determined using a kit from Upstate Biotechnology Inc. The high PKA activity (*C*) was correlated with a higher level of cytoplasmic Gli1.

paper, followed by autoradiography. Western blotting analysis was performed according to a previously published procedure (37).

Cellular PKA Activation Assay—COS7 cells were seeded into 6-well plates the day before the experiment. Cells were serum-starved for 12 h and then treated with 20 μM H89, 20 μM forskolin or both for 45 min. 100 μM IBMX was added for 30 min prior to treatment with forskolin. Cellular PKA activity in the above-described conditions was determined using a PKA activation assay (Upstate Biotechnology Inc.), in which Leu-Arg-Arg-Ala-Ser-Leu-Gly (Kemptide) was used as the substrate (38). In brief, cell lysates were prepared using Nonidet P-40 lysis buffer. After sonication, the cell lysates were collected at 12,000 rpm for 5 min. 10-μl cell lysates were incubated with 10 μM ATP containing 10μCi [γ-^{32}P]ATP (3,000 Ci/mmol)], 250 μM Kemptide substrate in ADBI buffer at 30 °C for 10 min. Background was determined from reactions without substrate, and the total PKA activity was estimated in reactions containing 20 μM dibutyryl-cAMP. Aliquots were spotted onto Whatman P-81 paper, and the filters were washed in 0.75% phosphoric acid three times for 5 min per wash. ^{32}P incorporation was determined by liquid scintillation counting. Protein concentration of the cell lysates was determined by a kit from Bio-Rad (Bio-Rad protein assay). Data are representative of three independent experiments.

Cell Fractionation—Following transfection, the COS7 cells were maintained in 10 cm cell culture dishes for 48 h. Before harvest, the cells were rinsed twice with cold phosphate-buffered saline, harvested by scraping with 1 ml of cold phosphate-buffered saline for each 10-cm dish, and collected by centrifugation at 3,000 × *g* for 30 s. One-fifth of the lysates were collected for detection of Gli1 expression by Western blotting. The cell pellets were incubated with 60 μl of buffer A (50 mM HEPES, pH 7.4, 10 mM KCl, 1 mM EDTA, 1 mM EGTA, 1 mM dithiothreitol, 0.1 μg of phenylmethylsulfonyl fluoride/ml, 1 μg of pepstatin A/ml, 1 μg of leupeptin/ml, 10 μg of soybean trypsin inhibitor/ml, 10 μg of aprotinin/ml, and 0.1% IGEPAL CA-630). After 10 min on ice, the lysates were centrifuged at 6,000 × *g* for 30 s at 4 °C. The supernatant fractions were saved as the cytoplasmic fraction. The pellet (containing the nuclei) was resuspended in buffer B (buffer A containing 1.0 M sucrose) and centrifuged at 15,000 × *g* for 10 min at 4 °C. The purified nuclei (pellets) were incubated in 30 μl buffer C (10% glycerol, 50 mM HEPES, pH 7.4, 400 mM KCl, 1 mM EDTA, 1 mM EGTA, 1 mM dithiothreitol, 0.1 μg of phenylmethylsulfonyl fluoride/ml, 1 μg of pepstatin A/ml, 1 μg of leupeptin/ml, 10 μg of soybean trypsin inhibitor/ml, 10 μg of aprotinin/ml) after vigorous vortex and centrifuged at 15,000 × *g* for 20 min at 4 °C, and supernatant fractions were collected. All extracts were normalized for protein amounts determined by Bio-Rad protein assay (Bio-Rad) and separated by 10% SDS-PAGE for further analysis (39). Antibodies to β-tubulin (Sigma) and Lamin A/C (Santa Cruz Biotechnology Inc.) were used to detect the purity of cytoplasmic (β-tubulin) and nuclear (Lamin A/C) fractions using Western blotting analysis.

Luciferase Reporter Gene Assay—For luciferase assay, NIH3T3 cells with stable expression of the Gli luciferase reporter were transfected with Gli1 constructs (0.5 μg/well) and the TK-*Renilla* control plasmid (5 ng/well) using Lipofectamine 2000. After 5 h, the medium was replaced with fresh growth medium and the cells were incubated in 5% CO_2 at 37 °C overnight. Following treatment with forskolin or other compounds, the cells were harvested, and luciferase activity was measured with the dual luciferase reporter assay system (Promega) according to the manufacturer's instruction. In brief, the transfected cells were lysed in the 6-well plates with 100 μl of reporter lysis buffer and the lysate transferred into Eppendorf tubes. Cell debris was removed by centrifugation at top speed for 10 min in a microcentrifuge. 20 μl of the supernatant was mixed with 100 μl of buffer LAR II, and the absorbance was immediately measured (the first reading). After 3 s, 100 μl of Stop & Glo® Reagent was added to measure the Renillar luciferase activity (the second reading). The value from the first reading was divided by the value from the second reading of each sample to obtain the luciferase activity. Each experiment was repeated three times with similar results.

RESULTS

Gli1 is not only a downstream effector but also a target gene of the hedgehog pathway (40). Thus, identification of the mechanism by which PKA phosphorylation regulates Gli1 functions will help us understand signal transduction of the hedgehog pathway in cancer.

First, we tested whether Gli1 protein localization can be altered by accumulation of the cellular cAMP level in COS7 cells. After transient transfection, the protein localization of Gli1 was detected by immunofluorescent staining of the C-MYC tag at the Gli1 N terminus and by cell fractionation. In the presence of 20 μM forskolin, which directly activates adenylyl cyclase and raises the cyclic AMP level (41), we observed that the percentage of cytoplasmic Gli1 was increased over 5-fold, whereas the percentage of nuclear Gli1 was reduced by 80% (Fig. 1, *A* and *B*). The effect seems to be direct because the change in Gli1 localization can be observed 20 min after forskolin treatment. Conversely, addition of PKA inhibitor H89 led to a shift of Gli1 localization to the nucleus (Fig. 1, *A* and *B*). As a consequence of forskolin treatment, the cellular PKA activity was increased 2-fold (Fig. 1*C*). Conversely, addition of H89 into the medium inhibited the cellular PKA activity by 70% (Fig. 1*C*). Thus, Gli1 localization was correlated with the cellular PKA activity. To confirm the data from the immunofluorescent staining, we performed cell fractionation analysis. As shown in Fig. 1*B*, more Gli1 were in the nuclear fraction following H89 treatment whereas forskolin caused an increase of cytoplasmic Gli1 (Fig. 1*B*). Furthermore, we monitored localization of Gli1-GFP fusion protein with a time-lapse microscope in the presence of H89 or forskolin. Forskolin retained Gli1-GFP in the cytoplasm whereas H89 promoted nuclear accumulation of this fusion protein (data not shown). All these data indicate that Gli1 localization can be regulated by modulating the cellular PKA activity.

Gli1 protein shuttling between the nucleus and the cytoplasm was interrupted by inhibition of nuclear export with LMB, a specific inhibitor for CRM1-mediated nuclear export, resulting in nuclear accumulation of all Gli1 proteins (Fig. 1, *A* and *B*), supporting that Gli1 localization is a dynamic process and is tightly regulated. Our data suggest that direct phosphorylation of Gli1 by PKA is responsible for regulation of Gli1 protein localization.

Sequence analysis predicts five putative PKA sites in Gli1. The sequence around these PKA sites is highly conserved among Gli proteins (Fig. 2*A*). Several point mutations of Gli1 were made to test Gli1 regulation by PKA (see the diagram in Fig. 2*B*). These mutations were made by *in situ* mutagenesis in our DNA Recombinant Laboratory Core Facility or by PCR-based mutagenesis.

Using these mutant constructs, we assessed Gli1 localization in cultured

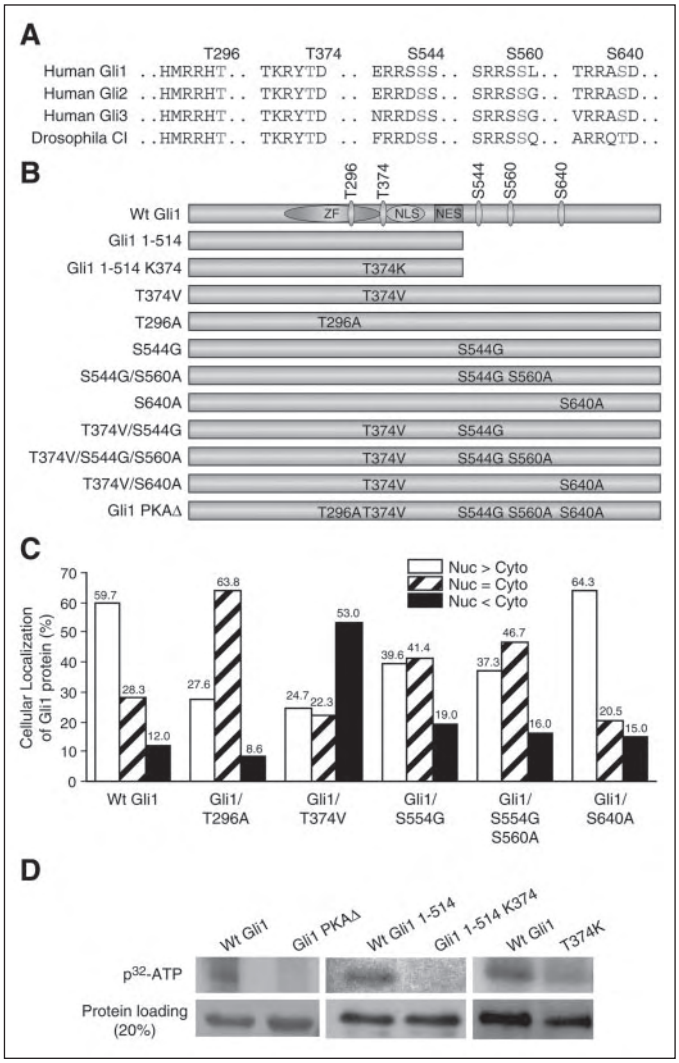

FIGURE 2. **Regulation of PKA phosphorylation and localization by cAMP/PKA. The five putative sites are conserved in all Gli molecules.** *A* shows the sequence alignment of CI and human Gli1, Gli2, and Gli3 at the five putative PKA sites. *B* shows the Gli1 constructs used in this study. Gli1 molecules with point mutations of one or more PKA sites were expressed in COS7 cells and their localization was detected by immunofluorescent staining. Full-length Gli1 with a mutation at Thr^{374} (T374V) had the most significant effect on Gli1 protein localization (*C*). In contrast, a mutation at Ser^{544} or other sites (*C* and see supplemental figure) had little effects on Gli1 protein localization. A Gli1 mutant Gli1/T374V/S544G/S560A with triple mutations at PKA sites behaved like Gli1/T374V (supplemental figure), indicating that Thr^{374} is a critical PKA site for determining Gli1 protein localization. Over 200 Gli1-positive cells were counted under a fluorescent microscope for Gli1 protein localization, and the experiment was repeated three times with similar results. The data were the average result from these experiments. *D* shows Gli1 phosphorylation *in vitro* by recombinant PKA. Wild type Gli1 and its mutant forms were expressed in COS7 cells and subsequently purified through immunoprecipitation. The ability of PKA to phosphorylate immunoprecipitated Gli1 proteins were performed *in vitro* (see "Materials and Methods"). The full-length Gli1, but not Gli1-PKAΔ (see *B*, the mutation sites), was highly phosphorylated by PKA *in vitro* (*D*, *left panels*). A single point mutation in a Gli1 fragment (1–514 aa, shown in *B*) prevented protein phosphorylation by PKA (*D*, *center panels*). This same mutation in the full-length Gli1 also dramatically reduced the level of phosphorylation (*D*, *right panels*).

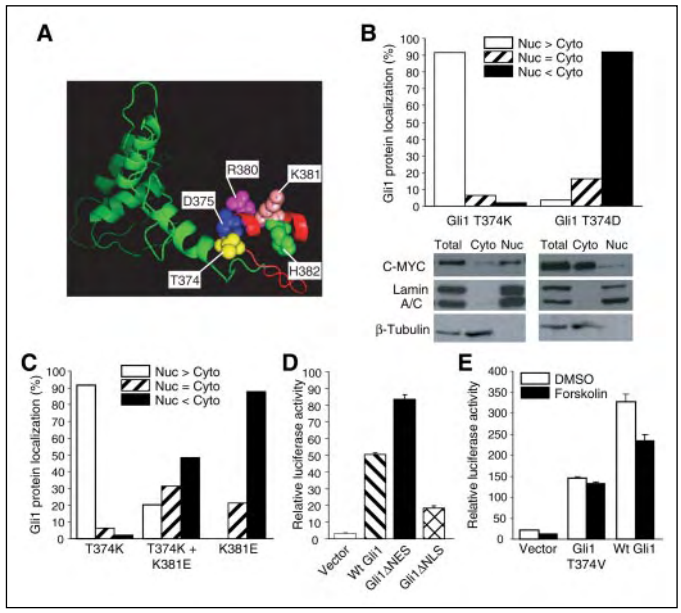

FIGURE 3. **Demonstration of Thr^{374} as the major site for Gli1 regulation.** *A*, a three-dimensional model of Gli1 fragment, showing the proximity of Thr^{374}/Asp^{375} to the basic residue cluster (Arg^{380}/Lys^{381}/His^{382}) of the Gli1 NLS. *B* shows the preferential nuclear localization of Gli1/T374K and the predominant cytoplasmic localization of Gli1/T374D. Localization was confirmed by cell fractionation. Immunofluorescent staining was done as described for Fig. 1*A*. *C* shows Gli1/T374K localization following an additional mutation at Lys^{381}. These experiments suggest that Thr^{374} is responsible for cAMP/PKA-mediated regulation of Gli1 localization, which may be achieved through affecting the NLS function. *D*, correlation of Gli1 localization with its transcriptional activity was examined in NIH3T3 cells with stable expression of a luciferase reporter under the control of Gli-responsive elements (see "Materials and Methods" for details). Gli1 with a Lys to Glu mutation at Lys^{381} (K381E) of the NLS motif, which predominantly localizes to the cytoplasm, was unable to activate this reporter. In contrast, Gli1 with mutations in the NES motif, which predominantly localizes to the nucleus, was more active than the wild type Gli1. *E*, transcriptional activity of Gli1/T374V was not responsive to forskolin treatment whereas the transcriptional activity of wild type Gli1 was reduced by 60% following forskolin treatment.

cells. We found that mutation at Thr^{374} (Gli1/T374V) significantly affects Gli1 localization (Fig. 2*C*). Furthermore, the response of Gli1/T374V to forskolin treatment was nearly diminished (in response to forskolin treatment, 5-fold increase in cytoplasmic protein for wild type Gli1 but only 40% increase for Gli1/T374V) (also see the supplemental figure). In contrast, the protein localization of Gli1/S544G and Gli1/S544G/S560A was not different from the wild type Gli1 (supplemental figure). A mutant Gli1 (Gli1/T374V/S544G/S560A) with triple mutations at the PKA sites behaved like Gli1/T374V (supplemental figure), indicating that Ser^{544} and Ser^{560} are not involved in regulation of Gli1 localization. On the other hand, a mutation at S640A had only slight effects on Gli1 protein localization in response to forskolin (supplemental figure). These data indicate that Thr^{374} is the major site responsible for Gli1 protein localization in cultured cells.

Consistent with the role of Thr^{374} for Gli1 protein localization, we also confirmed that Thr^{374} can be phosphorylated by recombinant PKA *in vitro* (Fig. 2*D*). We performed PKA phosphorylation with Gli1 protein purified by immunoprecipitation in the presence of [γ-^{32}P]ATP and recombinant PKA in test tube and found that Gli1 was highly phosphorylated by PKA *in vitro* (Fig. 2*D*, *left panels*, *first lane*). Gli1 with mutations of all five PKA sites (PKAΔ) could not be phosphorylated by PKA (Fig. 2*D*, *left panels*, *right lane*). To test whether the Thr^{374} site of Gli1 is phosophorylated by recombinant PKA, we used a Gli1 fragment containing only two PKA sites: Thr^{296} and Thr^{374}. We found that this Gli1 fragment (1–514 aa) with a mutation at Thr^{374} was not able to be phosphorylated by recombinant PKA *in vitro* (Fig. 2*D*, *center panels*). Even a single point mutation at Thr^{374} significantly reduced PKA-mediated phosphorylation of full-length Gli1 (Fig. 2*D*, *right panels*), indicating that the Thr^{374} site is a major PKA site of Gli1 phosphorylation. In addition, our data also suggested that Ser^{544}, Ser^{560}, and Ser^{640} can be phosphorylated by PKA *in vitro* (data not shown here). The above data indicate that Thr^{374} is a major PKA site involved in regulation of Gli1 protein localization.

In the three-dimensional structure, Thr^{374}, together with the adjacent Asp^{375}, is close to the first basic residue cluster (Arg^{380}/Lys^{381}/His^{382}) of the bipartite motif (the classic NLS) in Gli1 (Fig. 3*A*) (42). It is known that protein phosphorylation at the residue next to the bipartite motif inhibits its binding affinity to importins, leading to reduced nuclear localization of the target protein (43). We predict that phosphorylation of Thr^{374} will increase the local negative charge, leading to reduced NLS functions and accumulation of Gli1 in the cytoplasm. Indeed, Gli1/T374D was preferentially localized to the cytoplasm (Fig. 3*B*). Conversely, Gli1/T374K has a high local positive charge near the NLS, and we found that Gli1/T374K predominantly localized to the nucleus (Fig. 3*B*). Localization of these Gli1 proteins was further confirmed by

cell fractionation (Fig. 3*B*). These data support our hypothesis that one mechanism by which the cellular PKA activity regulates Gli1 localization is through altering the local charge nearby the NLS of Gli1.

If Gli1 nuclear localization is regulated by PKA phosphorylation through a NLS-dependent mechanism, disruption of the NLS should affect localization of these mutant Gli1 molecules. As shown in Fig. 3*C*, we found that Gli1/K381E, which is predicted to disrupt the NLS, was predominantly localized to the cytoplasm, confirming the role of NLS in Gli1 localization (12). Although Gli1/T374K localizes predominantly to the nucleus, additional mutation at K381 (K381E) retained Gli1/T374K to the cytoplasm (Fig. 3*C*), suggesting that regulation of Gli1 localization by T374 phosphorylation requires the intact NLS.

The ultimate effect of Gli1 is transcriptional activation of the downstream target genes. To assess whether Gli1 localization affects its transcriptional activity, we established stable expression of Gli1 luciferase reporter under the control of Gli responsive elements in NIH3T3 cells (13). By measuring the reporter luciferase activity, we examined the association of Gli1 localization with its transcriptional activity (Fig. 3*D*). If Gli1/K381E remains preferentially in the cytoplasm, the transcriptional activity was low. In contrast, Gli1 with a defective NES (Gli1/L496V/L498V), which localizes predominantly in the nucleus, was more active (Fig. 3*D*). Thus, the Gli1 luciferase reporter activity in these cells is very sensitive to Gli1 localization. We examined the effects of forskolin to Gli1-mediated transcriptional activity in this NIH3T3 stable cell line. Like the wild type Gli1, Gli1/T374V can activate the Gli luciferase reporter (Fig. 3*E*). Consistent with its cytoplasmic localization, the luciferase activity in cells expressing the wild type Gli1 was reduced after forskolin treatment (Fig. 3*E*). In contrast, Gli1/T374V-mediated reporter gene activity was not affected by forskolin (Fig. 3*E*). These data suggest that Thr^{374} is an important PKA site responsible for PKA phosphorylation and for the transcriptional activity of Gli1.

Based on these data, we proposed a mechanism by which the cAMP/PKA signaling axis mediates regulation of Gli1 localization. Gli1 enters the nucleus through a nuclear localization signal. With the accumulation of cAMP in the cell, Thr^{374} gets phosphorylated. Phosphorylation of Thr^{374} will increase the local negative charge nearby the NLS, which results in inhibition of NLS function. Consequently, Gli1 is retained in the cytoplasm and is unable to activate the target genes. Since this Thr residue is highly conserved among Gli proteins, we anticipate that the same mechanism is applicable to PKA regulation of other Gli molecules.

DISCUSSION

In our study, we provide direct evidence to support that the cAMP/PKA signaling axis regulates Gli1 protein localization primarily through a site at Thr^{374}. Our data further indicate that PKA-mediated regulation of Gli1 localization is through Thr^{374}, possibly through interfering with the NLS function.

Although our studies demonstrated that Thr^{374} is a major site for PKA-mediated regulation of Gli1 localization (Figs. 2 and 3 and supplemental figure), mutation at this site did not completely abolish the effects of forskolin (supplemental figure). To identify an additional site required for this regulation, we made double and triple point mutations of Gli1 at the PKA sites (Fig. 2*B*). Our data indicate that mutations at Thr^{374} and Ser^{640} completely abolished the response to forskolin treatment, indicating that Ser^{640} is another site involving PKA-mediated regulation of Gli1 localization (supplemental figure). However, mutation at Ser^{640} alone had no effect on Gli1 protein localization and had only a slight effect in response to forskolin treatment, suggesting that Ser^{640} is not a primary site for Gli1 regulation. This hypothesis was further supported by the fact that Gli1/S640E and Gli1/S640R, unlike Gli1/T374D and Gli1/T374K, did not alter Gli1 protein localization (data not shown here). Thus, we believe that additional structural information of Gli1 near the Ser^{640} region is required to understand the molecular mechanism by which PKA phosphorylation at Ser^{640} affects Gli1 localization.

Further studies of Gli1 phosphorylation can be facilitated by measuring the stoichiometry of phosphorylation for Gli1. Currently, a large amount of purified Gli1 protein is not available, making it difficult to calculate the stoichiometry of phosphorylation for such a large protein (150 kDa for Gli1). This issue may be addressed in the future using highly purified Gli1 fragments from bacteria.

In addition, our data indicate that Ser^{544} and Ser^{560} residues are not involved in regulation of Gli1 protein localization. It will be interesting to know how these two sites are involved in regulation of Gli1 functions.

Acknowledgments—We thank Drs. James Lee, Yigong Shi, Xiaodong Cheng, Mark Evers, and Min Chen for help with this project, Drs. H. Sasaki and Bert Vogelstein for providing reagents, and Karen Martin and Brenda Rubio for help with the manuscript.

REFERENCES

1. Taipale, J., and Beachy, P. A. (2001) *Nature* **411,** 349–354
2. Pasca di Magliano, M., and Hebrok, M. (2003) *Nat. Rev. Cancer* **3,** 903–911
3. Stone, D. M., Hynes, M., Armanini, M., Swanson, T. A., Gu, Q., Johnson, R. L., Scott, M. P., Pennica, D., Goddard, A., Phillips, H., Noll, M., Hooper, J. E., de Sauvage, F., and Rosenthal, A. (1996) *Nature* **384,** 129–134
4. Hooper, J. E., and Scott, M. P. (2005) *Nat. Rev. Mol. Cell Biol.* **6,** 306–317
5. Chuang, P. T., and McMahon, A. P. (1999) *Nature* **397,** 617–621
6. Lum, L., and Beachy, P. A. (2004) *Science* **304,** 1755–1759
7. Jia, J., Tong, C., and Jiang, J. (2003) *Genes Dev.* **17,** 2709–2720
8. Lum, L., Zhang, C., Oh, S., Mann, R. K., von Kessler, D. P., Taipale, J., Weis-Garcia, F., Gong, R., Wang, B., and Beachy, P. A. (2003) *Mol. Cell* **12,** 1261–1274
9. Ogden, S. K., Ascano, M., Jr., Stegman, M. A., Suber, L. M., Hooper, J. E., and Robbins, D. J. (2003) *Curr. Biol.* **13,** 1998–2003
10. Ruel, L., Rodriguez, R., Gallet, A., Lavenant-Staccini, L., and Therond, P. P. (2003) *Nat. Cell Biol.* **5,** 907–913
11. Kogerman, P., Grimm, T., Kogerman, L., Krause, D., Unden, A. B., Sandstedt, B., Toftgard, R., and Zaphiropoulos, P. G. (1999) *Nat. Cell Biol.* **1,** 312–319
12. Wang, Q. T., and Holmgren, R. A. (1999) *Development* (*Camb.*) **126,** 5097–5106
13. Sasaki, H., Hui, C., Nakafuku, M., and Kondoh, H. (1997) *Development* (*Camb.*) **124,** 1313–1322
14. Kinzler, K. W., and Vogelstein, B. (1990) *Mol. Cell. Biol.* **10,** 634–642
15. Jiang, J., and Struhl, G. (1995) *Cell* **80,** 563–572
16. Lepage, T., Cohen, S. M., Diaz-Benjumea, F. J., and Parkhurst, S. M. (1995) *Nature* **373,** 711–715
17. Li, W., Ohlmeyer, J. T., Lane, M. E., and Kalderon, D. (1995) *Cell* **80,** 553–562
18. Pan, D., and Rubin, G. M. (1995) *Cell* **80,** 543–552
19. Strutt, D. I., Wiersdorff, V., and Mlodzik, M. (1995) *Nature* **373,** 705–709
20. Chen, Y., Gallaher, N., Goodman, R. H., and Smolik, S. M. (1998) *Proc. Natl. Acad. Sci. U. S. A.* **95,** 2349–2354
21. Wang, G., Wang, B., and Jiang, J. (1999) *Genes Dev.* **13,** 2828–2837
22. Jia, J., Amanai, K., Wang, G., Tang, J., Wang, B., and Jiang, J. (2002) *Nature* **416,** 548–552
23. Aza-Blanc, P., Ramirez-Weber, F. A., Laget, M. P., Schwartz, C., and Kornberg, T. B. (1997) *Cell* **89,** 1043–1053
24. Kiger, J. A., Jr., and O'Shea, C. (2001) *Genetics* **158,** 1157–1166
25. Jia, J., Tong, C., Wang, B., Luo, L., and Jiang, J. (2004) *Nature* **432,** 1045–1050
26. Zhang, C., Williams, E. H., Guo, Y., Lum, L., and Beachy, P. A. (2004) *Proc. Natl. Acad. Sci. U. S. A.* **101,** 17900–17907
27. Wang, B., Fallon, J. F., and Beachy, P. A. (2000) *Cell* **100,** 423–434
28. Ruiz i Altaba, A. (1999) *Development* (*Camb.*) **126,** 3205–3216
29. Zhu, Y., James, R. M., Peter, A., Lomas, C., Cheung, F., Harrison, D. J., and Bader, S. A. (2004) *Cancer Lett.* **207,** 205–214
30. Ma, X., Chen, K., Huang, S., Zhang, X., Adegboyega, P. A., Evers, B. M., Zhang, H., and Xie, J. (2005) *Carcinogenesis* **26,** 1698–1705
31. Ma, X., Sheng, T., Zhang, Y., Zhang, X., He, J., Huang, S., Chen, K., Sultz, J., Adegboyega, P. A., Zhang, H., and Xie, J. (2006) *Int. J. Cancer* **118,** 139–148
32. Dahmane, N., Lee, J., Robins, P., Heller, P., and Ruiz i Altaba, A. (1997) *Nature* **389,** 876–881
33. Bonifas, J. M., Pennypacker, S., Chuang, P. T., McMahon, A. P., Williams, M., Rosenthal, A., De Sauvage, F. J., and Epstein, E. H., Jr. (2001) *J. Invest. Dermatol* **116,** 739–742
34. Xie, J., Aszterbaum, M., Zhang, X., Bonifas, J. M., Zachary, C., Epstein, E., and McCormick, F. (2001) *Proc. Natl. Acad. Sci. U. S. A.* **98,** 9255–9259
35. Toftgard, R. (2000) *Cell Mol. Life Sci.* **57,** 1720–1731
36. Regl, G., Neill, G. W., Eichberger, T., Kasper, M., Ikram, M. S., Koller, J., Hintner, H., Quinn, A. G., Frischauf, A. M., and Aberger, F. (2002) *Oncogene* **21,** 5529–5539
37. Athar, M., Li, C., Tang, X., Chi, S., Zhang, X., Kim, A. L., Tyring, S. K., Kopelovich, L., Hebert, J., Epstein, E. H., Jr., Bickers, D. R., and Xie, J. (2004) *Cancer Res.* **64,** 7545–7552
38. Cheng, X., Ma, Y., Moore, M., Hemmings, B. A., and Taylor, S. S. (1998) *Proc. Natl. Acad. Sci. U. S. A.* **95,** 9849–9854
39. He, N., Li, C., Zhang, X., Sheng, T., Chi, S., Chen, K., Wang, Q., Vertrees, R., Logrono, R., and Xie, J. (2005) *Mol. Carcinog* **42,** 18–28
40. Stecca, B., Mas, C., and Ruiz i Altaba, A. (2005) *Trends Mol. Med.* **11,** 199–203
41. Laurenza, A., Sutkowski, E. M., and Seamon, K. B. (1989) *Trends Pharmacol. Sci.* **10,** 442–447
42. Pavletich, N. P., and Pabo, C. O. (1993) *Science* **261,** 1701–1707
43. Harreman, M. T., Kline, T. M., Milford, H. G., Harben, M. B., Hodel, A. E., and Corbett, A. H. (2004) *J. Biol. Chem.* **279,** 20613–20621

Available online at www.sciencedirect.com
SCIENCE DIRECT®
ELSEVIER
Cancer Letters xx (xxxx) 1–7
CANCER Letters
www.elsevier.com/locate/canlet

Activation of the hedgehog pathway in a subset of lung cancers

Sumin Chi [a,1], Shuhong Huang [b,1], Chengxin Li [a,1], Xiaoli Zhang [b], Nonggao He [a], Manoop S. Bhutani [c], Dennie Jones [c], Claudia Y. Castro [d], Roberto Logrono [d], Abida Haque [d], Joseph Zwischenberger [e], Stephen K. Tyring [f], Hongwei Zhang [a,*], Jingwu Xie [b,*]

[a] *School of Life Sciences, Institute of Developmental Biology, Shandong University, Jinan, People's Republic of China*
[b] *Department of Pharmacology, Sealy Centers for Cancer Cell Biology, University of Texas Medical Branch, 301 University Boulevard, Galveston, TX 77555-1048, USA*
[c] *Department of Internal Medicine, Sealy Centers for Cancer Cell Biology, University of Texas Medical Branch, 301 University Boulevard, Galveston, TX 77555-1048, USA*
[d] *Department of Pathology, Sealy Centers for Cancer Cell Biology, University of Texas Medical Branch, 301 University Boulevard, Galveston, TX 77555-1048, USA*
[e] *Department of Surgery, Sealy Centers for Cancer Cell Biology, University of Texas Medical Branch, 301 University Boulevard, Galveston, TX 77555-1048, USA*
[f] *Department of Dermatology, University of Texas Health Science Center, Houston, TX 77030, USA*

Received 12 July 2005; received in revised form 19 October 2005; accepted 28 November 2005

Abstract

Activation of the hedgehog pathway is reported in lung cancer, but its frequency remains unknown. We examine activation of this pathway in lung cancers by in situ hybridization and immunohistochemstry, and find that less than 10% of the tumors have elevated hedgehog target gene expression. We further identify a cell line NCI-H209 and two primary tumors with no detectable Su(Fu), a negative regulator of the pathway. Ectopic expression of Su(Fu) in NCI-H209 cells down-regulates hedgehog target gene expression and leads to inhibition of cell proliferation. These data indicate that activation of the hedgehog pathway is activated through Shh over-expression or Su(Fu) inactivation in only a subset of lung cancers.

Keywords: Hedgehog; Lung cancer; Gli1; Su(Fu); PTCH1

1. Introduction

The hedgehog pathway plays a critical role in embryonic development and tissue formation, including foregut [1]. Targeted deletions of sonic hedgehog, Gli2 or Gli3 result in foregut malformation and embryo lethality in mice [2–4]. Secreted Hh molecules bind to the receptor patched (PTC-PTCH1, PTCH2), thereby alleviating PTC-mediated suppression of smoothened (SMO), a putative seven-transmembrane protein. SMO signaling triggers a cascade of intracellular events,

Abbreviations PTC, patched; PTCH1, human patched gene 1; NSCLC, non-small cell lung cancer; shh, sonic hedgehog; BCC, basal cell carcinoma; Su(Fu), suppressor of fused.

* Corresponding authors. Tel.: +1 409 747 1845; Fax: +1 409 747 1938.
E-mail addresses: zhw@sdu.edu.cn (H. Zhang), jinxie@utmb.edu (J. Xie).

[1] These authors contributed equally to this work.

0304-3835/$ - see front matter © 2005 Published by Elsevier Ireland Ltd.
doi:10.1016/j.canlet.2005.11.036

leading to activation of the pathway through GLI-dependent transcription [5,6]. Activation of Hh signaling, through loss-of-function mutations of PTCH1 or activated mutations of SMO, occurs frequently in human basal cell carcinomas (BCCs) and medulloblastomas [7–16]. More recently, abnormal activation of the sonic hedgehog pathway has been reported in subsets of small cell lung cancer, pancreatic cancer, prostate cancer, and gastrointestinal (GI) cancers [17–23].

Lung cancer is the leading cause of cancer-related death, claiming more than 150,000 lives every year in the US alone (which exceeds the combined mortality from breast, prostate, and colorectal cancers). Patients with advanced stage of lung cancer, which represents 75% of all new cases, have a median survival time of only 10 months. Thus, identifying an effective biomarker for early diagnosis of lung cancer is the first essential step to reduce the mortality. Activation of hedgehog signaling was reported in five of 10 small cell lung cancers and four of 40 non-small cell lung cancers (NSCLC) [17]. To determine if hedgehog signaling activation can be utilized for diagnosis and treatment of lung cancer, we performed a comprehensive study to assess hedgehog pathway activation in specimens from 172 lung cancer patients and five patients without lung cancer by in situ hybridization and immunohistochemistry.

2. Materials and methods

2.1. Patient material

A total of 177 patients (172 lung cancer patients and five patients without cancer) were included in our study with approval of Institutional Research Board. Specimens from 96 patients were received as discarded materials from University of Texas Medical Branch Surgical Pathology and the Shan Dong Qi Lu Hospital, Jinan, China. Lung cancers and the matched lung tissues were collected from each patient whenever possible. For tumors without matched normal tissues, a portion of lung tissue surrounding the tumor was used. Pathology reports and H&E stained slides from each specimen were reviewed to determine the nature of the disease and the tumor histology [24]. The randomly sorted samples with masked identity were evaluated by at least two independent certified pathologists. Lung cancers were divided into the following subtypes: adenocarcinoma, squamous cell carcinoma, alveolar cell carcinoma, adenosquamous cell carcinomas, large cell carcinoma, small cell carcinoma and carcinoid. For tissue microarray, we have triplicates for each specimen [25]. Both tumor tissues and the matched normal tissues (or the surrounding tissues) were included in our study.

In addition, we purchased a tissue microarray of lung cancer from Chaoying Biotechnology Co. Ltd (Xi'an, China), which contains 81 informative specimens (including five non-cancerous lung tissues as controls). Analyzes of these specimens were described in each experimental method.

2.2. In situ hybridization

Using probes for Gli1, PTCH1 and HIP was performed in specimens listed in Supplementary Table 1 according to our previously published protocol [26,27]. Matched normal lung tissues or tissues surrounding tumors were also included in the study. Sense and antisense probes were obtained by T3 and T7 in vitro transcription using a kit from Roche (Mannheim, Germany). Blue indicated strong hybridization. As negative controls, sense probes were used in all hybridization and no positive signals were observed.

2.3. RNA isolation, quantitative PCR and northern blotting

Total RNAs were extracted using a RNA extraction kit from Promega according to the manufacturer (Promega, Madison, WI). Real-time PCR analyzes were performed according to Ma et al. [26,27]. Northern blotting was performed as previously reported [28].

2.4. Immunohistochemistry

Representative formalin-fixed and paraffin embedded tissue sections (6 μm thickness) were used for immunohistochemistry with specific antibodies to human Shh, PTCH1, Su(Fu) and HIP [Catno. 9024 for Shh and Catno. 6149 for PTCH1, Catno. 10934 for Su(Fu), Santa Cruz Biotechnology, Inc.; Catno. AF1568 for HIP antibodies, R&D Systems, Inc.]. All primary antibodies have been previously tested for immunohistostaining [22,23]. Immunohistochemistry of PTCH1 and Shh was carried out as previously reported [22,29] on specimens listed in Supplementary Tables 1 and 2. HIP protein expression was also detected by immunohistochemistry in the specimens listed in Supplementary Table 2. Detection of Su(Fu) protein was only performed in several specimens with activated hedgehog signaling.

2.5. Cell culture, colony formation assay, BrdU labeling and MTT assay

Human lung cancer cell lines (A549, H82, H187, H196, H209, H460, H661, H1299, BEAS2-B and BZR-T33) were purchased from ATCC and cultured in the recommended media from ATCC [28]. Expression of Su(Fu), under the control of the CMV promoter, in NCI-H209 cells was achieved by retrovirus-mediated gene transfer [29]. BrdU labeling was performed as previously described [29]. Flow cytometry was performed in our core facility [28].

Colorimetric MTT assay was performed according to our published protocol in the presence of 0.5% FBS [30,31].

Student's *t*-test for two samples was performed for the difference between tumor groups: $P<0.05$ was considered statistically significant.

3. Results

To assess the frequency of hedgehog signaling activation in primary lung cancers, we initially examined expression of hedgehog target genes Gli1 and PTCH1 in 81 cases of lung specimens in a tissue microarray (see Supplementary Table 1 for specimen information). Increased levels of both PTCH1 and Gli1 transcripts indicate activation of the hedgehog pathway [5].

We first detected Gli1 and PTCH1 transcripts using in situ hybridization. In agreement with a published report [17], we did not detect Gli1 and PTCH1 in normal lung tissues, suggesting that the hedgehog pathway is not normally activated in adult normal lung tissues (Fig. 1A and A′). In contrast, we detected expression of both Gli1 and PTCH1 transcripts in 8 of 76 tumor specimens (Table 1; Fig. 1B, C, B′ and C′), suggesting that activation of the hedgehog pathway occurs in a subset of lung cancers. Further analyzes indicated that activation of the hedgehog pathway is not restricted to any specific subtypes of lung cancers (see Table 1, positive tumors include three adenocarcinomas, two squamous cell carcinomas, one small cell carcinoma, one large cell carcinoma and one alveolar cell carcinoma).

Expression of PTCH1 in lung cancer specimens (see Supplementary Table 1) was further confirmed by immunohistochemistry (Fig. 1E and F) [22,23]. All tissues with detectable PTCH1 protein had elevated PTCH1 transcript. With these data, we expanded the study to include additional 96 lung cancer specimens. Immunohistochemistry using antibodies identified additional eight tumors with detectable expression of both PTCH1 and HIP [22] (Fig. 1H; Table 2; Supplementary Table 2), indicating activation of the hedgehog pathway in 8 of 96 tumors. These data confirm that activation of the hedgehog pathway occurs only in a small subset of lung cancers.

In total, we found 15 out of 172 lung cancers (8.7%) harboring activated hedgehog signaling. Due to limited number of tumors with activated hedgehog signaling (detectable expression of at least two hedgehog target genes, PTCH1, Gli1 or HIP), it was not possible to perform statistical analysis. We also examined expression of PTCH1 protein by immunohistochemistry in lung cancer metastases (lymph node and intra-lung metastases) and identified 4 of 38 metastases of NSCLC with PTCH1 positive staining, suggesting that activation of the hedgehog pathway is not specifically

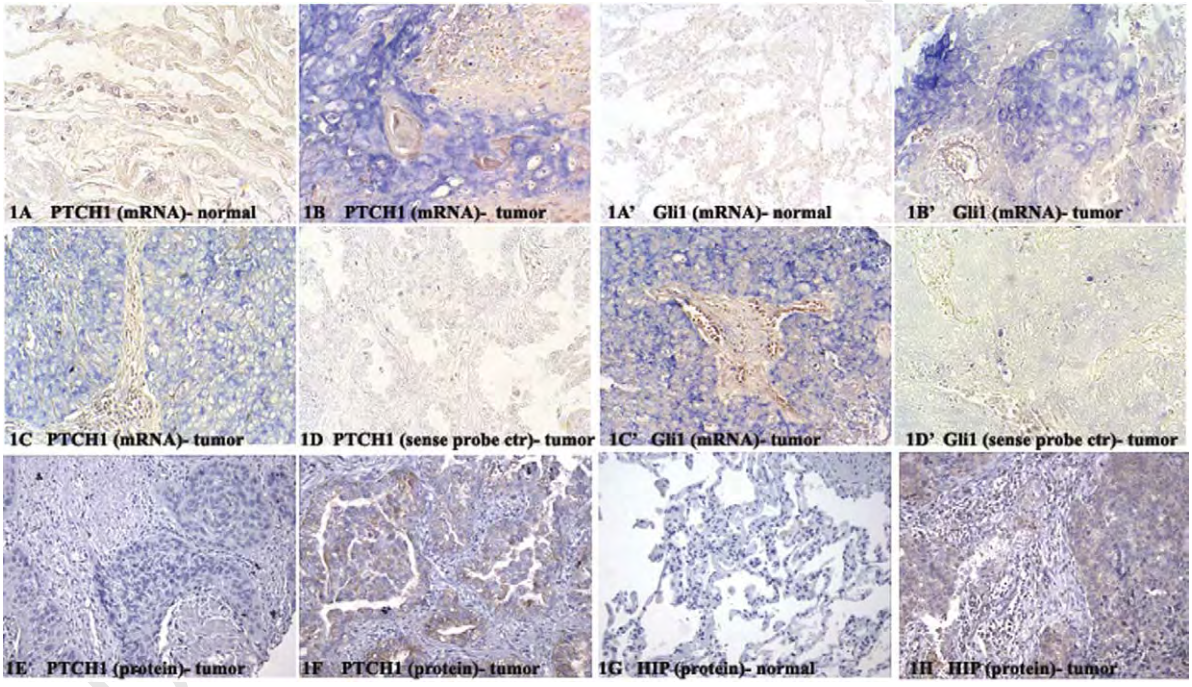

Fig. 1. Expression of hedgehog target genes in lung specimens. The levels of PTCH1 (1A–C), Gli1 (1A′–C′) transcripts (100×, blue as positive) were detected by in situ hybridization in normal and tumors (see Supplementary Table 1 for the list of specimens). The sense probe control did not give signal (see D and D′). The result was shown as '+++' for strong staining, as '++' for staining, as '+' for weak staining. Negative staining was shown as '−'. Protein expression of PTCH1 (1E and F), HIP (G and H) was detected by immunohistochemistry in all specimens with specific antibodies (see Section 2 for details, 100×) (brown–red as positive). The result was shown as '+++' for strong staining, as '++' for staining, as '+' for weak staining. Negative staining was shown as '−'. (For interpretation of the reference to colour in this legend, the reader is referred to the web version of this article.)

Table 1
Expression of Shh, PTCH1 and Gli1 in lung cancer (in situ hybridization)

	Tumor types	Total	Shh		PTCH1/Gli1	
			Positive	(%)	Positive	(%)
		76	64	84.2	8	10.5
Subtypes	Adenocarcinoma	27	21	80.8	3	11.1
	Alveolar cell carcinoma	9	7	77.8	1	11.1
	Large cell carcinoma	5	4	80.0	1	20.0
	Small cell carcinoma	10	8	80.0	1	10.0
	Squamous cell carcinoma	25	23	92.0	2	8.0
	Carcinoid	1	1		0	
Grade	Well differentiated	5	5	100	0	0
	Moderately differentiated	18	16	88.9	2	11.1
	Poorly differentiated	26	22	84.6	2	7.7
	UND[a]	27	21	77.8	4	14.8
Sex	Female	19	15	78.9	1	5.2
	Male	57	49	85.9	7	12.3

[a] Information not available.

associated with lung tumor metastases. Expression of hedgehog targets resides to the tumor nest, not to the stroma, suggesting that hedgehog signaling is not very active in the stroma, which is quite different from other situations such as during lung development [1] or in gastric cancers [27].

Next, we tested expression of molecules potentially involving in hedgehog signaling activation. It is reported that Shh over-expression is responsible for activation of the hedgehog pathway in pancreatic cancer [23], gastric cancer [18,27] and lung cancer [17]. To test this possibility, we first examined expression of Shh in lung specimens by in situ hybridization in lung cancer specimens listed in Supplementary Table 1. As expected, Shh expression was undetectable in all three normal lung tissues examined (Fig. 2A). In contrast, many primary tumors expressed Shh (Fig. 2B; Tables 1 and 2). In agreement with the in situ hybridization data, we detected Shh protein in tumors with detectable Shh transcript (Fig. 2C and D; Supplementary Table 1). Shh was detectable specifically in the tumor, not in the stroma (Fig. 2C and D), suggesting that that a paracrine signaling mechanism of sonic hedgehog does not play an important role in lung cancers. Furthermore, expression of Shh protein was also detected in specimens listed Supplementary Table 2. In all, over 73% of lung cancers had detectable Shh

Table 2
Expression of Shh, PTCH1 and HIP in lung cancer (immunohistochemistry)

	Tumor types	Total	Shh		PTCH1/Gli1	
			Positive	(%)	Positive	(%)
		96	63	65.6	8	8.3
Subtype	Adenocarcinoma	37	21	56.8	3	8.1
	Alveolar cell carcinoma	3	2		0	
	Large cell carcinoma	5	4	80.0	1	20.0
	Small cell carcinoma	3	2		0	
	Squamous cell carcinoma	42	31	73.8	4	9.5
	Carcinoid	2	1		0	
	Adenosquamous cell carcinoma	4	2		0	
Grade	Well differentiated	12	8	66.7	0	0
	Moderately differentiated	44	31	70.5	5	11.4
	Poorly differentiated	36	20	55.6	3	8.3
	UND[a]	3	3		0	
Stage	I	48	29	60.4	1	2.1
	II	24	16	66.7	3	12.5
	III/IV	20	15	75.0	4	20.0
	UND[a]	4	3		0	
Sex	Female	35	25	71.4	3	8.6
	Male	61	38	62.3	5	8.2

[a] Information not available.

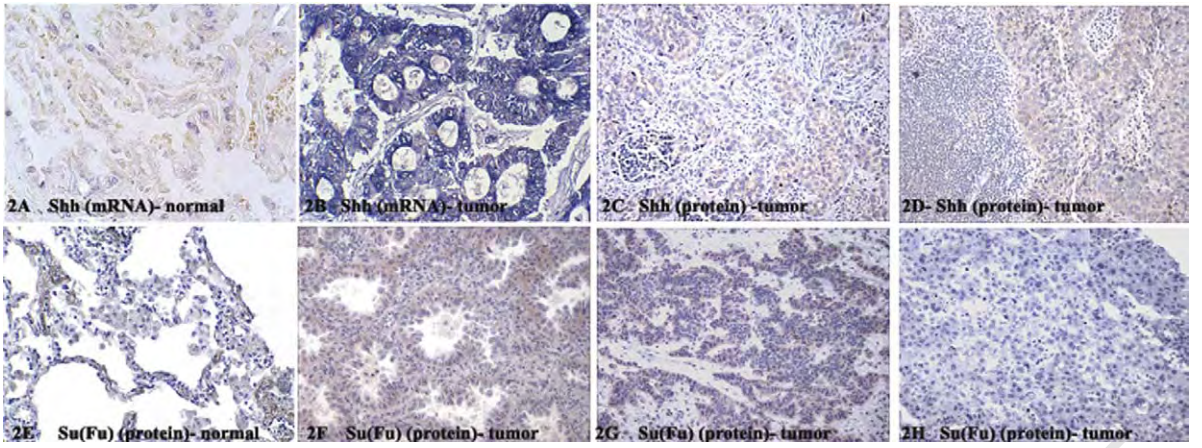

Fig. 2. Expression of Shh and Su(Fu) in lung specimens. The level of Shh transcript (A and B) was detected by in situ hybridization in the specimens listed in Supplementary Table 1 (100×, blue as positive) [25]. The proteins of Shh (C and D) and Su(Fu) (E–H) were assessed by immunohistochemistry (100×, Brown–red as positive). The result was shown as '+++' for strong staining, as '++' for staining, as '+' for weak staining. Negative staining was shown as '−'. (For interpretation of the reference to colour in this legend, the reader is referred to the web version of this article.)

expression (Tables 1 and 2). We found that expression of Shh is not always associated with expression of hedgehog target genes in lung cancers ($P = 0.8444$). Furthermore, 5 of the 16 tumors, which have detectable expression of at least two hedgehog target genes, did not have detectable expression of Shh (Supplementary Tables 1 and 2), suggesting that over-expression of Shh may be partially responsible for activating hedgehog signaling pathway in lung cancers.

To identify additional molecular mechanisms for hedgehog signaling activation, we detected expression of other components of the hedgehog pathway, including Su(Fu), a negative regulator of hedgehog signaling [32,33]. Like PTCH1, loss of Su(Fu) is reported to be responsible for hedgehog signaling activation in subset of medulloblastomas [12], prostate cancer [22] and basal cell carcinomas [11]. We found that two tumors with elevated levels of PTCH1 and Gli1 had no detectable levels of Su(Fu), one of the tumors had no Shh expression (Fig. 2E–H and Supplementary Table 2), suggesting that loss of Su(Fu) may be also responsible for hedgehog signaling activation in a small number of lung cancers.

To substantiate our findings in the tumors, we examined eight lung cancer cell lines for Su(Fu) expression and found one cell line NCI-H209 with no detectable Su(Fu) protein (Fig. 3A and Supplementary Fig. 1). Southern hybridization using Su(Fu) probe did not reveal dramatic genomic changes of the Su(Fu) gene in H209 cells (data not shown here). Northern analysis showed no detectable Su(Fu) transcript in NCI-H209 cells (Fig. 3A), indicating a possible transcriptional silencing mechanism, such as promoter methylation. Methylation of the promoter region causes gene transcription silencing, which can be reversed by 5-aza-2′-deoxycytidine. We found that Su(Fu) became detectable in NCI-H209 cells in the presence of 5-aza-2′-deoxycytidine for 6–8 days (Fig. 3B), confirming that the Su(Fu) gene was silenced through promoter methylation in these cells.

To demonstrate the tumor suppressing role of Su(Fu), we stably expressed wild type Su(Fu) in H209 cells using retrovirus-mediated gene transfer [29]. Protein expression was verified by western blot analysis (Fig. 3B). By comparison of the levels of PTCH1 and Gli1 transcripts using real-time PCR analysis [26], we found that stable expression of Su(Fu) caused dramatic reduction in hedgehog target genes GLi1 and PTCH1 (Fig. 3C), indicating that Su(Fu) is sufficient to inhibit hedgehog signaling in this cell line. To demonstrate the tumor suppressor activity of wild type Su(Fu), we performed colony formation analysis in Su(Fu) negative H209 cells. Cells with ectopic expression of wild type Su(Fu) or the control vector were selected with G418 for 2 weeks, and cell colonies were stained with violet blue. Expression of Su(Fu) caused reduction of both the colony number and the size (Fig. 3D), indicating that ectopic expression of Su(Fu) is sufficient to suppress cell proliferation of these tumor cells.

Next, we examined cell growth using MTT assay, and found that H209-Su(Fu) cells grow slower than H209-vector cells, confirming that Su(Fu) indeed can suppress cell growth (Fig. 3E). The effect of Su(Fu) on DNA synthesis was assessed with BrdU labeling (Fig. 3F). In H209 cells, we found around 24% of cells are positive for BrdU after 30 min labeling with BrdU. In contrast, we only observed that 15% of cells with stable expression of Su(Fu) were BrdU positive. The difference is significant ($P < 0.02$). In contrast, Su(Fu) has no effects on DNA synthesis of A549 cells, which have no activated hedgehog signaling (data not shown here). These data indicate that wild type Su(Fu) can inhibit DNA synthesis and cell growth in lung cancer cells.

Taken together, our findings indicate that activation of the hedgehog signaling pathway occurs only in 15 out of 172 lung cancers (8.7%) is not a very common event in lung cancer although sonic hedgehog is frequently over-expressed. Our data suggest that Shh over-expression or loss of Su(Fu) may be

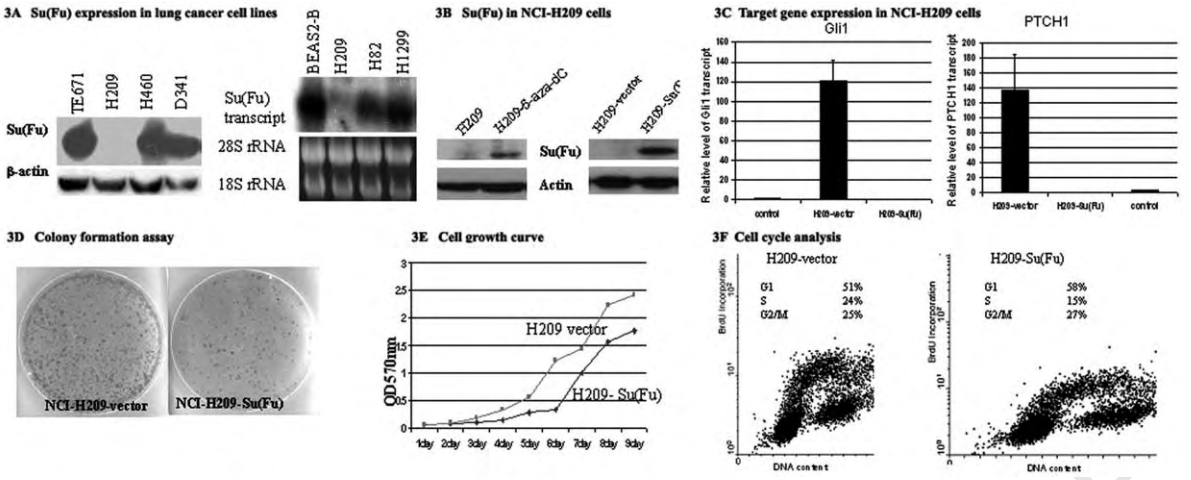

Fig. 3. Role of Su(Fu) in cancer cell lines Su(Fu) was detected by western blotting using Su(Fu) specific antibodies (see Section 2 for details). One of the eight lung cancer cell lines, NCI-H209, has no detectable Su(Fu) protein (A, also see Supplementary Fig. 1). Su(Fu) transcripts were undetectable in H209 cells by northern hybridization (A), indicating inactivation of the Su(Fu) gene. The inactivation of Su(Fu) was reversible in H209 cells in the presence of 5-aza-2′-deoxycytidine for over 6 days (B left), indicating an epigenetic mechanism of Su(Fu) silencing in these cells. Following expression of Su(Fu) in H209 cells, Su(Fu) protein was detected by western blotting (B right). Following stable expression of Su(Fu), levels of PTCH1 and Gli1 transcripts were detected by real-time PCR [25] and found to be dramatically reduced (2C), indicating that Su(Fu) expression was sufficient to suppress the hedgehog signaling pathway. In contrast, expression of Su(Fu) has no effects on A549 cells (data not shown). Colony formation assay was performed to test the role wild type Su(Fu) on cell growth in H209 cells. Cells transfected with Su(Fu) formed small and few colonies (D). To confirm this result, the cell growth curve from Su(Fu) stably expressed H209 cell line was compared with that from the control cell line (E). Su(Fu) expression slowed cell growth. Furthermore, we performed BrdU labeling in these two cell lines (F). Following BrdU labeling for 30 min, around 24% of H209-vector cells were BrdU positive. In contrast, only 15% BrdU positive cells were observed in H209-Su(Fu) cells ($P<0.02$), indicating that Su(Fu) inhibits cell growth and DNA synthesis in H209 cells.

responsible for hedgehog signaling activation in a small subset of lung cancers. Using a cell line with no detectable Su(Fu) protein, we demonstrated that expression of Su(Fu) is sufficient to inhibit the hedgehog signaling, leading to reduced DNA synthesis and inhibited cell growth. Thus, Su(Fu) inactivation appears to be another mechanism by which the hedgehog pathway is activated in subset of human lung cancer.

4. Discussion

Our data indicate that only a small proportion of lung tumors have expression of two hedgehog target genes (8.7%). We further find that loss of Su(Fu) was observed in 2 of the 16 tumors and one cell line NCI-H209, in which elevated hedgehog target genes were detected. The role of Su(Fu) is demonstrated in NCI-H209 cells. Thus, our data provide evidence that hedgehog signaling activation occurs in only a small percentage of lung cancer in which hedgehog signaling may be involved in cancer cell proliferation. Our studies further indicate that activation of the hedgehog pathway can be achieved by either Shh over-expression or Su(Fu) inactivation in a subset of lung cancer.

While activation of hedgehog signaling occurs infrequently, Shh is frequently over-expressed in lung cancers (Tables 1 and 2). Although Shh is weakly detectable in an inflammatory lung tissue (Supplementary Table 1), all three normal lung tissues had no detectable Shh, indicating that Shh expression may be a biomarker of abnormal lung pathology. Based on the fact that the target genes were not elevated in these tissues, it will be interesting to investigate the functions of Shh in preneoplastic lesions as well as in lung cancers. We speculate that Shh expression is induced during lung cancer development long before the induction of the target genes. An early report indicates that sonic hedgehog may be involved in generating progenitor cells of lung [17]. Further investigation of hedgehog expression in a large number of inflammatory lung tissues and other pathological conditions may provide additional clues of sonic hedgehog functions in lung tissues.

Acknowledgements

This research was supported by grants from the NIH (R01-CA94160, JX), Department of Defense (DOD-PC030429, JX), the NIEHS (ES06676) and National Science Foundation of China (30228031, JX and HWZ).

Supplementary Material

Supplementary data associated with this article can be found, in the online version, at doi:10.1016/j.canlet.2005.11.036.

References

[1] D. Warburton, J. Zhao, M.A. Berberich, M. Bernfield, Molecular embryology of the lung: then, now, and in the future, Am J. Physiol. 276 (1999) L697–L704.

[2] C.V. Pepicelli, P.M. Lewis, A.P. McMahon, Sonic hedgehog regulates branching morphogenesis in the mammalian lung, Curr. Biol. 8 (1998) 1083–1086.

[3] J. Motoyama, J. Liu, R. Mo, Q. Ding, M. Post, C.C. Hui, Essential function of Gli2 and Gli3 in the formation of lung, trachea and oesophagus, Nat. Genet. 20 (1998) 54–57.

[4] Y. Litingtung, L. Lei, H. Westphal, C. Chiang, Sonic hedgehog is essential to foregut development, Nat. Genet. 20 (1998) 58–61.

[5] M. Pasca di Magliano, M. Hebrok, Hedgehog signalling in cancer formation and maintenance, Nat. Rev. Cancer 3 (2003) 903–911.

[6] J. Xie, Hedgehog signaling in prostate cancer, Future Oncol. 1 (2005) 331–338.

[7] R. Toftgard, Hedgehog signalling in cancer, Cell. Mol. Life Sci. 57 (2000) 1720–1731.

[8] E. Epstein Jr, Genetic determinants of basal cell carcinoma risk, Med. Pediatr. Oncol. 36 (2001) 555–558.

[9] H. Hahn, C. Wicking, P.G. Zaphiropoulous, M.R. Gailani, S. Shanley, A. Chidambaram, et al., Mutations of the human homolog of Drosophila patched in the nevoid basal cell carcinoma syndrome, Cell 85 (1996) 841–851.

[10] R.L. Johnson, A.L. Rothman, J. Xie, L.V. Goodrich, J.W. Bare, J.M. Bonifas, et al., Human homolog of patched, a candidate gene for the basal cell nevus syndrome, Science 272 (1996) 1668–1671.

[11] J. Reifenberger, M. Wolter, C.B. Knobbe, B. Kohler, A. Schonicke, C. Scharwachter, et al., Somatic mutations in the PTCH, SMOH, SUFUH and TP53 genes in sporadic basal cell carcinomas, Br. J. Dermatol. 152 (2005) 43–51.

[12] M.D. Taylor, L. Liu, C. Raffel, C.C. Hui, T.G. Mainprize, X. Zhang, et al., Mutations in SUFU predispose to medulloblastoma, Nat. Genet. 31 (2002) 306–310.

[13] J. Xie, R.L. Johnson, X. Zhang, J.W. Bare, F.M. Waldman, P.H. Cogen, et al., Mutations of the PATCHED gene in several types of sporadic extracutaneous tumors, Cancer Res. 57 (1997) 2369–2372.

[14] J. Xie, M. Murone, S.M. Luoh, A. Ryan, Q. Gu, C. Zhang, et al., Activating smoothened mutations in sporadic basal-cell carcinoma, Nature 391 (1998) 90–92.

[15] J. Xie, R.L. Johnson, X. Zhang, J.W. Bare, F.M. Waldman, P.H. Cogen, et al., Mutations of the PATCHED gene in several types of sporadic extracutaneous tumors, Cancer Res. 57 (1997) 2369–2372.

[16] D.M. Berman, S.S. Karhadkar, A.R. Hallahan, J.I. Pritchard, C.G. Eberhart, D.N. Watkins, et al., Medulloblastoma growth inhibition by hedgehog pathway blockade, Science 297 (2002) 1559–1561.

[17] D.N. Watkins, D.M. Berman, S.G. Burkholder, B. Wang, P.A. Beachy, S.B. Baylin, Hedgehog signalling within airway epithelial progenitors and in small-cell lung cancer, Nature 422 (2003) 313–317.

[18] D.M. Berman, S.S. Karhadkar, A. Maitra, R. Montes De Oca, M.R. Gerstenblith, K. Briggs, et al., Widespread requirement for Hedgehog ligand stimulation in growth of digestive tract tumours, Nature 425 (2003) 846–851.

[19] L. Fan, C.V. Pepicelli, C.C. Dibble, W. Catbagan, J.L. Zarycki, R. Laciak, et al., Hedgehog signaling promotes prostate xenograft tumor growth, Endocrinology 145 (2004) 3961–3970.

[20] S.S. Karhadkar, G. Steven Bova, N. Abdallah, S. Dhara, D. Gardner, A. Maitra, et al., Hedgehog signalling in prostate regeneration, neoplasia and metastasis, Nature 431 (2004) 707–712.

[21] P. Sanchez, A.M. Hernandez, B. Stecca, A.J. Kahler, A.M. DeGueme, A. Barrett, et al., Inhibition of prostate cancer proliferation by interference with SONIC HEDGEHOG-GLI1 signaling, Proc. Natl Acad. Sci. USA 101 (2004) 12561–12566.

[22] T. Sheng, C. Li, X. Zhang, S. Chi, N. He, K. Chen, et al., Activation of the hedgehog pathway in advanced prostate cancer, Mol. Cancer 3 (2004) 29.

[23] S.P. Thayer, M.P. Di Magliano, P.W. Heiser, C.M. Nielsen, D.J. Roberts, G.Y. Lauwers, et al., Hedgehog is an early and late mediator of pancreatic cancer tumorigenesis, Nature 425 (2003) 851–856.

[24] A.K. Haque, W. Au, N. Cajas-Salazar, S. Khan, A.W. Ginzel, D.V. Jones, et al., CYP2E1 polymorphism, cigarette smoking, p53 expression, and survival in non-small cell lung cancer: a long term follow-up study, Appl. Immunohistochem. Mol. Morphol. 12 (2004) 315–322.

[25] J. Xie, Identifying biomarkers of lung cancer in the post-genomic era, Curr. Pharmacogenomics 3 (2005) 265–274.

[26] X. Ma, K. Chen, S. Huang, X. Zhang, P.A. Adegboyega, B.M. Evers, et al., Frequent activation of the hedgehog pathway in advanced gastric adenocarcinomas, Carcinogenesis 26 (2005) 1698–1705.

[27] X. Ma, K. Chen, S. Huang, X. Zhang, T. Sheng, P. Adegboyega, et al., Frequent activation of the hedgehog pathway in advanced gastric adenocarcinomas, Carcinogenesis (2005).

[28] N. He, C. Li, X. Zhang, T. Sheng, S. Chi, K. Chen, et al., Regulation of lung cancer cell growth and invasiveness by beta-TRCP, Mol. Carcinog. 42 (2005) 18–28.

[29] J. Xie, M. Aszterbaum, X. Zhang, J.M. Bonifas, C. Zachary, E. Epstein, et al., A role of PDGFRalpha in basal cell carcinoma proliferation, Proc. Natl Acad. Sci. USA 98 (2001) 9255–9259.

[30] C. Li, S. Chi, N. He, X. Zhang, O. Guicherit, R. Wagner, et al., IFNalpha induces Fas expression and apoptosis in hedgehog pathway activated BCC cells through inhibiting Ras-Erk signaling, Oncogene 23 (2004) 1608–1617.

[31] M. Athar, C. Li, X. Tang, S. Chi, X. Zhang, A.L. Kim, et al., Inhibition of smoothened signaling prevents ultraviolet B-induced basal cell carcinomas through regulation of fas expression and apoptosis, Cancer Res. 64 (2004) 7545–7552.

[32] P. Kogerman, T. Grimm, L. Kogerman, D. Krause, A.B. Unden, B. Sandstedt, et al., Mammalian suppressor-of-fused modulates nuclear-cytoplasmic shuttling of Gli-1, Nat. Cell Biol. 1 (1999) 312–319.

[33] D.M. Stone, M. Murone, S. Luoh, W. Ye, M.P. Armanini, A. Gurney, et al., Characterization of the human suppressor of fused, a negative regulator of the zinc-finger transcription factor Gli, J. Cell Sci. 112 (Pt 23) (1999) 4437–4448.

Carcinogenesis vol.27 no.7 pp.1334–1340, 2006
doi:10.1093/carcin/bgi378
Advance Access publication February 25, 2006

Activation of the hedgehog pathway in human hepatocellular carcinomas

Shuhong Huang[2,†], Jing He[†], Xiaoli Zhang[†], Yuehong Bian[2], Ling Yang[2], Guorui Xie[2], Kefei Zhang[3], Wendell Tang[1], Arwen A.Stelter, Qian Wang[3], Hongwei Zhang[2] and Jingwu Xie[*]

Department of Pharmacology and Toxicology, Sealy Center for Cancer Cell Biology and [1]Department of Pathology, University of Texas Medical Branch, 301 University Boulevard, Galveston, TX 77555-1048, USA, [2]Institute of Developmental Biology, School of Life Sciences, Shandong University, Jinan, P.R. China and [3]Department of Hepatobiliary Surgery, The First Affiliated Hospital, Sun Yat-Sen University, 58 Zhongshan Road, Guangzhou, 510080, P.R. China

[*]To whom correspondence should be addressed. Tel: (409) 747 1845; Fax: (409) 747 1938;
Email: jinxie@utmb.edu; wangqian_dr@126.com; zhw@sdu.edu.cn

Liver cancers, the majority of which are hepatocellular carcinomas (HCCs), rank as the fourth in cancer mortality worldwide and are the most rapidly increasing type of cancer in the United States. However, the molecular mechanisms underlying HCC development are not well understood. Activation of the hedgehog pathway is shown to be involved in several types of gastrointestinal cancers. Here, we provide evidence to indicate that hedgehog signaling activation occurs frequently in HCC. We detect expression of *Shh*, *PTCH1* and *Gli1* in 115 cases of HCC and in 44 liver tissues adjacent to the tumor. Expression of *Shh* is detectable in about 60% of HCCs examined. Consistent with this, hedgehog target genes *PTCH1* and *Gli1* are expressed in over 50% of the tumors, suggesting that the hedgehog pathway is frequently activated in HCCs. Of five cell lines screened, we found Hep3B, Huh7 and PLC/PRF/5 cells with detectable hedgehog target genes. Specific inhibition of hedgehog signaling in these three cell lines by smoothened (SMO) antagonist, KAAD-cyclopamine, or with Shh neutralizing antibodies decreases expression of hedgehog target genes, inhibits cell growth and results in apoptosis. In contrast, no effects are observed after these treatments in HCC36 and HepG2 cells, which do not have detectable hedgehog signaling. Thus, our data indicate that hedgehog signaling activation is an important event for development of human HCCs.

Abbreviations: DMEM, Dulbecco-modified essential medium; FBS, fetal bovine serum; HCCs, hepatocellular carcinomas; MTT, 1-(4,5-Dimethylthiazol-2-yl)-3,5-diphenylformazan; PCR, polymerase chain reaction; RT–PCR, reverse transcription–polymerase chain reaction; SMO, smoothened; TUNEL, terminal deoxynucleotidyl transferase-mediated dUTP nick end labeling.

[†]These authors contributed equally to this work.

Introduction

Liver cancer, with hepatocellular carcinoma (HCC) as the major tumor type, is a malignancy of worldwide significance (1–4). HCC ranks as the eighth cause of cancer-related death in American men with 14 000 deaths yearly and is the most rapidly increasing type of cancer in the United States (2). The medical oncology community is largely unprepared for this looming epidemic of HCC. Although the increase of HCC in the United States is correlated with the increasing prevalence of chronic infection with hepatitis C virus (HCV), the molecular understanding of HCC development remains elusive (2). A majority (70–85%) of patients present with advanced or unresectable disease, making the prognosis of HCC dismal, and systemic chemotherapy is quite ineffective in HCC treatment. The first essential step for development of effective therapeutic approaches is to identify specific signaling pathways involved in HCC.

The role of the hedgehog pathway in human cancers has been established through studies of basal cell nevus syndrome (BCNS) (5,6), a rare hereditary disorder with a high risk of basal cell carcinomas, and activation of the hedgehog pathway has been observed in other cancers such as prostate cancer and gastrointestinal cancers (7–17). Targeted inhibition of the hedgehog pathway results in growth inhibition in cancer cell lines with activated hedgehog signaling (10–17). The hedgehog pathway is essential for embryonic development, tissue polarity and cell differentiation (18). The hedgehog pathway is critical in the early development of the liver and contributes to differentiation between hepatic and pancreatic tissue formation, but the adult liver normally does not have detectable levels of hedgehog signaling (10,19). In this report, we characterize expression of sonic hedgehog and its target genes in 115 HCC specimens. The role of hedgehog signaling on cell growth is further demonstrated in five HCC cancer cell lines.

Materials and methods

Tissue samples

A total of 115 specimens of HCC tissues were used. Of these, 14 specimens were received as discarded materials from General Surgery of the Shan Dong Qi Lu Hospital, Jinan, China. Pathology reports and H&E stained sections of each specimen were reviewed to determine the nature of the disease and the tumor histology. The remaining 101 HCC specimens were from Sun Yat-Sen University. Forty-four liver tissues adjacent to the tumor were also included in this study. None of the patients had received chemotherapy or radiation therapy prior to specimen collection.

In situ hybridization

In situ hybridization was performed according to the manufacture's instructions (Roche Molecular Biochemicals, Indianapolis, IN) and our published protocol

(16,17). In brief, tissues were fixed with 4% paraformaldehyde in phosphate buffered saline (PBS) and embedded with paraffin. Then 6 μm thick tissue sections were mounted onto Poly-L-Lysine slides. Samples were treated with proteinase K (20 μg/ml) at 37°C for 15 min, refixed in 4% paraformaldehyde and hybridized overnight with a digoxigenin-labeled RNA probe (at a final concentration of 1 μg/ml). The hybridized RNA was detected by alkaline phosphatase-conjugated anti-digoxigenin antibodies (Roche Molecular Biochemicals, Indianapolis, IN), which catalyzed a color reaction with the substrate NBT/BCIP (Roche Molecular Biochemicals). Blue signal indicated positive hybridization. We regarded tissues without blue signals as negative. As negative controls, sense probes were used in the hybridization and no signals were observed. *In situ* hybridizations were repeated at least twice for each tissue sample with similar results.

RNA isolation and quantitative RT–PCR

Total RNA of cells was extracted using a RNA extraction kit from Promega according to the manufacturer (Promega, Madison, WI), and quantitative PCR analyses were performed according to a previously published procedure (17,20). Triplicate C_T values were analyzed in Microsoft Excel using the comparative $C_T(\Delta\Delta C_T)$ method as described by the manufacturer (Applied Biosystems, Foster City, CA). The amount of target ($2^{-\Delta\Delta CT}$) was obtained by normalization to an endogenous reference (18S RNA) and relative to a calibrator. We used the following primers for RT–PCR of *Shh*: forward primer—5′-ACCGAGGGCTGGGACGAAGA-3′; reverse primer—5′-ATTTGGCCGCCACCGAGTT -3′

Cell culture, transfection and drug treatment

HCC cell lines [Hep3B, HepG2, HCC36, PLC/PRF/5 (as PLC throughout this manuscript) and Huh7] were generously provided by Drs Chiaho Shih, Tien Ko and Kui Li at UTMB. All cells were cultured in Dulbecco-modified essential medium (DMEM) with 10% FBS and antibiotics. Cells were treated with 2 μM KAAD-cyclopamine, a specific antagonist of smoothened (SMO) (21) (dissolved in DMSO as 5 mM stock solution, Cat# K171000 from Toronto Research Chemicals, Canada), in 0.5% FBS in DMEM for indicated time mentioned in the figure legends. Previously, we performed toxicity assay with KAAD-cyclopamine in GI cancer cells and found that 10 μM of KAAD-cyclopamine can lead to non-specific toxicity (16). In fact, 5 or 10 μM KAAD-cyclopamine was quite toxic to cells regardless of hedgehog signaling status (our unpublished observation), and was, thus, not used in this study. Tomatidine (2 μM in 0.5% FBS DMEM, Sigma Cat# T2909), a structurally similar compound with non-specific inhibition on hedgehog signaling, was used as a negative control. In addition, the specific inhibition of hedgehog signaling in HCC cells was achieved by addition of Shh neutralizing antibodies (1 μg/ml in 0.5% FBS DMEM, Cat# SC-9024, Santa Cruz Biotechnology, Santa Cruz, CA). Most cell lines were treated with KAAD-cyclopamine (2μM) or Shh antibodies (1 μg/ml) in 0.5% FBS in DMEM medium for an indicated time (see figure legends for details). However, for Hep3B cells, we used 2% FBS in DMEM because Hep3B cells cannot grow in 0.5% FBS DMEM medium. Transient transfection of Gli1 in HCC cells was performed using LipofectAmine according to manufacturer's recommendation (Plasmid:LipofectAmine = 1:2.5). Cells with ectopic expression of Gli1 were subjected to drug treatment and to TUNEL (terminal deoxynucleotidyl transferase-mediated dUTP nick end labeling) assay.

Cell viability and TUNEL assays

For cell viability analysis, we used two methods: Trypan blue analysis and MTT assay. Trypan blue analysis was performed according to a procedure from the manufacturer (Invitrogen, CA) (22). The percentage of trypan blue positive cells (dead cells) was calculated under a microscope and triplicates of samples for each treatment were used. The experiment was repeated three times. MTT assay was performed using a previously published procedure (22). In brief, triplicates of samples for each treatment were used in a 96-well format. Twenty microliters of MTT (10 mg/ml in PBS) was added to each well (containing 100 μl cultured medium, 0.5% FBS DMEM in this study). Three hours later, medium was aspirated, and 100 μl of a mixture of isopropanol and DMSO (9:1) added into each well. Thirty minutes later, the 570 nm absorbance was measured with a microplate reader from Molecular Devices Co Sunnyvale, CA. BrdU labeling was for 1 h and immunofluorescent staining of BrdU was performed as reported previously (23). TUNEL assay was performed using a kit from Roche Biochemicals according to a published procedure (24). In brief, cells were fixed with 4% paraformaldehyde at room temperature for 1 h and permeated with 0.1% Triton X-100, 0.1% sodium citrate (freshly prepared) on ice for 2 min. After washing with PBS, each sample was incubated with 50 μl of TUNEL reaction mixture at 37°C for 30 min. TUNEL label solution (without enzyme) was used as a negative control. TUNEL positive cells were counted under a fluorescent microscope. The counting was repeated three times, and the percentage from each counting was calculated.

Statistical analysis

Statistical analysis was performed by Binomial proportions analysis. The association of mRNA transcript expression with various clinicopathological parameters was also analyzed; a P-value < 0.05 was considered to be statistically significant.

Results

Expression of PTCH1 and Gli1 in primary HCC

In order to assess hedgehog signaling activation in HCC, we assayed *PTCH1* and *Gli1* expression in 115 cases of HCC specimens. As the target genes of the hedgehog pathway, expression of *PTCH1* and *Gli1* transcripts indicate hedgehog signaling activation (25,26). Primarily, we used *in situ* hybridization to assess hedgehog signaling activation in our collected tissues ($n = 115$), which was further confirmed in selected specimens by real-time PCR. The results are summarized in Table I.

For *in situ* hybridization analysis, blue signal was regarded as detectable expression of the target. Tissues without blue signals were regarded as negative for the target. Using *in situ* hybridization, 79 of 110 (70%) tumor specimens had detectable expression of *Gli1* (representative images are shown in Figure 1A, and summarized in Table I, with additional images and data provided in Supplementary Table 1 and Supplementary Figures 1–6), indicating that *Gli1* expression is detectable in many HCCs. The sense probe gave no detectable signals (Figure 1A), confirming the specificity of *in situ* hybridization in our experiments. In most cases, *Gli1* expression was detectable in the tumor nest, not in the adjacent liver tissue (Figure 1A; Supplementary Figure 1 and Table 1) or in the stroma (arrows in Figure 1A).

In comparison with the *Gli1* transcript, the *in situ* hybridization signal of *PTCH1* was generally less intense (Figure 1B and Supplementary Figures 1–6), but 56% (60 of 107) of HCC specimens were positive for *PTCH1* transcript. We found a total of 51 tumors (out of 98 informative HCCs) (52%) with detectable expression of both *Gli1* and *PTCH1* (Table I, Supplementary Table 1), which suggests activated hedgehog signaling in these specimens. Our analysis indicates that activation of hedgehog signaling (as indicated by expression of both *Gli1* and *PTCH1* transcripts) occurs more frequently in HCC than in the adjacent liver tissue (Table I, Supplementary Table 1 and Supplementary Figure 1). There are several cases in which only *Gli1* or *PTCH1* was expressed (Supplementary Table 1), suggesting that expression of *Gli1* and *PTCH1* may be differentially regulated. Further analysis of our data did not reveal association of the hedgehog signaling activation with tumor size or tumor differentiation (Table I). Tumors with hepatocirrhosis were not significantly different from tumors without hepatocirrhosis in the expression of *Gli1* and *PTCH1* (Table I).

In situ hybridization data was further confirmed by real-time PCR in several tumor specimens in which 70% of the tissue mass was actually tumor tissue (Figure 1C and D). Consistent with *in situ* hybridization, expression of *Gli1* and *PTCH1* were detectable in the tumor, not in the adjacent liver tissue in most cases (will be discussed later in the Discussion). Our data indicate that expression of *Gli1* and *PTCH1* in the tumor was 3- to 30-fold higher than that in adjacent liver tissues (Figure 1C and D). The real-time PCR analyses further confirmed that activation of the hedgehog pathway is a common event in HCC.

Table I. Detection of *Shh*, *PTCH1* and *Gli1* expression in HCC and in adjacent liver tissue by *in situ* hybridization

	Shh			Hedgehog pathway activation						
				PTCH1		*Gli1*		Pathway activation		
	pos	neg	*P*-value	pos	neg	pos	neg	pos	neg	*P*-value
HCC	64/108	44/108	<0.01*	60/107	47/107	79/110	31/110	51/98	47/98	<0.01*
Adjacent tissues	5/41	36/41		18/43	25/43	15/44	29/44	9/43	34/43	
Tumor size										
Small (<3 cm)	16/31	15/31	0.316	17/31	14/31	25/32	7/32	16/31	15/31	0.896
Large (>3 cm)	46/74	28/74		42/74	32/74	52/75	23/75	35/66	31/66	
Tumor differentiation										
Well	34/52	18/52	0.107	30/51	21/51	43/52	9/52	29/51	22/51	0.264
Mod-poor	20/41	21/41		22/41	19/41	32/43	11/43	19/42	23/42	
Sex										
Male	47/81	34/81	0.651	43/81	38/81	58/83	25/83	35/72	37/72	0.258
Female	17/27	10/27		17/26	9/26	21/27	6/27	16/26	10/26	
Hepatocirrhosis										
+	14/19	5/19	0.163	14/20	6/20	14/20	6/20	11/17	6/17	0.251
–	49/87	38/87		43/83	40/83	63/87	24/87	39/79	40/79	

Statistical analysis was performed by Binomial proportions analysis. A P-value < 0.05 was considered to be statistically significant. The association of mRNA transcript expression with various clinicopathological parameters was also analyzed. Statistically significant difference was indicated by asterisk (*).

pos, positive signal; neg, negative signal; well, well-differentiated tumors; mod-poor, moderately to poorly differentiated tumors. Elevated expression of at least two hedgehog target genes was regarded as being positive (pos) in activation of the hedgehog pathway, whereas elevated expression of one hedgehog target gene was regarded as being negative (neg) in hedgehog signaling activation.

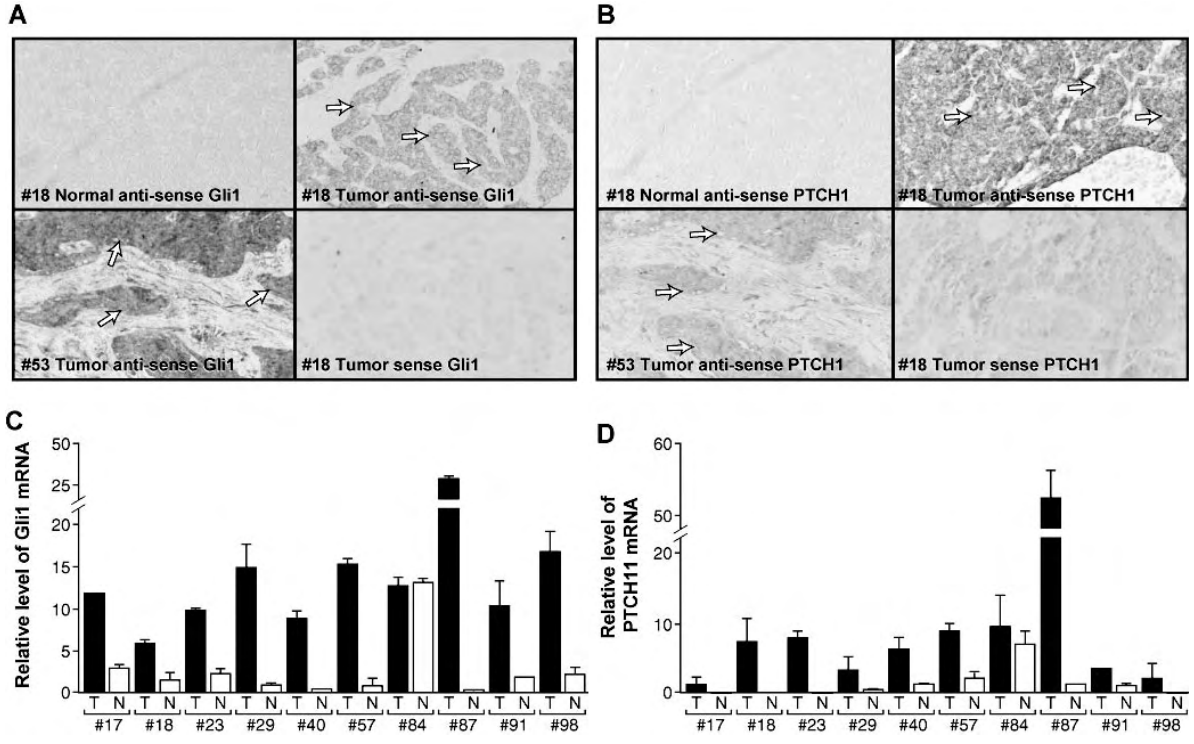

Fig. 1. Detection of *Gli1*, *PTCH1* expression in primary HCCs. *In situ* hybridization detection of *Gli1* (**A**) and *PTCH1* (**B**) transcripts in HCCs was performed as reported previously. Positive signals (dark grey staining) were observed in the tumor ('Tumor', tumor nests indicated by arrows), not in the stroma surrounding the tumor nests or in the liver tissue adjacent to the tumor ('Normal'). The sense probes did not give any positive signals (A and B), confirming the specificity of our *in situ* hybridization. Additional pictures have been included in the Supplementary Figures. Expression of *Gli1* and *PTCH1* was further confirmed by real-time PCR analysis done in triplicate (**C** and **D**) in selected tumor specimens in which 70% of the tissue mass was tumor tissue. Expression of *Gli1* (C) and *PTCH1* (D) from the tumor (T) was 3- to 30-fold higher than that from the adjacent liver tissue (N). Data indicates values relative to 18S RNA and to a calibrator. The data from this analysis are consistent with those from *in situ* hybridization analysis.

Expression of Shh in HCCs

To investigate if *Shh* is associated with hedgehog signaling activation in HCCs, *Shh* expression was first detected by *in situ* hybridization. We detected *Shh* transcripts in 64 of 108 HCC specimens, but not in the majority of liver tissues adjacent to the tumor (Figure 2A, Table I and Supplementary Figures 1, 4–6). *Shh* transcript was only detectable in the tumor nests, not in the stroma (dark grey signals in Figure 2A), suggesting that

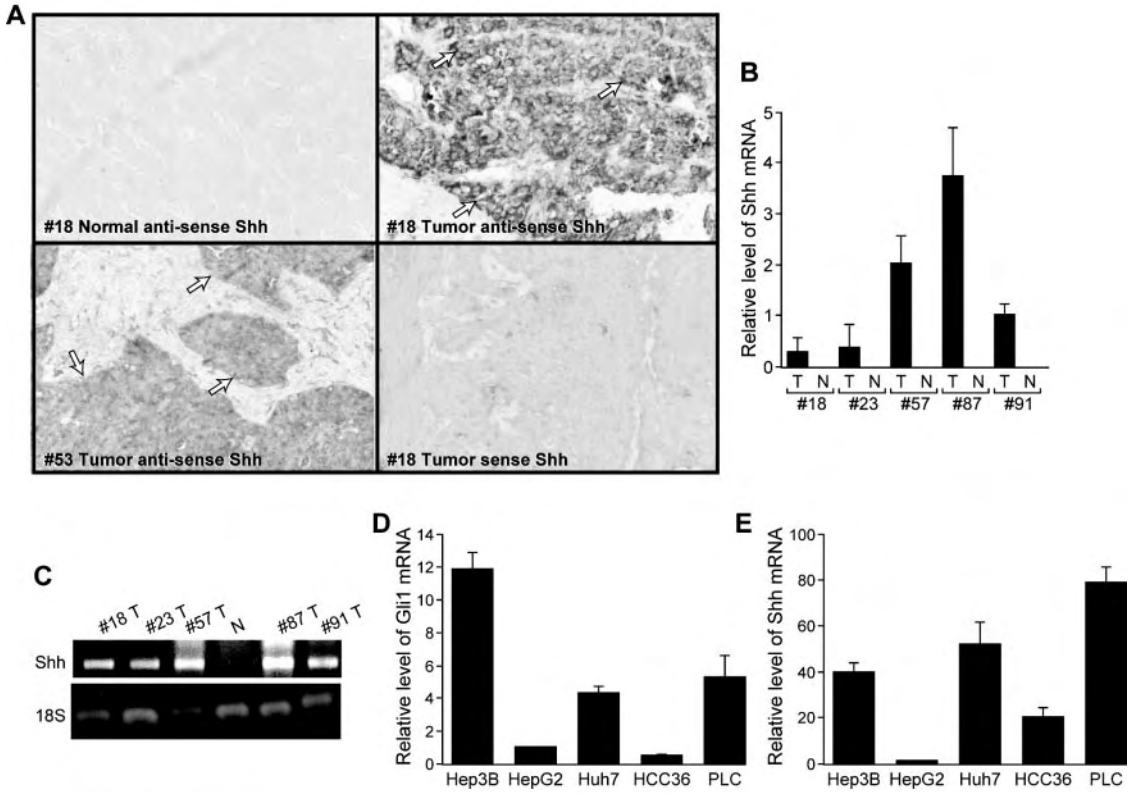

Fig. 2. Detection of *Shh* expression in HCCs. *In situ* hybridization (**A**), real-time PCR (**B**) and regular RT–PCR (**C**) were used to detect *Shh* transcript. *Shh* transcript (dark grey signals in A) resided in the tumor ('Tumor', tumor nests indicated by black arrows), not the stromal or adjacent liver tissue ('Normal') (A), suggesting that the tumor tissue is the major source for *Shh* expression. To confirm our *in situ* hybridization results, we used real-time PCR to detect *Shh* expression (B), which was further confirmed by RT–PCR (C). Shh transcripts were detected only in the tumor (T), not in the adjacent liver tissue (N). Tumors with detectable *Gli1* and *PTCH1* transcripts all had detectable *Shh*, suggesting a major role of *Shh* for activation of the hedgehog pathway in HCCs. Additional real-time PCR experiments showed a relatively high level of *Gli1* (**D**), *PTCH1* (not shown here) and *Shh* (**E**) in three HCC cell lines: Hep3B, Huh7 and PLC. Data indicates values relative to 18S RNA and to a calibrator.

cancer cells are the major source of *Shh* expression. Almost all tumors with detectable *Gli1* and *PTCH1* expression had detectable *Shh* transcript (Figures 1 and 2, Supplementary Table 1, Supplementary Figures 5 and 6). *Shh* expression in the tumor was further confirmed by real-time PCR and regular RT–PCR (Figure 2B and C). Thus, it appears that *Shh* induction may be the trigger for activated hedgehog signaling in HCCs. In support of this hypothesis, we detected expression of *Shh* in all three HCC cell lines with detectable transcript of *Gli1* (Figure 2D and E).

Targeted inhibition of hedgehog signaling in HCC cells

SMO is the major signal transducer of the hedgehog pathway; thus cancer cells with activated hedgehog signaling through *Shh* expression should be sensitive to treatment with the SMO antagonist, KAAD-cyclopamine (Toronto Research Chemicals, Cat# K171000, Toronto, Canada) (21). First, we screened HCC cell lines for hedgehog signaling activation by real-time PCR detection of *Gli1* and *PTCH1* and found that hedgehog signaling pathway was activated in Hep3B, PLC and Huh7 cells but not in HepG2 and HCC36 cells (Figure 2D shows the level of *Gli1* transcript). Addition of KAAD-cyclopamine (2 μM) greatly decreased the level of *Gli1* transcript in three cell lines (Hep3B, PLC and Huh7) (Figure 3A), whereas no changes on *Shh* expression were observed (Supplementary Figure 7). The closely related compound tomatidine, which does not affect SMO signaling and thus served as a negative control, had little discernible effect on hedgehog target genes. This data indicates specific inhibition of the hedgehog pathway by KAAD-cyclopamine in these cells.

As a result of inhibited hedgehog signaling by KAAD-cyclopamine treatment, we observed an inhibition on cell growth of Huh7 cells, but not on that of HepG2 cells (Figure 3B and C). The specificity of hedgehog signaling inhibition was further demonstrated using Shh neutralizing antibodies (Figure 3B and C). We found that addition of Shh antibodies at a concentration of 1 μg/ml reduced cell growth of Huh7 cells but had no effect on HepG2 cells (Figure 3B and C). Further analysis indicates that BrdU incorporation was also reduced after treatment with KAAD-cyclopamine in Huh7 cells (see Supplementary Figure 8).

Following treatment with KAAD-cyclopamine or Shh antibodies, we found that PLC cells underwent apoptosis whereas no apoptosis was observed in HepG2 cells (Figure 4A shows data from KAAD-cyclopamine treatment). Data from TUNEL assay was confirmed by Trypan blue staining (data not shown here). The percentage of apoptotic cells varied from cell line to cell line, with PLC being the most sensitive cell line (over 20% TUNEL positive cells after KAAD-cyclopamine treatment for 8 h, Figure 4B). Similar data were also observed after Shh antibody treatment (data not shown here). These data demonstrate that the HCC cells with activated hedgehog signaling are sensitive to targeted inhibition of the hedgehog pathway, whereas other HCC

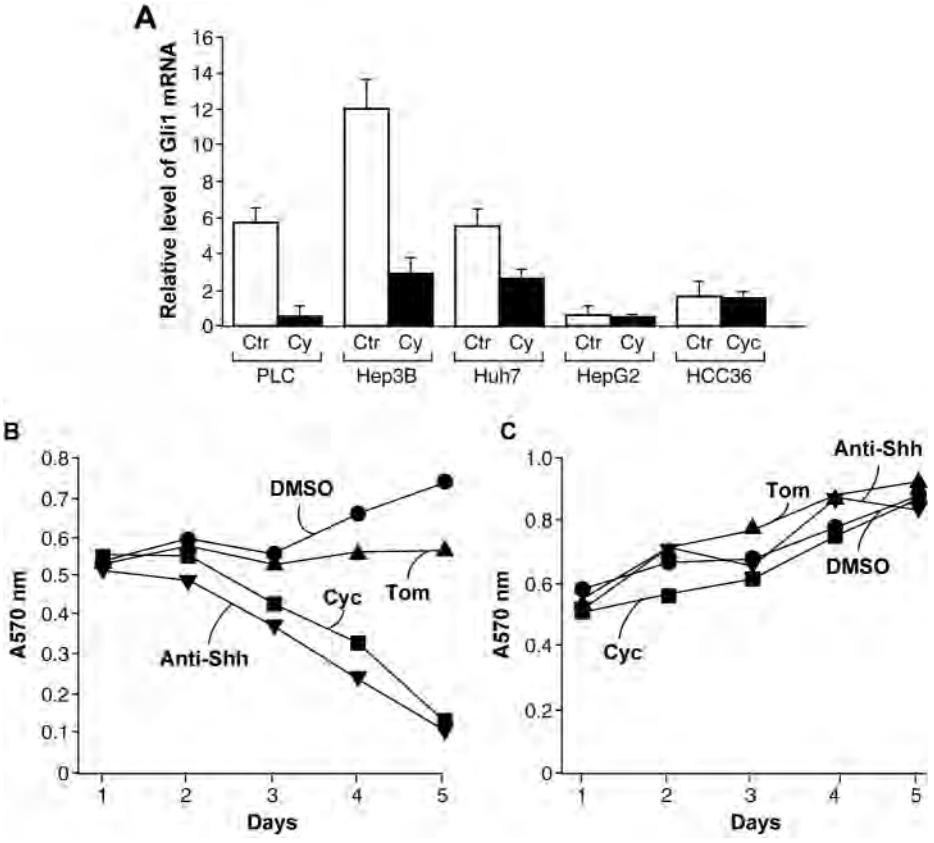

Fig. 3. Hedgehog signaling and growth of HCC cells. Real-time PCR data of *Gli1* transcript shows that in the presence of 2 μM KAAD-cyclopamine (**A**) or 1 μg/ml Shh neutralizing antibodies (data not shown here) for 12 h (see Materials and methods for details on drug-treatment conditions), the level of hedgehog target gene *Gli1* was decreased in the three cell lines with activated hedgehog signaling (PLC, Hep3B and Huh7). In contrast, no effects were observed in HCC36 and HepG2 cells, in which hedgehog signaling is not activated. Cell growth of Huh7 (**B**) and HepG2 (**C**) cell lines were examined by MTT assay. Huh7 cells were inhibited by 2 μM KAAD-cyclopamine (Cat# K317000, Toronto Research Chemicals) or 1 μg/ml Shh neutralizing antibodies (Cat# 9024, Santa Cruz Biotechnology) (Figure 2B). This inhibition was specific because addition of tomatidine, a structurally similar but non-specific compound for hedgehog signaling, did not affect cell growth. In contrast, cell growth of HepG2 was not affected by KAAD-cyclopamine (2 μM) or Shh neutralizing antibodies (1 μg/ml) (C), confirming the specific growth inhibition of HCC cells through targeted inactivation of hedgehog signaling.

cells (without activated hedgehog signaling) are resistant to these treatments.

Because KAAD-cyclopamine and Shh antibodies only affect signaling upstream of SMO, we hypothesize that cells with ectopic expression of the downstream effector Gli1 may prevent KAAD-cyclopamine-mediated apoptosis if these treatments are specific to the hedgehog pathway. In Huh7 cells, we transiently expressed Gli1 under the control of the CMV promoter (pLNCX vector) (23). After KAAD-cyclopamine treatment, we found that all Gli1-expressing cells ($n = 500$) were negative for TUNEL, demonstrating the specificity of KAAD-cyclopamine. Similarly, Gli1-expressing Huh7 cells were resistant to Shh antibody treatment (data not shown). This study also suggests that downregulation of *Gli1* may be an important mechanism by which targeted inhibition of hedgehog signaling mediates apoptosis in HCC cells.

Taken together, our findings indicate that activation of the hedgehog pathway is quite common in liver cancers. Expression of *Shh* and its target genes, *Gli1* and *PTCH1*, is more frequent in the tumor than in the adjacent liver tissue. This activation of hedgehog signaling is not associated with other clinicopathological parameters of the tumor. HCC cells with activation of the hedgehog pathway are sensitive to targeted inhibition of hedgehog signaling. These data support our hypothesis that activation of the hedgehog pathway is an important event in the development of HCC.

Discussion

Hedgehog signaling in liver cancer

Over 500 000 new cases of liver cancers are reported each year worldwide; most of them are HCCs. Most of HCC patients (70–80%) are diagnosed late in the progression of the disease and cannot be effectively treated. Understanding the molecular mechanisms underlying liver cancer development is an essential first step in early diagnosis of liver cancer. In this report, we present strong evidence to indicate that the hedgehog pathway is frequently activated in liver cancers. Our data further indicate that induced expression of *Shh* may be the major trigger for activated hedgehog signaling in HCCs. How was *Shh* expression induced in HCC? Our preliminary data indicate that the Shh promoter activity is high in Huh7 cells but low in HepG2 cells (our unpublished observation), suggesting that transcriptional upregulation of the *Shh* gene may be the major mechanism for induced expression of *Shh*.

Since hedgehog signaling is frequently activated in HCCs, markers for hedgehog signaling activation, including *Shh*, *PTCH1* and *Gli1*, may be useful for diagnosis of liver cancers. In most cases, *Gli1* and *PTCH1* were expressed in the tumor,

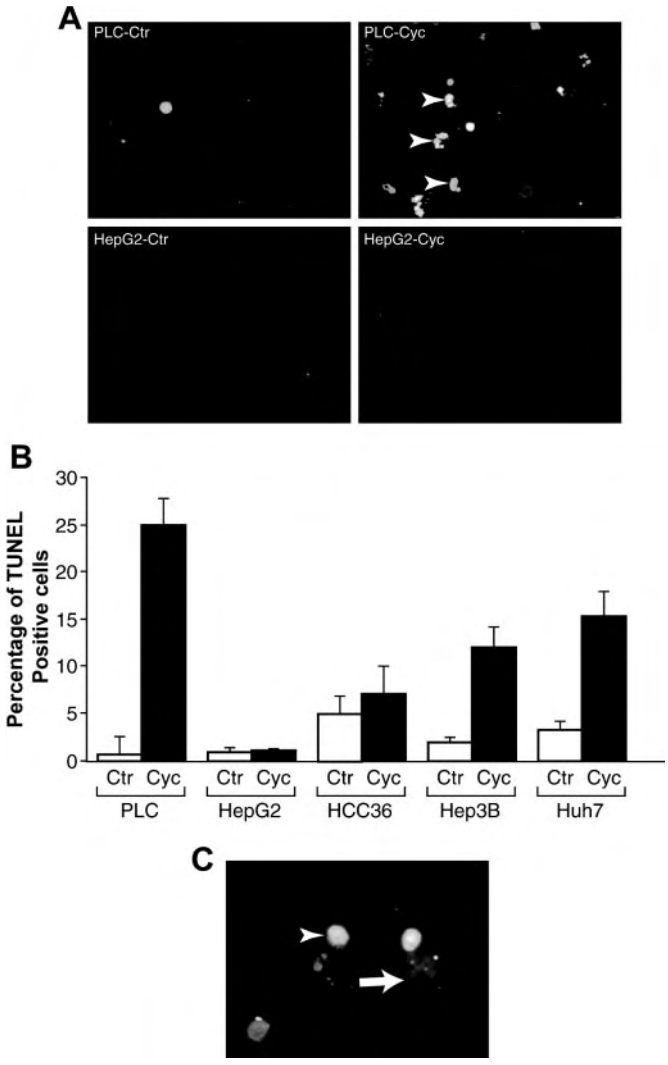

Fig. 4. Targeted inhibition of hedgehog signaling induces apoptosis in hepatocellular carcinoma cells. TUNEL assays (**A**) for detection of apoptosis were measured after treatment with 2 μM KAAD-cyclopamine (Cat# K317000, Toronto Research Chemicals) in PLC (8 h) and in HepG2 (36 h). During treatment, we used 0.5% FBS in DMEM for cell culture. TUNEL positive cells (light grey, indicated by arrowheads) were observed in PLC cells after KAAD-cyclopamine treatment. The percentages of TUNEL positive cells in all five cell lines are quantified in **B.** Please note that different cell lines have different sensitivities to KAAD-cyclopamine. Whereas treatment of 2 μM KAAD-cyclopamine for 8 h was sufficient to induce cell death in PLC cells, a longer treatment was needed for Hep3B (48 h) and Huh7 cells (36 h) (also see Materials and methods for drug treatment). TUNEL positive cells ($n = 500$) were counted under a fluorescent microscope, and the experiment was repeated three times with similar results. TUNEL assays following ectopic Gli1 expression and KAAD-cyclopamine treatment (**C**) demonstrated that cells positive for ectopic Gli1 expression [dark grey staining, detection by c-myc tag as reported previously (27)] were TUNEL negative. Gli1 was expressed in Huh7 cells under the control of the CMV promoter. Transfected cells were treated with 2 μM KAAD-cyclopamine or 2 μM tomatidine in 0.5% FBS in DMEM for 48 h. We found that Gli1-expressing cells ($n = 500$) were all TUNEL negative.

not in the liver tissues adjacent to the tumor. However, in nine cases, we detected expression of *Gli1* and *PTCH1* in both the tumor and the adjacent liver tissues, which were confirmed by real-time PCR in one case (#84) (see Supplementary Table 1 for details). Further analysis indicated that tissue abnormalities were present in these adjacent liver tissues with expression of *Gli1* and *PTCH1*, ranging from small cell dysplasia, dysplastic nodules to microscopic HCCs. In contrast, a non-cancerous liver tissue (as shown in supplementary Figures 2E, 3E and 4E) did not have any detectable expression of *Shh*, *PTCH1* and *Gli1*. Thus, it appears that hedgehog signaling activation occurs in early lesions of HCCs. Further studies of hedgehog signaling in different stages of HCCs, particularly early stages, will establish the basis for early diagnosis of HCC through detection of *Gli1*, *PTCH1* and *Shh*.

Another important pathway involved in HCC is the Wnt pathway via mutations of β-catenin or axin (28–31). We have investigated the association of hedgehog signaling with the Wnt pathway in liver cancer. We detected β-catenin protein localization by immunohistochemistry in tumors with activated hedgehog signaling. Only 1 in 20 tumors with hedgehog signaling activation had nuclear β-catenin, a major indicator for the canonical Wnt signaling, suggesting that hedgehog signaling activation may be a distinct abnormality from β-catenin activation in HCCs.

Therapeutic perspective of liver cancer through targeted inhibition of the hedgehog pathway

Our studies also indicate that targeted inhibition of hedgehog signaling may be effective in treatment of HCCs. We demonstrate in this report that SMO antagonist, KAAD-cyclopamine, or Shh neutralizing antibodies specifically induce apoptosis in HCC cells with activated hedgehog signaling. The hedgehog pathway is not activated in HepG2 cells, and these cells are not sensitive to these reagents. In our studies, variable sensitivities were observed in different cell lines. For PLC cells, treatment with 2 μM KAAD-cyclopamine for 8 h caused apoptosis in many cells. In contrast, a similar rate of cell death was observed in Huh7 cells after treatment (2 μM KAAD-cyclopamine) for 36 h. This difference may be due to other genetic alterations in different cell lines. Further understanding of the molecular basis for cell sensitivity to KAAD-cyclopamine will help us to design better ways to treat HCC in the future. Thus, it may be possible in the future to treat the subsets of liver cancer with hedgehog signaling inhibitors (e.g. KAAD-cyclopamine).

While this manuscript is being reviewed, two other groups have reported similar data on hedgehog signaling in HCCs (32,33).

Supplementary material

Supplementary material is available at: http://www.carcin.oxfordjournals.org/

Acknowledgements

This research was supported by grants from the NIH (R01-CA94160), Department of Defense (DOD-PC030429), The NIEHS (ES06676) and National Science Foundation of China (30228031). We thank Drs Chiaho Shih, Tien Ko and Kui Li for providing cell lines for this study and Huiping Guo for technical support in real-time PCR analysis and Karen Martin for help with the manuscript. Funding to pay the Open Access publication charges for this article was provided by National Cancer Institute (R01-CA94160).

Conflict of Interest Statement: None declared.

References

1. Bruix,J., Boix,L., Sala,M. and Llovet,J.M. (2004) Focus on hepatocellular carcinoma. *Cancer Cell*, **5**, 215–219.

2. El-Serag,H.B. and Mason,A.C. (2000) Risk factors for the rising rates of primary liver cancer in the United States. *Arch. Intern. Med.*, **160**, 3227–3230.
3. Pisani,P., Parkin,D.M., Bray,F. and Ferlay,J. (1999) Estimates of the worldwide mortality from 25 cancers in 1990. *Int. J. Cancer*, **83**, 18–29.
4. Srivatanakul,P., Sriplung,H. and Deerasamee,S. (2004) Epidemiology of liver cancer: an overview. *Asian Pac. J. Cancer Prev.*, **5**, 118–125.
5. Johnson,R.L., Rothman,A.L., Xie,J. *et al.* (1996) Human homolog of patched, a candidate gene for the basal cell nevus syndrome. *Science*, **272**, 1668–1671.
6. Hahn,H., Wicking,C., Zaphiropoulous,P.G. *et al.* (1996) Mutations of the human homolog of Drosophila patched in the nevoid basal cell carcinoma syndrome. *Cell*, **85**, 841–851.
7. Raffel,C., Jenkins,R.B., Frederick,L., Hebrink,D., Alderete,B., Fults,D.W. and James,C.D. (1997) Sporadic medulloblastomas contain PTCH mutations. *Cancer Res.*, **57**, 842–845.
8. Xie,J., Johnson,R.L., Zhang,X. *et al.* (1997) Mutations of the PATCHED gene in several types of sporadic extracutaneous tumors. *Cancer Res.*, **57**, 2369–2372.
9. Watkins,D.N., Berman,D.M., Burkholder,S.G., Wang,B., Beachy,P.A. and Baylin,S.B. (2003) Hedgehog signalling within airway epithelial progenitors and in small-cell lung cancer. *Nature*, **422**, 313–317.
10. Berman,D.M., Karhadkar,S.S., Maitra,A. *et al.* (2003) Widespread requirement for Hedgehog ligand stimulation in growth of digestive tract tumours. *Nature*, **425**, 846–851.
11. Thayer,S.P., Di Magliano,M.P., Heiser,P.W. *et al.* (2003) Hedgehog is an early and late mediator of pancreatic cancer tumorigenesis. *Nature*, **425**, 851–856.
12. Fan,L., Pepicelli,C.V., Dibble,C.C. *et al.* (2004) Hedgehog signaling promotes prostate xenograft tumor growth. *Endocrinology*, **145**, 3961–3970.
13. Sanchez,P., Hernandez,A.M., Stecca,B. *et al.* (2004) Inhibition of prostate cancer proliferation by interference with SONIC HEDGEHOG-GLI1 signaling. *Proc. Natl Acad. Sci. USA*, **101**, 12561–12566.
14. Karhadkar,S.S., Bova,G.S., Abdallah,N., Dhara,S., Gardner,D., Maitra,A., Isaacs,J.T., Berman,D.M. and Beachy,P.A. (2004) Hedgehog signalling in prostate regeneration, neoplasia and metastasis. *Nature*, **431**, 707–712.
15. Sheng,T., Li,C.-X., Zhang,X., Chi,S., He,N., Chen,K., McCormick,F., Gatalica,Z. and Xie,J. (2004) Activation of the hedgehog pathway in advanced prostate cancer. *Mol. Cancer*, **3**, 29.
16. Ma,X., Sheng,T., Zhang,Y. *et al.* (2006) Hedgehog signaling is activated in subsets of esophageal cancers. *Int. J. Cancer*, **118**, 139–148.
17. Ma,X., Chen,K., Huang,S., Zhang,X., Adegboyega,P.A., Evers,B.M., Zhang,H. and Xie,J. (2005) Frequent activation of the hedgehog pathway in advanced gastric adenocarcinomas. *Carcinogenesis*, **26**, 1698–1705.
18. Ingham,P.W. (1998) Transducing hedgehog: the story so far. *EMBO J*, **17**, 3505–3511.
19. Deutsch,G., Jung,J., Zheng,M., Lora,J. and Zaret,K.S. (2001) A bipotential precursor population for pancreas and liver within the embryonic endoderm. *Development*, **128**, 871–881.
20. Chi,S., Huang,S., Li,C. *et al.* (2006) Activation of the hedgehog pathway in a subset of lung cancers. *Cancer Lett.* Epub January 27, 2006.
21. Chen,J.K., Taipale,J., Cooper,M.K. and Beachy,P.A. (2002) Inhibition of Hedgehog signaling by direct binding of cyclopamine to Smoothened. *Genes Dev.*, **16**, 2743–2748.
22. Li,C., Chi,S., He,N., Zhang,X., Guicherit,O., Wagner,R., Tyring,S. and Xie,J. (2004) IFNalpha induces Fas expression and apoptosis in hedgehog pathway activated BCC cells through inhibiting Ras-Erk signaling. *Oncogene*, **23**, 1608–1617.
23. Xie,J., Aszterbaum,M., Zhang,X., Bonifas,J.M., Zachary,C., Epstein,E. and McCormick,F. (2001) A role of PDGFRalpha in basal cell carcinoma proliferation. *Proc. Natl Acad. Sci. USA*, **98**, 9255–9259.
24. Athar,M., Li,C-X, Chi,S. *et al.* (2004) Inhibition of smoothened signaling prevents ultraviolet B-induced basal cell carcinomas through induction of fas expression and apoptosis. *Cancer Res.*, **64**, 7545–7552.
25. Pasca di Magliano,M. and Hebrok,M. (2003) Hedgehog signalling in cancer formation and maintenance. *Nat. Rev. Cancer*, **3**, 903–911.
26. Xie,J. (2005) Hedgehog signaling in prostate cancer. *Future Oncol.*, **1**, 331–338.
27. Sheng,T., Chi,S., Zhang,X. and Xie,J. (2006) Regulation of Gli1 localization by the cAMP/protein kinase A signaling axis through a site near the nuclear localization signal. *J. Biol. Chem.*, **281**, 9–12.
28. Taniguchi,K., Roberts,L.R., Aderca,I.N. *et al.* (2002) Mutational spectrum of beta-catenin, AXIN1, and AXIN2 in hepatocellular carcinomas and hepatoblastomas. *Oncogene*, **21**, 4863–4871.
29. Satoh,S., Daigo,Y., Furukawa,Y. *et al.* (2000) AXIN1 mutations in hepatocellular carcinomas, and growth suppression in cancer cells by virus-mediated transfer of AXIN1. *Nat. Genet.*, **24**, 245–250.
30. Miyoshi,Y., Iwao,K., Nagasawa,Y., Aihara,T., Sasaki,Y., Imaoka,S., Murata,M., Shimano,T. and Nakamura,Y. (1998) Activation of the beta-catenin gene in primary hepatocellular carcinomas by somatic alterations involving exon 3. *Cancer Res.*, **58**, 2524–2527.
31. de La Coste,A., Romagnolo,B., Billuart,P. *et al.* (1998) Somatic mutations of the beta-catenin gene are frequent in mouse and human hepatocellular carcinomas. *Proc. Natl Acad. Sci. USA*, **95**, 8847–8851.
32. Patil,M.A., Zhang,J., Ho,C., Cheung,S.T., Fan,S.T. and Chen,X. (2006) Hedgehog signaling in human hepatocellular carcinoma. *Cancer Biol. Ther.*, **5**, 111–117.
33. Sicklick,J.K., Li,Y.X., Jayaraman,A. *et al.* (2005) Dysregulation of the hedgehog pathway in human hepatocarcinogenesis. *Carcinogenesis* Epub December 8, 2005.

Received September 1, 2005; revised February 4, 2006; accepted February 19, 2006

PO Box 2345, Beijing 100023, China
www.wjgnet.com
wjg@wjgnet.com

World J Gastroenterol 2007 March 21; 13(11): 1659-1665
World Journal of Gastroenterology ISSN 1007-9327

Sonic hedgehog-Gli1 pathway in colorectal adenocarcinomas

Yue-Hong Bian, Shu-Hong Huang, Ling Yang, Xiao-Li Ma, Jing-Wu Xie, Hong-Wei Zhang

Yue-Hong Bian, Shu-Hong Huang, Ling Yang, Xiao-Li Ma, Hong-Wei Zhang, Institute of Developmental Biology, College of Life Science, Shandong University, Jinan 250100, Shandong Province, China
Jing-Wu Xie, Sealy Centers for Cancer Cell Biology, Department of Pharmacology and Toxicology, University of Texas Medical Branch, Galveston, Texas 77555-1048, United States
Supported by the grants from National Natural Science Foundation of China, No. 30228031, No. 30671072
Correspondence to: Dr. Hong-Wei Zhang, Institute of Developmental Biology, College of Life Science, Shandong University, Jinan 250010, Shandong Province, China. zhw@sdu.edu.cn
Telephone: +86-531-88364935 Fax: +86-531-88565610
Received: 2006-10-09 Accepted: 2007-01-30

Abstract

AIM: To determine the role of Sonic hedgehog (Shh) pathway in colorectal adenocarcinomas through analysis of the expression of Shh pathway-related molecules, Shh, Ptch1, hedgehog-interacting protein (Hip), Gli1, Gli3 and PDGFRα.

METHODS: Expression of Shh in 25 colorectal adenocarcinomas was detected by RT-PCR, *in situ* hybridization and immunohistochemistry. Expression of Ptch1 was observed by *in situ* hybridization and immunohistochemistry. Expression of Hip, Gli1, Gli3 and PDGFRα was analyzed by *in situ* hybridization.

RESULTS: Expression of cytokeratin AE1/AE3 was observed in the cytoplasm of colorectal crypts. Members of the Hh signaling pathway were expressed in colorectal epithelium. Shh was expressed in cytoplasm of dysplastic epithelial cells, while expression of Ptch1, Hip and Gli1 were mainly detected in the malignant crypts of adenocarcinomas. In contrast, PDGFRα was expressed highly in aberrant crypts and moderately in the stroma. Expression of Gli3 could not be detected in colorectal adenocarcinomas.

CONCLUSION: These data suggest that Shh-Ptch1-Gli1 signaling pathway may play a role in the progression of colorectal tumor.

Key words: Sonic hedgehog pathway; Sonic hedgehog; Ptch1; Hedgehog-interacting protein; Gli1; Gli3; PDGFRα; Colorectal adenocarcinomas

Bian YH, Huang SH, Yang L, Ma XL, Xie JW, Zhang HW. Sonic hedgehog-Gli1 pathway in colorectal adenocarcinomas. *World J Gastroenterol* 2007; 13(11): 1659-1665

http://www.wjgnet.com/1007-9327/13/1659.asp

INTRODUCTION

Hedgehog (Hh) signaling plays key roles in embryonic organ patterning, cell differentiation and cell proliferation during embryonic development. Hh signaling is essential for the development of the limb, lung, brain and foregut. Single hedgehog gene in *Drosophila* and three hedgehog genes, Sonic (Shh), Indian (Ihh) and Desert (Dhh) in vertebrates have been identified. All three Hh proteins in vertebrates appear to be processed by the same mechanism, use the same receptors and can elicit similar biological responses, but their relative potencies differ in an assay-dependent manner[1-3]. Hhs bind to receptor Patched (Ptch), a 12-transmembrane protein. Ptch acts to inhibit the 7-transmembrane protein Smoothened (Smo), rendering the pathway inactive in the absence of Hh ligand. After binding of Hh to Ptch, the repression of Smo is released and the target genes (e.g. Ptch1, Gli, PDGFRα, Wnts, CyclinD1 and Bmp) are activated[4,5]. The Hh signaling is negatively regulated by a hedgehog-interacting protein (Hip), which is also inducible by hedgehog and is lost in hedgehog mutant[6].

In the mouse, both Shh and Ihh are expressed in the gut endoderm and have been shown to participate in radial axis patterning of the gut[7]. Recent studies have shown that Shh is expressed in the normal adult human gut[8]. Aberrant activation of Hh signaling pathway has been shown to cause the occurrence of basal-cell carcinoma (BCC) and medulloblastoma, and mutations of Hh pathway components have been found both in familial and sporadic cases[9-12]. More recently, small-cell lung cancer (SCLC), prostate cancer and pancreatic adenocarcinoma have been linked to Hh signaling pathway, providing a molecular mechanism for these aggressive diseases[13-15]. Dysregulation of Hh signaling pathway may also play a role in gastrointestinal (GI) tumors[16,17]. To better understand the mechanism of colorectal adenocarcinoma, a common cancer worldwide, we examined here the expression of several key molecules functioned in the Hh signaling pathway at protein and mRNA levels.

MATERIALS AND METHODS

Meterials

Twenty five tissue specimens of colorectal adenocarcinomas were obtained from Shandong Qilu Hospital, Jinan, China with approval from the local ethics research committee. Five of the 25 samples also included non-cancerous colorectal tissue as normal control. All of the samples were fixed in 4% paraformaldehyde with PBS at 4℃ overnight. The samples were dehydrated in gradated ethanol and stored in 70% ethanol at -20℃. The samples were embedded in paraffin and sectioned (6 μm). The sections were stained with H&E. Each sample was reviewed and confirmed by pathologists based on the clinical characteristics.

Immunohistochemistry

Immunohistochemistry was performed according to the protocol described by Ma *et al*[16,17]. Antigen unmasking was achieved by boiling sections in 0.01 mol/L sodium citrate; pH 6.0, for 10 min. Tissues were blocked in 10% sheep serum twice and incubated for 2 h at 37℃ with primary antibodies. Antibodies were applied at the following dilutions: Shh, and Ptch1 (1:100; Cat# 9024 for Shh and Cat# 6149 for Ptch1, Santa Cruz Biotechnology Inc, Santa Cruz, CA), PCNA (1:100; Santa Cruz Biotechnology, Inc., Santa Cruz, CA), cytokeratin AE1/AE3. (MAB 0049, Maixin Biotechnology, Inc., China). Negative controls were performed in all cases by omitting the first antibodies. All primary antibodies have been previously tested for immun ohistostaining[18].

In situ hybridization

The sense and antisense digoxigenin-labeled RNA probes were made using a DIG RNA labeling kit and following the manufacturer's instructions (Boehringer Mannherm). The *in situ* hybridization was performed as described previously[16,17]. In brief, rehydrated sections were treated with proteinase K (20 μg/mL) for 20 min and refixed in 4% paraformaldehyde with PBS for 5 min. Sections were washed with 50% formamide in 2 × SSC at 37℃ for 2 h and hybridization was performed at 42℃ overnight with 5 μg/mL of digoxigenin-labeled probe in the following hybridization buffer: 40% formamide, 10% dextran sulfate, 1 × Denhardt's solution, 1 mg/mL yeast RNA, 10 mmol/L Dithiothreit, and 4 × SSC. Washes were done in 4 × SSC, 2 × SSC, 20 μg/mL RNase A, 1 × SSC, 0.1 × SSC at 37℃, 3 × 15 min, and then in buffer 1 (100 mmol/L Tris-Cl, 150 mmol/L NaCl, pH 7.5). Sections were incubated for 30 min in blocking buffer -2% goat serum, 0.1% TritonX-100 in buffer 1 and left overnight at room temperature in alkaline phosphatase-conjugated anti-digoxigenin antibody (Roche) at 1:500 dilution in blocking buffer. Washes were done in buffer 2 (100 mmol/L Tris-Cl, 100 mmol/L NaCl, 50 mmol/L $MgCl_2$, pH 7.5) and 3 (100 mmol/L Tris-Cl, 100 mmol/L NaCl, 50 mmol/L $MgCl_2$, pH 9.5), 2 × 10 min. Color reaction was performed in the NBT/BCIP (Roche) solution containing 10 mmol/L levamisole in the dark. Blue staining indicated strong hybridization. Sense probes were used in all hybridization as negative controls and no positive signals were observed.

RT-PCR

RT-PCR was performed using RT-PCR system according to the manufacturer's protocol. Total RNA was isolated from paraffin-embedded tissue using an RNA isolation kit (Promega). Three micrograms of total RNA were reverse transcribed by using M-MLV reverse transcriptase (Promega) with a mixture of oligo $(dT)_{15}$ and random primers (Promega). One tenth of each RT reaction mixture was then subjected to PCR amplification using Taq DNA polymerase (TAKARA). The PCR primers for detecting specific transcripts were as follows: for Shh forward, 5'-ACCGAGGGCTGGGACGAAGA-3' and reverse, 5'-ATTTGGCCGCCACCGAGTT-3', respectively. Following denaturation at 94℃ for 10 min, 35 PCR cycles were performed at 94℃ for 60 s, at 52℃ for 50 s, and at 72℃ for 60 s.

For β-actin, forward: 5'-TCCTCCCTGGAGAAGAGC TA-3' reverse: 5'-TCAGGAGGAGCAATGATCTTG-3'. Following denaturation at 94℃ for 10 min, 35 PCR cycles were performed at 94℃ for 60 s, at 59℃ for 50 s, and at 72℃ for 60 s. The PCR products were analyzed by 0.7% agarose gel electrophoresis.

RESULTS

Cytokeratin AE1/AE3 expression in colorectal adenocarcinomas

To determine whether colorectal adenocarcinomas originate from epidermis, we analyzed the expression of an epidermic molecular marker, cytokeratin AE1/AE3. Expression of cytokeratin AE1/AE3 was observed in the cytoplasm of colorectal crypts (Figure 1A and B). In addition, we examined the expression of the proliferation marker, PCNA. The results showed nuclear staining in the base of crypts in both normal (Figure 1C) and colorectal adenocarcinoma tissue (Figure 1D). However, there were a great number of stained nuclei in malignant crypts in contrast to that in normal tissue, suggesting that malignant crypts had a high level proliferation compared with normal crypts. Taken together, these data indicate that primary colorectal adenocarcinomas originate in epidermis.

Shh expression and localization in primary colorectal adenocarcinomas

It has been shown that Shh is expressed in stomach and esophageal cancers[16,17]. To determine if Shh is expressed in colorectal adenocarcinomas, we examined the expression of Shh at mRNA and protein levels. The result of *in situ* hybridization revealed that Shh mRNA was well stained in the cytoplasm of epithelial cells throughout the section in 10 of 25 samples (Figure 2B). The sense probes gave no detectable signals (Figure 2C). This result was confirmed by immunohistochemistry and RT-PCR (Figure 2G, only in 9 of 25 samples). The pattern of staining of immunohistochemistry (13 out of 25 showed a positive reaction) was similar to that of *in situ* hybridization (Figure 2E). No staining was observed when secondary detection was performed in the absence of primary antibodies (Figure 3F). The cells except cancer cells showed a negative reaction, suggesting that the

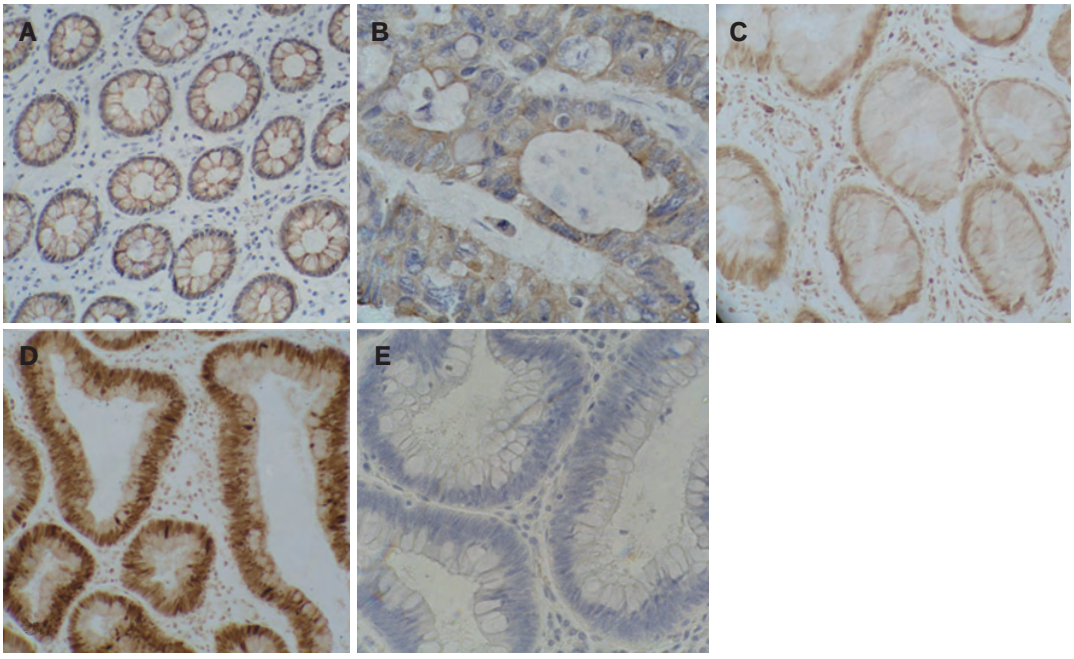

Figure 1 Expression of cytokeratin AE1/AE3 and PCNA in primary colorectal adenocarcinomas. We performed immunohistochemistry with cytokeratin AE1/AE3 antibodies showing positive staining in cytoplasm of colorectal normal crypts (A) and malignant crypts (B) (positive in brown). While the proliferation marker PCNA stained the nuclei of the normal (C) and tumor (D) tissues (positive in brown). E is the negative control.

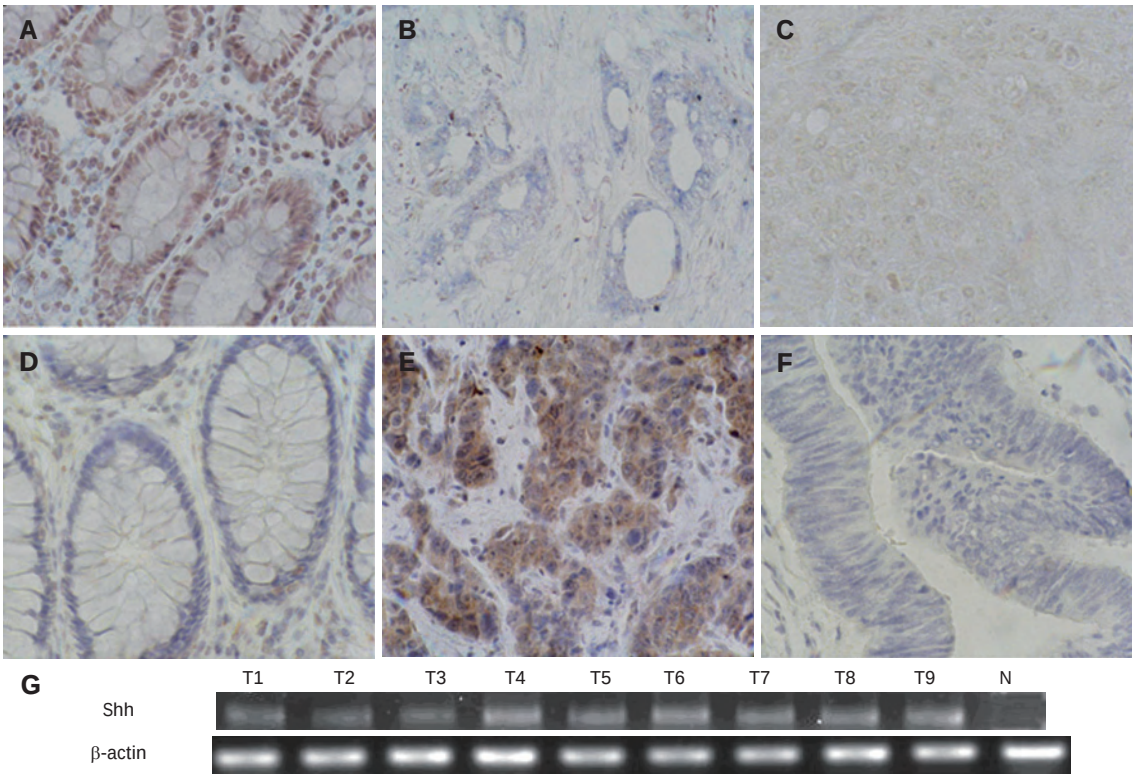

Figure 2 Expression of Shh in primary colorectal adenocarcinomas. *In situ* hybridization was performed to detect Shh transcript in normal (A) and cancerous (B) tissues (positive in blue), and the sense probe did not reveal any positive signals (C is the sense control of B). Results of *in situ* hybridization were confirmed by immunohistostaining in normal (D) and tumor (E) tissues (positive in brown, F is the negative control) and by RT-PCR (G).

expression of mRNA and protein was tumor specific. One normal tissue (the morphologically normal crypts close to the adenocarcinoma tissue) did not show the expression of Shh (Figure 2A and D). Our data demonstrated that, like other GI cancers, colorectal cancers expressed Shh in epithelial cells.

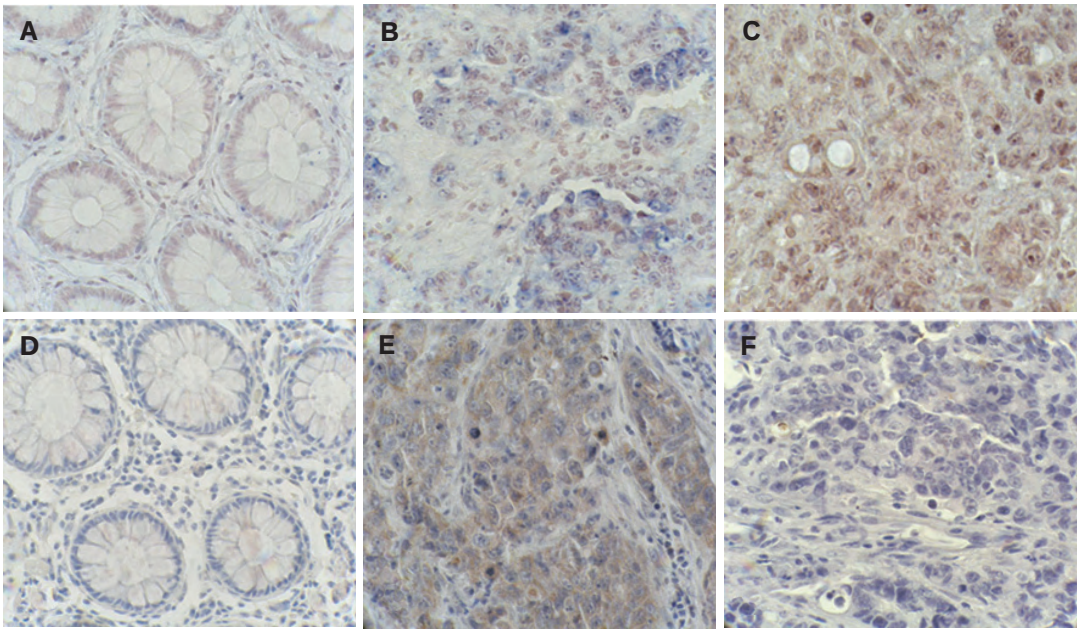

Figure 3 Expression of Ptch1 in primary colorectal adenocarcinomas. Ptch1 transcript (blue as positive) was detected by *in situ* hybridization in the normal control (A) and colorectal cancers (B). C is from the same tumor with B being derived from the Ptch1 sense probe. To confirm the *in situ* hybridization results, we performed immunohistochemistry with PTCH1 antibodies, showing positive staining of PTCH1 protein (positive in brown) in malignant crypts (E). D is the normal control and F is the negative control.

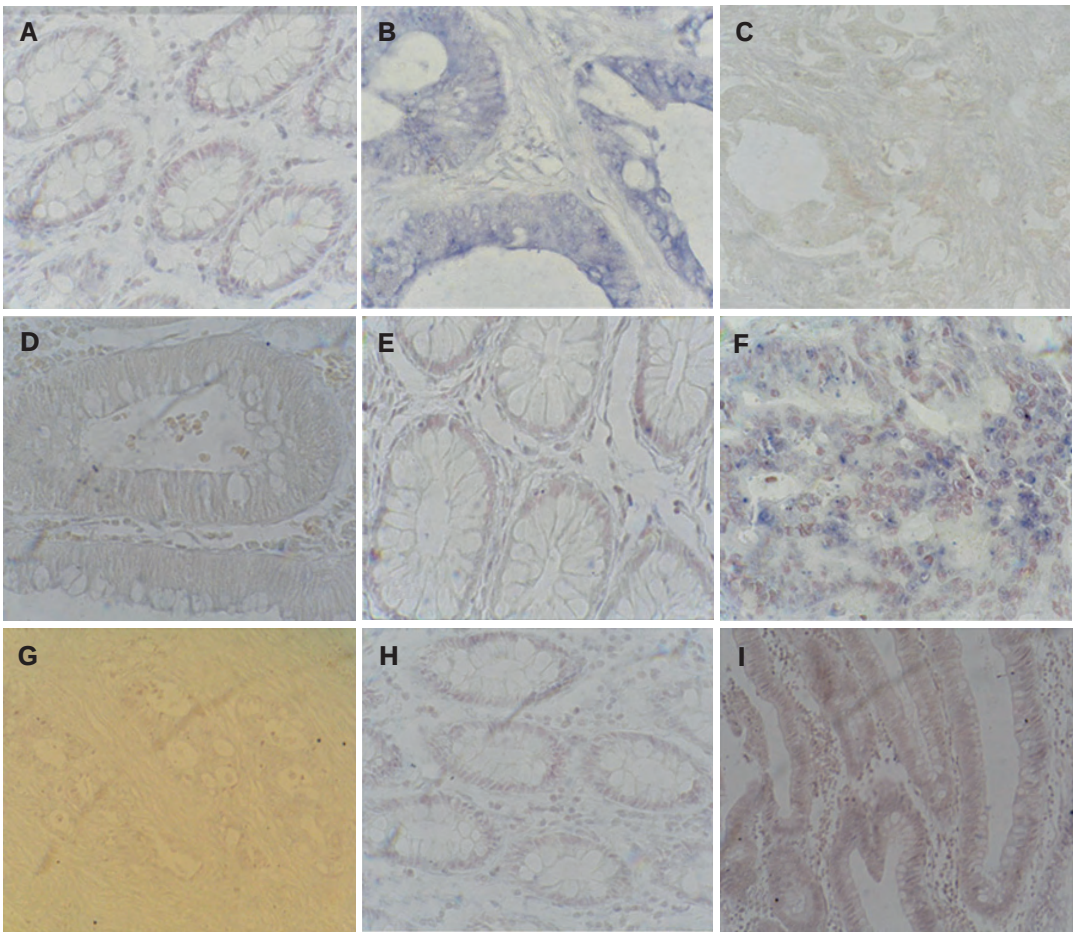

Figure 4 Expression of Gli1, Gli3 and Hip in primary colorectal adenocarcinomas. We detected expression patterns of Gli1, Gli3 and Hip transcripts by *in situ* hybridization (positive in blue). Gli1 (A) and Hip (E) were not expressed in normal control tissue. B: Gli1 was expressed in cytop-lasm of malignant crypt. The expression of Gli1 (C) and Hip (D) sense probe in tumor tissue. F: Hip was expressed in cytoplasm of tumor cells. G: Gli3 was not expressed in colorectal adenocarcinomas. H is the normal control of Gli3 and I is the sense control of Gli3.

Expression of the Hh signaling pathway components Ptch1, Gli1 and Hip, but not Gli3 in primary colorectal adenocarcinomas

The Hh signaling pathway can include Ptch receptor and Gli transcriptor, and it is also regulated by Hip. To determine if these genes are activated in colorectal cancer cells, the mRNAs of Ptch1, Gli1 and Hip were examined in colorectal adenocarcinoma tissue. The positive staining of Ptch1 (Figure 3A-C), Gli1 (Figure 4A-C) and Hip (Figure 4D-F) appeared in the majority of the malignant crypts in adenocarcinomas, but not in the stroma. The results (Table 1) indicate that there was no consistency in the expression of Ptch1, Hip and Gli1. Interestingly, we did not examine the expression of Gli3 by *in situ* hybridization

Table1 Colorectal adenocarcinoma specimens and summary of Shh, Ptch1, Smo Gli1, Sufu, PDGFRα and Hip expression

No	WHO Classification	Differentiation	Age	Gender	Shh -ish	SHH -ihc	Ptch1 -ish	PTCH1 -ihc	Gli1 -ish	PDGFRα -ish	Hip -ish
1	RAC	PD	50	M	+	+	-	+	+	+	-
2	RAC	WD	69	F	-	-	-	-	+-	-	-
3	RAC	PD	60	M	+	+	+	+	+	-	-
4	RAC	MD	69	F	+-	+	-	-	-	-	-
5	CAC	MD	50	F	-	-	-	-	-	-	-
6	RAC	WD	72	M	-	-	+-	+	+-	-	-
7	CAC	MD	60	F	-	-	-	-	-	-	-
8	RAC	MD	27	F	-	-	+-	+	-	-	-
9	RAC	MD	63	M	-	-	-	-	-	-	-
10	CAC	WD	55	M	-	-	-	-	+-	-	-
11	RAC	MD	66	F	-	+	-	-	+	-	-
12	CAC	PD	79	F	+	+	-	-	+	-	-
13	RAC	PD	54	M	-	-	-	-	-	-	-
14	RAC	WD	73	F	-	-	-	-	-	-	-
15	RAC	MD	68	F	+	+	+	+	-	-	-
16	RAC	MD	70	F	-	-	-	-	+-	+	-
17	RAC	MD	68	M	-	-	-	-	+	+	-
18	RAC	MD	67	F	-	-	-	-	-	-	-
19	CAC	PD	68	M	+	+	+	+	+	+	+
20	CAC	PD	48	F	-	+	+-	+	+-	-	-
21	RAC	PD	73	M	+	+	-	+	-	-	-
22	RAC	MD	51	M	-	-	-	-	+	-	-
23	RAC	MD	70	M	+	+	+	+	+	-	+
24	RAC	PD	37	F	+	+	+	+	-	-	+
25	RAC	PD	79	M	+	+	+	+	-	-	+

These data were derived from *in situ* hybridization (ish) and immunohistochemistry (ihc). + means positive result (ratio of positive cells to cancer cells ⩾ 25%), - means negative result (no positive cell or ratio of positive cells to cancer cells ⩽ 10%), +- means weakly positive result (10% < ratio of positive cells to cancer cells < 25%); WD: Well differentiated; MD: Moderately differentiated; PD: Poorly differentiated; CAC: Colonic adenocarcinoma; RAC: Rectal adenocarcinoma.

in any tissue (Figure 4G-I). To confirm the results of *in situ* hybridization, we detected Ptch1 protein by immunohistochemistry. The results were in agreement with the *in situ* hybridization data (Figure 3D-G). These findings indicate that the Shh-Ptch-Gli1 pathway was likely involved in colorectal adenocarcinomas. However, it should be noted that upregulation of Shh expression may not be the sole cause of enhanced Ptch1 or Gli1 expression, because, in some cases, upregulation of Ptch1 or Gli1 expression was not in accordance with the expression of Shh (Table 1). This suggests that the hedgehog signaling pathway might be activated by other regulatory mechanisms in colorectal carcinoma.

Expression of PDGFRα in primary colorectal adenocarcinomas

The platelet-derived growth factors (PDGFs) are a pleotrophic family of peptide growth factors that signal through cell surface tyrosine kinase receptors (PDGFR) and stimulate various cellular functions including growth, proliferation, and differentiation. In the past few years, the role of PDGF signaling has been demonstrated in cancer cell proliferation and tumor angiogenesis[19-22]. Only recently Xie *et al* found that in the hedgehog-responsive cell line C3H10T1/2, Gli1 activates PDGFRα expression and enhances its activity[19]. In the murine BCC cell line ASZ001 (Ptch1 null), DNA synthesis and cell proliferation can be slowed by re-expression of PTCH1 possibly through down-regulating PDGFRα expression, or by downstream inhibition with PDGFRα-neutralizing antibodies[19]. To test whether Shh signaling pathway in colorectal carcinomas is activated through expression of PDGFα, we analyzed mRNA of PDGFRα using *in situ* hybridization. PDGFRα was detected strongly in aberrant crypts and moderately in stroma of colorectal cancers (Figure 5B) that expressed Gli1. Thus, it may imply that Shh-Gli1 pathway in colorectal cancers is activated through increased expression of PDGFRα.

DISCUSSION

Hh signaling drives cell proliferation, promotes cell survival, and directs cell differentiation in the developing embryo. Abortive regulation of the pathway during development has been associated with significant human birth defects, including holoprosencephaly, basal cell nevus syndrome, and polydactyly[9,10,23-26]. Recent studies have shown that aberrant signaling of this pathway is involved in a variety of human cancers, such as basal cell carcinomas, medulloblastomas and small-cell lung cancer[9-12,15].

Onisu *et al* have studied the expression of Shh, Patch1 and Smo in colonic neoplasia by immunohistochemistry[18]. In the current study, we showed that overexpression of Shh at both mRNA and protein levels were similar in colonic adenocarcinoma and rectal adenocarcinoma tissue. To the best of our knowledge, this is the first report on the expression of Gli3, and Hip in colorectal cancer tissue. Since overexpression of Shh, Ptch1, Hip, Gli1 and PDGFRα occurred in colorectal cancers, whereas

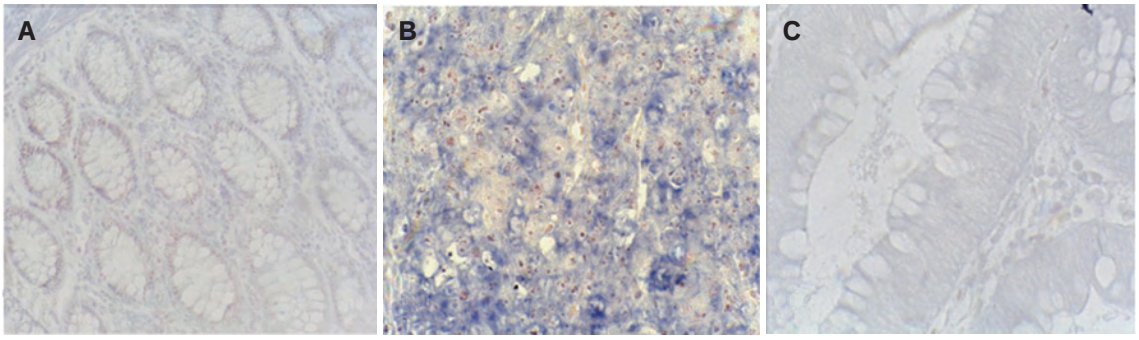

Figure 5 Expression of PDGFRα in primary colorectal adenocarcinomas. A: We analyzed expression pattern of PDGFRα transcript by *in situ* hybridization (blueas positive); B: Expression of PDGFRα in normal control was high in aberrant crypts and moderate in the stroma; C: The expression of PDGFR sense probe in tumor tissue.

no positive signal of Gli3 was observed at mRNA or protein levels, it may imply that the Shh-Gli1 pathway is activated in colorectal cancers. This supports the view that activation of the hedgehog pathway may play a role in the development of colorectal carcinoma.

We showed in this study that upregulation of Ptch1 or Gli1 expression, in some cases, was not consistent with the expression pattern of Shh (Table 1). This suggests that upregulation of Shh expression may not be the sole cause of activated Ptch1 or Gli1 expression, and that the hedgehog signaling pathway might be activated by other regulatory mechanisms in colorectal carcinoma. Furthermore, we unexpectedly found that the negative regulator, Hip, was expressed in several samples. This may support a model in which Hip, like Ptch1, modulates the responses to Hh signaling via a negative regulatory feedback loop.

The link between the hedgehog pathway, PDGFRα and human cancer was first revealed in Gorlin's syndrome, a disease with a high risk of basal cell carcinoma[19,26-28]. Those previous studies have shown that PDGFRα can be regulated by Gli1 and that PDGFRα mediates Gli1-induced Ras/Erk activation[19,26-28]. In our studies, we also detected the expression of PDGFRα in colorectal adenocarcinomas which expressed Gli1. Therefore, up-regulation of PDGFRα appears to be one of the mechanisms by which Sonic hedgehog-Gli1 signaling induces colorectal cancers.

Taken together, our findings suggest that activation of the Shh-Gli1 pathway may be involved in colorectal cancer progression.

ACKNOWLEDGMENTS

We appreciate the help from Dr. Shaojun Du, Center of Marine Biotechnology, University of Maryland Biotechnology Institute, in revising the manuscript.

REFERENCES

1 **Hammerschmidt M**, Bitgood MJ, McMahon AP. Protein kinase A is a common negative regulator of Hedgehog signaling in the vertebrate embryo. *Genes Dev* 1996; **10**: 647-658
2 **Johnson RL**, Scott MP. New players and puzzles in the Hedgehog signaling pathway. *Curr Opin Genet Dev* 1998; **8**: 450-456
3 **Pathi S**, Pagan-Westphal S, Baker DP, Garber EA, Rayhorn P, Bumcrot D, Tabin CJ, Blake Pepinsky R, Williams KP. Comparative biological responses to human Sonic, Indian, and Desert hedgehog. *Mech Dev* 2001; **106**: 107-117
4 **Denef N**, Neubuser D, Perez L, Cohen SM. Hedgehog induces opposite changes in turnover and subcellular localization of patched and smoothened. *Cell* 2000; **102**: 521-531
5 **Taipale J**, Cooper MK, Maiti T, Beachy PA. Patched acts catalytically to suppress the activity of Smoothened. *Nature* 2002; **418**: 892-897
6 **Chuang PT**, McMahon AP. Vertebrate Hedgehog signalling modulated by induction of a Hedgehog-binding protein. *Nature* 1999; **397**: 617-621
7 **van den Brink GR**, Hardwick JC, Nielsen C, Xu C, ten Kate FJ, Glickman J, van Deventer SJ, Roberts DJ, Peppelenbosch MP. Sonic hedgehog expression correlates with fundic gland differentiation in the adult gastrointestinal tract. *Gut* 2002; **51**: 628-633
8 **Nielsen CM**, Williams J, van den Brink GR, Lauwers GY, Roberts DJ. Hh pathway expression in human gut tissues and in inflammatory gut diseases. *Lab Invest* 2004; **84**: 1631-1642
9 **Johnson RL**, Rothman AL, Xie J, Goodrich LV, Bare JW, Bonifas JM, Quinn AG, Myers RM, Cox DR, Epstein EH Jr, Scott MP. Human homolog of patched, a candidate gene for the basal cell nevus syndrome. *Science* 1996; **272**: 1668-1671
10 **Hahn H**, Wicking C, Zaphiropoulous PG, Gailani MR, Shanley S, Chidambaram A, Vorechovsky I, Holmberg E, Unden AB, Gillies S, Negus K, Smyth I, Pressman C, Leffell DJ, Gerrard B, Goldstein AM, Dean M, Toftgard R, Chenevix-Trench G, Wainwright B, Bale AE. Mutations of the human homolog of Drosophila patched in the nevoid basal cell carcinoma syndrome. *Cell* 1996; **85**: 841-851
11 **Raffel C**, Jenkins RB, Frederick L, Hebrink D, Alderete B, Fults DW, James CD. Sporadic medulloblastomas contain PTCH mutations. *Cancer Res* 1997; **57**: 842-845
12 **Berman DM**, Karhadkar SS, Hallahan AR, Pritchard JI, Eberhart CG, Watkins DN, Chen JK, Cooper MK, Taipale J, Olson JM, Beachy PA. Medulloblastoma growth inhibition by hedgehog pathway blockade. *Science* 2002; **297**: 1559-1561
13 **Thayer SP**, di Magliano MP, Heiser PW, Nielsen CM, Roberts DJ, Lauwers GY, Qi YP, Gysin S, Fernandez-del Castillo C, Yajnik V, Antoniu B, McMahon M, Warshaw AL, Hebrok M. Hedgehog is an early and late mediator of pancreatic cancer tumorigenesis. *Nature* 2003; **425**: 851-856
14 **Sheng T**, Li C, Zhang X, Chi S, He N, Chen K, McCormick F, Gatalica Z, Xie J. Activation of the hedgehog pathway in advanced prostate cancer. *Mol Cancer* 2004; **3**: 29
15 **Watkins DN**, Berman DM, Burkholder SG, Wang B, Beachy PA, Baylin SB. Hedgehog signalling within airway epithelial progenitors and in small-cell lung cancer. *Nature* 2003; **422**: 313-317
16 **Ma X**, Sheng T, Zhang Y, Zhang X, He J, Huang S, Chen K,

Sultz J, Adegboyega PA, Zhang H, Xie J. Hedgehog signaling is activated in subsets of esophageal cancers. *Int J Cancer* 2006; **118**: 139-148

17 **Ma X**, Chen K, Huang S, Zhang X, Adegboyega PA, Evers BM, Zhang H, Xie J. Frequent activation of the hedgehog pathway in advanced gastric adenocarcinomas. *Carcinogenesis* 2005; **26**: 1698-1705

18 **Oniscu A**, James RM, Morris RG, Bader S, Malcomson RD, Harrison DJ. Expression of Sonic hedgehog pathway genes is altered in colonic neoplasia. *J Pathol* 2004; **203**: 909-917

19 **Xie J**, Aszterbaum M, Zhang X, Bonifas JM, Zachary C, Epstein E, McCormick F. A role of PDGFRalpha in basal cell carcinoma proliferation. *Proc Natl Acad Sci USA* 2001; **98**: 9255-9259

20 **Clarke ID**, Dirks PB. A human brain tumor-derived PDGFR-alpha deletion mutant is transforming. *Oncogene* 2003; **22**: 722-733

21 **Uhrbom L**, Hesselager G, Nister M, Westermark B. Induction of brain tumors in mice using a recombinant platelet-derived growth factor B-chain retrovirus. *Cancer Res* 1998; **58**: 5275-5279

22 **Heinrich MC**, Corless CL, Duensing A, McGreevey L, Chen CJ, Joseph N, Singer S, Griffith DJ, Haley A, Town A, Demetri GD, Fletcher CD, Fletcher JA. PDGFRA activating mutations in gastrointestinal stromal tumors. *Science* 2003; **299**: 708-710

23 **Roessler E**, Belloni E, Gaudenz K, Jay P, Berta P, Scherer SW, Tsui LC, Muenke M. Mutations in the human Sonic Hedgehog gene cause holoprosencephaly. *Nat Genet* 1996; **14**: 357-360

24 **Weed M**, Mundlos S, Olsen BR. The role of sonic hedgehog in vertebrate development. *Matrix Biol* 1997; **16**: 53-58

25 **Hill RE**, Heaney SJ, Lettice LA. Sonic hedgehog: restricted expression and limb dysmorphologies. *J Anat* 2003; **202**: 13-20

26 **Johnson RL**, Rothman AL, Xie J, Goodrich LV, Bare JW, Bonifas JM, Quinn AG, Myers RM, Cox DR, Epstein EH Jr, Scott MP. Human homolog of patched, a candidate gene for the basal cell nevus syndrome. *Science* 1996; **272**: 1668-1671

27 **Hahn H**, Wicking C, Zaphiropoulous PG, Gailani MR, Shanley S, Chidambaram A, Vorechovsky I, Holmberg E, Unden AB, Gillies S, Negus K, Smyth I, Pressman C, Leffell DJ, Gerrard B, Goldstein AM, Dean M, Toftgard R, Chenevix-Trench G, Wainwright B, Bale AE. Mutations of the human homolog of Drosophila patched in the nevoid basal cell carcinoma syndrome. *Cell* 1996; **85**: 841-851

28 **Xie J**, Quinn A, Zhang X, Bare J, Rothman A, Collins C, Cutone S, Rutter M, McCormick MK, Epstein E Jr. Physical mapping of the 5 Mb D9S196-D9S180 interval harboring the basal cell nevus syndrome gene and localization of six genes in this region. *Genes Chromosomes Cancer* 1997; **18**: 305-309

S- Editor Wang J **L- Editor** Zhu LH **E- Editor** Liu Y

Hedgehog signaling in prostate cancer

Jingwu Xie

University of Texas Medical Branch at Galveston, Sealy Centers for Cancer Cell Biology and Environmental Health, Department of Pharmacology and Toxicology, 301 University Blvd, Galveston, TX 77555-1048, USA
Tel.: +1 409 747 1935; Fax: +1 409 747 1938; jinxie@utmb.edu

Prostate cancer is the most common malignancy and the second leading cancer-related cause of death in men in the USA. Despite enormous efforts in understanding the molecular basis of prostate cancer, very little progress has been made in prevention and treatment of this often lethal cancer. Recent studies have demonstrated that hedgehog signaling is frequently activated in advanced or metastatic prostate cancers. With small molecule inhibitors available to analyze the hedgehog signaling pathway, a novel rationale for prostate cancer therapy can be devised.

Keywords: basal cell carcinoma, cyclopamine, prostate specific antigen, PTCH1, small interfering RNA, suppressor of fused, smoothened, sonic hedgehog, transurethral resection of the prostate

future medicine

Prostate cancer is the most common malignancy and the second leading cancer-related cause of death in men in the USA [1]. Aging is an important risk factor for prostate cancer, as over 70% of all prostate cancer cases are diagnosed in men over the age of 65 years. In addition, the incidence of prostate cancer in African–American men is significantly higher than that in Caucasian men. The most common method to diagnose prostate cancer is a measurement of the serum level of prostate-specific antigen (PSA). PSA screening has contributed to the increased 5-year survival rate of men diagnosed with prostate cancer. Radical prostatectomy is an effective treatment strategy for early prostate cancer; however, treatments for metastatic prostate cancer are generally not effective. For example, hormone therapy only temporarily reduces tumor size and, often, the tumor relapses a few years later due to androgen-independent tumor growth. Currently, little progress has been made on the prevention of prostate cancer [1]. Improved progress in these clinical areas will require a more detailed understanding of prostate cancer progression at the molecular level.

Development of prostate cancer is a multistep process, from precursor lesions, to invasive carcinoma, to metastatic tumor [2]. Gleason grading is the most commonly used system to define the aggressiveness of prostate cancer [3]. A high Gleason score suggests an aggressive tumor. Currently, the molecular alterations which accompany these morphologic changes remain poorly defined.

Cytogenetic and allelic loss studies have identified a number of chromosome regions potentially involved in prostate cancer development and progression [4,5] (**Figure 1**). Despite the significance of allelic loss for prostate carcinogenesis, no single tumor suppressor gene has been definitively assigned a role in cancer progression. The tumor suppressor protein phosphatase and tensin homolog deleted on chromosome ten (*PTEN*) has proven to be one of the best candidate tumor suppressors for prostate cancer [6]. In addition to genetic data, studies utilizing either clinical human specimens or mouse models have provided evidence of other molecules involving prostate cancer initiation and progression. Quantitative methylation-specific polymerase chain reaction (PCR) of the glutathione S-transferase P1 (*GSTP1*) promoter has demonstrated near perfect specificity for cancer detection in prostate biopsies, and these studies indicate that *GSTP1* promoter hypermethylation is one of the earliest biomarkers for prostate cancer [7]. Loss of $p27^{kip1}$ is another biomarker for prostate cancer [8]. The role of *p27* in prostate cancer progression is further supported by targeted gene disruption in mice, which results in hyperplasia of multiple tissues including the prostate, and by the synergism between *p27* losses with PTEN inactivation [9]. Overexpression of Bcl-2 is an important marker of advanced, hormone-refractory prostate cancer, and may be responsible for the resistance to apoptosis of late stage tumors [8]. Recent studies indicate a role of the hedgehog pathway in the development of prostate cancer and will serve as the focus of this review.

Hedgehog signaling in human cancers

The hedgehog pathway, initially identified in the fruit fly, is a master regulator of cell proliferation, tissue differentiation and tissue polarity. The hedgehog (Hh) pathway plays a critical role in embryonic development and tissue polarity. Activation of this pathway occurs frequently in human cancer, whereas inactivation of this pathway is associated with developmental disorders.

The current understanding of the hedgehog pathway will be discussed (**Figure 2**). There are

Figure 1. Major genetic alterations during prostate cancer progression.

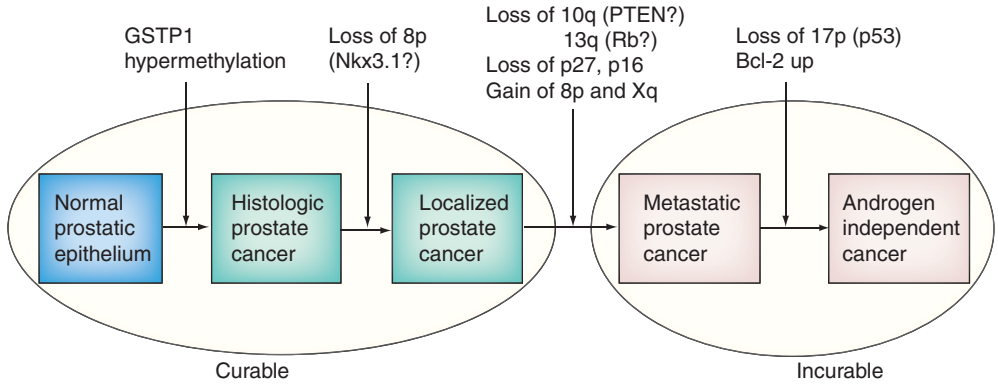

Several genetic alterations are reported in prostate cancer. Methylation of the GSTP1 promoter and loss of chromosome 8p (containing the *Nkx3.1* gene) are the early changes. Loss of 10q [containing the PTEN gene], 13q (containing the Rb gene), loss of p27, p16 and gain of 8p and Xq are frequently found in advanced prostate cancers. Loss of chromosome 17p (containing the *p53* gene) and elevated *Bcl-2* expression are markers for metastatic prostate cancers.
GSTP1: Glutathione S-transferase P1; PTEN: Phosphatase and tensin homolog deleted on chromosome ten; Rb: Retinoblastoma.

three distinct hedgehog (*Hh*) genes in humans, sonic hedgehog, desert hedgehog and Indian hedgehog). These hedgehog proteins undergo similar post-translational modifications [10]. Secreted Hh molecules bind to the receptor patched (PTC), thereby alleviating PTC-mediated suppression of smoothened (SMO). Expression of sonic hedgehog (Shh) appears to stabilize SMO protein possibly through post-translational modification of SMO. This effect of hedgehog molecules can be inhibited by hedgehog-interacting protein (HIP) through competitive association with PTC [11]. In *Drosophila*, SMO stabilization triggers complex formation with Costal-2, Fused and Gli homolog Cubitus interruptus (CI), which prevents CI degradation and formation of a transcriptional repressor. However, such a mechanism has not been established in mammalian cells. SMO ultimately activates transcription factors of the Gli family. There is genetic evidence indicating that several proteins link SMO to Gli. These signal transducers include Fu, Su(Fu), Rab23 and protein kinase A (PKA) [12]. As transcriptional factors, Gli molecules can regulate target gene expression by directly associating with a consensus binding site (5′-TTTGGTTGCA-3′) located in the promoter region of target genes.

There are several regulatory feedback loops in this pathway (**Figure 2**). *PTC*, *Gli1* and *HIP*, which are components of this pathway, are also the target genes. PTC and HIP provide a negative feedback mechanism to maintain the pathway activity at an appropriate level in a given cell. In contrast, Gli1 forms a positive-regulatory loop. Alteration of these loops will result in abnormal signaling of the hedgehog pathway.

Studies on hedgehog signaling are accelerated by availability of specific small molecular inhibitor cyclopamine, a natural product from *Veratrum californicum*, the corn lily [13]. Several synthetic compounds, which can promote or inhibit SMO signaling, are also available [14,15].

The link between the hedgehog pathway and human cancer was first identified in the Gorlin syndrome, a disease with a high risk of basal cell carcinomas (BCCs), medulloblastomata and meningiomas [16,17]. Loss-of-function mutations of the patched gene (*PTCH*)1 are the cause of Gorlin syndrome. BCC, the most common human cancer, consistently has abnormalities of the hedgehog pathway and has often lost the function of *PTCH1* via point mutations and loss of the remaining allele. Most *PTCH*1 mutations lead to loss of the protein function. Elevated expression of *Gli1* is an important indicator of this pathway activation in BCCs [18]. Mice heterozygous for a *PTCH*1 null mutation exhibit a high risk of cancers such as medulloblastomata, rhabdomyosarcomas and BCCs, confirming that *PTCH1* functions as a tumor suppressor. Currently, $Ptch1^{+/-}$ mice represent the most practical model of ultraviolet (UV)-mediated BCC formation. In addition to *PTCH1*, somatic mutations of *SMO* [19], a putative seven-transmembrane protein of the hedgehog pathway,

Figure 2. Components of the hedgehog pathway in mammals.

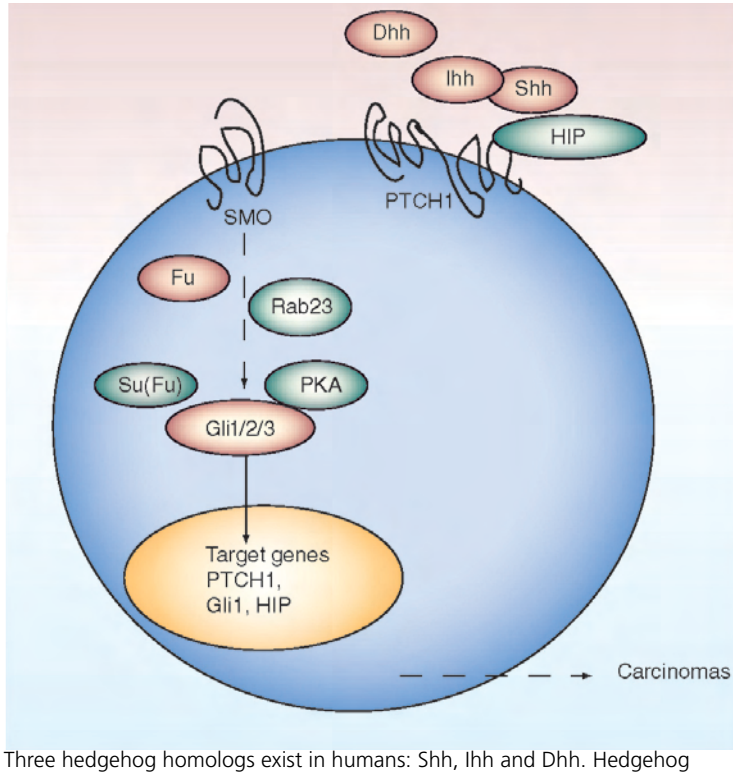

Three hedgehog homologs exist in humans: Shh, Ihh and Dhh. Hedgehog receptor PTCH1 (and its homolog PTCH2, not shown in this diagram) inhibits SMO signaling in the absence of hedgehog. Presence of hedgehog molecules, however, desuppresses SMO activities, which result in Gli-dependent transcription (three homologs exist in humans: Gli1, Gli2 and Gli3). Several other signaling molecules are also involved in hedgehog signaling, including Fu, Su(Fu), Rab23 and PKA. One unique feature of the hedgehog signaling pathway is the existence of several regulatory feedback loops: PTCH1, hedgehog-interacting protein (HIP) and Gli1. However, signal transduction from SMO to Gli1 is still not very clear. Presently, the molecular link from hedgehog signaling activation to tumor formation is not known.
Ihh: Indian hedgehog; Dhh: Desert hedgehog; Fu: Fused kinase; PKA: Protein kinase A; PTCH: Patched; Shh: Sonic hedgehog; SMO: Smoothened; Su(Fu): Suppressor of fused;

occur in sporadic BCCs. Activation of the hedgehog pathway is also found in medulloblastomata, small-cell lung cancer and gastrointestinal tract cancers (**Table 1**) [20–24]. These findings provide additional insight into the role of the sonic hedgehog pathway in human cancer.

In summary, the hedgehog pathway is not only one of the most important signaling pathways during embryonic development, but is also highly activated in nearly 30% of all human cancers. Recent studies from several groups indicate an important role of the hedgehog pathway in prostate cancer [25–28]. The authors shall summarize recent findings regarding hedgehog signaling during prostate development and in prostate cancer.

Hedgehog signaling during formation of prostate gland

Formation of the murine prostate gland is initiated through budding of the urogenital sinus epithelium (UGE) into the surrounding mesenchyme to form the main prostatic ducts in response to testosterone stimulation, which is followed by duct formation, elongation and branching. The mature prostate gland is an intensively branched ductal system enmeshed in a supporting stroma and connected to the urethra by approximately 25 main ducts. Expression of Shh and its target genes, *PTCH*1 and *Gli1*, is observed in the prebudding stage; peaks in the budding stage and then declines during ductal branching [29–31]. In contrast, Shh is expressed in the UGE, Ptch1, Gli1, and Gli2 are localized primarily to mesenchyme surrounding prostate buds. These observations suggest that epithelial hedgehog expression activates stroma-mediated signals and stimulate epithelial cell proliferation in a paracrine manner.

Expression of *Gli1* and *Ptch1* can be induced by an exogenous Shh peptide in the intact urogenital sinus or in the isolated urogenital mesenchyme [29–31]. In the presence of Shh antibodies or the hedgehog signaling inhibitor cyclopamine, ductal morphogenesis is inhibited. *Shh* mutant fetuses display abnormal urogenital development and fail to form prostate buds. Thus, *Shh* is critical for maintaining appropriate prostate growth, proliferation and tissue polarity during development of the prostate gland.

It is suggested that prostate progenitor cells contain activated hedgehog signaling [27]. Prostate regeneration can be observed in rodent ventral prostate through castration-induced androgen withdrawal for 7 days, followed by androgen supplementation. The ventral prostate regenerates to its normal size after a 10-day course of androgen supplementation. However, inhibition of the hedgehog signaling by cyclopamine (or Shh antibodies) prevents prostate regeneration, yielding a prostate gland similar to the one after castration [27]. This study demonstrates that hedgehog signaling is critical for regeneration of adult prostate. Thus, hedgehog-positive prostate epithelial cells can be regarded as prostate progenitor cells.

Activation of hedgehog signaling in prostate cancer

Evidence from several groups indicates that the hedgehog signaling pathway is activated in subsets of prostate cancer, particularly metastatic tumors [25–28]. *In vivo* and *in vitro* data using cultured prostate cancer cell lines demonstrate

Table 1. Aberrant hedgehog signaling in human cancer.

Cancer	Gene mutations	Gene overexpression	Activation identified	Refs
Basal cell nevus syndrome	*PTCH1, Su(Fu)*		yes	[16,17]
BCCs	*PTCH1, SMO*		yes	[16,17,19]
Medullbloastomata	*PTCH1, Su(Fu), SMO*		yes	[32]
Trichoepitheliomas	*PTCH1*		yes	[35]
Gastric cancer		*Shh*	yes	[22]
Esophageal cancer		*Shh*	yes	[22]
Pancreatic cancer		*Shh*	yes	[20,22]
Oral SCCs		*Shh*	yes	[36]
Prostate cancer	*Su(Fu)*	*Shh*	yes	[25–28]
SCLC		*Shh*	yes	[21]

BCC: Basal cell carcinoma; PTCH: Patched; Shh: Sonic hedgehog; SCC: Smalll cell carcinoma; SCLC: Small-cell lung carcinoma; SMO: Smoothened; Su(Fu): Suppressor of fused;

that inhibition of hedgehog signaling prevents cell growth, inhibits cell invasiveness and abrogates tumor metastasis in nude mice [25–28]. Thus, hedgehog signaling activation may be an important mechanism for the development and progression of prostate cancers.

Detection of hedgehog signaling activation in prostate cancers

Analyses of primary prostate cancers reveal elevated hedgehog signaling in subsets of prostate cancers [25–28]. Due to the heterogeneous nature of prostate cancer, a pure population of tumor cells is required for analysis of hedgehog target genes, which can be obtained through dissected transurethral resection of the prostate (TURP) or microdissected prostatectomy specimens. One group did not find a significant activation of the hedgehog target gene *Gli1* in the tumor samples [25], which could be due to a low percentage of tumor content in the specimens since only 5 to 30% of tumors exist in most prostatectomy specimens. Using real-time PCR analyses, elevated Gli1 and PTCH1 mRNA, indicators of the hedgehog signaling activation, are detected in all metastatic prostate tumors and subsets of locally metastasized tumors [25–28].

A large number of prostate cancer specimens can be readily analyzed by *in situ* hybridization and immunohistochemistry. *In situ* hybridization of Gli1 and PTCH1 indicates activation of the hedgehog pathway in subsets of prostate cancers. Expression of Gli1 mRNA is frequently detected in the epithelium [28], and stromal expression of Gli1 is also detected in some tumors [25]. Further thorough analyses using a large number of clinical specimens are needed to clarify these different observations. The authors suspect that these differences could be related to the known heterogeneity of prostate cancer. Immunohistochemistry studies indicate that expression of hedgehog target genes *PTCH1* and *HIP* is frequently observed in prostate cancers with high Gleason scores or distant metastases [26].

There are several mechanisms by which the hedgehog pathway can be activated. First, Shh expression is significantly higher in prostate cancers [25–28], suggesting that elevated Shh expression may contribute to the pathway activation in these tumors. However, Shh overexpression is unlikely to be the only trigger of hedgehog signaling activation since hedgehog signaling is tightly regulated by feedback mechanisms in a given cell (**Figure 2**).

Another possibility is the elevated expression of *SMO*, which is low in normal prostate [27]. The role of SMO for hedgehog signaling activation in prostate cancer cells is demonstrated in the prostate cell line Pre1 [27], which has no *SMO* expression and no hedgehog signaling activation. Following ectopic expression of *SMO*, hedgehog signaling activation is observed by luciferase reporter assays. This activity can be suppressed by cyclopamine or Shh antibodies. Further studies are needed to determine the mechanisms for SMO induction in primary prostate tumors.

The third mechanism is through mutations of other components of the hedgehog pathway. In the authors' studies, 11 of 27 PTCH1-positive prostate cancer specimens have no detectable Su(Fu) protein, a negative regulator of the hedgehog pathway [26]. Two of these 11 tumors were shown to contain *Su(Fu)* mutations [26]. Previously, mutations of *Su(Fu)* have been identified in a subset of medulloblastomata [32]. Thus, inactivation of the negative regulator *Su(Fu)* is another mechanism

for hedgehog signaling activation. The overall results from these studies indicate that the hedgehog pathway is frequently activated in advanced or metastatic prostate cancers.

Association of activated hedgehog signaling with cellular functions of prostate cancer

Several cell lines have been employed to demonstrate the involvement of hedgehog signaling for prostate cancer cellular functions, including PC3, LNCap, Du145, 22RV1 and several rodent prostate cancer cell lines. In comparison with immortalized prostate epithelial cell lines Pre1 and RWPE-1, all prostate cancer cell lines have relatively high levels of Gli1 and PTCH1 mRNA, suggesting increased hedgehog signaling. Thus, it is predicted that inhibition of the hedgehog pathway by the SMO antagonist, cyclopamine, would suppress cell proliferation and cell invasiveness.

Indeed, prostate cancer cells are often responsive to treatment of cyclopamine although variable inhibition is noted among different cell lines [25–28]. Following treatment with 5 μM cyclopamine in PC3 cells, expression of hedgehog target genes is dramatically suppressed, which is accompanied with a significant reduction in bromodeoxyuridine (BrdU) positive cells. This effect is specific because addition of tomatidine, a nonspecific compound with a similar structure to cyclopamine, had no effect on either target gene expression or DNA synthesis [26]. On the other hand, the prostate epithelial cell line, RWPE-1, which demonstrates no activation of the hedgehog signaling pathway, was not sensitive to cyclopamine, indicating that cyclopamine specifically affects cells with elevated hedgehog signaling. As a result, cell growth of PC3 cells can be inhibited by cyclopamine, but not by tomatidine.

Prostate cancer progression is accompanied by increased cell invasiveness, and hedgehog signaling is frequently activated in advanced prostate cancers. It is therefore predicted that cyclopamine may inhibit cell invasiveness of prostate cancer cells. Cell invasiveness can be examined by the cell's ability to penetrate a matrix gel. In all prostate cancer cell lines, but not in the control RWPE-1 cells, the authors demonstrate that cyclopamine can reduce cell invasiveness by 70% [26]. Thus, hedgehog signaling activation regulates both cell proliferation and invasiveness of prostate cancer cells.

Evidence indicates that Gli1 plays an important role during hedgehog signaling activation in prostate cancers [25–28]. First, Gli1 is highly elevated in primary prostate tumors and cancer cell lines. Second, cancer cells with ectopic expression of *Gli1* are resistant to cyclopamine treatment [26,27]. Third, normal prostate epithelial cell lines Pre1 and AT2.1, are significantly more aggressive following ectopic expression of Gli1 [26,27]. Furthermore, inactivation of *Gli1* by short interfering RNA (siRNA) is sufficient to inhibit DNA synthesis in prostate cancer cells [28].

Hedgehog signaling & tumor growth in nude mice

In vitro data from several prostate cell lines predict the importance of the hedgehog pathway in tumor growth *in vivo*. Using LNCap cells, Fan and colleagues have demonstrated the dependence of *Shh* expression on tumor growth in nude mice [25]. Elegant experiments by Beachy and co-workers have provided direct evidence for Shh and tumor growth [27]. First, tumors derived from human prostate cancer cell lines PC3 and 22RV1 in nude mice are all sensitive to cyclopamine treatment. By day 28 following subcutaneous injection, mice develop tumors with a mean size of 155 mm^3. In contrast, mice treated with cyclopamine following cancer cell inoculation have no visible tumors. Ectopic expression of Gli1 renders these cells resistant to cyclopamine treatment in mice, supporting the specificity of the cyclopamine effects [27]. Second, these investigators demonstrate, using a series of rodent prostate cancer cell lines with different metastatic potentials, that hedgehog signaling activity is associated with tumor metastasis. The high metastatic AT6.3 cells rapidly form tumors in nude mice. These tumors metastasize to the lung, resulting in death in a few weeks. Following intraperitoneal injection of cyclopamine, lung metastasis is dramatically decreased, and the mice survive for a longer period of time [27]. Conversely, AT2.1 cells, which have a low metastatic potential, do not metastasize to the lung following subcutaneous injection. However, ectopic expression of Gli1 in this cell line significantly increases metastasis, further supporting the role of hedgehog signaling in prostate cancer progression and metastasis [27].

Conclusion

Several recent studies demonstrate that the hedgehog pathway is activated in advanced prostate cancers, as indicated by high expression of hedgehog target genes. These results further demonstrate that hedgehog signaling is required for cell proliferation, invasion and tumor metastasis of prostate cancer cells. Thus, targeted inhibition of the hedgehog should be effective in inhibiting prostate cancer progression. The first clinical trial using hedgehog signaling inhibitor is

already being initiated by Genentech and Curis, Inc. It is anticipated that, in the next few years, hedgehog signaling-based cancer clinical trials will be carried by multiple pharmaceutical or biotechnology industries.

Future perspective

Although additional studies are needed to verify hedgehog signaling in a large number of prostate cancer specimens, recent studies provide a clear rationale for prostate cancer therapy using hedgehog signaling inhibitors.

Studies in other types of tumors have predicted the feasibility for cancer therapy using hedgehog signaling inhibitors. Using *p53*$^{-/-}$; *Ptch1*$^{+/-}$ mice as a model for medulloblastomata, hedgehog signaling inhibitors, HhAntag (Curis, Inc. and Genentech, Inc.) or cyclopamine, prevent tumor progression and prolong medulloblastoma-free survival of the mice [15,23,33]. Similarly, oral delivery of cyclopamine in drinking water prevents formation of UV-induced BCCs and reduces the number of mature BCCs [34]. In these experiments, long-term (20 weeks) treatment of mice with cyclopamine had no effect on the overall survival, suggesting that cyclopamine has few side effects. A pilot study using cyclopamine in patients with BCCs has also proven to be beneficial in the treatment of these cancers [35].

Currently, our understanding of the roles of the hedgehog pathway in prostate cancer is rather limited. Thus, several important issues need to be addressed before clinical therapeutics can be effectively performed. First, we need to:

- Understand how the hedgehog pathway interacts with other signaling pathways in prostate cancers
- Demonstrate in a model system that activation of the hedgehog pathway is sufficient to drive cancer progression in an organism [6,9]
- Understand the mechanism(s) by which inhibition of hedgehog signaling prevent tumor progression.

If encouraging results are obtained in these studies and following approval of Food and Drugs Administration (FDA), it will be possible to test the effectiveness of these inhibitors in clinical trials.

There are several considerations in the future treatment of prostate cancers using hedgehog inhibitors. First, hedgehog signaling should be tested in the needle core biopsies, which can be best utilized for *in situ* hybridization. Another possibility is to establish an enzyme-linked immunosorbent assay (ELISA)-based assay using patient's serum. Future studies in identifying sensitive and cost-effective methods for detecting hedgehog signaling will be extremely helpful.

Second, an effective agent should be selected. Currently, there are several possibilities: Shh antibodies, cyclopamine or its analogs and Gli1 siRNA [25–27]. Careful examination of Shh in normal prostate epithelium should be assessed before applying the antibodies because Shh is expressed in both the tumor and some normal epithelium of prostate [25]. Although cyclopamine or its analog KAAD-cyclopamine is effective in suppressing hedgehog signaling activation, a high concentration (at a micromolar concentration range) is often needed to observe biologic effects in cultured cells. Therefore, novel inhibitors with efficacy in the nanomolar ranges are needed for clinical application. Since cyclopamine mainly targets SMO, tumors with alterations downstream of SMO are expected to be resistant to cyclopamine. In fact, the authors have demonstrated inactivation of *Su(Fu)* in prostate cancers and other tumors [Unpublished Data] [26]. One possibility is to use Gli1 siRNA, since recent data indicate that downregulation of Gli1 may be an important mechanism by which inhibition of the hedgehog pathway by cyclopamine induces apoptosis [26,27]. Sanchez and colleagues also indicated that Gli1 SiRNA downregulated BrdU incorporation in prostate cancer cells. Future improvements of current *in vivo* delivery systems will be necessary for siRNA-based therapeutics [28].

Bibliography

Papers of special note have been highlighted as either of interest (•) or of considerable interest (••) to readers.

1. Jemal A, Murray T, Ward E *et al.:* Cancer statistics, 2005. *CA Cancer J. Clin.* 55(1), 10–30 (2005).
2. Deutsch E, Maggiorella L, Eschwege P *et al.:* Environmental, genetic, and molecular features of prostate cancer. *Lancet Oncol.* 5(5), 303–313 (2004).
3. Humphrey PA: Gleason grading and prognostic factors in carcinoma of the prostate. *Mod. Pathol.* 17(3), 292–306 (2004).
4. Dong JT: Chromosomal deletions and tumor suppressor genes in prostate cancer. *Cancer Met. Rev.* 20(3–4), 173–193 (2001).
5. Gonzalgo ML, Isaacs WB: Molecular pathways to prostate cancer. *J. Urol.* 170(6 Pt 1), 2444–2452 (2003).
6. Wang S, Gao J, Lei Q *et al.:* Prostate-specific deletion of the murine Pten tumor suppressor gene leads to metastatic prostate cancer. *Cancer Cell* 4(3), 209–221 (2003).

• **The tumor suppressor role of PTEN in prostate cancer is demonstrated in a murine model.**

7. Henrique R, Jeronimo C: Molecular detection of prostate cancer: a role for GSTP1 hypermethylation. Eur. Urol. 46(5), 660–669. Discussion 669 (2004).

Executive summary

Prostate cancer

- Prostate cancer is the most common malignancy and the second leading cancer-related cause of death in men in the USA. Despite enormous efforts in our understanding of the molecular basis of prostate cancer, very little progress has been made in prevention and treatment of this often lethal cancer. Recent studies have demonstrated that hedgehog signaling is frequently activated in advanced or metastatic prostate cancers.

Hedgehog signaling in human cancers

- The hedgehog pathway, initially identified in the fruit fly, is a master regulator of cell proliferation, tissue differentiation and polarity. The link between the hedgehog pathway and human cancer was first identified by the Gorlin syndrome, a disease with a high risk of basal cell carcinomas (BCCs) and medulloblastomata.
- Loss-of-function mutations of the tumor suppressor gene *PTCH1* or gain-of-functions of proto-oncogene smoothened (SMO) are the causes of hedgehog signaling activation in basal cell carcinomas (BCCs) and medulloblastomata.
- Activation of the hedgehog pathway is also found in small-cell lung cancer, pancreatic cancer and gastrointestinal tract cancers.
- Recent data from several groups indicate that hedgehog signaling is activated in advanced prostate cancers.

Hedgehog signaling during formation of prostate gland

- During development of the prostate gland, sonic hedgehog (*Shh*) is important for maintaining appropriate prostate growth, proliferation and tissue polarity. Evidence also suggests that hedgehog signaling is critical for regeneration of adult prostate.

Activation of hedgehog signaling in prostate cancer

- Analyses of primary prostate cancers reveal elevated hedgehog signaling in subsets of prostate cancers, particularly advanced and metastatic prostate cancers.
- There are several mechanisms by which the hedgehog pathway can be activated: overexpression of *Shh*, elevated expression of SMO or downregulation of Su(Fu). Using a specific hedgehog signaling inhibitor cyclopamine, in cultured cell lines, it is demonstrated that hedgehog signaling activation is required for cell proliferation and cancer cell invasiveness.
- Published *in vitro* data demonstrates that tumor formation and metastases of prostate cancer cells in nude mice are dependent on hedgehog signaling. Conversely, ectopic of Gli1, the downstream effector of the hedgehog pathway, in a nontumorigenic prostate epithelial cell line is sufficient to cause tumor formation in nude mice. Experiments using specific siRNA of Gli1 demonstrate the importance of hedgehog signaling for DNA synthesis in prostate cancer cells.
- These results demonstrate that hedgehog signaling is required for cell proliferation, invasion and tumor metastasis of prostate cancer cells. Thus, targeted inhibition of the hedgehog should be effective in inhibiting prostate cancer progression.

8. De Marzo AM, Meeker AK, Zha S *et al.:* Human prostate cancer precursors and pathobiology. *Urology* 62(5 Suppl. 1), 55–62 (2003).
9. Gao H, Ouyang X, Banach-Petrosky W *et al.:* A critical role for $p27^{kip1}$ gene dosage in a mouse model of prostate carcinogenesis. *Proc. Natl Acad. Sci. USA* 101(49), 17204–17209 (2004).
- **The synergism between PTEN and *p27* during prostate cancer metastasis is demonstrated in a mouse model.**
10. Taipale J, Beachy PA: The Hedgehog and Wnt signaling pathways in cancer. *Nature* 411(6835), 349–354 (2001).
11. Chuang PT, McMahon AP: Vertebrate Hedgehog signaling modulated by induction of a Hedgehog-binding protein. *Nature* 397(6720), 617–621 (1999).
12. Pasca di Magliano M, Hebrok M: Hedgehog signaling in cancer formation and maintenance. *Nature Rev. Cancer* 3(12), 903–911 (2003).
13. Bale AE: Sheep, lilies and human genetics. *Nature* 406(6799), 944–945 (2000).
14. Frank-Kamenetsky M, Zhang XM, Bottega S *et al.:* Small-molecule modulators of Hedgehog signaling: identification and characterization of Smoothened agonists and antagonists. *J. Biol.* 1(2), 10 (2002).
15. Romer JT, Kimura H, Magdaleno S *et al.:* Suppression of the Shh pathway using a small molecule inhibitor eliminates medulloblastoma in $Ptc1^{(+/-)}p53^{(-/-)}$ mice. *Cancer Cell* 6(3), 229–240 (2004).
•• **Demonstrates that targeted inhibition of hedgehog signaling is sufficient to prevent sporadic medulloblastomas in a mouse model.**
16. Hahn H, Wicking C, Zaphiropoulous PG *et al.:* Mutations of the human homolog of Drosophila patched in the nevoid basal cell carcinoma syndrome. *Cell* 85(6), 841–851 (1996).
17. Johnson RL, Rothman AL, Xie J *et al.* Human homolog of patched, a candidate gene for the basal cell nevus syndrome. *Science* 272(5268), 1668–1671 (1996).
18. Dahmane N, Lee J, Robins P, Heller P, Ruiz i Altaba A: Activation of the transcription factor Gli1 and the Sonic hedgehog signaling pathway in skin tumours. *Nature* 389(6653), 876–881 (1997).
19. Xie J, Murone M, Luoh SM *et al.:* Activating Smoothened mutations in sporadic basal-cell carcinoma. *Nature* 391(6662), 90–92 (1998).
20. Thayer SP, Di Magliano MP, Heiser PW *et al.:* Hedgehog is an early and late mediator of pancreatic cancer tumorigenesis. *Nature* 425(6960), 851–856 (2003).
- **Demonstrates that hedgehog signaling is involved in pancreatic cancers.**
21. Watkins DN, Berman DM, Burkholder SG *et al.:* Hedgehog signaling within airway epithelial progenitors and in small- cell lung cancer. *Nature* 422(6929), 313–317 (2003).
- **A role of hedgehog signaling in human small-cell lung cancer is revealed in this study.**
22. Berman DM, Karhadkar SS, Maitra A *et al.:* Widespread requirement for Hedgehog ligand stimulation in growth of digestive tract tumours. *Nature* 425, 846–851 (2003).
- **In this paper, the role of hedgehog signaling activation is shown to be involved in gastrointestinal tract cancers.**

23. Berman DM, Karhadkar SS, Hallahan AR *et al.:* Medulloblastoma growth inhibition by hedgehog pathway blockade. *Science* 297(5586), 1559–1561 (2002).
- **Reports that inhibition of hedgehog signaling by cyclopamine causes regression of medulloblastomas in nude mice.**

24. Dahmane N, Sanchez P, Gitton Y *et al.:* The Sonic Hedgehog-Gli pathway regulates dorsal brain growth and tumorigenesis. *Development* 128(24), 5201–5212 (2001).
- **First report of cyclopamine effects on medulloblastoma cells.**

25. Fan L, Pepicelli CV, Dibble C *et al.:* Hedgehog signaling promotes prostate xenograft tumor growth. *Endocrinology* 145, 3961–3970 (2004).
- **First report showing that prostate xenograft tumor growth is dependent on hedgehog signaling.**

26. Sheng T, Li C, Zhang X *et al.:* Activation of the hedgehog pathway in advanced prostate cancer. *Mol. Cancer* 3(1), 29 (2004).
- •• **Demonstrate that hedgehog signaling is activated in advanced prostate cancers. This report reveals that overexpression of Shh or lack of Su(Fu) expression occurs in tumors with activated hedgehog signaling. Inactivated mutations of *Su(Fu)* are revealed in two tumors. The relevance of hedgehog signaling to DNA synthesis and cell invasiveness is demonstrated in several cancer cell lines.**

27. Karhadkar SS, Bova GS, Abdallah N *et al.:* Hedgehog signaling in prostate regeneration, neoplasia and metastasis. *Nature* 431(7009), 707–712 (2004).
- •• **Comprehensive study demonstrating that hedgehog signaling is activated in metastatic prostate cancers. In addition to over-expression of Shh, elevated *SMO* expression is shown in prostate cancer cells. The relevance of hedgehog signaling to DNA synthesis, cell invasiveness and tumor growth of prostate cancer cells is demonstrated in several cancer cell lines. In addition, evidence is provided to suggest that Shh positive cells may represent prostate stem cells.**

28. Sanchez P, Hernandez AM, Stecca B *et al.:* Inhibition of prostate cancer proliferation by interference with Sonic hedgehog-GLI1 signaling. *Proc. Natl Acad. Sci. USA* 101, 12561–12566 (2004).
- •• **Demonstrates that hedgehog signaling is activated in subsets of prostate cancers. Overexpression of *Shh* is shown in tumors with activated hedgehog signaling. The relevance of hedgehog signaling to DNA synthesis of prostate cancer cells is shown in several cancer cell lines.**

29. Lamm ML, Catbagan WS, Laciak RJ *et al.:* Sonic hedgehog activates mesenchymal Gli1 expression during prostate ductal bud formation. *Dev. Biol.* 249(2), 349–366 (2002).

30. Freestone S, Marker P, Grace OC *et al.:* Sonic hedgehog regulates prostatic growth and epithelial differentiation. *Dev. Biol.* 264, 352–362 (2003).

31. Pu Y, Huang L, Prins GS: Sonic hedgehog-patched Gli signaling in the developing rat prostate gland: lobe-specific suppression by neonatal estrogens reduces ductal growth and branching. *Dev. Biol.* 273(2), 257–275 (2004).

32. Taylor MD, Liu L, Raffel C *et al.:* Mutations in SUFU predispose to medulloblastoma. *Nature Genet.* 31(3), 306–310 (2002).

33. Sanchez P, Ruiz IAA: *In vivo* inhibition of endogenous brain tumors through systemic interference of Hedgehog signaling in mice. *Mech. Dev.* 122(2), 223–230 (2005).
- •• **The effectiveness of cyclopamine in preventing medulloblastoma in a murine model is reported in this paper.**

34. Athar M, Li C, Tang X *et al.:* Inhibition of smoothened signaling prevents ultraviolet B-induced basal cell carcinomas through regulation of Fas expression and apoptosis. *Cancer Res.* 64(20), 7545–7552 (2004).
- •• **Demonstrates that long-term chronic treatment of mice with BCCs with cyclopamine prevents formation of microscopic tumors and regresses macroscopic tumors. Despite long-term treatment, no specific side effects (hair loss or changes of overall animal survival) are identified, suggesting a feasibility of cyclopamine for treatment of human cancers. Furthermore, a mechanism of cyclopamine-induced apoptosis in BCCs is reported.**

35. Tabs S, Avci O: Induction of the differentiation and apoptosis of tumor cells *in vivo* with efficiency and selectivity. *Eur. J. Dermatol.* 14(2), 96–102 (2004).
- •• **The first report of a pilot human clinical trial with cyclopamine on human BCCs. The result indicates that cyclopamine treatment is beneficial to basal cell carcinoma patients.**

36. Vorechovsky AB, Unden B, Sandstedt R, Toftgard, Stahle-Backdahl M: Trichoepitheliomas contain somatic mutations in the overexpressed PTCH gene: support for a gatekeeper mechanism in skin tumorigenesis. *Cancer Res.* 57, 4677–4681 (1997).

37. Koike C, Mizutani T, Ito T *et al.:* Introduction of wild-type patched gene suppresses the oncogenic potential of human squamous cell carcinoma cell lines including A431. *Oncogene* 21, 2670–2678 (2002).

Affiliation

- *Jingwu Xie*
  University of Texas Medical Branch at Galveston, Sealy Centers for Cancer Cell Biology and Environmental Health, Department of Pharmacology and Toxicology, 301 University Blvd, Galveston, TX 77555-1048, USA
  Tel.: +1 409 747 1935;
  Fax: +1 409 747 1938;
  jinxie@utmb.edu

Molecular Cancer

BioMed Central

Research

Open Access

Activation of the hedgehog pathway in advanced prostate cancer

Tao Sheng[†1], Chengxin Li[†1,2], Xiaoli Zhang[†1], Sumin Chi[1,2], Nonggao He[1], Kai Chen[1], Frank McCormick[3], Zoran Gatalica[4] and Jingwu Xie*[1]

Address: [1]Sealy Centers for Cancer Cell Biology and Environmental Health, Department of Pharmacology and Toxicology, University of Texas Medical Branch, Galveston, Texas, 77555-1048, USA, [2]Department of Dermatology, Xijing hospital, Xi'an 710032, China, [3]UCSF Cancer Center, 2340 Sutter Street, San Francisco, CA 94115, USA and [4]Department of Pathology, Creighton University Medical Center, 601 N 30th St. Omaha, NE 68131, USA

Email: Tao Sheng - tasheng@utmb.edu; Chengxin Li - cxli66@yahoo.com; Xiaoli Zhang - xiaolzha@utmb.edu; Sumin Chi - chisumin@yahoo.com; Nonggao He - nhe@utmb.edu; Kai Chen - kachen@utmb.edu; Frank McCormick - mccormick@cc.ucsf.edu; Zoran Gatalica - zgatalica@pathology.creighton.edu; Jingwu Xie* - jinxie@utmb.edu

* Corresponding author †Equal contributors

Published: 13 October 2004

Molecular Cancer 2004, **3**:29 doi:10.1186/1476-4598-3-29

Received: 22 September 2004
Accepted: 13 October 2004

This article is available from: http://www.molecular-cancer.com/content/3/1/29

Abstract

Background: The hedgehog pathway plays a critical role in the development of prostate. However, the role of the hedgehog pathway in prostate cancer is not clear. Prostate cancer is the second most prevalent cause of cancer death in American men. Therefore, identification of novel therapeutic targets for prostate cancer has significant clinical implications.

Results: Here we report that activation of the hedgehog pathway occurs frequently in advanced human prostate cancer. We find that high levels of hedgehog target genes, PTCH1 and hedgehog-interacting protein (HIP), are detected in over 70% of prostate tumors with Gleason scores 8–10, but in only 22% of tumors with Gleason scores 3–6. Furthermore, four available metastatic tumors all have high expression of PTCH1 and HIP. To identify the mechanism of the hedgehog signaling activation, we examine expression of Su(Fu) protein, a negative regulator of the hedgehog pathway. We find that Su(Fu) protein is undetectable in 11 of 27 PTCH1 positive tumors, two of them contain somatic loss-of-function mutations of *Su(Fu)*. Furthermore, expression of sonic hedgehog protein is detected in majority of PTCH1 positive tumors (24 out of 27). High levels of hedgehog target genes are also detected in four prostate cancer cell lines (TSU, DU145, LN-Cap and PC3). We demonstrate that inhibition of hedgehog signaling by smoothened antagonist, cyclopamine, suppresses hedgehog signaling, down-regulates cell invasiveness and induces apoptosis. In addition, cancer cells expressing Gli1 under the CMV promoter are resistant to cyclopamine-mediated apoptosis. All these data suggest a significant role of the hedgehog pathway for cellular functions of prostate cancer cells.

Conclusion: Our data indicate that activation of the hedgehog pathway, through loss of Su(Fu) or overexpression of sonic hedgehog, may involve tumor progression and metastases of prostate cancer. Thus, targeted inhibition of hedgehog signaling may have significant implications of prostate cancer therapeutics.

Background

The *hedgehog* (Hh) pathway plays a critical role in embryonic development and tissue polarity [1]. Secreted Hh molecules bind to the receptor *patched* (PTC-PTCH1, PTCH2), thereby alleviating PTC-mediated suppression of *smoothened* (SMO), a putative seven-transmembrane protein. SMO signaling triggers a cascade of intracellular events, leading to activation of the pathway through GLI-dependent transcription [2]. The hedgehog receptor PTCH1 is also a target gene of this pathway, which forms a negative feedback mechanism to maintain the pathway activity at an appropriate level in a given cell. Activation of Hh signaling through loss-of-function somatic mutations of PTCH1 in human basal cell carcinomas (BCCs) disrupts this feedback regulation, leading to uncontrolled SMO signaling. Activating mutations of SMO in BCCs, on the other hand, are resistant to PTCH1-mediated inhibition, leading to an outcome similar to PTCH1 inactivation [3-6]. More recently, abnormal activation of the sonic hedgehog pathway, through over-expression of sonic hedgehog, has been implicated in the development of subsets of medulloblastomas, small cell lung cancer and gastrointestinal tract (GI) cancers [7-10].

Development of prostate requires hedgehog signaling. Although the initial formation of prostate buds does not require sonic hedgehog signaling (shh), shh is critical for maintaining appropriate prostate growth, proliferation and tissue polarity [11-14]. In the adult prostate, however, the activity of the hedgehog pathway is quite low. It remains to be tested whether this hedgehog pathway is activated during development of prostate cancer, the second most prevalent cause of cancer death in American men. Activation of the hedgehog pathway is often indicated by elevated levels of PTCH1 and HIP. In addition to PTCH1 mutation, SMO activation and hedgehog over-expression, loss of Su(Fu) can result in activation of the hedgehog pathway. In the human, the Su(Fu) gene is localized at chromosome 10q24, a region with LOH in several types of cancer including prostate cancer, lung cancer, breast cancer and medulloblastomas [15,16]. As a negative regulator of the hedgehog pathway, Su(Fu) inhibits the function of Gli molecules, leading to inactivation of this pathway [17-19]. Su(Fu) is also reported to affect beta-catenin function [20]. In addition, over-expression of sonic hedgehog is shown to be involved in the development of GI cancers [9,10]. Here we report our findings that activation of the hedgehog pathway occurs frequently in advanced prostate cancers, possibly through loss of Su(Fu) protein or over-expression of sonic hedgehog.

Results

Elevated expression of hedgehog target genes in prostate cancer specimens

As an important regulator of tissue polarity, active hedgehog signaling is required for ductual morphogenesis and proliferation during prostate development [11-14]. The adult prostate, on the other hand, does not contain active hedgehog signaling. Because hedgehog signaling is an important regulator for epithelial-mesenchymal interaction, an event critical during prostate cancer development, we examined whether the hedgehog-signaling pathway is activated in prostate cancer.

Activation of hedgehog signaling causes elevated expression of target genes PTCH1 and HIP. Thus, increased protein expression of PTCH1 and HIP indicates activation of the hedgehog pathway. Using PTCH1 antibodies [10], we examined 59 prostate cancer samples for hedgehog signaling activation (see Table 1, Additional file 1 for details). We first tested the specificity of the PTCH1 antibodies in MEF cells. *Ptch1* null MEF cells have no active *Ptch1* gene, thus should not have positive staining with PTCH1 antibodies. Indeed, no staining was seen in *Ptch1* null MEF cells (Fig. 1A). After transfection of *PTCH1* expressing plasmid, transfected cells showed positive staining (Fig. 1A), indicating that the PTCH1 antibodies are specific to PTCH1. Furthermore, PTCH1 immunohistostining was abolished after addition of the specific peptide, from which the antibodies were raised (Fig. 1B,1c). We found that percentage of PTCH1 positive staining tumors increased in high grade tumors (Table 1, Additional file 1). In prostate cancers with Gleason scores 3–6, 4 out of 18 specimens were positive for PTCH1 (22%), whereas 16 out of 22 undifferentiated carcinomas (Gleason Scores of 8–10) expressed PTCH1 (73%, see Table 1, Additional file 1), suggesting that the hedgehog pathway is frequently activated in advanced prostate cancer. To confirm this data, we found that all four available metastatic prostate cancer specimens were all positive for PTCH1 staining.

To further confirm our data, we detected HIP protein expression, another marker of the hedgehog signaling activation. After transfection of HIP expressing plasmid into 293 cells, HIP antibodies recognize a single band around 75 KD (Fig. 3A), and an endogenous HIP protein with a similar size was also detected in two cancer tissues, in which hedgehog signaling is known to be activated (Fig. 3B and data not shown here). In contrast, the matched normal tissue did not express detectable HIP. Thus, HIP expression appears to be a good marker for hedgehog signaling activation. Immunohistostaining with HIP antibodies in prostate cancer specimens revealed a similar pattern to prostate specific antigen (PSA) and PTCH1 (Fig. 3C and Table 1, Additional file 1), further confirming that hedgehog pathway is activated in

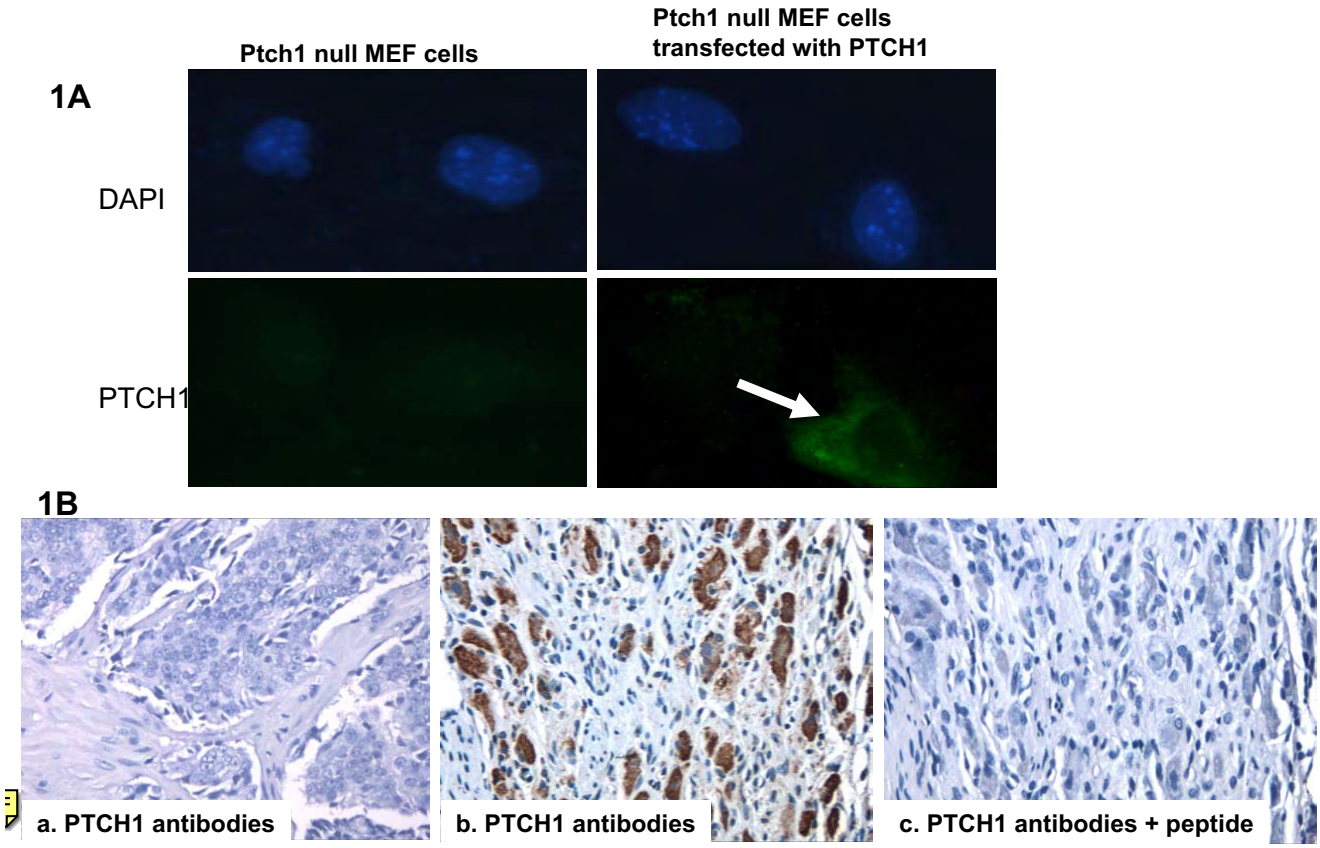

Figure 1
Detection of PTCH1 expression in prostate cancers. Protein expression of PTCH1 was detected by immunostaining. PTCH1 antibodies (Santa Cruz Biotechnology Cat# 9149) were tested in *Ptch1*$^{-/-}$ null MEF cells (**A**). While *Ptch1*$^{-/-}$ null MEF cells had no positive fluorescent staining with PTCH1 antibodies, transfection of PTCH1 expressing plasmid lead to positive staining (green, indicated by an arrow, 400×). Immunohistochemistry of prostate cancer specimens with PTCH1 gave negative (**B-a,** 200×) or positive (Red in **B-b,** 200×) signals. When PTCH1 antibodies were pre-incubated with the very peptide for raising the antibodies, no positive signals could be observed (**B-c**).

advanced prostate cancers. Thus the hedgehog pathway appears to be frequently activated in advanced or metastatic prostate cancers.

Altered expression of Su(Fu) and Shh in prostate cancer specimens

There are several mechanisms by which the hedgehog pathway in these prostate tumors can be activated, including loss of Su(Fu) or over-expression of hedgehog [6-10]. The Su(Fu) gene is localized at 10q24, a region with a frequent LOH in prostate cancer [15,16,18]. Mutations of Su(Fu) have been reported in other human cancers [6]. To test whether loss of Su(Fu) function is responsible for hedgehog signaling activation, we examined expression of Su(Fu) protein in these prostate cancer specimens. The antibodies of Su(Fu) recognize a single band at 52-kD in Western blotting analyses (Fig. 4A), which was reduced following treatment with Su(Fu) SiRNA (Fig. 4B), indicating the specificity of the antibodies. Furthermore, addition of the peptide, from which the antibodies were raised, prevented the antibody binding, further confirming the specificity of our Su(Fu) antibodies (data not shown). Of the 16 PTCH1 positive prostate cancer specimens with Gleason scores 8–10, 9 have no detectable Su(Fu) protein (Fig. 4C,4D,4E and Table 1, Additional file 1). In total, 11 of 27 PTCH1 positive prostate cancer specimens have no detectable Su(Fu) protein. Prostate cancers with low Gleason scores, however, frequently have

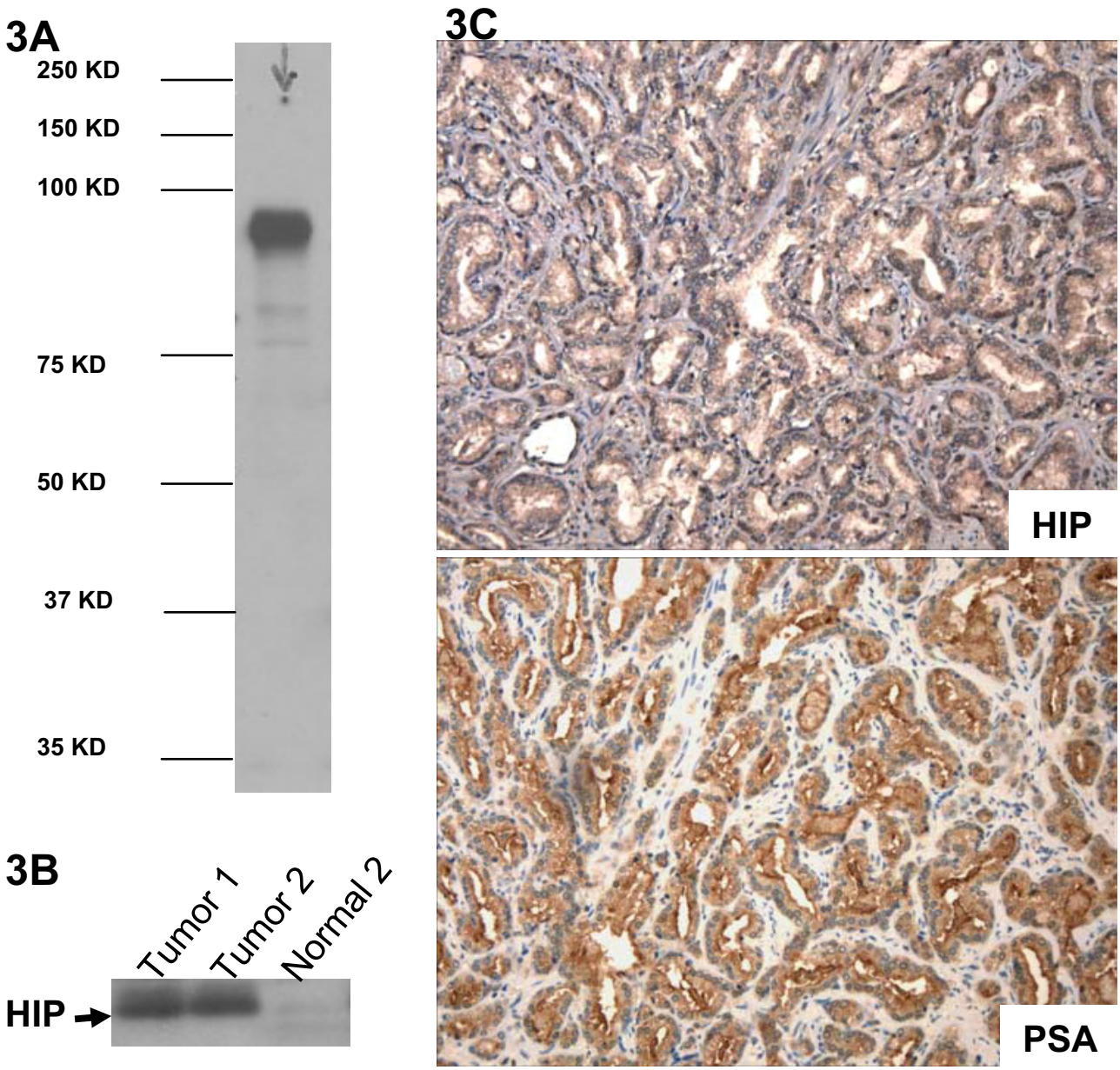

Figure 3
Detection of HIP in human cancer specimens. By Western blotting, HIP antibodies (R&D systems Cat# AF1568) recognized one band between 75 and100 KD (**A**). Expression of endogenous HIP was detected in two GI cancer tissues, which were known to contain activated hedgehog signaling (data not shown here), but not in the matched normal tissue (**B**). Immunohistostaining of HIP I prostate cancer showed a similar pattern to PSA (**C**, 200×)

detectable Su(Fu) protein (see Table 1, Additional file 1), suggesting that loss of Su(Fu) protein may be associated with prostate cancer progression.

To confirm the immunohistochemistry data, we performed immunoblotting analyses using several dissected TURP (Transurethral resection of the prostate) specimens in which tumor portion can be as high as 70% of the tissue mass. Prostatectomy specimens (most of our tumors), however, often contain a small percentage (5–10%) of tumor tissue and are therefore not suitable for Western blotting or real-time PCR analyses. As shown in Fig. 5A,

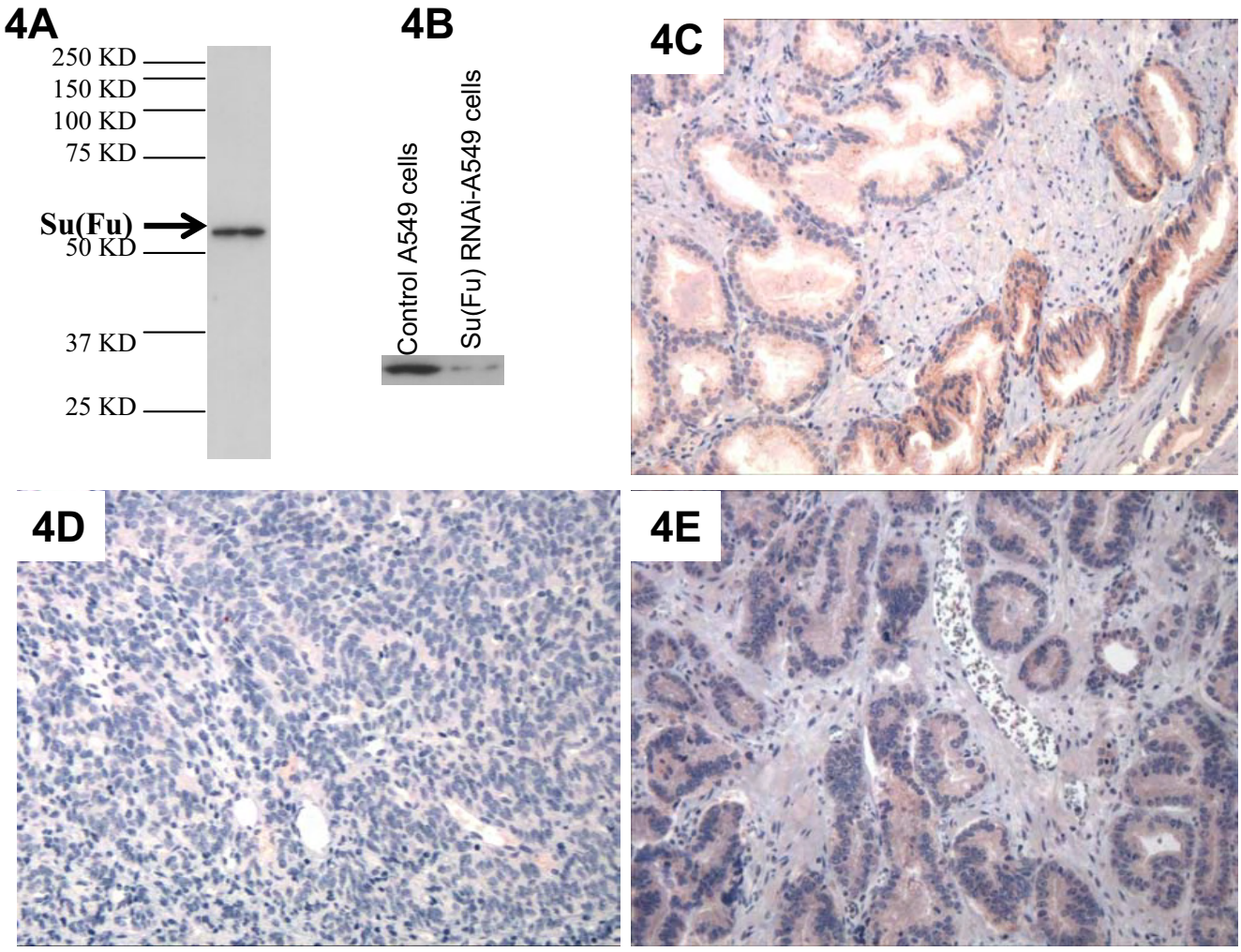

Figure 4
Detection of Su(Fu) in prostate cancer specimens. Su(Fu) antibodies (Santa Cruz Biotechnology Cat# 10933) recognized only one single band (54-Kd) in D283 cells (**A**). Following treatment of a specific SiRNA of Su(Fu), the endogenous Su(Fu) band was greatly reduced (**B**). Immunohistostaining with Su(Fu) antibodies in prostate cancer specimens revealed positive (**C**, in red, 200×), negative (**D**, 200×) or weak staining (**E**, red, 200×).

two tumors (PC48 and PC51) had no detectable Su(Fu) protein, which are consistent with our immunohistostaining, suggesting loss of Su(Fu) may be responsible for hedgehog pathway activation in these tumors. The matched normal tissues, however, retained expression of Su(Fu), indicating that alteration of Su(Fu) is a somatic event. Sequence analyses of these two tumors revealed genetic mutations in *Su(Fu)*, which are predicted to create STOP codons in the coding sequence (Fig. 5B and Table 1, Additional file 1). In PC48, a homozygous deletion of A1315 was detected, which results in a STOP codon at +1318 bp (Fig. 5B). In PC51, we detected two types of mutations, one with a deletion of C255, which results in a STOP codon at +294 bp whereas another with a deletion of C198, create a STOP codon (Picture not shown here, see Table 1, Additional file 1). These mutations were confirmed with 6 independent clones from two separate experiments, which exclude the possibility of PCR errors. No mutations were detected from the matched benign tissues, indicating the somatic nature of the mutations. Real-time PCR analyses indicated that target genes of the hedgehog pathway, PTCH1 and Gli1, were all elevated in these tumors (Fig. 5C), confirming activation of the hedgehog pathway in these tumors. Thus, Su(Fu) inactivation appears to contribute to activation of hedgehog signaling in these prostate tumors.

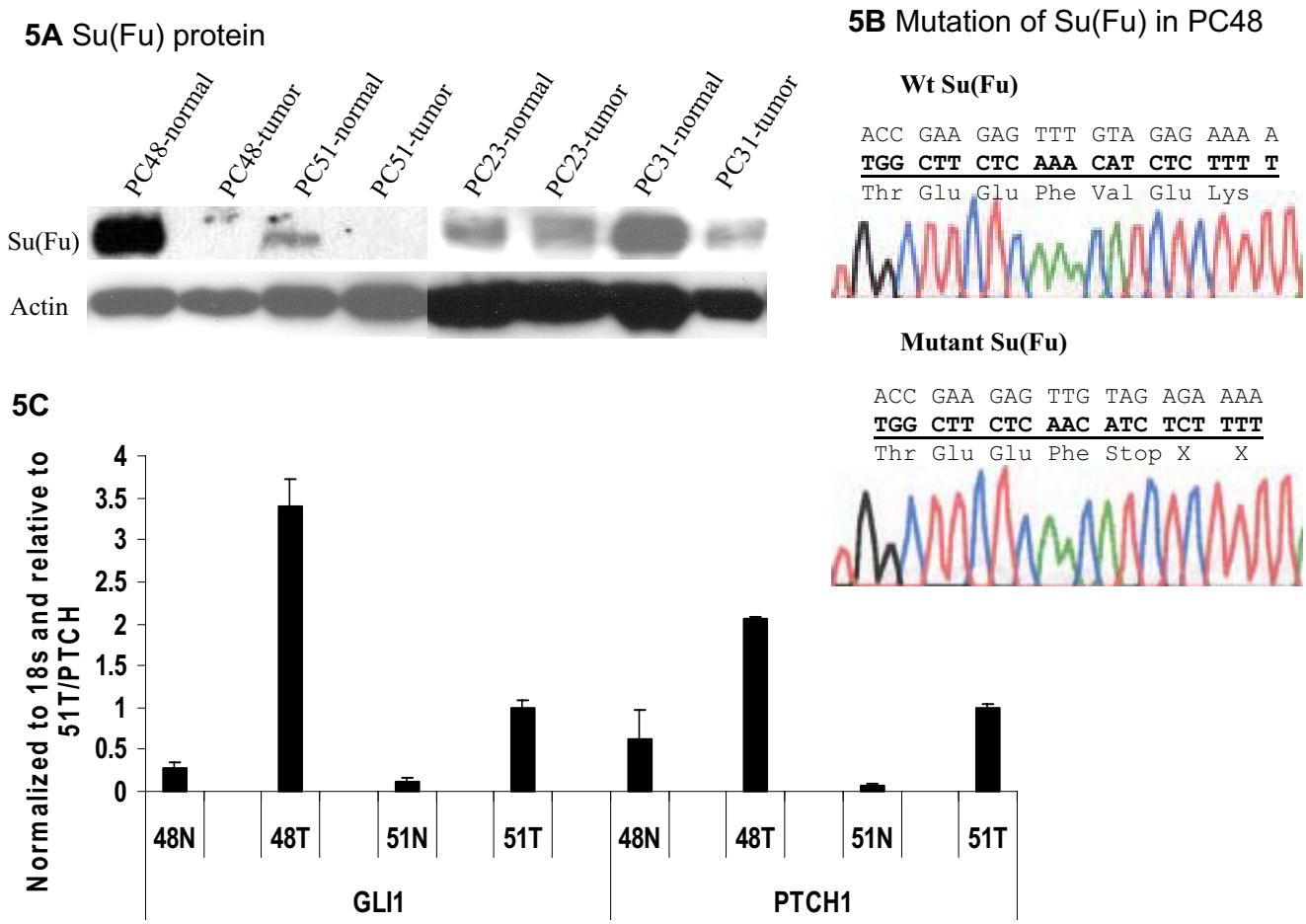

Figure 5

Inactivation of Su(Fu) in prostate cancer. Two TURP (Transurethral resection of the prostate) tumors with loss of Su(Fu) expression were confirmed by Western blotting (**A**). One mutation of Su(Fu) found in prostate cancer PC48 is shown in **B**, which is predicted to create a STOP codon in the Su(Fu) coding sequence +1318. The levels of Gli1 and PTCH1 transcripts in prostate tissues were detected by real-time PCR (see methods for details) (**C**). Tumor tissues had higher levels of the target gene transcripts.

For tumors with high level of PTCH1 expression, but no changes in Su(Fu) protein expression, we examined expression of sonic hedgehog. It is reported that expression of hedgehog may be responsible for hedgehog signaling activation in lung cancer and GI cancers. Immunohistostaining with sonic hedgehog antibodies indicate that sonic hedgehog is highly expressed in 24 of 27 advanced prostate tumors with elevated expression of PTCH1 and HIP (see Fig. 2 and Table 1, Additional file 1). Thus, activation of the hedgehog pathway, as indicated by elevated PTCH1 and HIP expression, is associated with loss of Su(Fu) expression or elevated hedgehog expression.

The role for activated hedgehog signaling for cellular functions of prostate cancer

To demonstrate the role of hedgehog pathway in prostate cancer, we screen five available cell lines for the expression of Gli1, PTCH1 and HIP. TSU, LNCap, Du145 and PC3 are prostate cancer cell lines whereas RWPE-1 is a prostate epithelial cell line. We found that the hedgehog target genes were significantly elevated in all cancer cell lines (Fig. 6A). Thus, we predicted that inhibition of the hedgehog pathway by smoothened antagonist, cyclopamine, would suppress cell proliferation and cell invasiveness.

Following treatment with 5 μM cycloapmine in PC3 cells, expression of hedgehog target genes were dramatically inhibited (data not shown here), which was accompanied

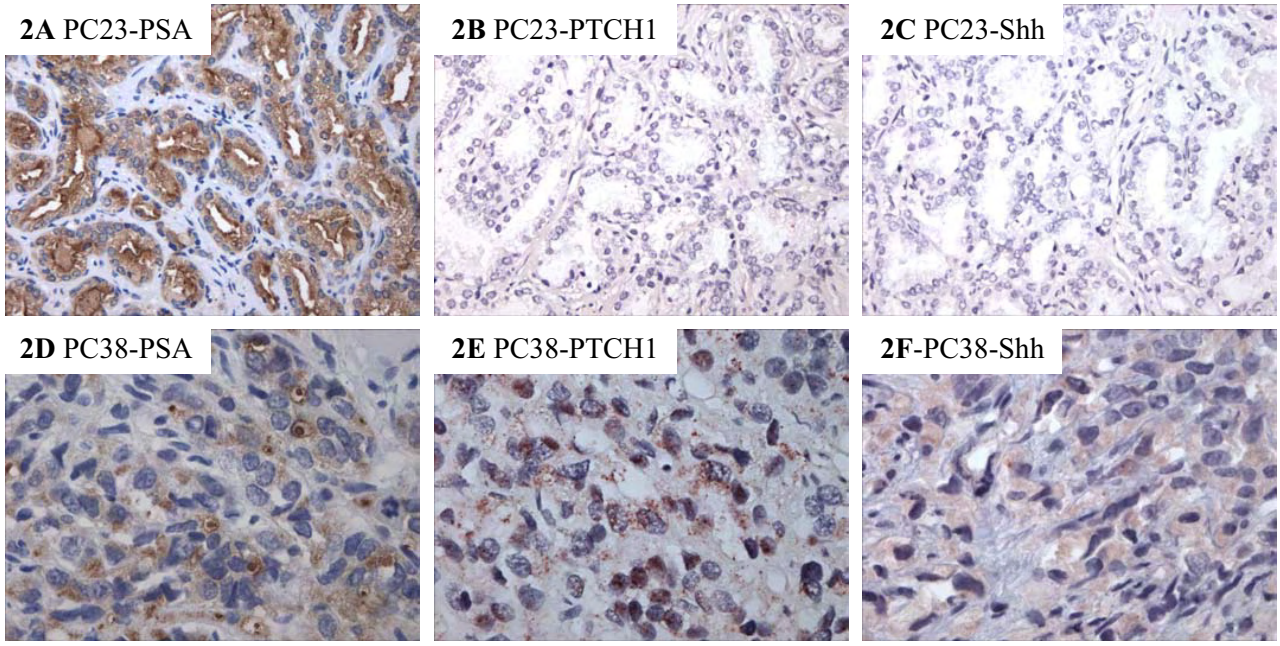

Figure 2
Co-expression of PTCH1, PSA and Shh in prostate cancer specimens. Immunohistochemistry of prostate cancer specimens with PSA was used to confirm the cancer region. Positive staining was in red. Positive staining patterns of PTCH1 and Shh antibodies (Santa Cruz Biotechnology Cat# 9024) were similar to that of PSA staining. PC23 (**A-C**) was from tumors with Gleason score 7 (200×). PC38 (**D-F**) was a tumor from Gleason score 10 (400×) (**see** Table 1, Additional file 1 for details).

with a significant reduction of BrdU positive cells (see Fig. 6B for details). This effect is specific because addition of tomotidine, a non specific compound with a similar structure to cycloapmine, had no effects on either target gene expression or DNA synthesis (indicated by BrdU labeling in Fig. 6B and 6C). The prostate epithelial RWPE-1 cells which have no activated hedgehog signaling, on the other hand, were not sensitive to cyclopamine (data not shown here), indicating that cyclopamine specifically affects cells with elevated hedgehog signaling. LN-CAP, Du145 and TSU cells, like PC3 cells were also sensitive to cyclopamine treatment (Fig. 6C).

Prostate cancer progression is accompanied by increased cell invasiveness. Because the hedgehog signaling activation occurs frequently in advanced prostate cancer, we examined if inhibition of the hedgehog signaling can reduce cell invasiveness. Using BD Bio-coat cell invasion chambers, we found that treatment of cyclopamine in PC3 cells reduced the percentage of invasive cells by 70% (Fig. 7A). Similar data were also observed in Du145, LN-CAP and TSU cells (Fig. 7B). Under the same condition, RWPE-1 cells were not very invasive. Thus, hedgehog signaling activation regulates both cell proliferation as well as cell invasiveness of prostate cancer cells.

It has been shown that cyclopamine induced apoptosis in cancer cells with activated hedgehog signaling [21]. We have shown that Gli1 down-regulation is necessary for cyclopamine-mediated apoptosis in basal cell carcinoma cells [21]. To test the significant role of Gli1, the downstream effector and the target gene of the hedgehog pathway, in cyclopamine-mediated apoptosis, we first transfected Gli1 expressing plasmid in to PC3 cells, and then treated the cells with 5 μM cyclopamine for 36 h. Since Gli1 is expressed under the control of the CMV promoter, we predicted that ectopic Gli1-expressing cells should be resistant to apoptosis, which is detected by TUNEL staining. As shown in Fig. 8, we found that all Gli1 positive cells (n = 500) were TUNEL negative, supporting our hypothesis that down-regulation of Gli1 may be an important mechanism by which cyclopamine mediates apoptosis in prostate cancer cells with activated hedgehog signaling.

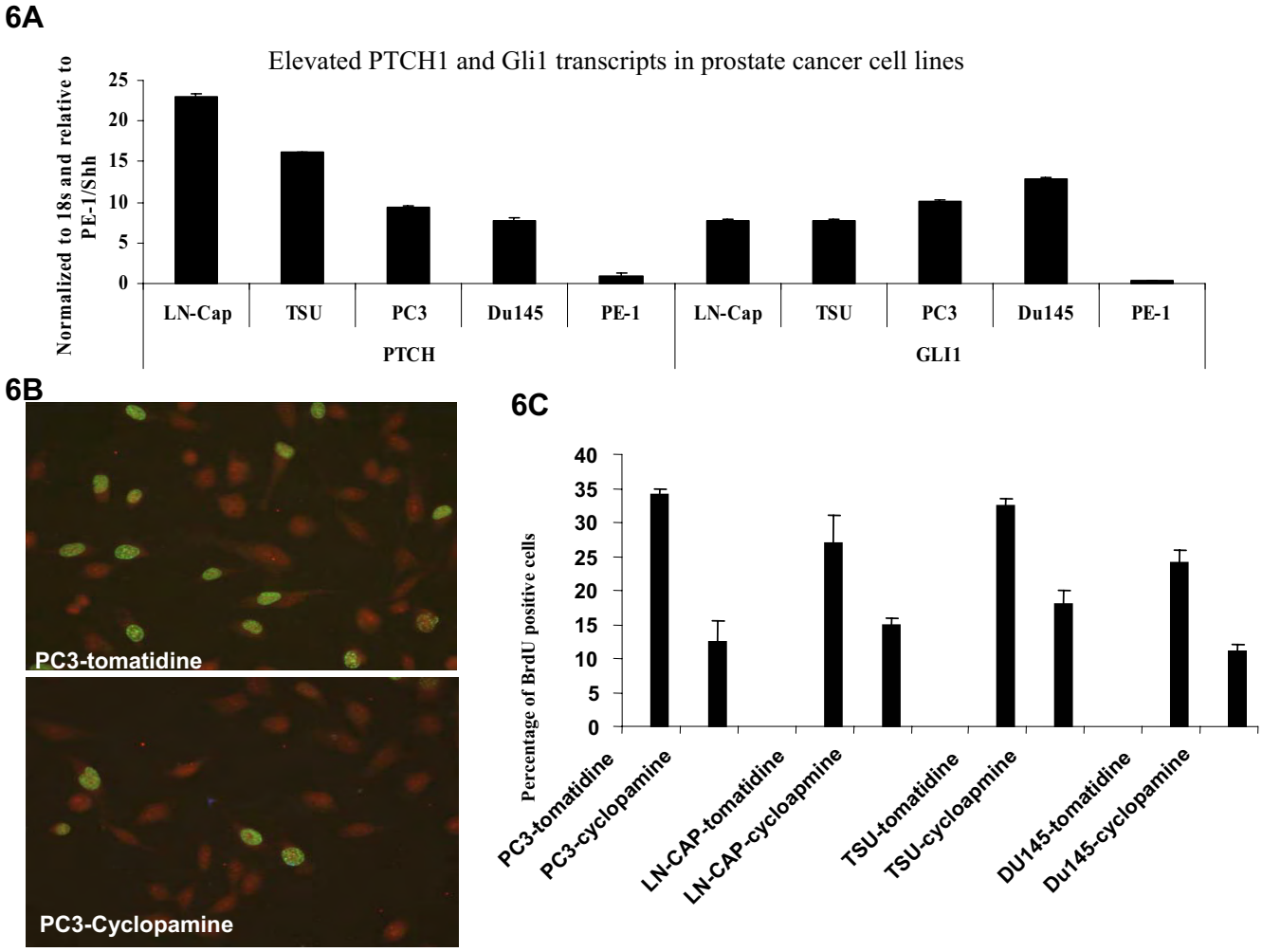

Figure 6

Cellular functions of the hedgehog pathway in prostate cancer cells. Expression of hedgehog target genes, PTCH1 and Gli1, were detected by real-time PCR (**A**). DNA synthesis was detected by BrdU labeling (**B**). Over 1000 cells were counted under fluorescent microscope for the percentage of BrdU positive cells, and the experiment was repeated twice (**C**).

All these data indicate that the hedgehog pathway is activated in advanced prostate cancers, as indicated by high expression of PTCH1 and HIP. Our results also indicate that hedgehog signaling is required for cell proliferation and cell invasion of prostate cancer cells. Thus, targeted inhibition of the hedgehog pathway may be effective in future prostate cancer therapeutics.

Discussion

Hedgehog signaling pathway regulates cell proliferation, tissue polarity and cell differentiation during normal development. Abnormal signaling of this pathway has been reported in a variety of human cancers, including basal cell carcinomas, medulloblastomas, small cell lung cancer and GI cancers [3,4,6-10,22,23]. Our findings in this report indicate a role of the sonic hedgehog pathway in prostate cancer. We detected a high expression of hedgehog target genes, PTCH1 and HIP, in advanced or metastatic prostate cancers. In contrast, only 22% of prostate tumors with Gleason scores 3–6 have elevated expression of PTCH1 and HIP. While our manuscript is being reviewed, three independent groups have recently reported similar results [24-26]. Thus, the hedgehog signaling pathway is frequently activated in advanced or metastatic prostate cancers.

Alterations of genes in the hedgehog pathway in prostate cancer

In our studies, we found that some prostate tumors had no detectable Su(Fu) protein expression while others

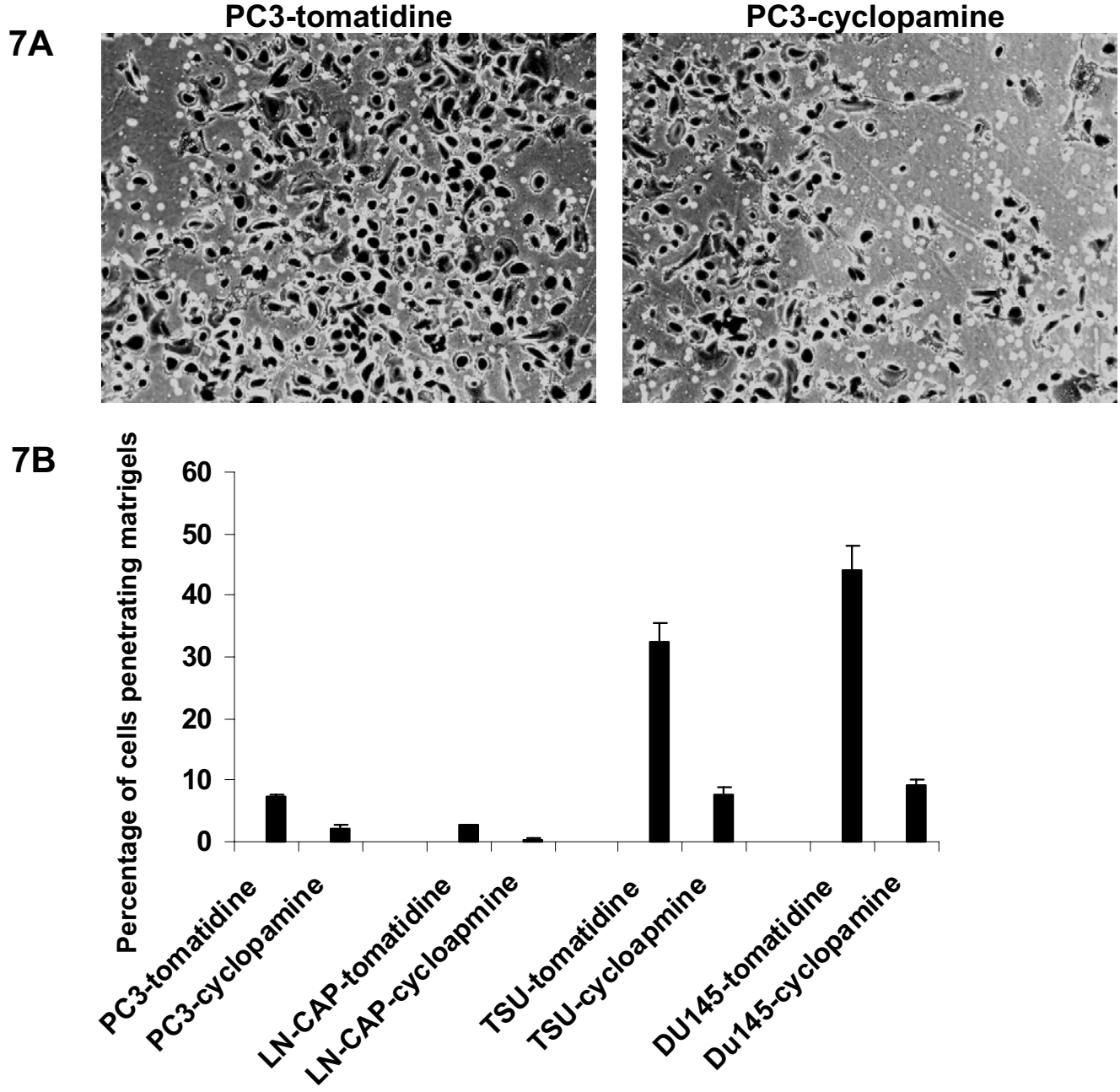

Figure 7
Effects of cyclopamine on cell invasiveness of prostate cancer cells. Cell invasion assay of prostate cancer cells was performed using BD Bio-coat cell invasion chambers (**A**). The rate of cell invasion was calculated by dividing cell numbers penetrated the matrigels by the number of cell in the control chambers (without matrigels) (**B**).

contained high levels of Shh protein expression. We further identified inactivated mutations of *Su(Fu)* in two prostate cancers. In addition to inactivated mutations in the coding region, Su(Fu) may be inactivated through promoter methylation. The heterogeneous nature of prostate cancer makes it difficult to screen prostate cancer specimens for Su(Fu) mutations since the tumor content is often less than 5% of the specimens. Future improve-

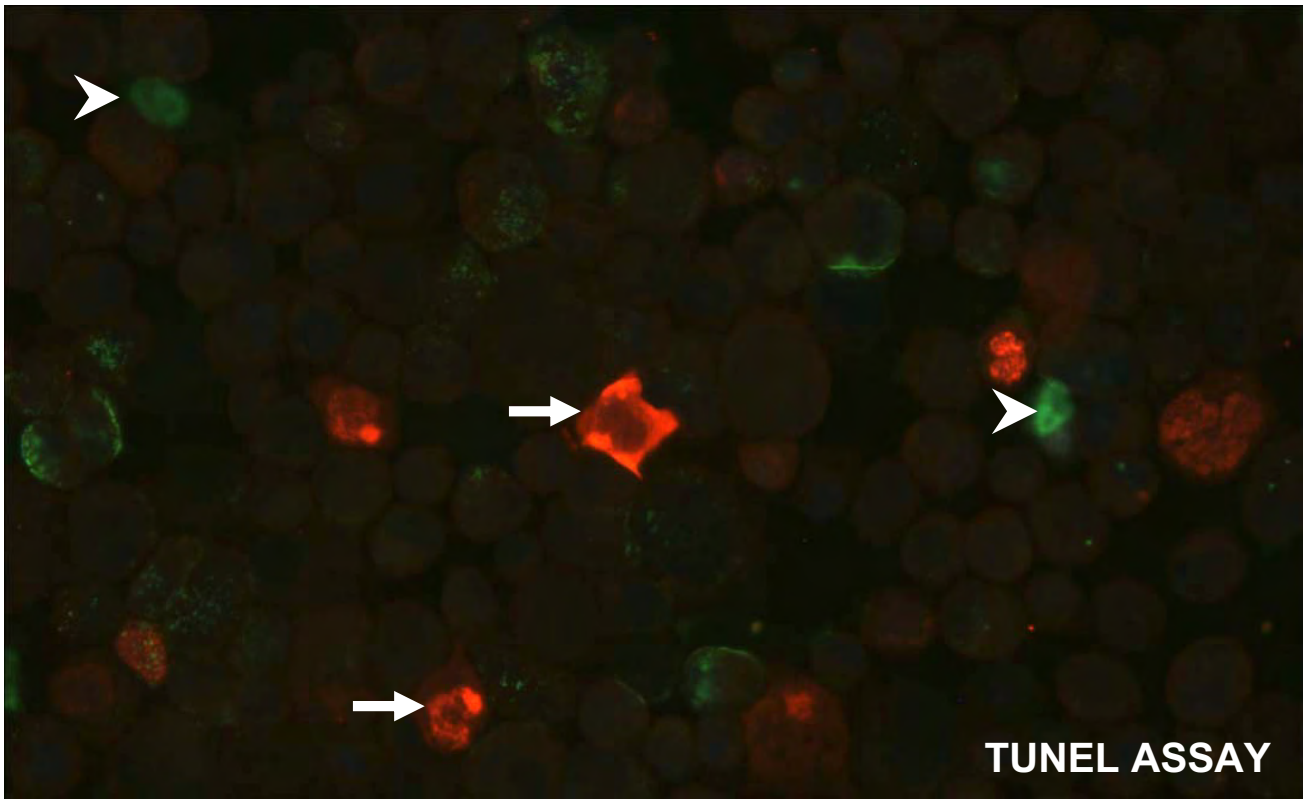

Figure 8
Cyclopamine induces apoptosis in prostate cancer cells. Cyclopamine-mediated apoptosis in prostate cancer cells was analyzed by TUNEL assay. TUNEL positive cells were indicated by arrowheads. Cells with expression of Gli1 under the CMV promoter (indicated by the arrows) did not undergo apoptosis (n = 500).

ment can be achieved using microdissection techniques for collecting pure population of tumor cells in gene mutation analysis.

Since all available prostate cancer cell lines express Su(Fu) at a high level, the role of Su(Fu) on cellular functions of prostate cancer cannot be investigated in these cells. It appears that over-expression of sonic hedgehog may be responsible for hedgehog signaling activation in these cell lines [our unpublished data and [24-26]]. After screening over 30 human cancer cell lines, we identified non-prostate cancer cell line with elevated hedgehog target genes and no detectable Su(Fu) expression (data not shown here). The growth suppression effects of Su(Fu) was demonstrated in this cell line, in which Su(Fu) expression down-regulated hedgehog target genes, inhibited DNA synthesis and cell growth (data not shown here). Thus, inactivation of Su(Fu) can contribute to active hedgehog signaling in prostate cancer.

Su(Fu) is reported to affect β-catenin signaling [27,28]. We analyzed expression of β-catenin and E-cadherin in our prostate cancer array and detected cytoplasmic distribution of E-cadherin and β-catenin only in PC51 (data not shown), indicating that Su(Fu) may be able to affect both the wnt pathway and the hedgehog pathway in prostate cancer.

In addition to Su(Fu) inactivation, over-expression of Shh is another mechanism by which the hedgehog pathway is activated in cancer [7-10]. We noticed that sonic hedgehog expression varies from tumor to tumor, which may be resulted from the heterogeneity of prostate cancer. Our immunohistostaining also revealed that three tumors (PC14, PC20 and PC36) expressed PTCH1 and HIP at high levels, but had no alterations of Shh and Su(Fu). This could be due to elevated expression of indian hedgehog, or even alterations of other components of the pathway (such as Rab23 or Fused).

Once hedgehog pathway is activated, the target gene expression will be up-regulated. Thus, analysis of target gene expression using immunohistochemistry will be an effective way to detect hedgehog pathway activation in prostate cancer. Currently, PTCH1, Gli1 and HIP are good markers for the hedgehog pathway.

Perspectives on prostate cancer therapy

Our findings not only provide novel basic understanding of prostate cancer, but also allow us to design new ways to treat prostate cancer. With a specific SMO antagonist, cyclopamine, it will be possible in the future to treat prostate cancers, which have over-expressed sonic hedgehog. However, as a downstream molecule, tumors with Su(Fu) inactivation may not respond to cyclopamine treatment. Therefore, additional small molecule inhibitors appear to be necessary to treat Su(Fu) inactivated prostate cancer. One possibility is to use Gli1 SiRNA since we have indicated that down-regulation of Gli1 may be an important mechanism by which inhibition of the hedgehog pathway by cyclopamine induces apoptosis (Fig. 8). Sanchez et al also indicated that Gli1 SiRNA down-regulated DNA synthesis in prostate cancer cells [24].

Conclusion

Taken together, our findings suggest that activation of the hedgehog pathway involves prostate cancer progression. There might be several mechanisms by which the hedgehog pathway is activated in advanced prostate cancers, including loss of Su(Fu) protein expression, over-expression of sonic hedgehog or other alterations. We demonstrate that activation of the hedgehog pathway is associated with DNA synthesis and cell invasiveness in prostate cancer cells. Inhibition of the hedgehog pathway, on the other hand, causes apoptosis possibly through down-regulation of Gli1. Our studies predict that targeted inhibition of the hedgehog pathway may be an effective way to prevent prostate cancer progression.

Materials and methods

Tissue Microarray of Prostate Cancer

A total of 55 paraffin-embedded tissue blocks from patients with prostate cancer were obtained from UTMB Surgical pathology with approval from the Institutional Review Board (IRB). Pathological reports, H#E staining of each specimen were reviewed to determine the nature of the disease and the Gleason scores. Of 55 specimens, 18 were from tumors with Gleason scores 3–6, 15 with Gleason score 7 and 22 with Gleason scores 8–10. The tumor area was first identified before tissue microarray (1.5 mm in diameter for specimens) was assembled with Beecher's Tissue arrayer-I® according to manufacturer's instruction http://www.beecherinstruments.com.

Immunohistochemistry and Western blotting

A standard avidin-biotin immunostaining technique was performed using a kit from Vector laboratories using specific antibodies to Su(Fu) (Santa Cruz Biotechnology Cat# 10933), PTCH1 (Santa Cruz Biotechnology Cat# 6149), HIP (R&D systems Cat# AF1568) and Shh (Santa Cruz Biotechnology Cat# 9024) and PSA (Vector laboratories). Positive staining was in red or brown. The specificity of antibodies was tested using the very peptide used for raising the antibodies, which abolished the specific staining. Hematoxylin was used for counterstaining (in blue). Protein was analyzed by Western analysis with appropriate antibodies [Su(Fu) antibodies were from Santa Cruz, beta-actin antibody was purchased from Sigma). The signals were visualized with the enhanced chemiluminescence detection system (Amersham).

Cell lines and Cell invasion assay

Cell lines (RWPE-1, Du145, PC3, LN-CAP were purchase from ATCC and cultured according to the suggested conditions. TSU was kindly provided by Dr. Allen Gao. Cell invasion assay was performed with BD Bio-coat cell invasion chambers according to manufacturer's instruction (BD Bioscience, Inc., Franklin Lakes, NJ), with triplicates for each sample and the experiment was repeated three times with the similar results. Cell were treated with 5 μM cyclopamine (or tomatidine) before (for 12 h) and during cell invasion assay (for 24 h). The rate of cell invasion was calculated by dividing cell numbers penetrated the matrigels by the number of cell in the control chambers (without matrigels).

RT-PCR and sequencing analysis

Total RNA was isolated using Trizol® reagent (Invitrogen), and RT-PCR was performed using Promega's RT-PCR system according to the manufacturer's protocol. Two pairs of Su(Fu) primers were used (the first set with the forward primer 5'-cctacgcaccccgatggcg-3" and the reverse primer 5'-agccaaaaccactacctcca-3'; the second set with the forward primer 5'-tccaggttaccgctatcgtc-3' ad the reverse primer 5'-tagtgtagcggactgtcg-3'). PCR products were first purified using Qiagen's Gel Extraction Kit. Due to existence of possible Su(Fu) splicing isoforms in humans, Su(Fu) genetic mutations were screened after the PCR products were cloned into TOPO® TA cloning vectors (Invitrogen). Several independent clones (from three experiments) of each PCR product were selected for sequencing analysis in UTMB sequencing facility. All mutations were confirmed by at least six independent clones.

Real-time PCR We used Applied Biosystems' assays-by-demand 20× assay mix of primers and TaqMan probes (FAM™ dye-labeled) for the target genes (human Gli and PTCH1, the sequences have been patented by Applied Biosystems, Foster City, CA) and pre-developed 18S rRNA

(VIC™-dye labled probe) TaqMan® assay reagent (P/N 4319413E) for an internal control. The primers are designed to span exon-exon junctions so as not to detect genomic DNA and the primers and probe sequences were searched against the Celera database to confirm specificity. To obtain the relative quantitation of gene expression, a validation experiment was performed to test the efficiency of the target amplification and the efficiency of the reference amplification. All absolute values of the slope of log input amount vs. ΔC_T were <0.1. Separate tubes (singleplex) one-step RT-PCR was performed with 20 ng RNA for both target genes and endogenous control. The reagent we used was TaqMan one-step RT-PCR master mix reagent kit (P/N 4309169). The cycling parameters for one-step RT-PCR was: reverse transcription 48°C for 30 min, AmpliTaq activation 95°C for 10 min, denaturation 95°C for 15 sec and annealing/extension 60°C for 1 min (repeat 40 times) on ABI7000. Triplicate C_T values were analyzed in Microsoft Excel using the comparative $C_T(\Delta\Delta C_T)$ method as described by the manufacturer(Applied Biosystems, Foster City, CA). The amount of target ($2^{-\Delta\Delta CT}$) was obtained by normalization to an endogenous reference (18sRNA) and relative to a calibrator.

BrdU labeling and TUNEL assay

BrdU labeling was performed using an *in situ* cell proliferation kit (Roche Molecular Biochemicals) [22]. Cells were treated with 5μM cyclopamine (or tomatidine) for 12 h before BrdU labeling (1 h at 37°C). The percentage of BrdU positive cells was obtained by counting over 1000 cells under microscope, and the experiment was repeated twice with similar results. TUNEL assay was performed using an *in situ* cell death kit (Roche Molecular Biochemicals) [21,29]. Cells were treated with 5 μM cyclopamine (or tomatidine) for 36 h before TUNEL assay).

List of abbreviations

PSA – prostate specific antigen; HIP – hedgehog-interacting protein; Su(Fu) – suppressor of fused; PTCH1 – human homologue of *patched* 1; Shh – sonic hedgehog; SMO – smoothened, BCC – basal cell carcinoma.

Authors' contributions

Tao Sheng contributed to Figures 6, 7, 8, cellular functions of the hedgehog pathway in prostate cancer cells. Chegxin Li contributed to primary tumor protein expression, particularly on Su(Fu) expression. Xiaoli Zhang contributed to mutation analyses of Su(Fu) in prostate cancer and real-time PCR analyses. Sumin Chi contributed to HIP antibody test (Fig. 3A and 3B). Nonggao He contributed to HIP antibody staining (Fig. 3C). Kai Chen contributed to PTCH1 antibody test (Fig. 1A). Frank McCormick involved in the initial project discussion. Zoran Gatalica contributed to prostate cancer histology and Gleason scores of the tumors.

Additional material

Additional File 1

Table 1 Prostate cancer specimens and protein expression. *Prostate cancer specimens and expression of several hedgehog signaling proteins are summarized in this table (A). A total of 55 specimens were used in this study. The Gleason scores and protein expression of Shh, PTCH1 and Su(Fu) are shown (B).*

Click here for file

[http://www.biomedcentral.com/content/supplementary/1476-4598-3-29-S1.doc]

Acknowledgements

we thank Dr. Huiping Guo for technical support of real-time PCR. J.X. was supported by grants from a NIH R01 grant, a DOD grant and the Sealy Foundation for biomedical Sciences.

References

1. Ingham PW: **Transducing Hedgehog: the story so far.** *Embo J* 1998, **17:**3505-3511.
2. Taipale J, Beachy PA: **The Hedgehog and Wnt signalling pathways in cancer.** *Nature* 2001, **411:**349-354.
3. Johnson RL, Rothman AL, Xie J, Goodrich LV, Bare JW, Bonifas JM, Quinn AG, Myers RM, Cox DR, Epstein E. H., Jr., Scott MP: **Human homolog of patched, a candidate gene for the basal cell nevus syndrome.** *Science* 1996, **272:**1668-1671.
4. Hahn H, Wicking C, Zaphiropoulous PG, Gailani MR, Shanley S, Chidambaram A, Vorechovsky I, Holmberg E, Unden AB, Gillies S, Negus K, Smyth I, Pressman C, Leffell DJ, Gerrard B, Goldstein AM, Dean M, Toftgard R, Chenevix-Trench G, Wainwright B, Bale AE: **Mutations of the human homolog of Drosophila patched in the nevoid basal cell carcinoma syndrome.** *Cell* 1996, **85:**841-851.
5. Xie J, Murone M, Luoh SM, Ryan A, Gu Q, Zhang C, Bonifas JM, Lam CW, Hynes M, Goddard A, Rosenthal A, Epstein E. H., Jr., de Sauvage FJ: **Activating Smoothened mutations in sporadic basal-cell carcinoma.** *Nature* 1998, **391:**90-92.
6. Taylor MD, Liu L, Raffel C, Hui CC, Mainprize TG, Zhang X, Agatep R, Chiappa S, Gao L, Lowrance A, Hao A, Goldstein AM, Stavrou T, Scherer SW, Dura WT, Wainwright B, Squire JA, Rutka JT, Hogg D: **Mutations in SUFU predispose to medulloblastoma.** *Nat Genet* 2002, **31:**306-310.
7. Berman DM, Karhadkar SS, Hallahan AR, Pritchard JI, Eberhart CG, Watkins DN, Chen JK, Cooper MK, Taipale J, Olson JM, Beachy PA: **Medulloblastoma growth inhibition by hedgehog pathway blockade.** *Science* 2002, **297:**1559-1561.
8. Watkins DN, Berman DM, Burkholder SG, Wang B, Beachy PA, Baylin SB: **Hedgehog signalling within airway epithelial progenitors and in small- cell lung cancer.** *Nature* 2003, **422:**313-317.
9. Berman DM, Karhadkar SS, Maitra A, Montes De Oca R, Gerstenblith MR, Briggs K, Parker AR, Shimada Y, Eshleman JR, Watkins DN, Beachy PA: **Widespread requirement for Hedgehog ligand stimulation in growth of digestive tract tumours.** *Nature* 2003, **425:**846-851.
10. Thayer SP, Di Magliano MP, Heiser PW, Nielsen CM, Roberts DJ, Lauwers GY, Qi YP, Gysin S, Fernandez-Del Castillo C, Yajnik V, Antoniu B, McMahon M, Warshaw AL, Hebrok M: **Hedgehog is an early and late mediator of pancreatic cancer tumorigenesis.** *Nature* 2003, **425:**851-856.
11. Berman DM, Desai N, Wang X, Karhadkar SS, Reynon M, Abate-Shen C, et al.: **Roles for Hedgehog signaling in androgen production and prostate ductal morphogenesis.** *Dev Biol* 2004, **267:**: 387-398.

12. Podlasek CA, Barnett DH, Clemens JQ, Bak PM, Bushman W: **Prostate development requires Sonic hedgehog expressed by the urogenital sinus epithelium.** *Dev Biol* 1999, **209:**28-39.
13. Wang BE, Shou J, Ross S, Koeppen H, De Sauvage FJ, Gao WQ: **Inhibition of epithelial ductal branching in the prostate by sonic hedgehog is indirectly mediated by stromal cells.** *J Biol Chem* 2003, **278:**18506-18513.
14. Freestone SH, Marker P, Grace OC, Tomlinson DC, Cunha GR, Harnden P and Thomson AA.: **Sonic hedgehog regulates prostatic growth and epithelial differentiation.** *Dev Biol* 2003, **264:**: 352-362.
15. Latini JM, Rieger-Christ KM, Wang DS, Silverman ML, Libertino JA, Summerhayes IC: **Loss of heterozygosity and microsatellite instability at chromosomal sites 1Q and 10Q in morphologically distinct regions of late stage prostate lesions.** *J Urol* 2001, **166:**1931-1936.
16. Leube B, Drechsler M, Muhlmann K, Schafer R, Schulz WA, Santourlidis S, Anastasiadis A, Ackermann R, Visakorpi T, Muller W, Royer-Pokora B: **Refined mapping of allele loss at chromosome 10q23-26 in prostate cancer.** *Prostate* 2002, **50:**135-144.
17. Ding Q, Fukami S, Meng X, Nishizaki Y, Zhang X, Sasaki H, et al.: **Mouse suppressor of fused is a negative regulator of sonic hedgehog signaling and alters the subcellular distribution of Gli1.** *Curr Biol* 1999, **9:**1119-1122.
18. Kogerman P, Grimm T, Kogerman L, Krause D, Unden AB, Sandstedt B, et al.: **Mammalian suppressor-of-fused modulates nuclear-cytoplasmic shuttling of Gli-1.** *Nat Cell Biol* 1999, **1:**312-319.
19. Stone DM, Murone M, Luoh S, Ye W, Armanini MP, Gurney A, Phillips H, Brush J, Goddard A, de Sauvage FJ, Rosenthal A: **Characterization of the human suppressor of fused, a negative regulator of the zinc-finger transcription factor Gli.** *J Cell Sci* 1999, **112:**4437-4448.
20. Meng X, Poon R, Zhang X, Cheah A, Ding Q, Hui CC, Alman B: **Suppressor of fused negatively regulates beta-catenin signaling.** *J Biol Chem* 2001, **276:**40113-40119.
21. Athar M, Li CX, Chi S, Tang X, Zhang X, Kim AL, Tyring SK, Kopelovich L, Epstein EH Jr, Blickers DR, Xie J: **Inhibition of smoothened signaling prevents ultraviolet B-induced basal cell carcinomas through induction of fas expression and apoptosis.** *Cancer Res* 2004, **64:**7545-7552.
22. Xie J, Aszterbaum M, Zhang X, Bonifas JM, Zachary C, Epstein E, McCormick F: **A role of PDGFRalpha in basal cell carcinoma proliferation.** *Proc Natl Acad Sci U S A* 2001, **98:**9255-9259.
23. Xie J, Johnson RL, Zhang X, Bare JW, Waldman FM, Cogen PH, Menon AG, Warren RS, Chen LC, Scott MP, Epstein E. H., Jr.: **Mutations of the PATCHED gene in several types of sporadic extracutaneous tumors.** *Cancer Res* 1997, **57:**2369-2372.
24. Sanchez P, Hernandez AM, Stecca B, Kahler AJ, DeGueme AM, Barrett A, et al.: **Inhibition of prostate cancer proliferation by interference with SONIC HEDGEHOG-GLI1 signaling.** *Proc Natl Acad Sci U S A* 2004, **101:**12561-12566.
25. Karhadkar SS, Steven Bova G, Abdallah N, Dhara S, Gardner D, Maitra A, et al.: **Hedgehog signalling in prostate regeneration, neoplasia and metastasis.** *Nature* 2004, **431:**707-712.
26. Fan L, Pepicelli CV, Dibble CC, Catbagan W, Zarycki JL, Laciak R, et al.: **Hedgehog signaling promotes prostate xenograft tumor growth.** *Endocrinology* 2004, **145:**3961-3970.
27. Meng X, Poon R, Zhang X, Cheah A, Ding Q, Hui CC and Alman B.: **Suppressor of fused negatively regulates beta-catenin signaling.** *J Biol Chem* 2001, **276:**40113-40119.
28. Taylor MD, Zhang X, Liu L, Hui CC, Mainprize TG, Scherer SW, et al.: **Failure of a medulloblastoma-derived mutant of SUFU to suppress WNT signaling.** *Oncogene* 2004, **23:**4577-4583.
29. Li C, Chi S, He N, Zhang X, Guicherit O, Wagner R, Tyring S, Xie J: **IFNalpha induces Fas expression and apoptosis in hedgehog pathway activated BCC cells through inhibiting Ras-Erk signaling.** *Oncogene* 2004, **23:**1608-1617.

ACCELERATED PUBLICATION

This paper is available online at www.jbc.org

THE JOURNAL OF BIOLOGICAL CHEMISTRY VOL. 281, NO. 1, pp. 9–12, January 6, 2006

Regulation of Gli1 Localization by the cAMP/Protein Kinase A Signaling Axis through a Site Near the Nuclear Localization Signal*[S]

Received for publication, June 28, 2005, and in revised form, November 14, 2005
Published, JBC Papers in Press, November 17, 2005, DOI 10.1074/jbc.C500300200

Tao Sheng, Sumin Chi, Xiaoli Zhang, and Jingwu Xie[1]

From the Sealy Center for Cancer Cell Biology and Department of Pharmacology, University of Texas Medical Branch, Galveston, Texas 7555-1048

The *hedgehog* (Hh) pathway plays a critical role during development of embryos and cancer. Although the molecular basis by which protein kinase A (PKA) regulates the stability of hedgehog downstream transcription factor cubitus interruptus, the *Drosophila* homologue of vertebrate Gli molecules, is well documented, the mechanism by which PKA inhibits the functions of Gli molecules in vertebrates remains elusive. Here, we report that activation of PKA retains Gli1 in the cytoplasm. Conversely, inhibition of PKA activity promotes nuclear accumulation of Gli1. Mutation analysis identifies Thr^{374} as a major PKA site determining Gli1 protein localization. In the three-dimensional structure, Thr^{374} resides adjacent to the basic residue cluster of the nuclear localization signal (NLS). Phosphorylation of this Thr residue is predicted to alter the local charge and consequently the NLS function. Indeed, mutation of this residue to Asp (Gli1/T374D) results in more cytoplasmic Gli1 whereas a mutation to Lys (Gli1/T374K) leads to more nuclear Gli1. Disruption of the NLS causes Gli1/T374K to be more cytoplasmic. We find that the change of Gli1 localization is correlated with the change of its transcriptional activity. These data provide evidence to support a model that PKA regulates Gli1 localization and its transcriptional activity, in part, through modulating the NLS function.

Hedgehog (Hh)[2] proteins are a group of secreted proteins whose active forms are derived from a unique protein cleavage process and at least two post-translational modifications (1, 2). Secreted Hh molecules bind to the receptor patched (PTC), thereby alleviating PTC-mediated suppression of smoothened (SMO) (2, 3). Expression of sonic hedgehog (Shh) appears to stabilize SMO protein possibly through post-translational modification of SMO (4). The effect of hedgehog molecules can be inhibited by hedgehog-interacting protein (HIP) through competitive association with PTC (5, 6). In *Drosophila*, SMO stabilization triggers complex formation with Costal-2, Fused, and Gli homologue cubitus interruptus (CI), which prevents CI degradation and formation of a transcriptional repressor (7–10). SMO ultimately activates transcription factors of the Gli family. Gli molecules enter nucleus through a nuclear localization signal (11, 12), but little is known about the regulatory mechanism for this process. As transcriptional factors, Gli molecules can regulate target gene expression by direct association with a consensus binding site (5′-tgggtggtc-3′) located in the promoter region of the target genes (13, 14).

Protein kinase A (PKA) was first identified as an inhibitory component of the Hh pathway in *Drosophila* (15–19). PKA fulfills its negative role by phosphorylating full-length Ci (Ci155) at several Ser/Thr residues, priming it for further phosphorylation by glycogen synthase kinase 3 (GSK3) and casein kinase I (CKI) (20–22). Hyperphosphorylation of Ci155 targets it for proteolytic processing to generate the repressor form (Ci75) (23). Consistent with this, overexpressing a constitutively active form of PKA catalytic subunit (PKAc), mC*, blocks Ci155 accumulation and Hh target gene expression (24). In addition to its inhibitory effects, PKA phosphorylation at the C terminus of SMO in *Drosophila*, but not in mammals, enhances hedgehog-mediated signaling (25, 26).

While the regulation of CI cleavage by PKA phosphorylation is well documented, very little is known about the role of PKA in Gli regulation. In vertebrates, there are three Gli molecules, Gli1, Gli2, and Gli3. Gli3 can be processed in a manner similar to CI, a process regulated by PKA (27, 28). The fact that Gli3 expression is often not detectable in human cancer suggests that Gli3 does not play a significant role in hedgehog-driven carcinogenesis (29–31). In contrast, Gli1 and Gli2 are expressed in tumors with activated hedgehog signaling (2, 29–36). Here, we report that the cAMP/PKA signaling axis regulates Gli1 protein localization, in part, through phosphorylation of Gli1 at a site near the nuclear localization signal (NLS). We propose that this unique regulation is an important mechanism by which PKA inhibits transcriptional activity of Gli molecules.

MATERIALS AND METHODS

Cell Culture and Plasmids—COS7 and NIH3T3 cells were purchased from the American Type Culture Collection (Manassas, VA) and were maintained in Dulbecco's modified Essential medium supplemented with 10% fetal bovine serum (Invitrogen). Transfection was performed using Lipofectamine 2000 (Invitrogen) according to the manufacturer's instructions (the ratio of plasmid (μg) to lipid (μl) was 1:2.5). Stable expression of a luciferase reporter under the control of Gli responsive elements in NIH3T3 cells was achieved through selection with G418 for 3 weeks after transient transfection with Lipofectamine 2000 (Invitrogen). Two clones with good responses to Gli1 expression (over 20-fold) were selected from a total of 80 clones.

Cells with expression of Gli1 (with C-MYC tag) were treated with 10 μM H89 (Calbiochem) or 0.4 ng/ml leptomycin B (LMB, Sigma) for 8 h. For forskolin treatment (20 μM for 8 h), cells were pretreated with phosphodiesterase inhibitor IBMX (100 μM) for 30 min before addition of forskolin. Immunofluorescent detection of C-MYC-tagged Gli1 was performed as described previously with Cy3-conjugated MYC antibody 9e10 (Sigma) (1:100 dilution) (37). Gli1 localization was detected under a fluorescent microscope; the percentage of Gli1 in the nucleus or the cytoplasm was calculated for each experiment from over 200 Gli1-expressing cells, and the experiment was repeated three times.

Gli1 cDNA was generously provided by Dr. Bert Vogelstein and cloned into pCDNA3.1 with a C-MYC tag at the N terminus. Gli1-GFP construct was made by subcloning Gli1 cDNA into pEGFP-3C using *BamHI* (5′) and NotI (3′) sites. Point mutations of Gli1 were made by *in situ* mutagenesis in our DNA Recombinant Laboratory Core Facility or by PCR-based mutagenesis. All mutations were confirmed by sequencing of the entire coding region. Clones containing only the targeted mutations were used in the studies.

Immunoprecipitation and in Vitro Kinase Assay—Cells were lysed using Nonidet P-40 cell lysis buffer 48 h following Gli1 transfection. C-MYC-tagged Gli1 proteins were immunoprecipitated with an anti-MYC 9B11 antibody (Cell Signaling Inc.) for 3 h followed by incubation with A/G plus beads (Bethyl Laboratories, Inc.) for 1 h. The immunocomplexes were divided into two portions. One portion (20%) was separated by 10% SDS-PAGE and analyzed by Western blotting using an anti-MYC antibody 9B11. The remaining 80% of them were incubated with 0.6 ng of recombinant PKA catalytic subunit with ADBI buffer (20 mM MOPS, pH 7.2, 25 mM β-glycerol phosphate, 5 mM EGTA, 1 mM sodium orthovanadate, 1 mM dithionthreitol) containing 1 mg/ml bovine serum albumin, and 10 μCi of [γ-^{32}P]ATP at 30 °C for 30 min. The kinase reactions were terminated by adding 4× SDS sample buffer, and the samples were separated by 10% SDS-PAGE. Gels were dried on Whatman

* This work was supported by NCI/National Institutes of Health Grant R01CA94160, Department of Defense Grant DOD-PC030429, and NIEHS/National Institutes of Health Grant ES06676. The costs of publication of this article were defrayed in part by the payment of page charges. This article must therefore be hereby marked "*advertisement*" in accordance with 18 U.S.C. Section 1734 solely to indicate this fact.

[S] The on-line version of this article (available at http://www.jbc.org) contains a supplemental figure.

[1] To whom correspondence should be addressed: Sealy Center for Cancer Cell Biology, MRB 9.104, UTMB, 301 University Blvd., Galveston, TX 77555-1048. Tel.: 409-747-1845; Fax: 409-747-1938; E-mail: jinxie@utmb.edu.

[2] The abbreviations used are: Hh, hedgehog; PTC, patched; SMO, smoothened; PKA, protein kinase A; CI, cubitus interruptus; Shh, sonic hedgehog; NLS, nuclear localization signal; NES, nuclear export signal; aa, amino acid; LMB, leptomycin B; IBMX, isobutylmethylxanthine; GFP, green fluorescent protein; MOPS, 4-morpholinepropanesulfonic acid.

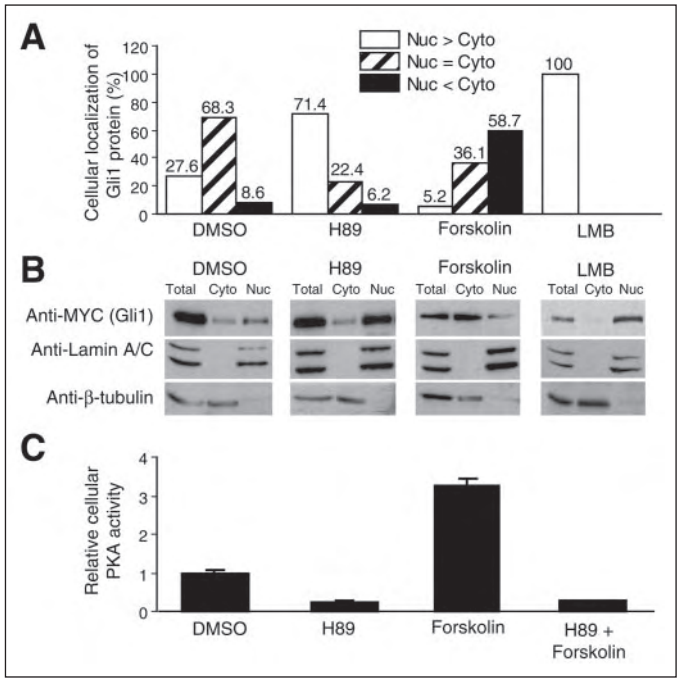

FIGURE 1. **Regulation of Gli1 localization by forskolin-mediated PKA activation in COS7 cells.** *A*, Gli1 was detected by immunofluorescent staining. Following treatment with forskolin (8 h), H89 (8 h), or LMB (8 h) (see "Materials and Methods"), Gli1 protein localization was assessed under a fluorescent microscope in over 200 Gli1-expressing cells, and the experiment was repeated three times with similar results. The percentage of Gli1 in each cellular compartment was calculated from these experiments (see supplemental figure for typical pictures of Gli1 staining). *Nuc > Cyto* indicates preferential nuclear localization, *Nuc = Cyto* indicates localization both in the nucleus and in the cytoplasm, and *Nuc < Cyto* indicates predominant cytoplasmic localization. *B*, Gli1 was detected after cell fractionation (see "Materials and Methods"). Both the nuclear fraction and the cytoplasmic fraction were collected for Western blotting analysis. The purity of cell fractionation was assessed using lamin A/C for the nuclear fraction and β-tubulin for the cytoplasmic fraction. *C*, the cellular PKA activity in COS7 cells was determined using a kit from Upstate Biotechnology Inc. The high PKA activity (*C*) was correlated with a higher level of cytoplasmic Gli1.

paper, followed by autoradiography. Western blotting analysis was performed according to a previously published procedure (37).

Cellular PKA Activation Assay—COS7 cells were seeded into 6-well plates the day before the experiment. Cells were serum-starved for 12 h and then treated with 20 μM H89, 20 μM forskolin or both for 45 min. 100 μM IBMX was added for 30 min prior to treatment with forskolin. Cellular PKA activity in the above-described conditions was determined using a PKA activation assay (Upstate Biotechnology Inc.), in which Leu-Arg-Arg-Ala-Ser-Leu-Gly (Kemptide) was used as the substrate (38). In brief, cell lysates were prepared using Nonidet P-40 lysis buffer. After sonication, the cell lysates were collected at 12,000 rpm for 5 min. 10-μl cell lysates were incubated with 10 μM ATP containing 10μCi [γ-^{32}P]ATP (3,000 Ci/mmol)], 250 μM Kemptide substrate in ADBI buffer at 30 °C for 10 min. Background was determined from reactions without substrate, and the total PKA activity was estimated in reactions containing 20 μM dibutyryl-cAMP. Aliquots were spotted onto Whatman P-81 paper, and the filters were washed in 0.75% phosphoric acid three times for 5 min per wash. ^{32}P incorporation was determined by liquid scintillation counting. Protein concentration of the cell lysates was determined by a kit from Bio-Rad (Bio-Rad protein assay). Data are representative of three independent experiments.

Cell Fractionation—Following transfection, the COS7 cells were maintained in 10 cm cell culture dishes for 48 h. Before harvest, the cells were rinsed twice with cold phosphate-buffered saline, harvested by scraping with 1 ml of cold phosphate-buffered saline for each 10-cm dish, and collected by centrifugation at 3,000 × *g* for 30 s. One-fifth of the lysates were collected for detection of Gli1 expression by Western blotting. The cell pellets were incubated with 60 μl of buffer A (50 mM HEPES, pH 7.4, 10 mM KCl, 1 mM EDTA, 1 mM EGTA, 1 mM dithiothreitol, 0.1 μg of phenylmethylsulfonyl fluoride/ml, 1 μg of pepstatin A/ml, 1 μg of leupeptin/ml, 10 μg of soybean trypsin inhibitor/ml, 10 μg of aprotinin/ml, and 0.1% IGEPAL CA-630). After 10 min on ice, the lysates were centrifuged at 6,000 × *g* for 30 s at 4 °C. The supernatant fractions were saved as the cytoplasmic fraction. The pellet (containing the nuclei) was resuspended in buffer B (buffer A containing 1.0 M sucrose) and centrifuged at 15,000 × *g* for 10 min at 4 °C. The purified nuclei (pellets) were incubated in 30 μl buffer C (10% glycerol, 50 mM HEPES, pH 7.4, 400 mM KCl, 1 mM EDTA, 1 mM EGTA, 1 mM dithiothreitol, 0.1 μg of phenylmethylsulfonyl fluoride/ml, 1 μg of pepstatin A/ml, 1 μg of leupeptin/ml, 10 μg of soybean trypsin inhibitor/ml, 10 μg of aprotinin/ml) after vigorous vortex and centrifuged at 15,000 × *g* for 20 min at 4 °C, and supernatant fractions were collected. All extracts were normalized for protein amounts determined by Bio-Rad protein assay (Bio-Rad) and separated by 10% SDS-PAGE for further analysis (39). Antibodies to β-tubulin (Sigma) and Lamin A/C (Santa Cruz Biotechnology Inc.) were used to detect the purity of cytoplasmic (β-tubulin) and nuclear (Lamin A/C) fractions using Western blotting analysis.

Luciferase Reporter Gene Assay—For luciferase assay, NIH3T3 cells with stable expression of the Gli luciferase reporter were transfected with Gli1 constructs (0.5 μg/well) and the TK-*Renilla* control plasmid (5 ng/well) using Lipofectamine 2000. After 5 h, the medium was replaced with fresh growth medium and the cells were incubated in 5% CO_2 at 37 °C overnight. Following treatment with forskolin or other compounds, the cells were harvested, and luciferase activity was measured with the dual luciferase reporter assay system (Promega) according to the manufacturer's instruction. In brief, the transfected cells were lysed in the 6-well plates with 100 μl of reporter lysis buffer and the lysate transferred into Eppendorf tubes. Cell debris was removed by centrifugation at top speed for 10 min in a microcentrifuge. 20 μl of the supernatant was mixed with 100 μl of buffer LAR II, and the absorbance was immediately measured (the first reading). After 3 s, 100 μl of Stop & Glo® Reagent was added to measure the Renillar luciferase activity (the second reading). The value from the first reading was divided by the value from the second reading of each sample to obtain the luciferase activity. Each experiment was repeated three times with similar results.

RESULTS

Gli1 is not only a downstream effector but also a target gene of the hedgehog pathway (40). Thus, identification of the mechanism by which PKA phosphorylation regulates Gli1 functions will help us understand signal transduction of the hedgehog pathway in cancer.

First, we tested whether Gli1 protein localization can be altered by accumulation of the cellular cAMP level in COS7 cells. After transient transfection, the protein localization of Gli1 was detected by immunofluorescent staining of the C-MYC tag at the Gli1 N terminus and by cell fractionation. In the presence of 20 μM forskolin, which directly activates adenylyl cyclase and raises the cyclic AMP level (41), we observed that the percentage of cytoplasmic Gli1 was increased over 5-fold, whereas the percentage of nuclear Gli1 was reduced by 80% (Fig. 1, *A* and *B*). The effect seems to be direct because the change in Gli1 localization can be observed 20 min after forskolin treatment. Conversely, addition of PKA inhibitor H89 led to a shift of Gli1 localization to the nucleus (Fig. 1, *A* and *B*). As a consequence of forskolin treatment, the cellular PKA activity was increased 2-fold (Fig. 1*C*). Conversely, addition of H89 into the medium inhibited the cellular PKA activity by 70% (Fig. 1*C*). Thus, Gli1 localization was correlated with the cellular PKA activity. To confirm the data from the immunofluorescent staining, we performed cell fractionation analysis. As shown in Fig. 1*B*, more Gli1 were in the nuclear fraction following H89 treatment whereas forskolin caused an increase of cytoplasmic Gli1 (Fig. 1*B*). Furthermore, we monitored localization of Gli1-GFP fusion protein with a time-lapse microscope in the presence of H89 or forskolin. Forskolin retained Gli1-GFP in the cytoplasm whereas H89 promoted nuclear accumulation of this fusion protein (data not shown). All these data indicate that Gli1 localization can be regulated by modulating the cellular PKA activity.

Gli1 protein shuttling between the nucleus and the cytoplasm was interrupted by inhibition of nuclear export with LMB, a specific inhibitor for CRM1-mediated nuclear export, resulting in nuclear accumulation of all Gli1 proteins (Fig. 1, *A* and *B*), supporting that Gli1 localization is a dynamic process and is tightly regulated. Our data suggest that direct phosphorylation of Gli1 by PKA is responsible for regulation of Gli1 protein localization.

Sequence analysis predicts five putative PKA sites in Gli1. The sequence around these PKA sites is highly conserved among Gli proteins (Fig. 2*A*). Several point mutations of Gli1 were made to test Gli1 regulation by PKA (see the diagram in Fig. 2*B*). These mutations were made by *in situ* mutagenesis in our DNA Recombinant Laboratory Core Facility or by PCR-based mutagenesis.

Using these mutant constructs, we assessed Gli1 localization in cultured

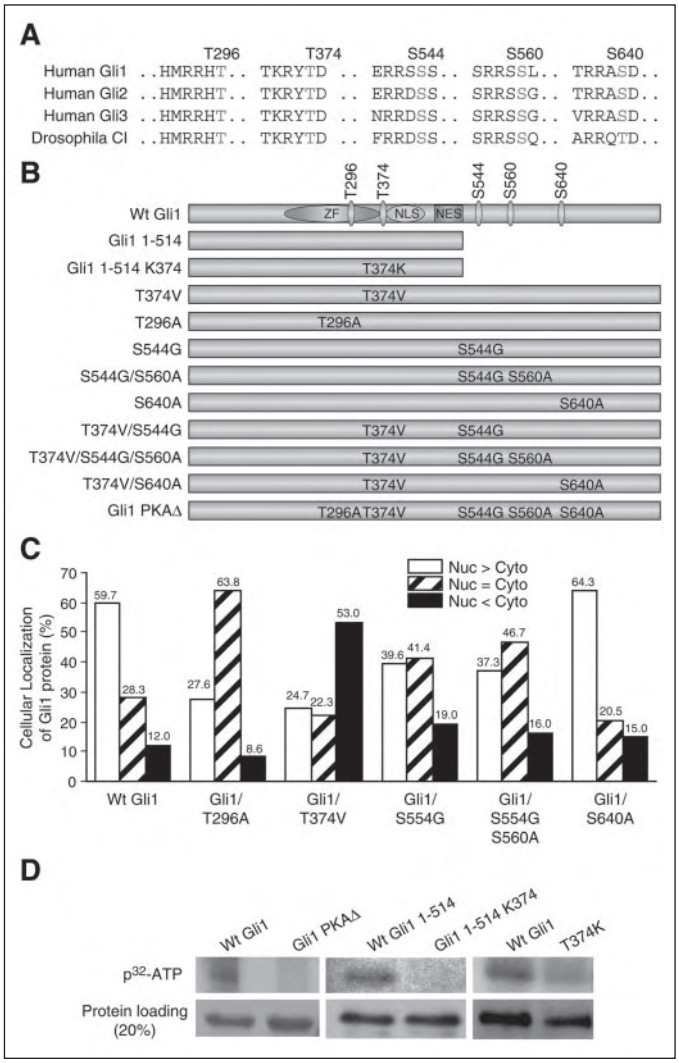

FIGURE 2. **Regulation of PKA phosphorylation and localization by cAMP/PKA. The five putative sites are conserved in all Gli molecules.** *A* shows the sequence alignment of CI and human Gli1, Gli2, and Gli3 at the five putative PKA sites. *B* shows the Gli1 constructs used in this study. Gli1 molecules with point mutations of one or more PKA sites were expressed in COS7 cells and their localization was detected by immunofluorescent staining. Full-length Gli1 with a mutation at Thr^{374} (T374V) had the most significant effect on Gli1 protein localization (*C*). In contrast, a mutation at Ser^{544} or other sites (*C* and see supplemental figure) had little effects on Gli1 protein localization. A Gli1 mutant Gli1/T374V/S544G/S560A with triple mutations at PKA sites behaved like Gli1/T374V (supplemental figure), indicating that Thr^{374} is a critical PKA site for determining Gli1 protein localization. Over 200 Gli1-positive cells were counted under a fluorescent microscope for Gli1 protein localization, and the experiment was repeated three times with similar results. The data were the average result from these experiments. *D* shows Gli1 phosphorylation *in vitro* by recombinant PKA. Wild type Gli1 and its mutant forms were expressed in COS7 cells and subsequently purified through immunoprecipitation. The ability of PKA to phosphorylate immunoprecipitated Gli1 proteins were performed *in vitro* (see "Materials and Methods"). The full-length Gli1, but not Gli1-PKAΔ (see *B*, the mutation sites), was highly phosphorylated by PKA *in vitro* (*D*, *left panels*). A single point mutation in a Gli1 fragment (1–514 aa, shown in *B*) prevented protein phosphorylation by PKA (*D*, *center panels*). This same mutation in the full-length Gli1 also dramatically reduced the level of phosphorylation (*D*, *right panels*).

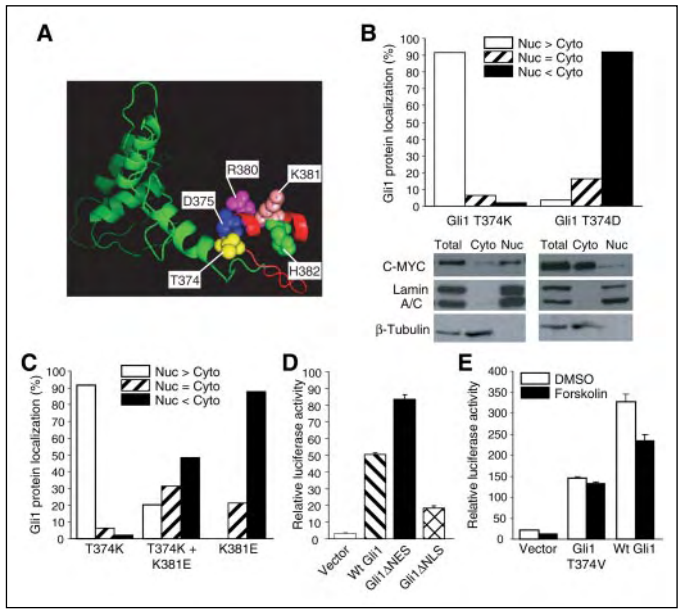

FIGURE 3. **Demonstration of Thr^{374} as the major site for Gli1 regulation.** *A*, a three-dimensional model of Gli1 fragment, showing the proximity of Thr^{374}/Asp^{375} to the basic residue cluster (Arg^{380}/Lys^{381}/His^{382}) of the Gli1 NLS. *B* shows the preferential nuclear localization of Gli1/T374K and the predominant cytoplasmic localization of Gli1/T374D. Localization was confirmed by cell fractionation. Immunofluorescent staining was done as described for Fig. 1*A*. *C* shows Gli1/T374K localization following an additional mutation at Lys^{381}. These experiments suggest that Thr^{374} is responsible for cAMP/PKA-mediated regulation of Gli1 localization, which may be achieved through affecting the NLS function. *D*, correlation of Gli1 localization with its transcriptional activity was examined in NIH3T3 cells with stable expression of a luciferase reporter under the control of Gli-responsive elements (see "Materials and Methods" for details). Gli1 with a Lys to Glu mutation at Lys^{381} (K381E) of the NLS motif, which predominantly localizes to the cytoplasm, was unable to activate this reporter. In contrast, Gli1 with mutations in the NES motif, which predominantly localizes to the nucleus, was more active than the wild type Gli1. *E*, transcriptional activity of Gli1/T374V was not responsive to forskolin treatment whereas the transcriptional activity of wild type Gli1 was reduced by 60% following forskolin treatment.

cells. We found that mutation at Thr^{374} (Gli1/T374V) significantly affects Gli1 localization (Fig. 2*C*). Furthermore, the response of Gli1/T374V to forskolin treatment was nearly diminished (in response to forskolin treatment, 5-fold increase in cytoplasmic protein for wild type Gli1 but only 40% increase for Gli1/T374V) (also see the supplemental figure). In contrast, the protein localization of Gli1/S544G and Gli1/S544G/S560A was not different from the wild type Gli1 (supplemental figure). A mutant Gli1 (Gli1/T374V/S544G/S560A) with triple mutations at the PKA sites behaved like Gli1/T374V (supplemental figure), indicating that Ser^{544} and Ser^{560} are not involved in regulation of Gli1 localization. On the other hand, a mutation at S640A had only slight effects on Gli1 protein localization in response to forskolin (supplemental figure). These data indicate that Thr^{374} is the major site responsible for Gli1 protein localization in cultured cells.

Consistent with the role of Thr^{374} for Gli1 protein localization, we also confirmed that Thr^{374} can be phosphorylated by recombinant PKA *in vitro* (Fig. 2*D*). We performed PKA phosphorylation with Gli1 protein purified by immunoprecipitation in the presence of [γ-^{32}P]ATP and recombinant PKA in test tube and found that Gli1 was highly phosphorylated by PKA *in vitro* (Fig. 2*D*, *left panels*, *first lane*). Gli1 with mutations of all five PKA sites (PKAΔ) could not be phosphorylated by PKA (Fig. 2*D*, *left panels*, *right lane*). To test whether the Thr^{374} site of Gli1 is phosophorylated by recombinant PKA, we used a Gli1 fragment containing only two PKA sites: Thr^{296} and Thr^{374}. We found that this Gli1 fragment (1–514 aa) with a mutation at Thr^{374} was not able to be phosphorylated by recombinant PKA *in vitro* (Fig. 2*D*, *center panels*). Even a single point mutation at Thr^{374} significantly reduced PKA-mediated phosphorylation of full-length Gli1 (Fig. 2*D*, *right panels*), indicating that the Thr^{374} site is a major PKA site of Gli1 phosphorylation. In addition, our data also suggested that Ser^{544}, Ser^{560}, and Ser^{640} can be phosphorylated by PKA *in vitro* (data not shown here). The above data indicate that Thr^{374} is a major PKA site involved in regulation of Gli1 protein localization.

In the three-dimensional structure, Thr^{374}, together with the adjacent Asp^{375}, is close to the first basic residue cluster (Arg^{380}/Lys^{381}/His^{382}) of the bipartite motif (the classic NLS) in Gli1 (Fig. 3*A*) (42). It is known that protein phosphorylation at the residue next to the bipartite motif inhibits its binding affinity to importins, leading to reduced nuclear localization of the target protein (43). We predict that phosphorylation of Thr^{374} will increase the local negative charge, leading to reduced NLS functions and accumulation of Gli1 in the cytoplasm. Indeed, Gli1/T374D was preferentially localized to the cytoplasm (Fig. 3*B*). Conversely, Gli1/T374K has a high local positive charge near the NLS, and we found that Gli1/T374K predominantly localized to the nucleus (Fig. 3*B*). Localization of these Gli1 proteins was further confirmed by

cell fractionation (Fig. 3*B*). These data support our hypothesis that one mechanism by which the cellular PKA activity regulates Gli1 localization is through altering the local charge nearby the NLS of Gli1.

If Gli1 nuclear localization is regulated by PKA phosphorylation through a NLS-dependent mechanism, disruption of the NLS should affect localization of these mutant Gli1 molecules. As shown in Fig. 3*C*, we found that Gli1/K381E, which is predicted to disrupt the NLS, was predominantly localized to the cytoplasm, confirming the role of NLS in Gli1 localization (12). Although Gli1/T374K localizes predominantly to the nucleus, additional mutation at K381 (K381E) retained Gli1/T374K to the cytoplasm (Fig. 3*C*), suggesting that regulation of Gli1 localization by T374 phosphorylation requires the intact NLS.

The ultimate effect of Gli1 is transcriptional activation of the downstream target genes. To assess whether Gli1 localization affects its transcriptional activity, we established stable expression of Gli1 luciferase reporter under the control of Gli responsive elements in NIH3T3 cells (13). By measuring the reporter luciferase activity, we examined the association of Gli1 localization with its transcriptional activity (Fig. 3*D*). If Gli1/K381E remains preferentially in the cytoplasm, the transcriptional activity was low. In contrast, Gli1 with a defective NES (Gli1/L496V/L498V), which localizes predominantly in the nucleus, was more active (Fig. 3*D*). Thus, the Gli1 luciferase reporter activity in these cells is very sensitive to Gli1 localization. We examined the effects of forskolin to Gli1-mediated transcriptional activity in this NIH3T3 stable cell line. Like the wild type Gli1, Gli1/T374V can activate the Gli luciferase reporter (Fig. 3*E*). Consistent with its cytoplasmic localization, the luciferase activity in cells expressing the wild type Gli1 was reduced after forskolin treatment (Fig. 3*E*). In contrast, Gli1/T374V-mediated reporter gene activity was not affected by forskolin (Fig. 3*E*). These data suggest that Thr^{374} is an important PKA site responsible for PKA phosphorylation and for the transcriptional activity of Gli1.

Based on these data, we proposed a mechanism by which the cAMP/PKA signaling axis mediates regulation of Gli1 localization. Gli1 enters the nucleus through a nuclear localization signal. With the accumulation of cAMP in the cell, Thr^{374} gets phosphorylated. Phosphorylation of Thr^{374} will increase the local negative charge nearby the NLS, which results in inhibition of NLS function. Consequently, Gli1 is retained in the cytoplasm and is unable to activate the target genes. Since this Thr residue is highly conserved among Gli proteins, we anticipate that the same mechanism is applicable to PKA regulation of other Gli molecules.

DISCUSSION

In our study, we provide direct evidence to support that the cAMP/PKA signaling axis regulates Gli1 protein localization primarily through a site at Thr^{374}. Our data further indicate that PKA-mediated regulation of Gli1 localization is through Thr^{374}, possibly through interfering with the NLS function.

Although our studies demonstrated that Thr^{374} is a major site for PKA-mediated regulation of Gli1 localization (Figs. 2 and 3 and supplemental figure), mutation at this site did not completely abolish the effects of forskolin (supplemental figure). To identify an additional site required for this regulation, we made double and triple point mutations of Gli1 at the PKA sites (Fig. 2*B*). Our data indicate that mutations at Thr^{374} and Ser^{640} completely abolished the response to forskolin treatment, indicating that Ser^{640} is another site involving PKA-mediated regulation of Gli1 localization (supplemental figure). However, mutation at Ser^{640} alone had no effect on Gli1 protein localization and had only a slight effect in response to forskolin treatment, suggesting that Ser^{640} is not a primary site for Gli1 regulation. This hypothesis was further supported by the fact that Gli1/S640E and Gli1/S640R, unlike Gli1/T374D and Gli1/T374K, did not alter Gli1 protein localization (data not shown here). Thus, we believe that additional structural information of Gli1 near the Ser^{640} region is required to understand the molecular mechanism by which PKA phosphorylation at Ser^{640} affects Gli1 localization.

Further studies of Gli1 phosphorylation can be facilitated by measuring the stoichiometry of phosphorylation for Gli1. Currently, a large amount of purified Gli1 protein is not available, making it difficult to calculate the stoichiometry of phosphorylation for such a large protein (150 kDa for Gli1). This issue may be addressed in the future using highly purified Gli1 fragments from bacteria.

In addition, our data indicate that Ser^{544} and Ser^{560} residues are not involved in regulation of Gli1 protein localization. It will be interesting to know how these two sites are involved in regulation of Gli1 functions.

Acknowledgments—We thank Drs. James Lee, Yigong Shi, Xiaodong Cheng, Mark Evers, and Min Chen for help with this project, Drs. H. Sasaki and Bert Vogelstein for providing reagents, and Karen Martin and Brenda Rubio for help with the manuscript.

REFERENCES

1. Taipale, J., and Beachy, P. A. (2001) *Nature* **411,** 349–354
2. Pasca di Magliano, M., and Hebrok, M. (2003) *Nat. Rev. Cancer* **3,** 903–911
3. Stone, D. M., Hynes, M., Armanini, M., Swanson, T. A., Gu, Q., Johnson, R. L., Scott, M. P., Pennica, D., Goddard, A., Phillips, H., Noll, M., Hooper, J. E., de Sauvage, F., and Rosenthal, A. (1996) *Nature* **384,** 129–134
4. Hooper, J. E., and Scott, M. P. (2005) *Nat. Rev. Mol. Cell Biol.* **6,** 306–317
5. Chuang, P. T., and McMahon, A. P. (1999) *Nature* **397,** 617–621
6. Lum, L., and Beachy, P. A. (2004) *Science* **304,** 1755–1759
7. Jia, J., Tong, C., and Jiang, J. (2003) *Genes Dev.* **17,** 2709–2720
8. Lum, L., Zhang, C., Oh, S., Mann, R. K., von Kessler, D. P., Taipale, J., Weis-Garcia, F., Gong, R., Wang, B., and Beachy, P. A. (2003) *Mol. Cell* **12,** 1261–1274
9. Ogden, S. K., Ascano, M., Jr., Stegman, M. A., Suber, L. M., Hooper, J. E., and Robbins, D. J. (2003) *Curr. Biol.* **13,** 1998–2003
10. Ruel, L., Rodriguez, R., Gallet, A., Lavenant-Staccini, L., and Therond, P. P. (2003) *Nat. Cell Biol.* **5,** 907–913
11. Kogerman, P., Grimm, T., Kogerman, L., Krause, D., Unden, A. B., Sandstedt, B., Toftgard, R., and Zaphiropoulos, P. G. (1999) *Nat. Cell Biol.* **1,** 312–319
12. Wang, Q. T., and Holmgren, R. A. (1999) *Development* (*Camb.*) **126,** 5097–5106
13. Sasaki, H., Hui, C., Nakafuku, M., and Kondoh, H. (1997) *Development* (*Camb.*) **124,** 1313–1322
14. Kinzler, K. W., and Vogelstein, B. (1990) *Mol. Cell. Biol.* **10,** 634–642
15. Jiang, J., and Struhl, G. (1995) *Cell* **80,** 563–572
16. Lepage, T., Cohen, S. M., Diaz-Benjumea, F. J., and Parkhurst, S. M. (1995) *Nature* **373,** 711–715
17. Li, W., Ohlmeyer, J. T., Lane, M. E., and Kalderon, D. (1995) *Cell* **80,** 553–562
18. Pan, D., and Rubin, G. M. (1995) *Cell* **80,** 543–552
19. Strutt, D. I., Wiersdorff, V., and Mlodzik, M. (1995) *Nature* **373,** 705–709
20. Chen, Y., Gallaher, N., Goodman, R. H., and Smolik, S. M. (1998) *Proc. Natl. Acad. Sci. U. S. A.* **95,** 2349–2354
21. Wang, G., Wang, B., and Jiang, J. (1999) *Genes Dev.* **13,** 2828–2837
22. Jia, J., Amanai, K., Wang, G., Tang, J., Wang, B., and Jiang, J. (2002) *Nature* **416,** 548–552
23. Aza-Blanc, P., Ramirez-Weber, F. A., Laget, M. P., Schwartz, C., and Kornberg, T. B. (1997) *Cell* **89,** 1043–1053
24. Kiger, J. A., Jr., and O'Shea, C. (2001) *Genetics* **158,** 1157–1166
25. Jia, J., Tong, C., Wang, B., Luo, L., and Jiang, J. (2004) *Nature* **432,** 1045–1050
26. Zhang, C., Williams, E. H., Guo, Y., Lum, L., and Beachy, P. A. (2004) *Proc. Natl. Acad. Sci. U. S. A.* **101,** 17900–17907
27. Wang, B., Fallon, J. F., and Beachy, P. A. (2000) *Cell* **100,** 423–434
28. Ruiz i Altaba, A. (1999) *Development* (*Camb.*) **126,** 3205–3216
29. Zhu, Y., James, R. M., Peter, A., Lomas, C., Cheung, F., Harrison, D. J., and Bader, S. A. (2004) *Cancer Lett.* **207,** 205–214
30. Ma, X., Chen, K., Huang, S., Zhang, X., Adegboyega, P. A., Evers, B. M., Zhang, H., and Xie, J. (2005) *Carcinogenesis* **26,** 1698–1705
31. Ma, X., Sheng, T., Zhang, Y., Zhang, X., He, J., Huang, S., Chen, K., Sultz, J., Adegboyega, P. A., Zhang, H., and Xie, J. (2006) *Int. J. Cancer* **118,** 139–148
32. Dahmane, N., Lee, J., Robins, P., Heller, P., and Ruiz i Altaba, A. (1997) *Nature* **389,** 876–881
33. Bonifas, J. M., Pennypacker, S., Chuang, P. T., McMahon, A. P., Williams, M., Rosenthal, A., De Sauvage, F. J., and Epstein, E. H., Jr. (2001) *J. Invest. Dermatol* **116,** 739–742
34. Xie, J., Aszterbaum, M., Zhang, X., Bonifas, J. M., Zachary, C., Epstein, E., and McCormick, F. (2001) *Proc. Natl. Acad. Sci. U. S. A.* **98,** 9255–9259
35. Toftgard, R. (2000) *Cell Mol. Life Sci.* **57,** 1720–1731
36. Regl, G., Neill, G. W., Eichberger, T., Kasper, M., Ikram, M. S., Koller, J., Hintner, H., Quinn, A. G., Frischauf, A. M., and Aberger, F. (2002) *Oncogene* **21,** 5529–5539
37. Athar, M., Li, C., Tang, X., Chi, S., Zhang, X., Kim, A. L., Tyring, S. K., Kopelovich, L., Hebert, J., Epstein, E. H., Jr., Bickers, D. R., and Xie, J. (2004) *Cancer Res.* **64,** 7545–7552
38. Cheng, X., Ma, Y., Moore, M., Hemmings, B. A., and Taylor, S. S. (1998) *Proc. Natl. Acad. Sci. U. S. A.* **95,** 9849–9854
39. He, N., Li, C., Zhang, X., Sheng, T., Chi, S., Chen, K., Wang, Q., Vertrees, R., Logrono, R., and Xie, J. (2005) *Mol. Carcinog* **42,** 18–28
40. Stecca, B., Mas, C., and Ruiz i Altaba, A. (2005) *Trends Mol. Med.* **11,** 199–203
41. Laurenza, A., Sutkowski, E. M., and Seamon, K. B. (1989) *Trends Pharmacol. Sci.* **10,** 442–447
42. Pavletich, N. P., and Pabo, C. O. (1993) *Science* **261,** 1701–1707
43. Harreman, M. T., Kline, T. M., Milford, H. G., Harben, M. B., Hodel, A. E., and Corbett, A. H. (2004) *J. Biol. Chem.* **279,** 20613–20621

[CANCER RESEARCH 64, 7545–7552, October 15, 2004]

Inhibition of *Smoothened* Signaling Prevents Ultraviolet B-Induced Basal Cell Carcinomas through Regulation of Fas Expression and Apoptosis

Mohammad Athar,[1] Chengxin Li,[5,6] Xiuwei Tang,[1] Sumin Chi,[5,6] Xiaoli Zhang,[6] Arianna L. Kim,[1] Stephen K. Tyring,[4] Levy Kopelovich,[2] Jennifer Hebert,[3] Ervin H. Epstein Jr.,[3] David R. Bickers,[1] and Jingwu Xie[5]

[1]Department of Dermatology, College of Physicians and Surgeons, Columbia University, New York, New York; [2]Division of Cancer Prevention, National Cancer Institute, Bethesda, Maryland; [3]Department of Dermatology and Comprehensive Cancer Center, University of California San Francisco, San Francisco, California; [4]Department of Dermatology, University of Texas Health Science Center, Houston, Texas; [5]Sealy Centers for Cancer Cell Biology and Environmental Health, Department of Pharmacology and Toxicology, University of Texas Medical Branch at Galveston, Galveston, Texas; and [6]Xijing Hospital, Xi'an 710032, China

ABSTRACT

Abnormal activation of the hedgehog-signaling pathway is the pivotal abnormality driving the growth of basal cell carcinomas (BCCs), the most common type of human cancer. Antagonists of this pathway such as cyclopamine may therefore be useful for treatment of basal cell carcinomas and other hedgehog-driven tumors. We report here that chronic oral administration of cyclopamine dramatically reduces (~66%) UVB-induced basal cell carcinoma formation in *Ptch1*$^{+/-}$ mice. Fas expression is low in human and murine basal cell carcinomas but is up-regulated in the presence of the smoothened (SMO) antagonist, cyclopamine, both *in vitro* in the mouse basal cell carcinoma cell line ASZ001 and *in vivo* after acute treatment of mice with basal cell carcinomas. This parallels an elevated rate of apoptosis. Conversely, expression of activated SMO in C3H10T1/2 cells inhibits Fas expression. Fas/Fas ligand interactions are necessary for cyclopamine-mediated apoptosis in these cells, a process involving caspase-8 activation. Our data provide strong evidence that cyclopamine and perhaps other SMO antagonists are potent *in vivo* inhibitors of UVB-induced basal cell carcinomas in *Ptch1*$^{+/-}$ mice and likely in humans because the majority of human basal cell carcinomas manifest mutations in PTCH1 and that a major mechanism of their inhibitory effect is through up-regulation of Fas, which augments apoptosis.

INTRODUCTION

The *hedgehog* (Hh) pathway plays a critical role in embryonic development and tissue polarity (1). Secreted Hh molecules bind to the receptor patched (PTC), thereby alleviating PTC-mediated suppression of smoothened (SMO), a putative seven-transmembrane protein. SMO signaling triggers a cascade of intracellular events, leading to activation of the pathway through GLI-dependent transcription (2). Considerable insight into the role of the Hh pathway in vertebrate development and human cancers has come from the discovery that mutations of the *patched* gene (*PTCH1*) underlie the basal cell nevus syndrome, a rare hereditary disorder in which patients are highly susceptible to the development of large numbers of basal cell carcinomas and other tumors (3, 4). Activation of Hh signaling, usually due to loss-of-function somatic mutations of *PTCH1* and less often to activating mutations of *SMO*, is the pivotal abnormality in sporadic basal cell carcinomas (5–7). Therefore, targeted inhibition of SMO signaling should afford mechanistically based prevention/therapy of basal cell carcinomas, as well as of other tumors driven by Hh signaling abnormalities, including certain medulloblastomas, small-cell lung carcinomas, and gastrointestinal tract cancers (8–11). One such inhibitor is the naturally occurring plant extract cyclopamine, and there are additional synthetic compounds that directly associate with the transmembrane domains of SMO (12–14). Therefore, these small molecular weight compounds have significant promise for the prevention and treatment of basal cell carcinomas and other human malignancies.

Ptch1$^{+/-}$ mice (15) provided the first practical animal model for inducing basal cell carcinomas using UV and ionizing radiation (16). We report here that chronic oral administration of cyclopamine dramatically inhibits basal cell carcinoma growth in these mice. We also have tested the *in vitro* effects of cyclopamine and of the synthetic SMO inhibitor Cur61414 on the mouse basal cell carcinoma cell line ASZ001 and have demonstrated that both compounds elevate Fas expression and augment apoptosis. The clinical relevance of our data for treatment of basal cell carcinomas is supported by the low baseline Fas expression in basal cell carcinomas of both humans and mice and by the *in vivo* induction of high level Fas expression by short-term administration of cyclopamine in murine basal cell carcinomas. Thus, our studies support the idea that treatment of human basal cell carcinomas with specific inhibitors of the Hh pathway may offer a mechanism-driven approach to the chemoprevention of these tumors.

MATERIALS AND METHODS

Animals. *Ptch1*$^{+/-}$ heterozygous knockout mice have been developed by deleting exons 1 and 2 and inserting the LacZ gene at the deletion site (15). *Ptch1-lacZ*-transgenic mice were genotyped by PCR amplification of genomic DNA extracted from tail biopsies (15, 16). The animals were housed under standard conditions (fluorescent lighting 12 hours per day, room temperature 23°C to 25°C, and relative humidity 45 to 55%). The mice were provided tap water and Purina Laboratory Chow 5001 diet (Ralston-Purina Co., St. Louis, MO).

UV Light Source. An UV Irradiation unit (Daavlin Co., Bryan, OH) equipped with an electronic controller to regulate dosage was routinely used for these studies. The UVB source consisted of eight FS72T12-UVB-HO lamps emitting UVB (290 to 320 nm, 75 to 80% of total energy) and UVA (320 to 380 nm, 20 to 25% of total energy). We used a Kodacel cellulose film (Kodacel TA401/407) to eliminate UVC radiation. A UVC sensor (Oriel's Goldilux UVC Probe) was used during each exposure to confirm the lack of UVC emission. The UVB dose was quantified using a UVB Spectrum 305 Dosimeter obtained from the Daavlin Co. The radiation was additionally calibrated using an IL1700 Research Radiometer/Photometer from International Light, Inc. (Newburyport, MA). The distance between the radiation source and targets was maintained at 30 cm. The irradiation assembly is kept in an air-conditioned room, and a fan is placed inside the exposure chamber to minimize temperature fluctuations during irradiation.

Carcinogenesis Protocol and Statistical Analyses. Mice were irradiated with a UV Irradiation unit (240 mJ/cm^2 three times a week) from age 6 to 32 weeks, at which time, ~50% of the animals had one or more visible skin tumors. The mice (25 mice per group) were given either cyclopamine (10 μg/day as a cyclodextran complex) or the vehicle control in drinking water,

Received 4/20/04; revised 6/20/04; accepted 8/18/04.

Grant support: National Cancer Institute Grants CA 94160 (J. Xie), CA81888 (M. Athar, A. Kim, J. Hebert, E. Epstein, D. Bickers), and CA101061 (M. Athar), Department of Defense Grant PC030429 (J. Xie), the American Cancer Society (J. Xie), the National Institute of Environmental Health Sciences Center at University of Texas Medical Branch (J. Xie), and the John Sealy Memorial Endowment Fund for Biomedical Research (J. Xie).

The costs of publication of this article were defrayed in part by the payment of page charges. This article must therefore be hereby marked *advertisement* in accordance with 18 U.S.C. Section 1734 solely to indicate this fact.

Note: M. Athar and C. Li contributed equally to this article.

Requests for reprints: Jingwu Xie, Sealy Center for Cancer Cell Biology, Department of Pharmacology and Toxicology, University of Texas Medical Branch at Galveston, 301 University Blvd., Galveston, TX 77555-1048. E-mail: jinxie@utmb.edu; or Mohammad Athar, Department of Dermatology, College of Physicians and Surgeons, Columbia University, 630 West 168th Street, New York, NY 10032. E-mail: ma493@columbia.edu

and the number of tumors was recorded weekly. Mice treated with cyclopamine or with the vehicle control were sacrificed at 52 weeks, their dorsal skin removed, and tumors harvested and collected for the histologic and immunohistochemical studies. The microscopic basal cell carcinoma areas were assessed by histologic evaluation of three dorsal skin sections per mouse from a total of seven mice ($n = 7$) in the vehicle-treated water group and a total of six mice ($n = 6$) in the cyclopamine-treated group. The basal cell carcinoma areas were measured by microscopic assessment using the Axiovision 3.1 analysis program (Carl Zeiss MicroImaging, Inc., Thornwood, NY). Results were analyzed using the Student's t test or a nonparametric test (Mann-Whitney test): $P < 0.05$ was considered statistically significant.

For evaluation of Fas expression and apoptosis *in vivo*, cyclopamine was injected (at 100 pg s.c. or intratumorally) into mice with visible basal cell carcinomas (>1 cm in diameter). Seventy-two hours later, basal cell carcinomas were embedded in OCT compound (Tissue-Tek; Sakura, Torrance, CA), and stored in −20°C for additional analyses. Stromal cells were used as the control for basal cell carcinoma cells.

β-Galactosidase Staining. Tissues were fixed in 0.2% glutaraldehyde (Sigma-Aldrich, St. Louis, MO)/2% formaldehyde (Fisher Scientific Co., Pittsburgh, PA) in 1× PBS for 20 minutes at 4°C, then washed twice in 1× PBS. Tissues were incubated with 5% 5-bromo-4-chloro-3-indolyl-β-D-galactopyranoside in 95% iron buffer solution for 24 hours at 37°C using a β-galactosidase staining set (Roche Applied Science, Indianapolis, IN), according to the manufacturer's guideline. The tissues were washed twice in 3% DMSO in 1× PBS and then three times in 70% etomidate. The tissues were embedded in paraffin and processed for counterstaining.

Terminal Deoxynucleotidyl Transferase-Mediated Nick End Labeling (TUNEL) and Immunofluorescent Staining. TUNEL analysis was performed using a kit from Roche Applied System according to the manufacturer's guideline. Immunofluorescent staining of Fas in basal cell carcinomas was performed with an antibody specific to mouse Fas (M20; Santa Cruz Biotechnology, Inc., Santa Cruz, CA).

Cell Culture and Cell Viability Assay. The mouse basal cell carcinoma cell line ASZ001 was maintained in 154CF medium as reported previously (17). Ectopic expression of Gli1 in ASZ001 cells was induced using LipofectAmine 2000, and the transfected cells were enriched by cell sorting after coexpression of green fluorescence protein and Gli1 (green fluorescence protein to Gli1 plasmid ratio = 1:4). C3H10T1/2 cells were cultured in basal medium containing 10% heat-inactivated fetal bovine serum. GLI-transformed baby rat kidney cells were cultured in DMEM containing 10% fetal bovine serum (18). ASZ001 cells were first treated with 2 μmol/L 3-keto-N-aminoethylaminoethylcaproyldihydrocinnamoyl cyclopamine (KAAD-cyclopamine) for 36 hours in the presence or absence of 10 μg/mL epidermal growth factor or platelet-derived growth factor (PDGF)-AA (R&D Systems, Inc., Minneapolis, MN) or treated with U0126 alone (10 μmol/L; EMD Biosciences, Inc., San Diego, CA) for 36 hours. Cells were then harvested for protein expression and cell viability analyses. Cell viability was assessed by trypan blue exclusion and colorimetric 3-(4,5-dimethylthiazol-2-yl)-2,5-diphenyltetrazolium bromide assay (19). The proliferation inhibition was calculated by dividing the mean test value by the respective PBS control. The background absorbance, obtained from the wells treated with DMSO only, was subtracted from the test- and control-well values to yield corrected absorbance. Triplicates for each sample were used, and all experiments were performed in triplicate (19).

Flow Cytometry and Cell Sorting. Cells were plated at 3,000,000 cells per 10-cm plate in 154CF without growth supplements the day before treatment. KAAD-cyclopamine (Toronto Research Chemicals, Inc., North York, Ontario, Canada) was added to the medium to achieve a final concentration of 2 μmol/L, and the cells were incubated for 36 hours. Epidermal growth factor and PDGF-A were used at a final concentration of 10 μg/mL, U0126 at a final concentration of 10 μmol/L, and Fas ligand (FasL)–neutralizing antibodies at a final concentration of 20 μg/mL were added to the medium. Subsequently, cells were collected and fixed overnight in 70% etomidate and treated with 50 ng/mL propidium iodide in the presence of 10 μg/mL RNase A (in PBS). Cell cycle profiles were determined by a fluorescence-activated cell sorter (FACSCaliber; Becton Dickinson, Franklin Lakes, NJ). At least 20,000 gated events were recorded for each sample, and the data were analyzed with Multicycle software for Windows (Phoenix Flow Systems, San Diego, CA). ASZ001 cells with ectopic Gli1 expression were enriched through cell sorting, resulting in >90% of the cells with Gli1 expression (from a starting population of 5% positive cells). Both positive and negative fractions were collected for Western blot analysis.

Western Blot Analysis and ELISA. Western blotting was performed as previously reported (17), with specific antibodies [anti-PDGFR-α and anti-mouse Fas antibodies from Upstate Biotechnology (Lake Placid, NY); anti-Erk, anti-phospho-Erk and anti-caspase-3 antibodies from Cell Signaling Technology (Beverly, MA); anti-β-actin from Sigma-Aldrich (St. Louis, MO); and antihuman Fas and anti-FasL from BD Transduction Laboratories (San Diego, CA)]. ELISA detection of secreted FasL protein in the growth medium was performed using a kit from R&D Systems, Inc., according to the manufacturer's protocol.

Real-time PCR Analyses. Total RNAs from ASZ001 cells were extracted using RNAqueous from Ambion, Inc. (Austin, TX). We used Applied Biosystems' (Foster City, Ca) assays-by-design 20× assay mix of primers and TaqMan probes (carboxyfluorescein dye-labeled probe) for the target genes [mouse Gli1, hedgehog interacting protein (HIP)] and predeveloped 18S rRNA (VIC dye-labeled probe) TaqMan assay reagent (P/N 4319413E) for an internal control. Mouse Gli1 and HIP primers are designed to span exon-exon junctions so as not to detect genomic DNA, and the primers and probe sequences were searched against the Celera database to confirm specificity. The primer and probe sequences of mouse Gli1 and HIP are as follows.

To obtain the relative quantitation of gene expression, a validation experiment was performed to test the efficiency of the target amplification and the efficiency of the reference amplification. All absolute values of the slope of log input amount *versus* ΔC_T were <0.1. Separate tubes (singleplex) one-step reverse transcription-PCR was performed with 20 ng of RNA for both target gene (mGli1 or mHIP) and endogenous control. The reagent we used was TaqMan one-step reverse transcription-PCR master mix reagent kit (P/N 4309169). The cycling parameters for one-step reverse transcription-PCR was reverse transcription 48°C for 30 minutes, AmpliTaq activation 95°C for 10 minutes, denaturation 95°C for 15 seconds, and annealing/extension 60°C for 1 minute (repeat 40 times) on ABI7000. Triplicate C_T values were analyzed in Microsoft Excel using the comparative C_T ($\Delta\Delta C_T$) method as described by the manufacturer (Applied Biosystems). The amount of target ($2^{-\Delta\Delta CT}$) was obtained by normalization to an endogenous reference (18 rRNA) and relative to a calibrator.

RESULTS

Cyclopamine Inhibits Basal Cell Carcinoma Development in *Ptch1*$^{+/-}$ Mice. The Hh pathway is constitutively activated in essentially all human and mouse basal cell carcinomas (3, 20). Because PTCH1, which is frequently inactivated in human basal cell carcinomas, is known to be upstream of SMO (21), inhibiting SMO functions should be an effective way to treat basal cell carcinomas. To test the effects of a SMO antagonist on development of basal cell carcinomas, we administered cyclopamine orally to basal cell carcinoma-bearing *Ptch1*$^{+/-}$ mice. We UV-irradiated *Ptch1*$^{+/-}$ mice from age 6 to 32 weeks, at which time, approximately half of the mice had developed one or more macroscopic tumors: basal cell carcinomas, squamous cell carcinomas, and/or spindle cell tumors (fibrosarcomas). UV irradiation was then stopped and the mice were randomized (25 mice per group) to receive either vehicle or cyclopamine (as cyclodextran complex) in the drinking water for the ensuing 20 weeks. The survival of these two groups of animals was similar, indicating that cyclopamine does not affect the overall survival of *Ptch*1$^{+/-}$ mice (data not shown). At age 52 weeks, we measured microscopic basal cell carcinoma areas per tissue area (mm^2) in these two groups after β-galactosidase staining (see Materials and Methods for details) and found a 90% reduction of microscopic basal cell carcinomas in the cyclopamine-treated animals (Fig. 1, *A* and *B*). Cyclopamine-treated mice also had fewer visible basal cell carcinomas at age 52 weeks than did the vehicle-treated controls (Fig. 2, *A* and *B*). Thus, the mice receiving vehicle alone continued to develop visible tumors, and the number of tumors had tripled by week 52. We

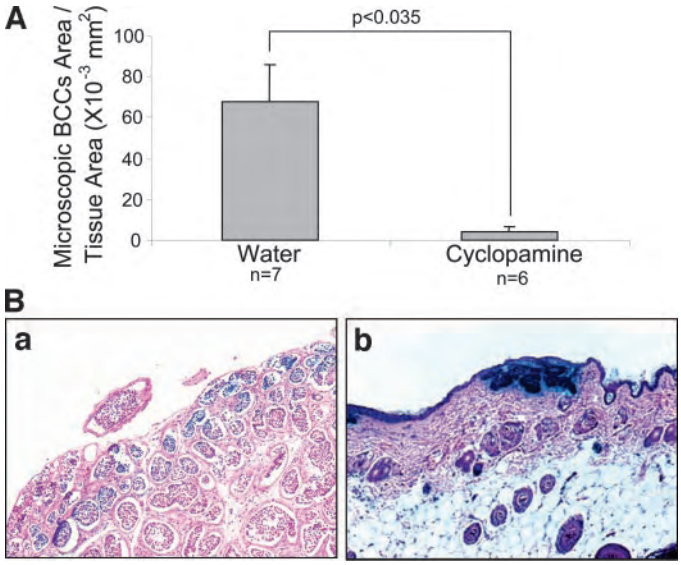

Fig. 1. Effect of cyclopamine on UVB-induced microscopic basal cell carcinomas (BCCs) in *Ptch1*$^{+/-}$ mice. *A*, effect of orally administered cyclopamine on the number of UVB-induced microscopic BCC-like lesions in *Ptch1*$^{+/-}$ mice. Microscopic BCC-like lesions were counted as total tumor area/mm^2 skin and assessed by histologic evaluation of three dorsal skin sections per mouse from a total of seven mice ($n = 7$) in the vehicle-treated group and a total of 6 mice ($n = 6$) in the cyclopamine-treated group. Results of microscopic BCCs in the two groups were statistically analyzed using the Student's *t* test (two-tailed): $P < 0.05$ was considered statistically significant. *B*, β-galactosidase and H&E staining showing the effect of orally administered cyclopamine on UVB-induced microscopic BCC lesions in *Ptch1*$^{+/-}$ mice. Representative staining from UVB-irradiated (*a*) and UVB-irradiated cyclopamine-treated (*b*) *Ptch1*$^{+/-}$ mice. These skin samples were fixed in 10% buffered formalin before staining with H&E and detection of β-galactosidase activities.

found that mice receiving cyclopamine developed 50% fewer new basal cell carcinomas than did the control group at week 52 (Fig. 2, *A* and *C*), and the difference is statistically significant ($P = 0.0078$ by nonparametric test, Mann-Whitney test). More importantly, the number of visible squamous cell carcinomas and spindle cell tumors did not differ between the two groups, showing the specificity of cyclopamine for basal cell carcinomas in this mouse model (Fig. 2*C*).

Cyclopamine Inhibits the Hh Pathway and Induces Apoptosis in Basal Cell Carcinoma Cells. To investigate the mechanism whereby cyclopamine prevents basal cell carcinoma development in *Ptch1*$^{+/-}$ mice, we used the mouse basal cell carcinoma cell line ASZ001, which is derived from basal cell carcinoma-bearing *Ptch1*$^{+/-}$ mice. Both copies of the *Ptch1* gene are lost in this cell line, resulting in constitutive activation of the Hh pathway (16, 17). Incubation with 2 μmol/L KAAD-cyclopamine, a cyclopamine analogue, for 12 hours reduced the levels of Hh target genes (Gli1 and Hip) by >70% (Fig. 3*A*), confirming that cyclopamine inhibits the Hh pathway in these cells. Treatment of ASZ001 cells for 36 hours with cyclopamine or Cur61414 caused a dose-dependent decrease in cell viability (Fig. 3*B*). A SMO antagonist, Cur61414, showed an effect similar to that of cyclopamine (Fig. 3*B*). A similar result was also obtained from the trypan blue exclusion analysis (data not shown). The closely related compound tomatidine, which does not affect SMO signaling and thus served as a negative control, had little discernible effect on the viability of the ASZ001 cells (Fig. 3*B*). Additional evidence that cyclopamine-mediated inhibition of cell growth is dependent on activated Hh signaling came from studies in primary mouse keratinocytes (Hh pathway inactivated), which did not respond to cyclopamine treatment (data not shown). In ASZ001 cells, cyclopamine treatment did not promote cellular differentiation, and hence, the dramatic reduction in the number of living cells suggested that cyclopamine might be inducing apoptosis.

We next assessed cyclopamine-induced apoptosis using flow cytometry analysis and found that treatment of cells with cyclopamine for 36 hours caused a 3-fold increase in the sub-G_1 cell population and a decrease in the S phase (Fig. 3*C*), suggesting that cyclopamine is a potent inducer of apoptosis in basal cell carcinomas. Treatment of ASZ001 cells with either cyclopamine or Cur61414 for 36 hours (see Materials and Methods for details) increased the level of activated caspase-3, a major executioner of cysteinyl aspartate-specific proteinases for apoptosis (Fig. 3*C*).

Confirming our *in vitro* findings, direct injection of cyclopamine into basal cell carcinoma-bearing mice for 72 hours enhanced apoptosis (an increase in TUNEL-positive cells) of basal cell carcinoma tumor cells *in vivo* (Fig. 3*D*).

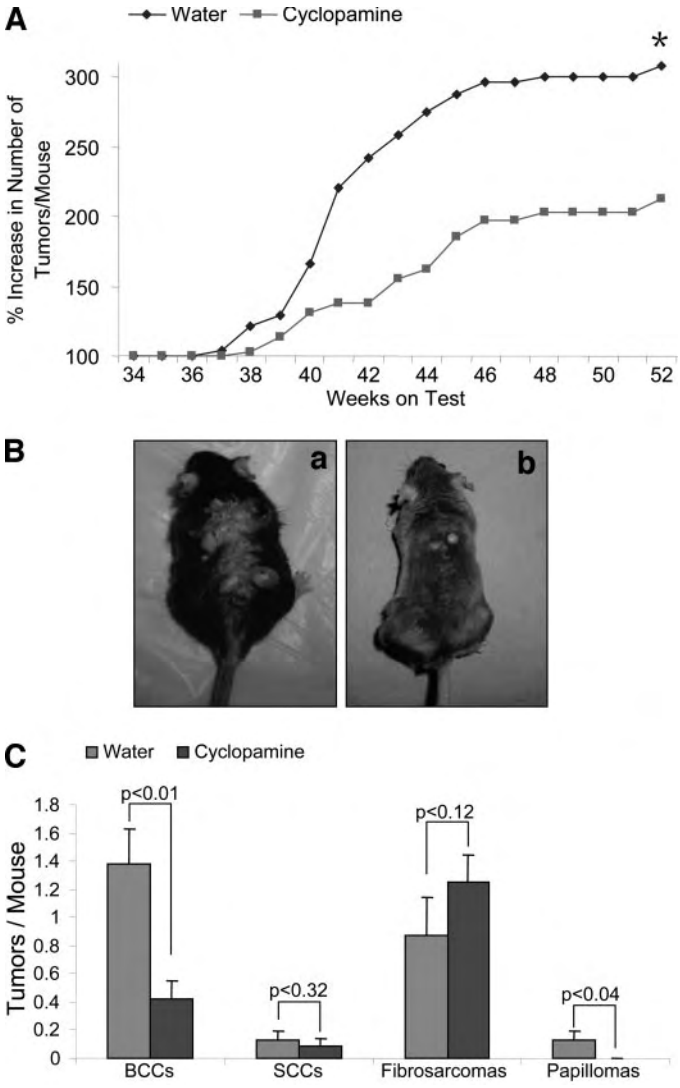

Fig. 2. Effect of cyclopamine on UVB-induced macroscopic basal cell carcinomas (BCCs) in *Ptch1*$^{+/-}$ mice. *A*, effect of cyclopamine administration on the growth of UVB-induced skin tumors in *Ptch1*$^{+/-}$ mice is shown as percent increase in number of tumors per mouse. The statistical analysis was performed using the nonparametric Mann-Whitney test (two-tailed) and obtained $P = 0.0078$ (*) at week 52. $P < 0.05$ is considered statistically significant. *B*, *Ptch1*$^{+/-}$ mice showing effects of cyclopamine treatment on UVB-induced skin tumors. Representative pictures of UVB-irradiated, vehicle-treated control mouse (*a*) and UVB-irradiated, cyclopamine-treated (*b*) mouse at week 52. *C*, effect of orally administered cyclopamine on the growth of UVB-induced BCCs, squamous cell carcinomas (SCCs), and fibrosarcomas in *Ptch1*$^{+/-}$ mice. The statistical analysis was performed using the Student's *t* test: $P < 0.05$ is considered statistically significant.

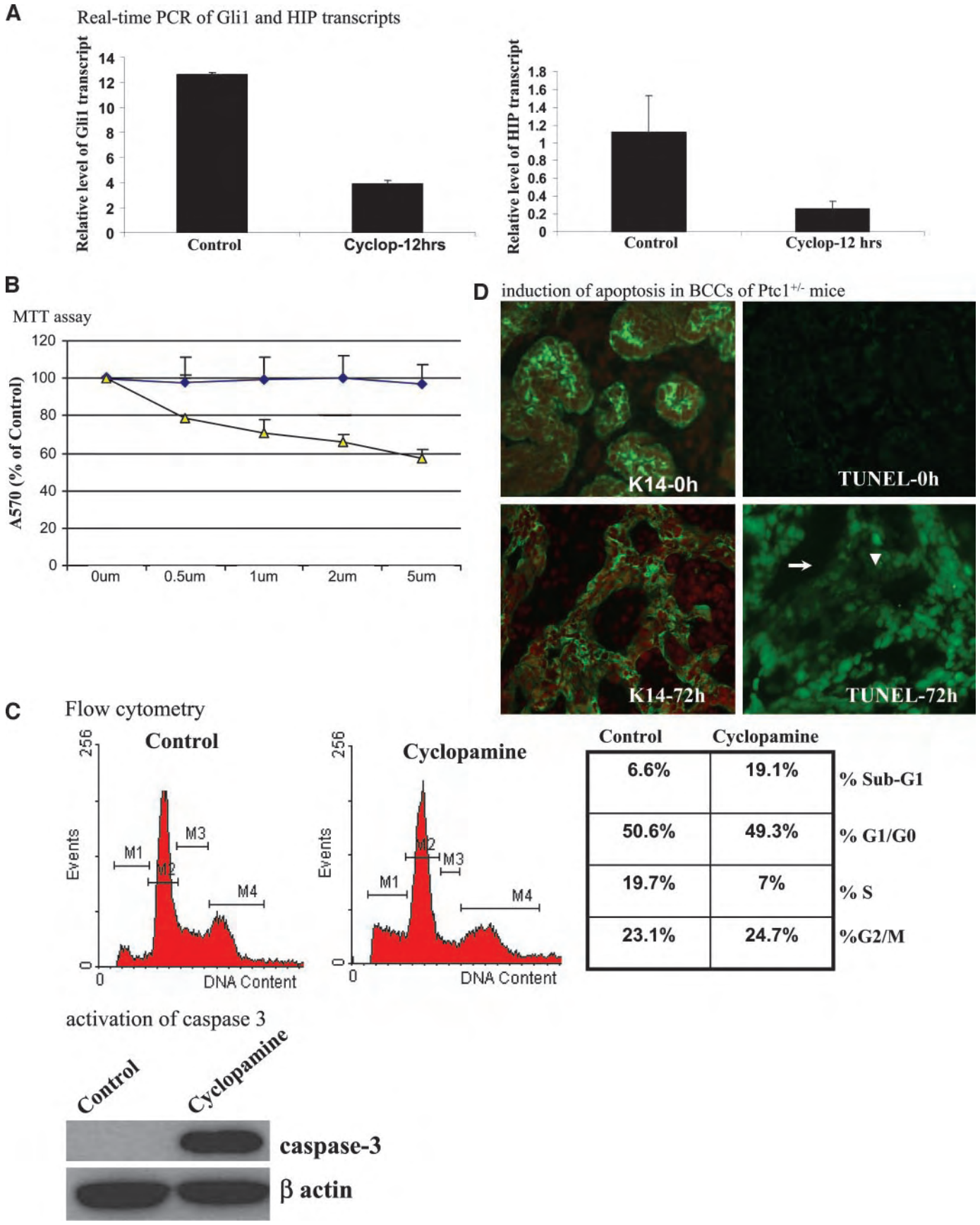

Fig. 3. Cyclopamine inhibits the Hh pathway and induces apoptosis in ASZ001 cells. *A*. Gli1 and HIP transcripts were detected by real-time PCR analysis. Cells were treated with 2 μmol/L KAAD-cyclopamine for 12 hours. After RNA extraction, real-time PCR analysis was performed (see Materials and Methods for details). *B*, 3-(4,5-dimethylthiazol-2-yl)-2,5-diphenyltetrazolium bromide (MTT) assay of ASZ001 cells in the presence of SMO antagonists. ASZ001 cells were treated with cyclopamine, or the control compound tamotidine for 36 hours, and the cell viability was examined by MTT assay. *C*, cell cycle and protein analyses of ASZ001 cells. The percentage of cell population in each cell cycle

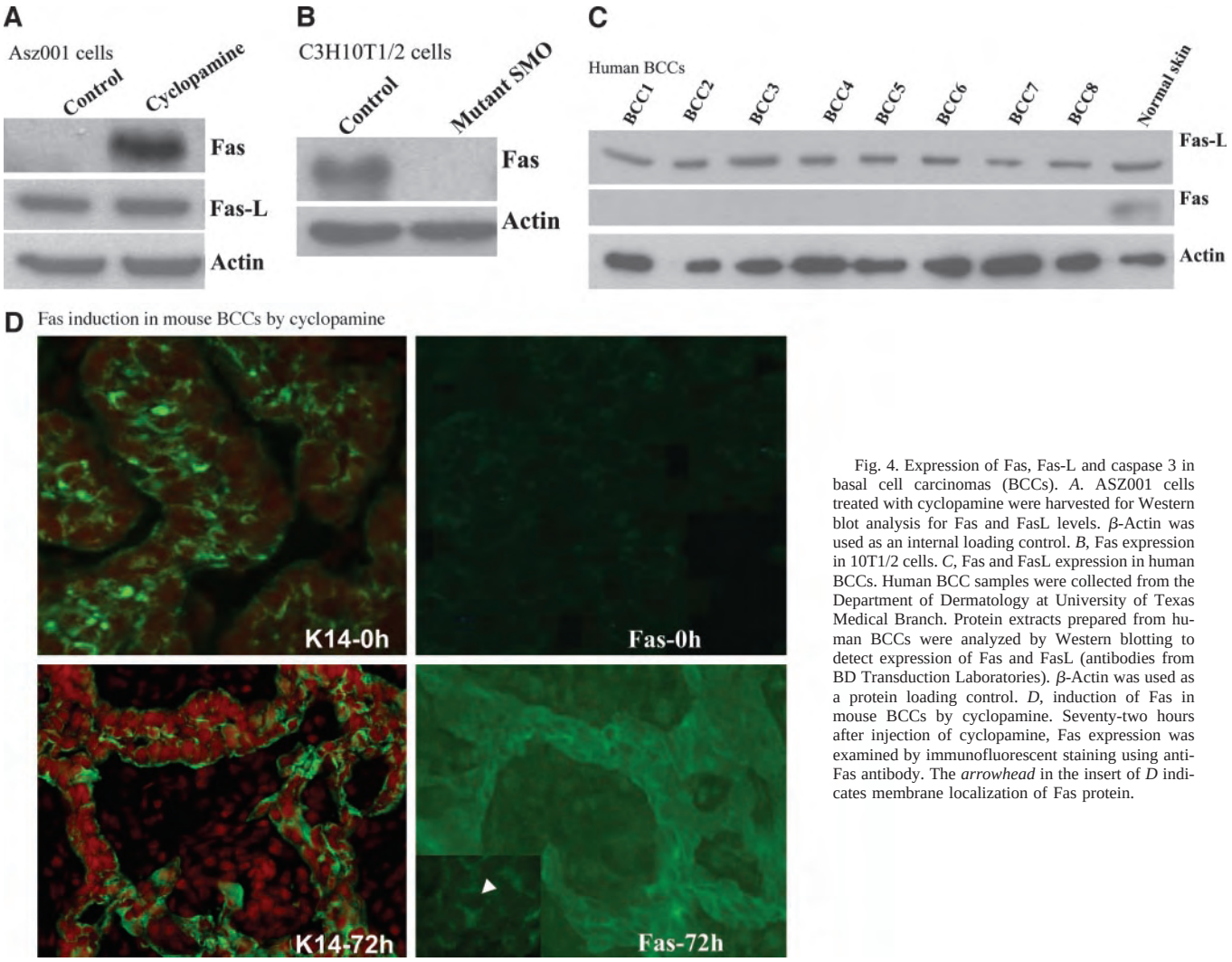

Fig. 4. Expression of Fas, Fas-L and caspase 3 in basal cell carcinomas (BCCs). *A.* ASZ001 cells treated with cyclopamine were harvested for Western blot analysis for Fas and FasL levels. β-Actin was used as an internal loading control. *B,* Fas expression in 10T1/2 cells. *C,* Fas and FasL expression in human BCCs. Human BCC samples were collected from the Department of Dermatology at University of Texas Medical Branch. Protein extracts prepared from human BCCs were analyzed by Western blotting to detect expression of Fas and FasL (antibodies from BD Transduction Laboratories). β-Actin was used as a protein loading control. *D,* induction of Fas in mouse BCCs by cyclopamine. Seventy-two hours after injection of cyclopamine, Fas expression was examined by immunofluorescent staining using anti-Fas antibody. The *arrowhead* in the insert of *D* indicates membrane localization of Fas protein.

Active Fas/FasL Interactions Are Necessary for Cyclopamine-induced Cell Death. Because treatment of human basal cell carcinomas with IFN-α may be accompanied by increased Fas expression in the tumor (19, 22), we tested whether cyclopamine, too, can augment Fas expression. Indeed, cyclopamine substantially increased the level of Fas protein in ASZ001 cells (Fig. 4*A*). In contrast, we detected FasL protein irrespective of cyclopamine treatment (Fig. 4*A*). Using an ELISA assay, we detected FasL in the culture medium of ASZ001 cells, indicating that these basal cell carcinoma cells indeed secrete FasL protein (see Fig. 5*B* for details). Thus, Fas would appear to be the limiting factor for the FasL/Fas signaling axis in this basal cell carcinoma cell line. Conversely, Fas is down-regulated in C3H10T1/2 cells with stable expression of activated SMO via retrovirus-mediated gene transfer (Fig. 4*B*).

The *in vivo* relevance of the data obtained from the experiments with the ASZ001 cell line is supported by the low level baseline expression of Fas in human basal cell carcinomas (refs. 23, 24; Fig. 4*C*) and the induction of Fas expression and apoptosis in *Ptch1*$^{+/-}$ mouse basal cell carcinomas by treatment with either cyclopamine (Fig. 4*D*) or by Cur 61414 (data not shown). Specifically, Fas protein expression increased after cyclopamine injection (either s.c. injection or intratumoral injection), and this was accompanied by increased TUNEL-positive cells (Figs. 3*F* and 4*D*). Immunofluorescent staining revealed a membrane localization of Fas protein in basal cell carcinoma cells (indicated by the arrowhead in the insert of Fig. 4*D*). Thus, it appears that Fas expression is elevated in the presence of SMO antagonists both in cultured cell lines and in basal cell carcinomas induced in *Ptch1*$^{+/-}$ mice.

On the basis of these results, we predicted that either (*a*) interruption of the FasL/Fas signaling axis or (*b*) inhibition of the downstream apoptosis-effector caspase 8 activity would prevent cyclopamine-induced apoptosis. To test this hypothesis, we inactivated FasL/Fas signaling using neutralizing antibodies against FasL. By depleting FasL molecules (Fig. 5*B*), the cyclopamine-mediated decrease in cell viability was rescued (Fig. 6, *C* and *D*). Neutralizing antibodies against FasL also decreased the level of caspase-3 (Fig. 5*C*). Furthermore, administration of the caspase-8 inhibitor Z-IETD-FMK (25) abrogated the cyclopamine-mediated activation of caspase-3 (Fig. 5*C*). Thus, our data provide direct evidence that the FasL/Fas signaling axis is an important mediator of cyclopamine-induced apoptosis in basal cell carcinomas.

phase was shown at the bottom. The level of caspase-3 in ASZ001 cells, a marker for apoptosis, was detected by immunoblotting with a specific antibody from Cell Signaling Technology (*C*). *D*, TUNEL analyses of basal cell carcinomas (BCCs) from *Ptch1*$^{+/-}$ mice. BCCs were induced in *Ptch1*$^{+/-}$ mice as reported previously (16). Cyclopamine was injected s.c. into BCC-bearing *Ptch1*$^{+/-}$ mice or directly into the tumor. Tumor specimens were collected at 72 hours after injection and embedded in OCT. Cryostat tissue sections were used for TUNEL analysis. *Green,* TUNEL or K14; *red,* nuclear staining. —◆—, Tomatidine; —■—, Cur61414; —△—, Cyclopamine.

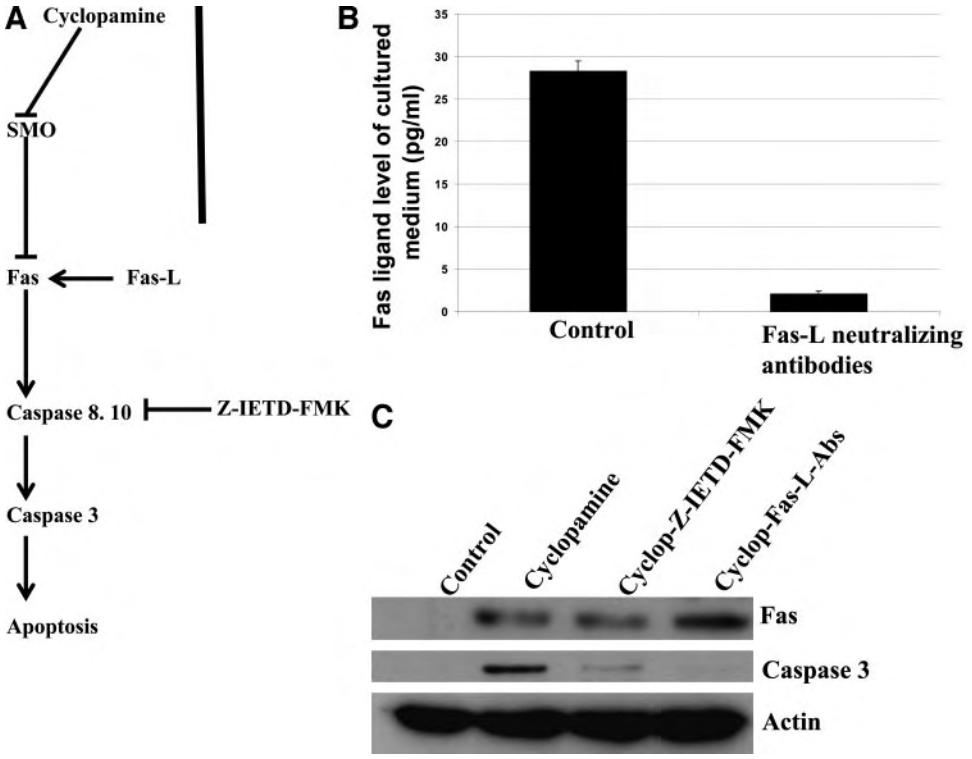

Fig. 5. Inhibition of cyclopamine-induced apoptosis by FasL-neutralizing antibodies. *A*, pathway for cyclopamine-mediated apoptosis. *B*. ASZ001 cells were cultured in 154CF medium without growth supplements during treatment with 2 μmol/L cyclopamine. The level of FasL in the culture medium of ASZ001 cells was detected by ELISA with a kit from R&D Systems, Inc. *C*, detection of Fas and caspase-3 in ASZ001 cells by Western blotting.

The Molecular Basis of Cyclopamine-mediated Induction of Fas. To investigate the mechanism whereby inhibition of the Hh pathway induces Fas expression, we assessed whether this regulation occurs directly as opposed to indirectly by altering other signaling pathways. It has been reported that several signaling pathways, including the Ras-Erk pathway and the p53 pathway, can regulate Fas expression (26–28). We have previously reported that Hh activation augments Ras-Erk signaling (17). Consistent with those findings, we observed that cyclopamine decreased the levels of PDGFR-α and phospho-Erk, indicating an inhibitory effect on Ras-Erk signaling in ASZ001 cell (Fig. 6*B*). As a result, PDGF-A had no effect on cyclopamine-mediated caspase-3 activation, Fas induction, or cell death (see Fig. 6, *D* and *E*, for details). In contrast, epidermal growth factor, which can activate the Ras-Erk pathway through the epidermal growth factor receptor, did inhibit cyclopamine-mediated accumulation of the sub-G_1 population (Fig. 6*C*), Fas expression (Fig. 6*D*), caspase-3 activation (Fig. 6*D*), and cell death (Fig. 6*E*). Furthermore, addition of the mitogen-activated protein kinase kinase inhibitor U0126 alone was sufficient to induce caspase-3 in ASZ001 cells (Fig. 6*D*). Consistent with these data, ASZ001 cells in which PDGFR-α and active Raf were overexpressed resisted cyclopamine treatment (data not shown), providing additional information that inhibition of PDGFR-α and subsequent down-regulation of Ras-Erk signaling is an important mechanism whereby cyclopamine induces apoptosis in basal cell carcinomas.

Our model predicts that overexpression of Gli1 in ASZ001 cells under a strong promoter (such as the cytomegalovirus promoter) would constitutively activate the Hh pathway, which could render these basal cell carcinoma cells resistant to cyclopamine treatment. Indeed, cyclopamine did not induce apoptosis in constitutive Gli1-expressing ASZ001 cells, as indicated by lack of TUNEL staining and of procaspase-3 cleavage (Fig. 6, *F* and *G*). As a result of constitutive Gli1 overexpression, PDGFR-α remained unchanged even after cyclopamine treatment (Fig. 6*G*). In addition, Fas protein was not induced by cyclopamine in constitutive Gli1-expressing ASZ001 cells (Fig. 6*G*). The ability of Gli-1 overexpression to abrogate cyclopamine-mediated cell death was additionally confirmed by flow cytometry analysis (data not shown). Although cyclopamine caused an increase in the sub-G_1 population in Gli1-negative cells, no such change was observed in Gli1-expressing ASZ001 cells. These data indicate that ectopic expression of Gli1 under the cytomegalovirus promoter prevents cyclopamine-induced changes in the expression of PDGFR-α, Fas, and apoptosis.

DISCUSSION

The identification of SMO antagonists has created the opportunity to consider mechanism-driven anticancer strategies for effective treatment of common malignancies in which Hh activation is thought to be important, including basal cell carcinomas, as well as subsets of medulloblastomas, lung cancer, and gastrointestinal cancers (3, 8–11). Basal cell carcinomas frequently contain mutations of the *PTCH1* gene, most of which lead to inactivated *PTCH1* and consequently uncontrolled SMO signaling. Because PTCH1 is upstream of SMO (21),[7] we reasoned that administration of the SMO inhibitor cyclopamine to *Ptch1*$^{+/-}$ mice could specifically and effectively inhibit the development of basal cell carcinomas *in vivo*. Our studies indicate that orally administered cyclopamine is a potent inhibitor of basal cell carcinomas in *Ptch1*$^{+/-}$ mice and that this natural substance does not cause significant toxicity because the overall survival of the treated mice was unaffected. These data are consistent with the observation in sheep that cyclopamine toxicity is limited to Hh signaling-dependent teratogenicity (2, 29) and with the fact that most normal adult mouse and human tissues appear to have very low expression of Hh target genes (30). Basal cell carcinomas would appear to be good candidates for the cutaneous application of SMO antagonists because our data indicate that direct injection of cyclopamine into mouse basal cell carcinomas induces Fas expression and apoptosis. Thus, it should be possible to design topical formulations of

[7] Unpublished observation.

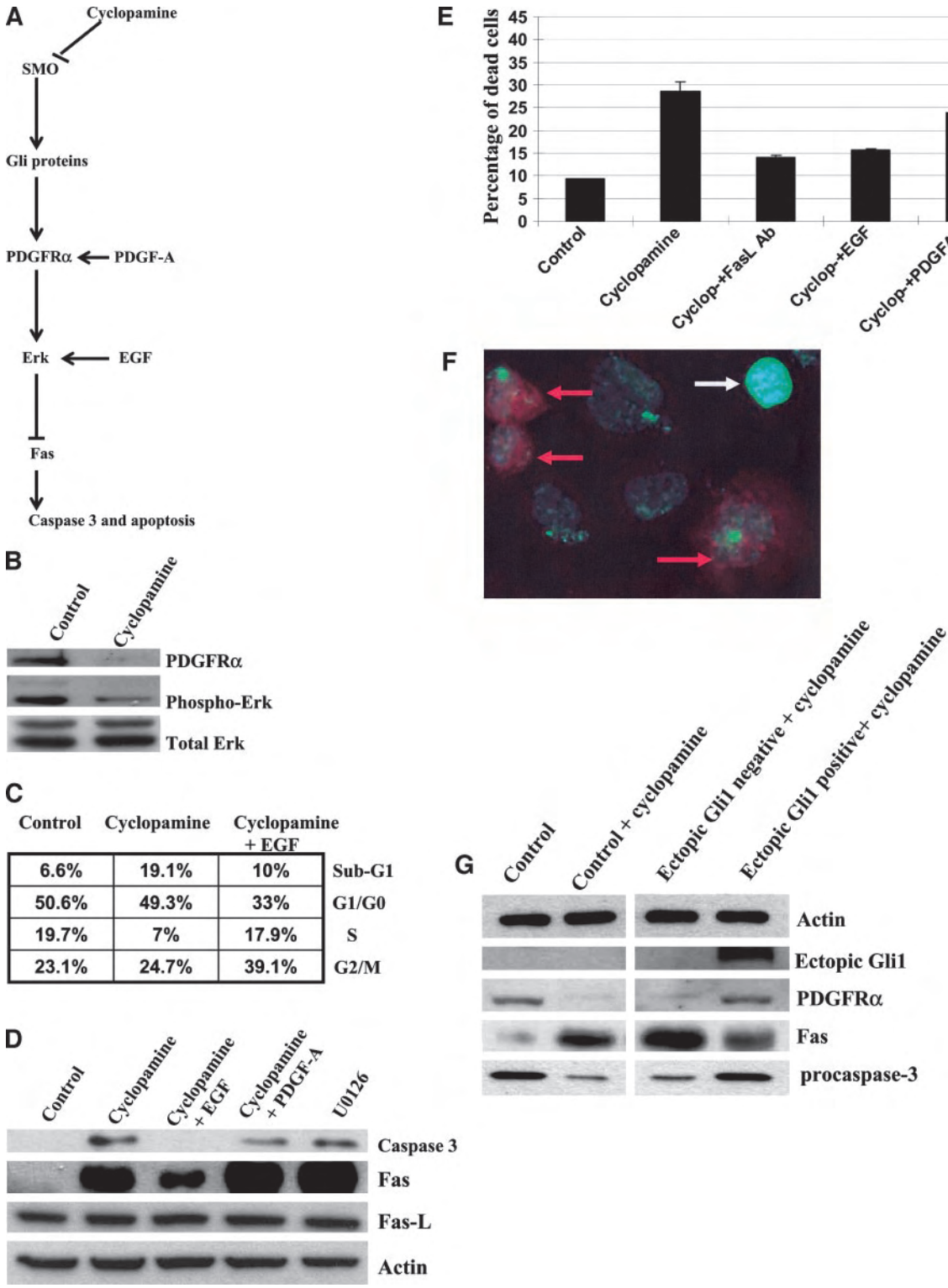

Fig. 6. Regulation of Fas expression by cyclopamine through the Ras-Erk pathway. *A*, pathway for cyclopamine-mediated apoptosis. *B*. In the presence of cyclopamine, the levels of PDGFR-α and phospho-Erk were down-regulated. *C*, epidermal growth factor (EGF) abrogated cyclopamine-mediated sub-G_1 accumulation in ASZ001 cells. *D*. The protein levels of Fas, FasL, and activated caspase-3 were detected by Western blotting after 36 hours treatment with 2 μmol/L KAAD-cyclopamine in the presence of other reagents or with U0126 alone (10 μmol/L). *E*. Cell viability was assessed by trypan blue analysis. Each experiment was repeated three times with similar results. *F*, detection of apoptosis by TUNEL assay in ASZ001 cells with Gli1 expression under the cytomegalovirus promoter. *Red arrows* indicate Gli1-positive cells, and the *white arrow* indicates TUNEL-positive cells. *G*. After enrichment of Gli1-overexpressing cells through cell sorting, the protein levels of PDGFR-α, Fas, and caspase-3 were detected by Western blotting.

cyclopamine or other SMO antagonists for treating basal cell carcinomas, initially in *Ptch1*$^{+/-}$ mice and eventually in humans.

Our data indicate that cyclopamine inhibits the Hh pathway in basal cell carcinomas, as indicated by down-regulation of the target genes HIP and Gli1 (Fig. 3, *A* and *B*). We additionally demonstrate that induction of Fas expression (both the protein and the RNA levels) and consequent activation of the FasL/Fas signaling axis is necessary for cyclopamine-mediated apoptosis because cell death is blocked *in vitro*

by anti-FasL antibodies. Thus, it appears that Fas expression is suppressed by the activity of the Ras-Erk pathway in basal cell carcinoma cells, and overexpression of Gli1, PDGFR-α, or active Raf (all downstream of Ptch1) renders ASZ001 cells resistant to cyclopamine-induced apoptosis (Fig. 6, *E* and *F*).[8] Furthermore, addition of a mitogen-activated protein kinase kinase inhibitor U0126 alone is sufficient to induce Fas expression and apoptosis in ASZ001 cells (Fig. 6, *C* and *D*). We have analyzed promoter sequences of human and mouse Fas genes and found multiple copies of serum response elements and Ras-responsive elements, suggesting that the Ras/Erk pathway can regulate transcription of murine and human Fas directly.[9] These data are consistent with a previous report showing that cyclopamine causes apoptosis in subsets of small-cell lung cancer and medulloblastomas in the presence of low concentrations of newborn bovine serum in which growth factor content is quite low (9, 11).[10] Because Fas is regulated at multiple levels, it will be interesting to determine whether other mechanisms, including altered Fas membrane translocation, could be involved in cyclopamine-mediated Fas up-regulation.

Because cyclopamine exerts its effects through direct association with SMO, tumors with genetic mutations downstream of SMO may not be sensitive to cyclopamine treatment. We have found that cyclopamine does not cause apoptosis in ASZ001 cells with Gli1 overexpression under the cytomegalovirus promoter (Fig. 6, *F* and *G*) or in Gli1-transformed RK3E cells.[11] Similarly, cells expressing activated SMO are resistant to cyclopamine (31). Thus, studies on the genetic mutations in specific target tumors could be helpful in predicting the effectiveness of cyclopamine treatment. Effective treatment of tumors with mutations of genes encoding proteins acting downstream of Smo will require identification of novel small molecular weight compounds acting downstream of SMO signaling. However, because most basal cell carcinomas do contain loss-of-function mutations of PTCH1, cyclopamine should represent an effective and specific agent for basal cell carcinoma therapy, as well as for those visceral cancers with Hh signaling activation, which thus far appears to be driven by overexpression of sonic Hh.

In summary, our results indicate that chronic administration of the SMO antagonist cyclopamine is effective in preventing basal cell carcinoma development *in vivo*. We demonstrate that cyclopamine inhibits Hh signaling and thereby exerts its effects through induction of Fas expression, leading to activation of the FasL/Fas signaling axis and apoptosis. It is likely that SMO antagonists capable of inhibiting Hh activation and inducing Fas expression hold great promise as a mechanism-directed approach for the treatment of basal cell carcinomas.

ACKNOWLEDGMENTS

We thank Brent Norris and Huiping Guo for technical support and Drs. Michelle Azsterbaum, Eric Fearon, and William Gaffield for providing reagents. We also thank Nonggao He, Tao Sheng, and Josh Sultz for support.

[8] Unpublished data.
[9] Unpublished observation.
[10] Unpublished data.
[11] J. Xie and C. Li, unpublished data.

REFERENCES

1. Ingham PW. Transducing Hedgehog: the story so far. EMBO J 1998;17:3505–11.
2. Taipale J, Beachy PA. The Hedgehog and Wnt signalling pathways in cancer. Nature (Lond.) 2001;411:349–54.
3. Epstein E Jr. Genetic determinants of basal cell carcinoma risk. Med Pediatr Oncol 2001;36:555–8.
4. Toftgard R. Hedgehog signalling in cancer. Cell Mol Life Sci 2000;57:1720–31.
5. Johnson RL, Rothman AL, Xie J, et al. Human homolog of patched, a candidate gene for the basal cell nevus syndrome Science (Wash. DC) 1996;272:1668–71.
6. Hahn H, Wicking C, Zaphiropoulous PG, et al. Mutations of the human homolog of Drosophila patched in the nevoid basal cell carcinoma syndrome. Cell 1996;85:841–51.
7. Xie J, Murone M, Luoh SM, et al. Activating Smoothened mutations in sporadic basal-cell carcinoma Nature (Lond.) 1998;391:90–2.
8. Thayer SP, di Magliano MP, Heiser PW, et al. Hedgehog is an early and late mediator of pancreatic cancer tumorigenesis. Nature (Lond.) 2003;425:851–6.
9. Berman DM, Karhadkar SS, Hallahan AR, et al. Medulloblastoma growth inhibition by hedgehog pathway blockade. Science (Wash. DC) 2002;297:1559–61.
10. Berman DM, Karhadkar SS, Maitra A, et al. Widespread requirement for Hedgehog ligand stimulation in growth of digestive tract tumours. Nature (Lond.) 2003;425:846–51.
11. Watkins DN, Berman DM, Burkholder SG, Wang B, Beachy PA, Baylin SB. Hedgehog signalling within airway epithelial progenitors and in small-cell lung cancer. Nature (Lond.) 2003;422:313–7.
12. Chen JK, Taipale J, Cooper MK, Beachy PA. Inhibition of Hedgehog signaling by direct binding of cyclopamine to Smoothened. Genes Dev 2002;16:2743–8.
13. Williams JA, Guicherit OM, Zaharian BI, et al. Identification of a small molecule inhibitor of the hedgehog signaling pathway: effects on basal cell carcinoma-like lesions. Proc Natl Acad Sci USA 2003;100:4616–21.
14. Frank-Kamenetsky M, Zhang XM, Bottega S, et al. Small-molecule modulators of Hedgehog signaling: identification and characterization of Smoothened agonists and antagonists. J Biol 2002;1:10.
15. Goodrich LV, Milenkovic L, Higgins KM, Scott MP. Altered neural cell fates and medulloblastoma in mouse patched mutants. Science (Wash. DC) 1997;277:1109–13.
16. Aszterbaum M, Epstein J, Oro A, et al. Ultraviolet and ionizing radiation enhance the growth of BCCs and trichoblastomas in patched heterozygous knockout mice. Nat Med 1999;5:1285–91.
17. Xie J, Aszterbaum M, Zhang X, et al. A role of PDGFRalpha in basal cell carcinoma proliferation. Proc Natl Acad Sci USA 2001;98:9255–9.
18. Louro ID, Bailey EC, Li X, et al. Comparative gene expression profile analysis of GLI and c-MYC in an epithelial model of malignant transformation. Cancer Res 2002;62:5867–73.
19. Li C, Chi S, He N, et al. IFNalpha induces Fas expression and apoptosis in hedgehog pathway activated BCC cells through inhibiting Ras-Erk signaling. Oncogene 2004;23:1608–17.
20. Bonifas JM, Pennypacker S, Chuang PT, et al. Activation of expression of hedgehog target genes in basal cell carcinomas. J Investig Dermatol 2001;116:739–42.
21. Zhang XM, Ramalho-Santos M, McMahon AP. Smoothened mutants reveal redundant roles for Shh and Ihh signaling including regulation of L/R asymmetry by the mouse node. Cell 2001;105:781–92.
22. Buechner SA, Wernli M, Harr T, Hahn S, Itin P, Erb P. Regression of basal cell carcinoma by intralesional interferon-alpha treatment is mediated by CD95 (Apo-1/Fas)-CD95 ligand-induced suicide. J Clin Investig 1997;100:2691–6.
23. Lee S, Jang JJ, Lee JY, et al. Fas ligand is expressed in normal skin and in some cutaneous malignancies. Br J Dermatology 1998;139:186–91.
24. Filipowicz E, Adegboyega P, Sanchez RL, Gatalica Z. Expression of CD95 (Fas) in sun-exposed human skin and cutaneous carcinomas. Cancer (Phila.) 2002;94:814–9.
25. Thornberry NA, Lazebnik Y. Caspases: enemies within. Science (Wash. DC) 1998;281:1312–6.
26. Fenton RG, Hixon JA, Wright PW, Brooks AD, Sayers TJ. Inhibition of Fas (CD95) expression and Fas-mediated apoptosis by oncogenic Ras. Cancer Res 1998;58:3391–400.
27. Kannan KAN, Rechavi G, Jakob-Hirsch J, et al. DNA microarrays identification of primary and secondary target genes regulated by p53. Oncogene 2001;20:2225–34.
28. Kazama H, Yonehara S. Oncogenic K-Ras and basic fibroblast growth factor prevent Fas-mediated apoptosis in fibroblasts through activation of mitogen-activated protein kinase. J Cell Biol 2000;148:557–66.
29. Cooper MK, Porter JA, Young KE, Beachy PA. Teratogen-mediated inhibition of target tissue response to Shh signaling. Science (Wash. DC) 1998;280:1603–7.
30. Hu Z, Bonifas JM, Aragon G, et al. Evidence for lack of enhanced hedgehog target gene expression in common extracutaneous tumors. Cancer Res 2003;63:923–8.
31. Taipale J, Chen JK, Cooper MK, et al. Effects of oncogenic mutations in Smoothened and Patched can be reversed by cyclopamine. Nature (Lond.) 2000;406:1005–9.

Carcinogenesis vol.00 no.00 pp.1–7, 2006
doi:10.1093/carcin/bgi378

Activation of the hedgehog pathway in human hepatocellular carcinomas

Shuhong Huang[2,†], Jing He[†], Xiaoli Zhang[†], Yuehong Bian[2], Ling Yang[2], Guorui Xie[2], Kefei Zhang[3], Wendell Tang[1], Arwen A.Stelter, Qian Wang[3,*], Hongwei Zhang[2,*] and Jingwu Xie[*]

Department of Pharmacology and Toxicology, Sealy Center for Cancer Cell Biology and [1]Department of Pathology, University of Texas Medical Branch, 301 University Boulevard, Galveston, TX 77555-1048, USA, [2]Institute of Developmental Biology, School of Life Sciences, Shandong University, Jinan, P.R. China and [3]Department of Hepatobiliary Surgery, The First Affiliated Hospital, Sun Yat-Sen University, 58 Zhongshan Road, Guangzhou, 510080, P.R. China

*To whom correspondence should be addressed. Tel: (409) 747 1845; Fax: (409) 747 1938;
Email: jinxie@utmb.edu

Liver cancers, the majority of which are hepatocellular carcinomas (HCCs), rank as the fourth in cancer mortality worldwide and are the most rapidly increasing type of cancer in the United States. However, the molecular mechanisms underlying HCC development are not well understood. Activation of the hedgehog pathway is shown to be involved in several types of gastrointestinal cancers. Here, we provide evidence to indicate that hedgehog signaling activation occurs frequently in HCC. We detect expression of *Shh*, *PTCH1* and *Gli1* in 115 cases of HCC and in 44 liver tissues adjacent to the tumor. Expression of *Shh* is detectable in about 60% of HCCs examined. Consistent with this, hedgehog target genes *PTCH1* and *Gli1* are expressed in over 50% of the tumors, suggesting that the hedgehog pathway is frequently activated in HCCs. Of five cell lines screened, we found Hep3B, Huh7 and PLC/PRF/5 cells with detectable hedgehog target genes. Specific inhibition of hedgehog signaling in these three cell lines by smoothened (SMO) antagonist, KAAD-cyclopamine, or with Shh neutralizing antibodies decreases expression of hedgehog target genes, inhibits cell growth and results in apoptosis. In contrast, no effects are observed after these treatments in HCC36 and HepG2 cells, which do not have detectable hedgehog signaling. Thus, our data indicate that hedgehog signaling activation is an important event for development of human HCCs.

Abbreviations: DMEM, Dulbecco-modified essential medium; HCCs, hepatocellular carcinomas; PCR, polymerase chain reaction; RT–PCR, reverse transcription–polymerase chain reaction; SMO, smoothened; TUNEL, terminal deoxynucleotidyl transferase-mediated dUTP nick end labeling.

[†]These authors contributed equally to this work.

Introduction

Liver cancer, with hepatocellular carcinoma (HCC) as the major tumor type, is a malignancy of worldwide significance (1–4). HCC ranks as the eighth cause of cancer-related death in American men with 14 000 deaths yearly and is the most rapidly increasing type of cancer in the United States (2). The medical oncology community is largely unprepared for this looming epidemic of HCC. Although the increase of HCC in the United States is correlated with the increasing prevalence of chronic infection with hepatitis C virus (HCV), the molecular understanding of HCC development remains elusive (2). A majority (70–85%) of patients present with advanced or unresectable disease, making the prognosis of HCC dismal, and systemic chemotherapy is quite ineffective in HCC treatment. The first essential step for development of effective therapeutic approaches is to identify specific signaling pathways involved in HCC.

The role of the hedgehog pathway in human cancers has been established through studies of basal cell nevus syndrome (BCNS) (5,6), a rare hereditary disorder with a high risk of basal cell carcinomas, and activation of the hedgehog pathway has been observed in other cancers such as prostate cancer and gastrointestinal cancers (7–17). Targeted inhibition of the hedgehog pathway results in growth inhibition in cancer cell lines with activated hedgehog signaling (10–17). The hedgehog pathway is essential for embryonic development, tissue polarity and cell differentiation (18). The hedgehog pathway is critical in the early development of the liver and contributes to differentiation between hepatic and pancreatic tissue formation, but the adult liver normally does not have detectable levels of hedgehog signaling (10,19). In this report, we characterize expression of sonic hedgehog and its target genes in 115 HCC specimens. The role of hedgehog signaling on cell growth is further demonstrated in five HCC cancer cell lines.

Materials and methods

Tissue samples

A total of 115 specimens of HCC tissues were used. Of these, 14 specimens were received as discarded materials from General Surgery of the Shan Dong Qi Lu Hospital, Jinan, China. Pathology reports and H&E stained sections of each specimen were reviewed to determine the nature of the disease and the tumor histology. The remaining 101 HCC specimens were from Sun Yat-Sen University. Forty-four liver tissues adjacent to the tumor were also included in this study. None of the patients had received chemotherapy or radiation therapy prior to specimen collection.

In situ hybridization

In situ hybridization was performed according to the manufacture's instructions (Roche Molecular Biochemicals) and our published protocol (16,17). In brief,

tissues were fixed with 4% paraformaldehyde in phosphate buffered saline (PBS) and embedded with paraffin. Then 6 μm thick tissue sections were mounted onto Poly-L-Lysine slides. Samples were treated with proteinase K (20 μg/ml) at 37°C for 15 min, refixed in 4% paraformaldehyde and hybridized overnight with a digoxigenin-labeled RNA probe (at a final concentration of 1 μg/ml). The hybridized RNA was detected by alkaline phosphatase-conjugated anti-digoxigenin antibodies (Roche Molecular Biochemicals), which catalyzed a color reaction with the substrate NBT/BCIP (Roche Molecular Biochemicals). Blue signal indicated positive hybridization. We regarded tissues without blue signals as negative. As negative controls, sense probes were used in the hybridization and no signals were observed. *In situ* hybridizations were repeated at least twice for each tissue sample with similar results.

RNA isolation and quantitative RT–PCR

Total RNA of cells was extracted using a RNA extraction kit from Promega according to the manufacturer (Promega, Madison, WI), and quantitative PCR analyses were performed according to a previously published procedure (17,20). Triplicate C_T values were analyzed in Microsoft Excel using the comparative $C_T(\Delta\Delta C_T)$ method as described by the manufacturer (Applied Biosystems, Foster City, CA). The amount of target ($2^{-\Delta\Delta CT}$) was obtained by normalization to an endogenous reference (18S RNA) and relative to a calibrator. We used the following primers for RT–PCR of *Shh*: forward primer—5′-ACCGAGGGCTGGGACGAAGA-3′; reverse primer—5′-ATTTGGCCGCCACCGAGTT -3′

Cell culture, transfection and drug treatment

HCC cell lines [Hep3B, HepG2, HCC36, PLC/PRF/5 (as PLC throughout this manuscript) and Huh7] were generously provided by Drs Chiaho Shih, Tien Ko and Kui Li at UTMB. All cells were cultured in Dulbecco-modified essential medium (DMEM) with 10% FBS and antibiotics. Cells were treated with 2 μM KAAD-cyclopamine, a specific antagonist of smoothened (SMO) (21) (dissolved in DMSO as 5 mM stock solution, Cat# K171000 from Toronto Research Chemicals, Canada), in 0.5% FBS in DMEM for indicated time mentioned in the figure legends. Previously, we performed toxicity assay with KAAD-cyclopamine in GI cancer cells and found that 10 μM of KAAD-cyclopamine can lead to non-specific toxicity (16). In contrast, 5 or 10 μM KAAD-cyclopamine was quite toxic to cells regardless of hedgehog signaling status (our unpublished observation), and was, thus, not used in this study. Tomatidine (2 μM in 0.5% FBS DMEM, Sigma Cat# T2909), a structurally similar compound with non-specific inhibition on hedgehog signaling, was used as a negative control. In addition, the specific inhibition of hedgehog signaling in HCC cells was achieved by addition of Shh neutralizing antibodies (1 μg/ml in 0.5% FBS DMEM, Santa Cruz Biotechnology, Cat# SC-9024). Most cell lines were treated with KAAD-cyclopamine (2μM) or Shh antibodies (1 μg/ml) in 0.5% FBS in DMEM medium for an indicated time (see figure legends for details). However, for Hep3B cells, we used 2% FBS in DMEM because Hep3B cells cannot grow in 0.5% FBS DMEM medium. Transient transfection of Gli1 in HCC cells was performed using LipofectAmine according to manufacturer's recommendation (Plasmid:LipofectAmine = 1:2.5). Cells with ectopic expression of Gli1 were subjected to drug treatment and to TUNEL (terminal deoxynucleotidyl transferase-mediated dUTP nick end labeling) assay.

Cell viability and TUNEL assays

For cell viability analysis, we used two methods: Trypan blue analysis and MTT assay. Trypan blue analysis was performed according to a procedure from the manufacturer (Invitrogen, CA) (22). The percentage of trypan blue positive cells (dead cells) was calculated under a microscope and triplicates of samples for each treatment were used. The experiment was repeated three times. MTT assay was performed using a previously published procedure (22). In brief, triplicates of samples for each treatment were used in a 96-well format. Twenty microliters of MTT (10 mg/ml in PBS) was added to each well (containing 100 μl cultured medium, 0.5% FBS DMEM in this study). Three hours later, medium was aspirated, and 100 μl of a mixture of isopropanol and DMSO (9:1) added into each well. Thirty minutes later, the 570 nm absorbance was measured with a microplate reader from Molecular Devices Co. BrdU labeling was for 1 h and immunofluorescent staining of BrdU was performed as reported previously (23). TUNEL assay was performed using a kit from Roche Biochemicals according to a published procedure (24). In brief, cells were fixed with 4% paraformaldehyde at room temperature for 1 h and permeated with 0.1% Triton X-100, 0.1% sodium citrate (freshly prepared) on ice for 2 min. After washing with PBS, each sample was incubated with 50 μl of TUNEL reaction mixture at 37°C for 30 min. TUNEL label solution (without enzyme) was used as a negative control. TUNEL positive cells were counted under a fluorescent microscope. The counting was repeated three times, and the percentage from each counting was calculated.

Statistical analysis

Statistical analysis was performed by Binomial proportions analysis. The association of mRNA transcript expression with various clinicopathological parameters was also analyzed; a P-value < 0.05 was considered to be statistically significant.

Results

Expression of PTCH1 and Gli1 in primary HCC

In order to assess hedgehog signaling activation in HCC, we assayed *PTCH1* and *Gli1* expression in 115 cases of HCC specimens. As the target genes of the hedgehog pathway, expression of *PTCH1* and *Gli1* transcripts indicate hedgehog signaling activation (25,26). Primarily, we used *in situ* hybridization to assess hedgehog signaling activation in our collected tissues ($n = 115$), which was further confirmed in selected specimens by real-time PCR. The results are summarized in Table I.

For *in situ* hybridization analysis, blue signal was regarded as detectable expression of the target. Tissues without blue signals were regarded as negative for the target. Using *in situ* hybridization, 79 of 110 (70%) tumor specimens had detectable expression of *Gli1* (representative images are shown in Figure 1A, and summarized in Table I, with additional images and data provided in Supplementary Table 1 and Supplementary Figures 1–6), indicating that *Gli1* expression is detectable in many HCCs. The sense probe gave no detectable signals (Figure 1A), confirming the specificity of *in situ* hybridization in our experiments. In most cases, *Gli1* expression was detectable in the tumor nest, not in the adjacent liver tissue (Figure 1A; Supplementary Figure 1 and Table 1) or in the stroma (arrows in Figure 1A).

In comparison with the *Gli1* transcript, the *in situ* hybridization signal of *PTCH1* was generally less intense (Figure 1B and Supplementary Figures 1–6), but 56% (60 of 107) of HCC specimens were positive for *PTCH1* transcript. We found a total of 51 tumors (out of 98 informative HCCs) (52%) with detectable expression of both *Gli1* and *PTCH1* (Table I, Supplementary Table 1), which suggests activated hedgehog signaling in these specimens. Our analysis indicates that activation of hedgehog signaling (as indicated by expression of both *Gli1* and *PTCH1* transcripts) occurs more frequently in HCC than in the adjacent liver tissue (Table I, Supplementary Table 1 and Supplementary Figure 1). There are several cases in which only *Gli1* or *PTCH1* was expressed (Supplementary Table 1), suggesting that expression of *Gli1* and *PTCH1* may be differentially regulated. Further analysis of our data did not reveal association of the hedgehog signaling activation with tumor size or tumor differentiation (Table I). Tumors with hepatocirrhosis were not significantly different from tumors without hepatocirrhosis in the expression of *Gli1* and *PTCH1* (Table I).

In situ hybridization data was further confirmed by real-time PCR in several tumor specimens in which 70% of the tissue mass was actually tumor tissue (Figure 1C and D). Consistent with *in situ* hybridization, expression of *Gli1* and *PTCH1* were detectable in the tumor, not in the adjacent liver tissue in most cases (will be discussed later in the Discussion). Our data indicate that expression of *Gli1* and *PTCH1* in the tumor was 3- to 30-fold higher than that in adjacent liver tissues (Figure 1C and D). The real-time PCR analyses further confirmed that activation of the hedgehog pathway is a common event in HCC.

Table I. Detection of *Shh*, *PTCH1* and *Gli1* expression in HCC and in adjacent liver tissue by *in situ* hybridization

	Shh			Hedgehog pathway activation						
				PTCH1		*Gli1*		Pathway activation		
	pos	neg	*P*-value	pos	neg	pos	neg	pos	neg	*P*-value
HCC	64/108	44/108	<0.01*	60/107	47/107	79/110	31/110	51/98	47/98	<0.01*
Adjacent tissues	5/41	36/41		18/43	25/43	15/44	29/44	9/43	34/43	
Tumor size										
Small (<3 cm)	16/31	15/31	0.316	17/31	14/31	25/32	7/32	16/31	15/31	0.896
Large (>3 cm)	46/74	28/74		42/74	32/74	52/75	23/75	35/66	31/66	
Tumor differentiation										
Well	34/52	18/52	0.107	30/51	21/51	43/52	9/52	29/51	22/51	0.264
Mod-poor	20/41	21/41		22/41	19/41	32/43	11/43	19/42	23/42	
Sex										
Male	47/81	34/81	0.651	43/81	38/81	58/83	25/83	35/72	37/72	0.258
Female	17/27	10/27		17/26	9/26	21/27	6/27	16/26	10/26	
Hepatocirrhosis										
+	14/19	5/19	0.163	14/20	6/20	14/20	6/20	11/17	6/17	0.251
–	49/87	38/87		43/83	40/83	63/87	24/87	39/79	40/79	

Statistical analysis was performed by Binomial proportions analysis. A P-value < 0.05 was considered to be statistically significant. The association of mRNA transcript expression with various clinicopathological parameters was also analyzed. Statistically significant difference was indicated by asterisk (*).

pos, positive signal; neg, negative signal; well, well-differentiated tumors; mod-poor, moderately to poorly differentiated tumors. Elevated expression of at least two hedgehog target genes was regarded as being positive (pos) in activation of the hedgehog pathway, whereas elevated expression of one hedgehog target gene was regarded as being negative (neg) in hedgehog signaling activation.

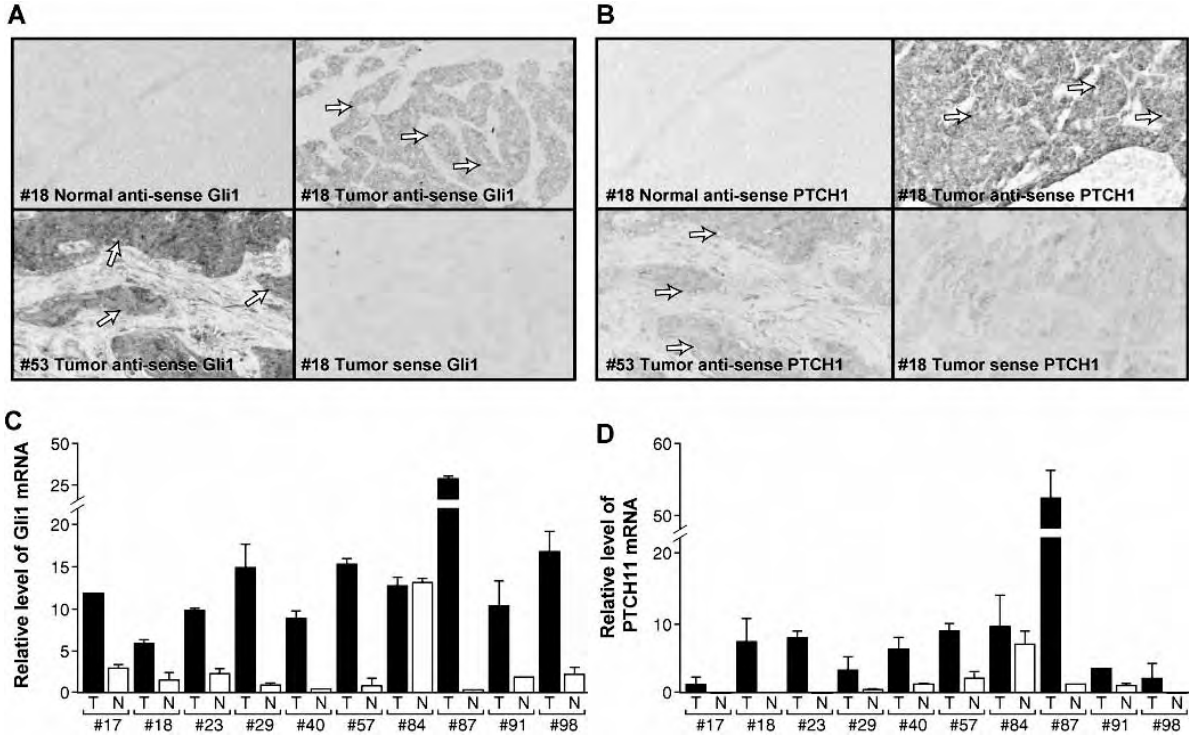

Fig. 1. Detection of *Gli1*, *PTCH1* expression in primary HCCs. *In situ* hybridization detection of *Gli1* (**A**) and *PTCH1* (**B**) transcripts in HCCs was performed as reported previously. Positive signals (dark grey staining) were observed in the tumor ('Tumor', tumor nests indicated by arrows), not in the stroma surrounding the tumor nests or in the liver tissue adjacent to the tumor ('Normal'). The sense probes did not give any positive signals (A and B), confirming the specificity of our *in situ* hybridization. Additional pictures have been included in the Supplementary Figures. Expression of *Gli1* and *PTCH1* was further confirmed by real-time PCR analysis done in triplicate (**C** and **D**) in selected tumor specimens in which 70% of the tissue mass was tumor tissue. Expression of *Gli1* (C) and *PTCH1* (D) from the tumor (T) was 3- to 30-fold higher than that from the adjacent liver tissue (N). Data indicates values relative to 18S RNA and to a calibrator. The data from this analysis are consistent with those from *in situ* hybridization analysis.

Expression of Shh in HCCs

To investigate if *Shh* is associated with hedgehog signaling activation in HCCs, *Shh* expression was first detected by *in situ* hybridization. We detected *Shh* transcripts in 64 of 108 HCC specimens, but not in the majority of liver tissues adjacent to the tumor (Figure 2A, Table I and Supplementary Figures 1, 4–6). *Shh* transcript was only detectable in the tumor nests, not in the stroma (dark grey signals in Figure 2A), suggesting that

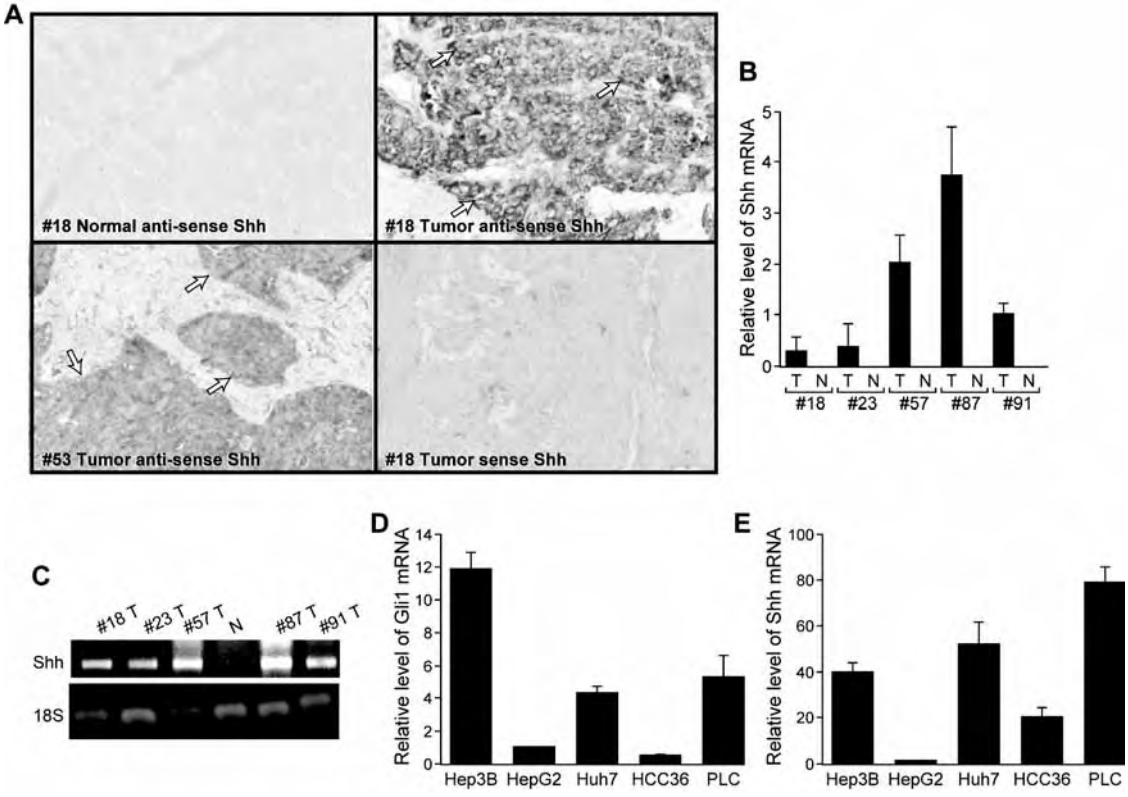

Fig. 2. Detection of *Shh* expression in HCCs. *In situ* hybridization (**A**), real-time PCR (**B**) and regular RT–PCR (**C**) were used to detect *Shh* transcript. *Shh* transcript (dark grey signals in A) resided in the tumor ('Tumor', tumor nests indicated by black arrows), not the stromal or adjacent liver tissue ('Normal') (A), suggesting that the tumor tissue is the major source for *Shh* expression. To confirm our *in situ* hybridization results, we used real-time PCR to detect *Shh* expression (B), which was further confirmed by RT–PCR (C). Shh transcripts were detected only in the tumor (T), not in the adjacent liver tissue (N). Tumors with detectable *Gli1* and *PTCH1* transcripts all had detectable *Shh*, suggesting a major role of *Shh* for activation of the hedgehog pathway in HCCs. Additional real-time PCR experiments showed a relatively high level of *Gli1* (**D**), *PTCH1* (not shown here) and *Shh* (**E**) in three HCC cell lines: Hep3B, Huh7 and PLC. Data indicates values relative to 18S RNA and to a calibrator.

cancer cells are the major source of *Shh* expression. Almost all tumors with detectable *Gli1* and *PTCH1* expression had detectable *Shh* transcript (Figures 1 and 2, Supplementary Table 1, Supplementary Figures 5 and 6). *Shh* expression in the tumor was further confirmed by real-time PCR and regular RT–PCR (Figure 2B and C). Thus, it appears that *Shh* induction may be the trigger for activated hedgehog signaling in HCCs. In support of this hypothesis, we detected expression of *Shh* in all three HCC cell lines with detectable transcript of *Gli1* (Figure 2D).

Targeted inhibition of hedgehog signaling in HCC cells

SMO is the major signal transducer of the hedgehog pathway; thus cancer cells with activated hedgehog signaling through *Shh* expression should be sensitive to treatment with the SMO antagonist, KAAD-cyclopamine (Toronto Research Chemicals, Cat# K171000) (21). First, we screened HCC cell lines for hedgehog signaling activation by real-time PCR detection of *Gli1* and *PTCH1* and found that hedgehog signaling pathway was activated in Hep3B, PLC and Huh7 cells but not in HepG2 and HCC36 cells (Figure 2D shows the level of *Gli1* transcript). Addition of KAAD-cyclopamine (2 μM) greatly decreased the level of *Gli1* transcript in three cell lines (Hep3B, PLC and Huh7) (Figure 3A), whereas no changes on *Shh* expression were observed (Supplementary Figure 7). The closely related compound tomatidine, which does not affect SMO signaling and thus served as a negative control, had little discernible effect on hedgehog target genes. This data indicates specific inhibition of the hedgehog pathway by KAAD-cyclopamine in these cells.

As a result of inhibited hedgehog signaling by KAAD-cyclopamine treatment, we observed an inhibition on cell growth of Huh7 cells, but not on that of HepG2 cells (Figure 3B and C). The specificity of hedgehog signaling inhibition was further demonstrated using Shh neutralizing antibodies (Figure 3B and C). We found that addition of Shh antibodies at a concentration of 1 μg/ml reduced cell growth of Huh7 cells but had no effect on HepG2 cells (Figure 3B and C). Further analysis indicates that BrdU incorporation was also reduced after treatment with KAAD-cyclopamine in Huh7 cells (see Supplementary Figure 8).

Following treatment with KAAD-cyclopamine or Shh antibodies, we found that PLC cells underwent apoptosis whereas no apoptosis was observed in HepG2 cells (Figure 4A shows data from KAAD-cyclopamine treatment). Data from TUNEL assay was confirmed by Trypan blue staining (data not shown here). The percentage of apoptotic cells varied from cell line to cell line, with PLC being the most sensitive cell line (over 20% TUNEL positive cells after KAAD-cyclopamine treatment for 8 h, Figure 4B). Similar data were also observed after Shh antibody treatment (data not shown here). These data demonstrate that the HCC cells with activated hedgehog signaling are sensitive to targeted inhibition of the hedgehog pathway, whereas other HCC

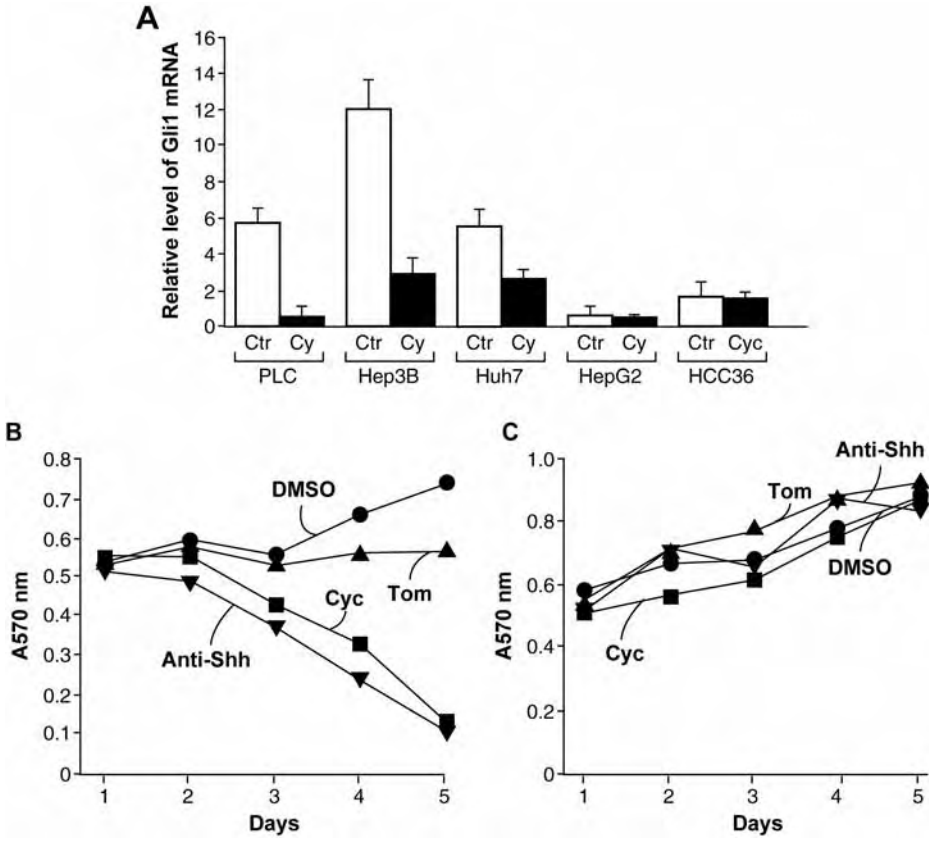

Fig. 3. Hedgehog signaling and growth of HCC cells. Real-time PCR data of *Gli1* transcript shows that in the presence of 2 μM KAAD-cyclopamine (**A**) or 1 μg/ml Shh neutralizing antibodies (data not shown here) for 12 h (see Materials and methods for details on drug-treatment conditions), the level of hedgehog target gene *Gli1* was decreased in the three cell lines with activated hedgehog signaling (PLC, Hep3B and Huh7). In contrast, no effects were observed in HCC36 and HepG2 cells, in which hedgehog signaling is not activated. Cell growth of Huh7 (**B**) and HepG2 (**C**) cell lines were examined by MTT assay. Huh7 cells were inhibited by 2 μM KAAD-cyclopamine (Cat# K317000, Toronto Research Chemicals) or 1 μg/ml Shh neutralizing antibodies (Cat# 9024, Santa Cruz Biotechnology) (Figure 2B). This inhibition was specific because addition of tomatidine, a structurally similar but non-specific compound for hedgehog signaling, did not affect cell growth. In contrast, cell growth of HepG2 was not affected by KAAD-cyclopamine (2 μM) or Shh neutralizing antibodies (1 μg/ml) (C), confirming the specific growth inhibition of HCC cells through targeted inactivation of hedgehog signaling.

cells (without activated hedgehog signaling) are resistant to these treatments.

Because KAAD-cyclopamine and Shh antibodies only affect signaling upstream of SMO, we hypothesize that cells with ectopic expression of the downstream effector Gli1 may prevent KAAD-cyclopamine-mediated apoptosis if these treatments are specific to the hedgehog pathway. In Huh7 cells, we transiently expressed Gli1 under the control of the CMV promoter (pLNCX vector) (23). After KAAD-cyclopamine treatment, we found that all Gli1-expressing cells ($n = 500$) were negative for TUNEL, demonstrating the specificity of KAAD-cyclopamine. Similarly, Gli1-expressing Huh7 cells were resistant to Shh antibody treatment (data not shown). This study also suggests that downregulation of *Gli1* may be an important mechanism by which targeted inhibition of hedgehog signaling mediates apoptosis in HCC cells.

Taken together, our findings indicate that activation of the hedgehog pathway is quite common in liver cancers. Expression of *Shh* and its target genes, *Gli1* and *PTCH1*, is more frequent in the tumor than in the adjacent liver tissue. This activation of hedgehog signaling is not associated with other clinicopathological parameters of the tumor. HCC cells with activation of the hedgehog pathway are sensitive to targeted inhibition of hedgehog signaling. These data support our hypothesis that activation of the hedgehog pathway is an important event in the development of HCC.

Discussion

Hedgehog signaling in liver cancer

Over 500 000 new cases of liver cancers are reported each year worldwide; most of them are HCCs. Most of HCC patients (70–80%) are diagnosed late in the progression of the disease and cannot be effectively treated. Understanding the molecular mechanisms underlying liver cancer development is an essential first step in early diagnosis of liver cancer. In this report, we present strong evidence to indicate that the hedgehog pathway is frequently activated in liver cancers. Our data further indicate that induced expression of *Shh* may be the major trigger for activated hedgehog signaling in HCCs. How was *Shh* expression induced in HCC? Our preliminary data indicate that the Shh promoter activity is high in Huh7 cells but low in HepG2 cells (our unpublished observation), suggesting that transcriptional upregulation of the *Shh* gene may be the major mechanism for induced expression of *Shh*.

Since hedgehog signaling is frequently activated in HCCs, markers for hedgehog signaling activation, including *Shh*, *PTCH1* and *Gli1*, may be useful for diagnosis of liver cancers. In most cases, *Gli1* and *PTCH1* were expressed in the tumor,

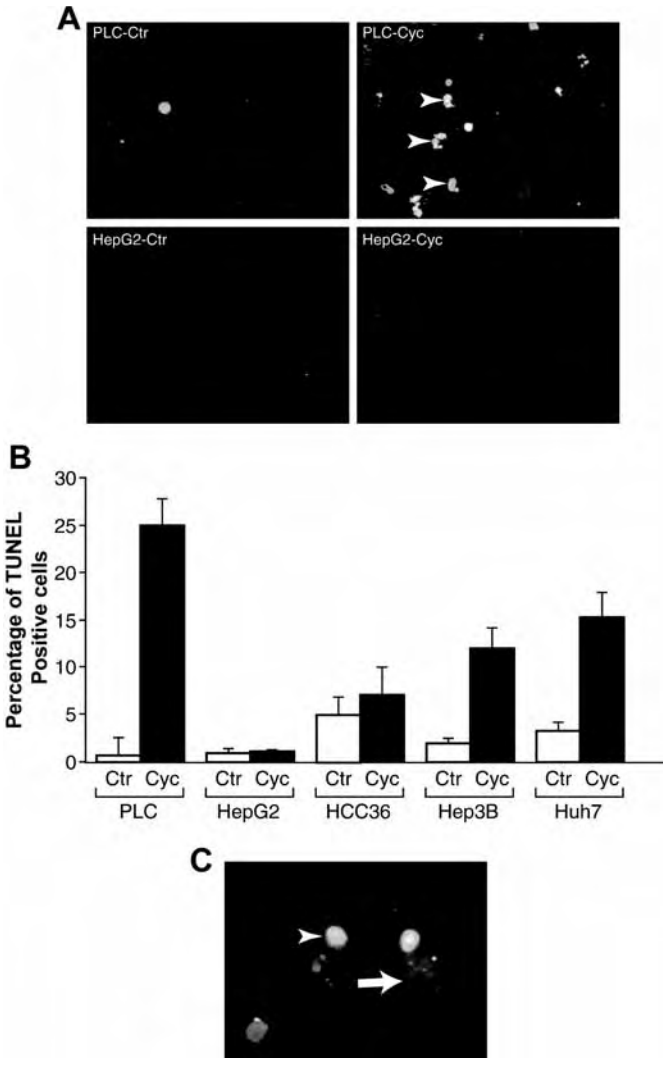

Fig. 4. Targeted inhibition of hedgehog signaling induces apoptosis in hepatocellular carcinoma cells. TUNEL assays (**A**) for detection of apoptosis were measured after treatment with 2 μM KAAD-cyclopamine (Cat# K317000, Toronto Research Chemicals) in PLC (8 h) and in HepG2 (36 h). During treatment, we used 0.5% FBS in DMEM for cell culture. TUNEL positive cells (light grey, indicated by arrowheads) were observed in PLC cells after KAAD-cyclopamine treatment. The percentages of TUNEL positive cells in all five cell lines are quantified in **B.** Please note that different cell lines have different sensitivities to KAAD-cyclopamine. Whereas treatment of 2 μM KAAD-cyclopamine for 8 h was sufficient to induce cell death in PLC cells, a longer treatment was needed for Hep3B (48 h) and Huh7 cells (36 h) (also see Materials and methods for drug treatment). TUNEL positive cells ($n = 500$) were counted under a fluorescent microscope, and the experiment was repeated three times with similar results. TUNEL assays following ectopic Gli1 expression and KAAD-cyclopamine treatment (**C**) demonstrated that cells positive for ectopic Gli1 expression [dark grey staining, detection by c-myc tag as reported previously (27)] were TUNEL negative. Gli1 was expressed in Huh7 cells under the control of the CMV promoter. Transfected cells were treated with 2 μM KAAD-cyclopamine or 2 μM tomatidine in 0.5% FBS in DMEM for 48 h. We found that Gli1-expressing cells ($n = 500$) were all TUNEL negative.

not in the liver tissues adjacent to the tumor. However, in nine cases, we detected expression of *Gli1* and *PTCH1* in both the tumor and the adjacent liver tissues, which were confirmed by real-time PCR in one case (#84) (see Supplementary Table 1 for details). Further analysis indicated that tissue abnormalities were present in these adjacent liver tissues with expression of *Gli1* and *PTCH1*, ranging from small cell dysplasia, dysplastic nodules to microscopic HCCs. In contrast, a non-cancerous liver tissue (as shown in supplementary Figures 2E, 3E and 4E) did not have any detectable expression of *Shh*, *PTCH1* and *Gli1*. Thus, it appears that hedgehog signaling activation occurs in early lesions of HCCs. Further studies of hedgehog signaling in different stages of HCCs, particularly early stages, will establish the basis for early diagnosis of HCC through detection of *Gli1*, *PTCH1* and *Shh*.

Another important pathway involved in HCC is the Wnt pathway via mutations of β-catenin or axin (28–31). We have investigated the association of hedgehog signaling with the Wnt pathway in liver cancer. We detected β-catenin protein localization by immunohistochemistry in tumors with activated hedgehog signaling. Only 1 in 20 tumors with hedgehog signaling activation had nuclear β-catenin, a major indicator for the canonical Wnt signaling, suggesting that hedgehog signaling activation may be a distinct abnormality from β-catenin activation in HCCs.

Therapeutic perspective of liver cancer through targeted inhibition of the hedgehog pathway

Our studies also indicate that targeted inhibition of hedgehog signaling may be effective in treatment of HCCs. We demonstrate in this report that SMO antagonist, KAAD-cyclopamine, or Shh neutralizing antibodies specifically induce apoptosis in HCC cells with activated hedgehog signaling. The hedgehog pathway is not activated in HepG2 cells, and these cells are not sensitive to these reagents. In our studies, variable sensitivities were observed in different cell lines. For PLC cells, treatment with 2 μM KAAD-cyclopamine for 8 h caused apoptosis in many cells. In contrast, a similar rate of cell death was observed in Huh7 cells after treatment (2 μM KAAD-cyclopamine) for 36 h. This difference may be due to other genetic alterations in different cell lines. Further understanding of the molecular basis for cell sensitivity to KAAD-cyclopamine will help us to design better ways to treat HCC in the future. Thus, it may be possible in the future to treat the subsets of liver cancer with hedgehog signaling inhibitors (e.g. KAAD-cyclopamine).

While this manuscript is being reviewed, two other groups have reported similar data on hedgehog signaling in HCCs (32,33).

Supplementary material

Supplementary material is available at: http://www.carcin.oxfordjournals.org/

Acknowledgements

This research was supported by grants from the NIH (R01-CA94160), Department of Defense (DOD-PC030429), The NIEHS (ES06676) and National Science Foundation of China (30228031). We thank Drs Chiaho Shih, Tien Ko and Kui Li for providing cell lines for this study and Huiping Guo for technical support in real-time PCR analysis and Karen Martin for help with the manuscript.

Conflict of Interest Statement: None declared.

References

1. Bruix,J., Boix,L., Sala,M. and Llovet,J.M. (2004) Focus on hepatocellular carcinoma. *Cancer Cell*, **5**, 215–219.

2. El-Serag,H.B. and Mason,A.C. (2000) Risk factors for the rising rates of primary liver cancer in the United States. *Arch. Intern. Med.*, **160**, 3227–3230.
3. Pisani,P., Parkin,D.M., Bray,F. and Ferlay,J. (1999) Estimates of the worldwide mortality from 25 cancers in 1990. *Int. J. Cancer*, **83**, 18–29.
4. Srivatanakul,P., Sriplung,H. and Deerasamee,S. (2004) Epidemiology of liver cancer: an overview. *Asian Pac. J. Cancer Prev.*, **5**, 118–125.
5. Johnson,R.L., Rothman,A.L., Xie,J. *et al.* (1996) Human homolog of patched, a candidate gene for the basal cell nevus syndrome. *Science*, **272**, 1668–1671.
6. Hahn,H., Wicking,C., Zaphiropoulous,P.G. *et al.* (1996) Mutations of the human homolog of Drosophila patched in the nevoid basal cell carcinoma syndrome. *Cell*, **85**, 841–851.
7. Raffel,C., Jenkins,R.B., Frederick,L., Hebrink,D., Alderete,B., Fults,D.W. and James,C.D. (1997) Sporadic medulloblastomas contain PTCH mutations. *Cancer Res.*, **57**, 842–845.
8. Xie,J., Johnson,R.L., Zhang,X. *et al.* (1997) Mutations of the PATCHED gene in several types of sporadic extracutaneous tumors. *Cancer Res.*, **57**, 2369–2372.
9. Watkins,D.N., Berman,D.M., Burkholder,S.G., Wang,B., Beachy,P.A. and Baylin,S.B. (2003) Hedgehog signalling within airway epithelial progenitors and in small-cell lung cancer. *Nature*, **422**, 313–317.
10. Berman,D.M., Karhadkar,S.S., Maitra,A. *et al.* (2003) Widespread requirement for Hedgehog ligand stimulation in growth of digestive tract tumours. *Nature*, **425**, 846–851.
11. Thayer,S.P., Di Magliano,M.P., Heiser,P.W. *et al.* (2003) Hedgehog is an early and late mediator of pancreatic cancer tumorigenesis. *Nature*, **425**, 851–856.
12. Fan,L., Pepicelli,C.V., Dibble,C.C. *et al.* (2004) Hedgehog signaling promotes prostate xenograft tumor growth. *Endocrinology*, **145**, 3961–3970.
13. Sanchez,P., Hernandez,A.M., Stecca,B. *et al.* (2004) Inhibition of prostate cancer proliferation by interference with SONIC HEDGEHOG-GLI1 signaling. *Proc. Natl Acad. Sci. USA*, **101**, 12561–12566.
14. Karhadkar,S.S., Bova,G.S., Abdallah,N., Dhara,S., Gardner,D., Maitra,A., Isaacs,J.T., Berman,D.M. and Beachy,P.A. (2004) Hedgehog signalling in prostate regeneration, neoplasia and metastasis. *Nature*, **431**, 707–712.
15. Sheng,T., Li,C.-X., Zhang,X., Chi,S., He,N., Chen,K., McCormick,F., Gatalica,Z. and Xie,J. (2004) Activation of the hedgehog pathway in advanced prostate cancer. *Mol. Cancer*, **3**, 29.
16. Ma,X., Sheng,T., Zhang,Y. *et al.* (2006) Hedgehog signaling is activated in subsets of esophageal cancers. *Int. J. Cancer*, **118**, 139–148.
17. Ma,X., Chen,K., Huang,S., Zhang,X., Adegboyega,P.A., Evers,B.M., Zhang,H. and Xie,J. (2005) Frequent activation of the hedgehog pathway in advanced gastric adenocarcinomas. *Carcinogenesis*, **26**, 1698–1705.
18. Ingham,P.W. (1998) Transducing hedgehog: the story so far. *EMBO J*, **17**, 3505–3511.
19. Deutsch,G., Jung,J., Zheng,M., Lora,J. and Zaret,K.S. (2001) A bipotential precursor population for pancreas and liver within the embryonic endoderm. *Development*, **128**, 871–881.
20. Chi,S., Huang,S., Li,C. *et al.* (2006) Activation of the hedgehog pathway in a subset of lung cancers. *Cancer Lett.* Epub January 27, 2006.
21. Chen,J.K., Taipale,J., Cooper,M.K. and Beachy,P.A. (2002) Inhibition of Hedgehog signaling by direct binding of cyclopamine to Smoothened. *Genes Dev.*, **16**, 2743–2748.
22. Li,C., Chi,S., He,N., Zhang,X., Guicherit,O., Wagner,R., Tyring,S. and Xie,J. (2004) IFNalpha induces Fas expression and apoptosis in hedgehog pathway activated BCC cells through inhibiting Ras-Erk signaling. *Oncogene*, **23**, 1608–1617.
23. Xie,J., Aszterbaum,M., Zhang,X., Bonifas,J.M., Zachary,C., Epstein,E. and McCormick,F. (2001) A role of PDGFRalpha in basal cell carcinoma proliferation. *Proc. Natl Acad. Sci. USA*, **98**, 9255–9259.
24. Athar,M., Li,C-X, Chi,S. *et al.* (2004) Inhibition of smoothened signaling prevents ultraviolet B-induced basal cell carcinomas through induction of fas expression and apoptosis. *Cancer Res.*, **64**, 7545–7552.
25. Pasca di Magliano,M. and Hebrok,M. (2003) Hedgehog signalling in cancer formation and maintenance. *Nat. Rev. Cancer*, **3**, 903–911.
26. Xie,J. (2005) Hedgehog signaling in prostate cancer. *Future Oncol.*, **1**, 331–338.
27. Sheng,T., Chi,S., Zhang,X. and Xie,J. (2006) Regulation of Gli1 localization by the cAMP/protein kinase A signaling axis through a site near the nuclear localization signal. *J. Biol. Chem.*, **281**, 9–12.
28. Taniguchi,K., Roberts,L.R., Aderca,I.N. *et al.* (2002) Mutational spectrum of beta-catenin, AXIN1, and AXIN2 in hepatocellular carcinomas and hepatoblastomas. *Oncogene*, **21**, 4863–4871.
29. Satoh,S., Daigo,Y., Furukawa,Y. *et al.* (2000) AXIN1 mutations in hepatocellular carcinomas, and growth suppression in cancer cells by virus-mediated transfer of AXIN1. *Nat. Genet.*, **24**, 245–250.
30. Miyoshi,Y., Iwao,K., Nagasawa,Y., Aihara,T., Sasaki,Y., Imaoka,S., Murata,M., Shimano,T. and Nakamura,Y. (1998) Activation of the beta-catenin gene in primary hepatocellular carcinomas by somatic alterations involving exon 3. *Cancer Res.*, **58**, 2524–2527.
31. de La Coste,A., Romagnolo,B., Billuart,P. *et al.* (1998) Somatic mutations of the beta-catenin gene are frequent in mouse and human hepatocellular carcinomas. *Proc. Natl Acad. Sci. USA*, **95**, 8847–8851.
32. Patil,M.A., Zhang,J., Ho,C., Cheung,S.T., Fan,S.T. and Chen,X. (2006) Hedgehog signaling in human hepatocellular carcinoma. *Cancer Biol. Ther.*, **5**.
33. Sicklick,J.K., Li,Y.X., Jayaraman,A. *et al.* (2005) Dysregulation of the hedgehog pathway in human hepatocarcinogenesis. *Carcinogenesis* Epub December 8, 2005.

Received 00, 0000; revised 00, 0000;
accepted 00, 0000